Sea Change To Nature-based Solutions

Tiggeloven, Timothy

2022

document version
Publisher's PDF, also known as Version of record

Sea Change To Nature-based Solutions

A Coastal Flood Risk Perspective

Timothy Tiggeloven

Sea Change to Nature-based Solutions: a coastal flood risk perspective

PhD thesis, Vrije Universiteit Amsterdam, The Netherlands
ISBN: 978-94-6458-644-2
Artwork: Mirjam Tiggeloven
Printed by: Ridderprint

Timothy Tiggeloven, Amsterdam, November 2022

This research was conducted under the auspices of the Graduate School for Socio-Economic and Natural Sciences of the Environment (SENSE). The research for this thesis was carried out at the Institute for Environmental Studies (IVM), Vrije Universiteit Amsterdam.

VRIJE UNIVERSITEIT

SEA CHANGE TO NATURE-BASED SOLUTIONS

A Coastal Flood Risk Perspective

ACADEMISCH PROEFSCHRIFT

ter verkrijging van de graad Doctor of Philosophy aan
de Vrije Universiteit Amsterdam,
op gezag van de rector magnificus
prof.dr. J.J.G. Geurts,
in het openbaar te verdedigen
ten overstaan van de promotiecommissie
van de Faculteit der Bètawetenschappen
op woensdag 2 november 2022 om 9.45 uur
in een bijeenkomst van de universiteit,
De Boelelaan 1105

door
Timothy Tiggeloven
geboren te Amsterdam

promotor:	prof.dr. P.J. Ward
copromotor:	dr. H. de Moel
promotiecommissie:	prof.dr. W.J.W. Botzen prof.dr. D. Coumou dr.ir. J.M. Kaspersma dr.ir. J.M. van Loon-Steensma prof.dr. A.T. Vafeidis

I see nothing.

We may sink and settle on the waves. The sea will drum in my ears. The white petals will be darkened with seawater. They will float for a moment and then sink. Rolling over the waves will shoulder me under. Everything falls in a tremendous shower,

Dissolving me.

- Virginia Woolf

Table of Contents

Summary 13

Samenvatting 17

Key Concepts 22

1 Introduction 27

1.1 Coastal flood risk and adaptation 28

1.2 Research challenges 30

1.3 Main goal and research questions 36

2 Surge predictions in coastal areas 39

2.1 Introduction 40

2.2 Methods 42

2.3 Results 50

2.4 Discussion 59

2.5 Conclusion and outlook 62

3 Coastal flood adaptation using structural measures 65

3.1 Introduction 66

3.2 Methods 67

3.3 Results and Discussion 78

3.4 Conclusion 93

4 Benefits of conserving foreshore vegetation 95

4.1 Introduction 96

4.2 Methods 98

4.3 Results 104

4.4 Discussion 110

4.5 Conclusion 113

5 Benefits of Mangrove Restoration 115

5.1 Introduction 116

5.2 Global scale flood risk benefits of mangrove restoration ____ 118
5.3 Regional scale flood risk benefits of mangrove restoration ____ 118
5.4 Benefit and cost analysis of mangrove restoration ____ 120
5.5 Poverty analysis of mangrove restoration ____ 122
5.6 Discussion ____ 124
5.7 Methods ____ 126
6 Hybrid Solutions ____ 133
6.1 Introduction ____ 134
6.2 Methods ____ 136
6.3 Results ____ 141
6.4 Outlook ____ 145
7 Synthesis ____ 147
7.1 Key research questions ____ 148
7.2 Remaining scientific challenges and the way forward ____ 152
7.3 Societal context and policy implications ____ 155
Appendices ____ 159
References ____ 187
List of Publications ____ 209
Acknowledgments ____ 211
About the author ____ 218

Summary

Coastal floods are one of the deadliest and costliest of natural hazards, triggering or contributing to economic disruption, displacement, (mental) health implications, environmental disasters, poverty traps, and geomorphic change. In the coming century, coastal communities are projected to face increases in coastal flood risk, even if the Paris Agreement's aim of keeping global warming below a 2°C increase by the end of the 21st century will be met. Together, the increases in sea level and a possible change in storminess will lead to increased flood hazards, as well as threats to shorelines, wetlands, and coastal development. Moreover, flood hazard is expected to increase because of subsidence, for instance due to groundwater extraction in many deltas and estuaries. Such climate shocks may exacerbate current poverty levels and catalyse the formation of poverty traps in low- and middle-income countries. Global coastal flood risk is also expected to increase in the future because of increasing exposure, due to growth in population and wealth, and economic activities in flood-prone areas.

To prevent this increase in coastal flood risk, or even reduce risk below today's levels, adaptation strategies are necessary. Given the need for coastal adaptation to tackle the expected increase in coastal flood risk, it is critical to improve our understanding of global coastal flood risk and the effectiveness of adaptation strategies on flood risk benefits. Flood risk can be reduced in many ways, including structural measures, ecosystem-based adaptation, or a combination of these (so-called hybrid solutions). To make informed decisions on what measures to take, it is important to better understand the effectiveness of such coastal flood risk adaptation strategies, preferably beyond just monetary terms. Moreover, it is essential to improve understanding of coastal flood hazard prediction. Therefore, the overall aim of this thesis is to disentangle drivers of coastal flood risk and assess costs and benefits of adaptation strategies. By doing so, the thesis improves upon conventional flood risk assessments by taking steps into the direction of integrated and holistic assessments that include Nature-based Solutions and valuing of adaptation beyond monetary terms.

A better understanding and prediction of the characteristics of sea levels can contribute to improving coastal adaptation and management. Therefore, in chapter 2, deep learning approaches are explored for predicting surge levels at the global scale. For 738 tide stations, an ensemble approach was developed and applied to predict hourly surges using four different types of Neural Networks (NN), using various atmospheric variables as predictors. To evaluate the NN model performance at each station, the results were benchmarked against a simple probabilistic model based on climatology. To explore how increasing the NN design complexity affects model performance, hidden layers were added, and the spatial footprint used around each station to extract the predictor variables was enlarged. Our results show that the NN models are able to capture the temporal evolution of surges using a deep learning architecture of two hidden layers, a spatial footprint of 1.25 degrees centred on the station of interest with input variables of

mean sea level pressure, wind speed parameters, and their derivatives. We found that they outperform large-scale hydrodynamic models, and we observe similar performance patterns across all the NN ensemble models.

Chapter 3 explores benefit-cost analysis for coastal flood protection and attributes this to different drivers of flood risk: sea-level rise, socio-economic change, subsidence, and optimizing to current conditions. A methodological framework has been created to assess the following steps: (1) flood risk estimation; (2) adaptation costs estimation; (3) benefit-cost analysis for four adaptation objectives; and (4) attribution of the total costs to the different drivers. The results of chapter 3 show that Expected Annual Damage (EAD) increases by a factor of 150 between 2010 and 2080, if no adaptation were to take place, and that 15 countries account for approximately 90% of this increase. All four adaptation objectives show potential to significantly reduce (future) coastal flood risk at the global scale in a cost-effective manner.

To make an informed decision on adaptation measures, it is also important to understand how non-structural measures like Nature-based Solutions, can reduce that risk. This is addressed in chapters 4-6, which present novel methods of global scale assessments on reduction of future flood risk through Nature-based Solutions and hybrid strategies. These studies extend on the coastal flood risk assessment framework developed in chapter 3 by assessing the effects of both foreshore vegetation and structural measures on global flood risk reduction under socioeconomic and climate change. In chapter 4, we show that conserving foreshore vegetation is an effective measure and can result in considerable flood risk reduction under future projections of sea-level rise and socioeconomic change. Chapter 5 presents the first global-scale assessment of mangrove restoration and (future) potential flood risk reduction. We show that a large share of future flood risk of US$40-90 billion (~9% of total EAD for both scenarios assessed) may be reduced by implementing mangrove restoration and that restoring mangroves could place up to 820,000 people at a lower risk of coastal flooding. Chapter 6 combines previous chapters into an assessment of hybrid adaptation strategies at the global scale. Implementing Nature-based Solutions will increase the feasibility of adaptation strategies for two-thirds (68%) of the regions assessed. Globally, we estimate a total reduction in adaptation costs of 8% by implementing Nature-based Solutions, compared to using structural measures only.

In chapter 5 and 6, this thesis shows the importance of using more indicators than economic ones alone, in order to assess the benefits of measures. Here, we use poverty indicators to understand the range of impacts of adaptation on different people. We show that the effects of Nature-based Solutions and flood hazards are unevenly distributed across the population in terms of poverty. Specifically, in many places the poorest people are relatively more exposed to flood hazards but can correspondingly benefit relatively much from Nature-based Solutions. As such, implementing adaptation

measures, such as mangrove restoration, in Low- and Middle-Income Countries (LMICs) can contribute to the resilience of people in poverty, poverty alleviation and help tackle poverty traps.

The results of this thesis indicate that it is important to enrich traditional flood risk strategies with Nature-based Solutions and more holistic hybrid approaches. In order to further advance this direction in the future, several remaining scientific challenges include: (1) enhanced hazard prediction by improving flood inundation models, paving the way towards improved early warning systems; (2) refining flood risk assessment by using object-based assessments instead of aggregation methods for protection levels and exposure information; (3) improving the simulation of adaptation strategies by including a myriad of adaptation measures and expanding on this by using dynamic approaches; and (4) next to including poverty analysis, incorporate further co-benefits of adaptation measures into flood risk assessments, such as ecosystems services related to NBS. Overall, the results of this thesis contribute to international initiatives such as the Sendai Framework for Disaster Risk Reduction and can be used to inform policy makers and development agencies on risks from global to regional level. For example, the flood risk estimates, costs and benefits of dikes and levees of chapter 3 are used in the Aqueduct Floods web tool (www.wri.org/floods), which enables users to assess risk and adaptation options anywhere in the world.

Samenvatting

Kustoverstromingen behoren tot de dodelijkste en duurste natuurrampen en veroorzaken of dragen bij tot economische ontwrichting, ontheemding, gevolgen voor de (geestelijke) gezondheid, milieurampen, armoedevallen en geomorfische veranderingen. In de komende eeuw zullen kustgemeenschappen naar verwachting te maken krijgen met een toename van het overstromingsrisico, zelfs als de doelstelling van de Overeenkomst van Parijs om de opwarming van de aarde tegen het einde van de 21e eeuw onder de 2°C te houden, wordt gehaald. De stijging van de zeespiegel en een mogelijke verandering van de stormintensiteit zullen samen leiden tot een verhoogd overstromingsgevaar, alsook tot bedreigingen voor kustlijnen, watergebieden en kustontwikkeling. Bovendien wordt verwacht dat het overstromingsgevaar zal toenemen door bodemdaling, bijvoorbeeld als gevolg van grondwateronttrekking in vele delta's en estuaria. Dergelijke klimaatschokken kunnen de huidige armoedeniveaus verergeren en de vorming van armoedevallen in lage- en midden-inkomenslanden katalyseren. Verwacht wordt dat het mondiale overstromingsrisico aan de kust in de toekomst ook zal toenemen door de toenemende blootstelling als gevolg van de bevolkings- en welvaartsgroei en de economische activiteiten in overstromingsgevoelige gebieden.

Om deze toename van het overstromingsrisico in kustgebieden te voorkomen of zelfs het risico te verminderen tot onder het huidige niveau, zijn adaptatiestrategieën nodig. Gezien de noodzaak van adaptatie aan de kust om de verwachte toename van het overstromingsrisico aan te pakken, is het van cruciaal belang ons inzicht in het wereldwijde overstromingsrisico aan de kust en de doeltreffendheid van adaptatiestrategieën op het gebied van overstromingsrisico vermindering te verbeteren. Het overstromingsrisico kan op vele manieren worden verminderd, onder meer via structurele maatregelen, adaptatie op basis van ecosystemen, of een combinatie daarvan (de zogenaamde hybride oplossingen). Om met kennis van zaken te kunnen beslissen welke maatregelen moeten worden genomen, is het van belang een beter inzicht te krijgen in de doeltreffendheid van dergelijke strategieën voor adaptatie om het overstromingsrisico te verminderen aan de kust, bij voorkeur in meer dan alleen geldelijke termen. Bovendien is het van essentieel belang om meer inzicht te krijgen in de voorspelling van het overstromingsgevaar aan de kust. Daarom is het algemene doel van dit proefschrift om de drijvende krachten achter het overstromingsrisico van kustgebieden te ontwarren en de kosten en baten van adaptatiestrategieën te beoordelen. Op deze manier verbetert de dissertatie conventionele overstromingsrisicobeoordelingen door stappen te zetten in de richting van geïntegreerde en holistische beoordelingen die ook op de natuur gebaseerde oplossingen omvatten en adaptatie niet alleen in geldelijke termen waarderen.

Een beter begrip en voorspelling van de karakteristieken van stormvloeden kan bijdragen aan het verbeteren van kustadaptatie en -beheer. Daarom worden in hoofdstuk 2 deep learning-benaderingen onderzocht voor het voorspellen van

stormvloeden op wereldschaal. Voor 738 getijdenstations is een ensemble-benadering ontwikkeld en toegepast voor het voorspellen van de temporele evolutie van stormvloeden per uur met behulp van vier verschillende typen Neurale Netwerken (NN), waarbij verschillende atmosferische variabelen als voorspellers zijn gebruikt. Om de prestaties van het NN-model op elk station te evalueren, werden de resultaten vergeleken met een eenvoudig probabilistisch model op basis van klimatologie. Om na te gaan hoe de complexiteit van het NN-ontwerp de prestaties van het model beïnvloedt, werden verborgen lagen toegevoegd in de NN en werd de ruimtelijke voetafdruk die rond elk station werd gebruikt om de voorspellende variabelen te extraheren, vergroot. Onze resultaten tonen aan dat de NN-modellen in staat zijn de temporele evolutie van vloedgolven te vatten met behulp van een deep learning architectuur van twee verborgen lagen, een ruimtelijke voetafdruk van 1,25 graden gecentreerd rond het betrokken station met inputvariabelen van gemiddelde zeespiegeldruk, windsnelheidsparameters en hun derivaten. We ontdekten dat ze soms beter presteren dan grootschalige hydrodynamische modellen, en we nemen vergelijkbare prestatiepatronen waar bij alle NN-ensemble-modellen.

Hoofdstuk 3 verkent de baten-kosten analyse voor kustbescherming tegen overstromingen en schrijft dit toe aan verschillende drijvende krachten achter het overstromingsrisico: zeespiegelstijging, sociaal-economische veranderingen, bodemdaling, en optimalisatie naar de huidige omstandigheden. Er is een methodologisch kader gecreëerd om de volgende stappen te beoordelen: (1) schatting van het overstromingsrisico; (2) schatting van de adaptatiekosten; (3) baten-kostenanalyse voor vier adaptatiedoelstellingen; en (4) toerekening van de totale kosten aan de verschillende drijvende krachten. Uit de resultaten van hoofdstuk 3 blijkt dat de verwachte jaarlijkse schade tussen 2010 en 2080 met een factor 150 toeneemt als er geen adaptatie plaatsvindt, en dat 15 landen gezamenlijk ongeveer 90% van deze toename zullen ervaren. Alle vier adaptatiedoelstellingen bieden de mogelijkheid om het (toekomstige) risico van kustoverstromingen op mondiale schaal op een kosteneffectieve manier aanzienlijk te verminderen.

Om een weloverwogen beslissing over adaptatiemaatregelen te kunnen nemen, is het ook belangrijk te begrijpen hoe niet-structurele maatregelen, zoals op de natuur gebaseerde oplossingen, dat risico kunnen verminderen. Dit wordt behandeld in de hoofdstukken 4 t/m 6, waarin nieuwe methoden worden gepresenteerd voor beoordelingen op wereldschaal van de vermindering van het toekomstige overstromingsrisico door middel van op de natuur gebaseerde oplossingen en hybride strategieën. Deze studies breiden het in hoofdstuk 3 ontwikkelde raamwerk voor de beoordeling van overstromingsrisico's aan de kust uit door de effecten van zowel vooroevervegetatie als structurele maatregelen op de wereldwijde vermindering van het overstromingsrisico onder sociaaleconomische en klimaatveranderingen te beoordelen.

In hoofdstuk 4 tonen we aan dat de instandhouding van de vooroevervegetatie een effectieve maatregel is en kan resulteren in een aanzienlijke overstromingsrisicovermindering onder toekomstige projecties van zeespiegelstijging en sociaaleconomische veranderingen. Hoofdstuk 5 presenteert de eerste beoordeling op wereldschaal van mangroveherstel en de (toekomstige) potentiële overstromingsrisicovermindering. Hierin toon ik aan dat een groot deel van het toekomstige overstromingsrisico van 40-90 miljard US$ (~9% van de totale EAD voor beide beoordeelde scenario's) kan worden verminderd door de uitvoering van mangroveherstel en dat herstel van de mangroven tot 820.000 mensen een lager risico op overstromingen van de kust kan opleveren. Hoofdstuk 6 combineert de voorgaande hoofdstukken tot een beoordeling van hybride adaptatiestrategieën op wereldschaal. De implementatie van op de natuur gebaseerde oplossingen zal de haalbaarheid van adaptatiestrategieën voor tweederde (68%) van de beoordeelde regio's vergroten. Wereldwijd schatten we een totale reductie in adaptatiekosten van 8% door het implementeren van op de natuur gebaseerde oplossingen, vergeleken met het gebruik van alleen structurele maatregelen.

In hoofdstuk 5 en 6 laat dit proefschrift zien dat het belangrijk is om meer indicatoren te gebruiken dan alleen economische, om de voordelen van maatregelen te beoordelen. Hier gebruiken we armoede-indicatoren om de verschillende effecten van adaptatie op verschillende mensen te begrijpen. We laten zien dat de effecten van adaptatie en overstromingsrisico's ongelijk verdeeld zijn over de bevolking in termen van armoede. Met name op veel plaatsen zijn de armste mensen relatief meer blootgesteld aan overstromingsgevaren, maar kunnen dienovereenkomstig relatief veel profiteren van op de natuur gebaseerde oplossingen. Als zodanig kan de uitvoering van adaptatiemaatregelen, zoals het herstel van mangroves, in lage- en middeninkomenslanden bijdragen aan de veerkracht van mensen die in armoede leven, aan armoedeverlichting en aan het aanpakken van armoedevallen.

De resultaten van dit proefschrift geven aan dat het belangrijk is om traditionele overstromingsrisicostrategieën te verrijken met op de natuur gebaseerde oplossingen en meer holistische hybride benaderingen. Om deze richting in de toekomst verder uit te werken, zijn er nog verschillende wetenschappelijke uitdagingen, zoals (1) verbeterde voorspelling van overstromingen door verbetering van inundatiemodellen, waarmee de weg wordt vrijgemaakt voor verbeterde systemen voor vroegtijdige waarschuwing; (2) verfijning van de beoordeling van overstromingsrisico's door gebruik te maken van objectgebaseerde beoordelingen in plaats van aggregatiemethoden voor beschermingsniveaus en blootstellingsinformatie; (3) verbetering van de simulatie van adaptatiestrategieën door een groot aantal adaptatiemaatregelen op te nemen en dit uit te breiden door gebruik te maken van dynamische benaderingen; en (4) naast het opnemen van armoedeanalyse, het opnemen van verdere nevenvoordelen van

adaptatiemaatregelen in overstromingsrisicobeoordelingen, zoals ecosysteemdiensten gerelateerd aan natuur gebaseerde oplossingen. Over het geheel genomen dragen de resultaten van dit proefschrift bij aan internationale initiatieven zoals het Sendai Framework for Disaster Risk Reduction en kunnen ze worden gebruikt om beleidsmakers en ontwikkelingsorganisaties te informeren over risico's van mondiaal tot regionaal niveau. De schattingen van overstromingsrisico's, kosten en baten van structurele maatregelen, zoals dijken, van hoofdstuk 3 worden bijvoorbeeld gebruikt in de Aqueduct Floods webtool (www.wri.org/floods), waarmee gebruikers risico's en aanpassingsopties overal ter wereld kunnen beoordelen.

Key Concepts

Glossary	Definitions
Adaptation	Measures, strategies, and objectives. Disaster Risk Reduction (DRR) measures focusing on flood impact reduction through implementation of one or more **Adaptation Measures** (i.e., structural measures, mangrove restoration, and conserving foreshore vegetation). A measure could be implemented to reach certain **Adaptation Objectives** (i.e., keeping protection standards or EAD constant through time). Combination of measures to reach adaptation objectives are defines as **Adaptation Strategies** (such as Nature-based and Hybrid Solutions).
Benefit-Cost Ratio (BCR)	Economic indicator to evaluate efficiency of certain adaptation measures, objectives, or strategies in which the ratio between total discounted benefits and costs over a certain time horizon is calculated.
Conservation of foreshore vegetation	Adaptation measure that focusses on maintenance of existing foreshore vegetation.
Continuous Ranked Probability Score (CRPS)	The **Continuous Ranked Probability Score (CRPS)** is a widely used metric within hydrology and coastal science for probabilistic prediction. This CRPS is sensitive to the entire permissible range of the parameter of interest and has a clear interpretation as for deterministic prediction it boils down to the **Mean Absolute Error (MAE)**, which is a common measure of errors by taking the mean of absolute deviations between paired observations. The CRPS can de decomposed into three components: 1) the **Reliability (RELI)** component indicates whether the distribution of the predicted values have similar statistical properties to the observed time series; 2) the **Uncertainty component (U)** represents the CRPS if only a reference (e.g., climatological) probabilistic prediction is available; and 3) **Resolution (Resol)** component evaluates the improvement of the neural network model ensemble predictions to the average ensemble spread and the observed outliers. To improve interpretation of the results we used the **Scaled**

	CRPS (CRPSS) that shows the skill gain compared to that of the reference ensemble predictions from the probabilistic climatology distribution (*based on Chapter 2 and Hersbach, 2000*).
Expected Annual Affected Population (EAAP) / Expected Annual Population Exposed (EAPE)	**Expected Annual Affected Population (EAAP)** or **Expected Annual Population Exposed (EAPE)** is the total estimated people exposed to flooding per year if all impacts of events would be spread out equally over time.
Expected Annual Damages (EAD)	**Expected Annual Damages (EAD)** are the estimated damages per year if all damages of flood events would be equally spread out over time. For example, a flood event that statistically occurs every 100 years would contribute to the estimation of EAD by dividing the damages of this event by 100 (because EAD is estimated as annual).
Flood Risk	The potential damages of a flooding events to assets which could occur to a system, society, or a community in a specific period of time, determined probabilistically as a function of flood hazard, exposure, and vulnerability (*based on UNDRR, 2016*).
Foreshore vegetation	Foreshore vegetation consists of the vegetation, such as mangroves and salt marshes, present in lagoons, estuaries, and deltas. It can provide flood protection benefits as it decreases wave runup due to frictional forces.
Hybrid Solutions	Adaptation strategy that combines structural measures with ecosystem-based approaches or Nature-based Solutions.
Low- and Middle-Income Countries (LMICs)	Countries that have a gross national income lower than a certain threshold (*as defined by the World Bank*).
Nature-based Solutions	Nature-based Solutions are management actions where people make use of nature and ecosystems protect people and assets, and safeguard biodiversity. In this thesis Nature-based Solutions consist of conserving foreshore vegetation (mangroves and salt marshes) and mangrove restoration.
Nature Contribution to People (NCP)	**Nature Contributions to People (NCP)** consists of positive and negative contributions to people's quality of life through a cultural and socioeconomic context in space and time. Examples of positive contributions of NCP for

	foreshore vegetation are carbon storage, enhancing fisheries, and flood protection (*based on Díaz et al., 2018*).
Neural Network (NN)	A **Neural Network (NN)** is a series of algorithms consisting of structured neurons that captures nonlinear processes by mimicking the way the human brain operates. The **Artificial Neural Network (ANN)**, the most general form of NN, has been extensively applied in various fields of science to capture nonlinear underlying relationships. The **Long Short-Term Memory (LSTM)** is a derivation of the Recurrent Neural Network (RNN) in that it captures sequence-to-sequence patterns in their internal state as memory but has advantages over the conventional RNN as they can selectively store long term information. The **Convolutional Neural Network (CNN)** is a class of NN models that works well in capturing spatial features, shapes, and texture due to its shared weight architecture and is thus often applied for image recognition purposes. The **Convolutional LSTM (ConvLSTM)** combines sequence-to-sequence learning with convolutional layers and emerges in current studies with promising applications in capturing spatiotemporal relationships (*defined as such in chapter 2*).
Net Present Value (NPV)	Economic indicator to evaluate efficiency of certain adaptation measures, objectives, or strategies in which the difference between total discounted benefits and costs over a certain time horizon is calculated.
Protection standard	Safety standards for flooding are expressed in **protection standards**, which denotes the exceedance probability of a flood occurring. For example, with a protection standard of 100-years is meant that protection is designed to withstand a flooding that statistically occurs once every 100 years.
Representative Concentration Pathway (RCP)	**Representative Concentration Pathways (RCP)** were developed to explore the magnitude and extent of climate change under different levels of forcing that contains emissions and land-use trajectories (*based on van Vuuren et al., 2014*).
Restoration of mangroves	Adaptation measure that focusses on restoring former degraded mangroves in areas that show potential that restoration can take place based on key environmental

	components that influence the ease of restoration (*based on Worthington et al., 2018).*
Scenario	Plausible future narratives or storylines describing the combination of changes in climate system (RCP) and socioeconomic aspect of society (SSP). For this thesis the combinations of RCP4.5/SSP2, narrative aligning with the Paris Agreement (Hope et al., 2017), and RCP8.5/SSP5, a fossil-fueled world (Kriegler et al., 2017), has been used often.
Shared Socioeconomic Pathways (SSP)	**Shared Socioeconomic Pathways (SSP)** describe plausible alternative changes in aspects of society such as demographic, economic, technological, social, governance and environmental factors, that include both qualitative descriptions of broad trends in development over large world regions (narratives) as well as quantification of key variables that can serve as inputs to land-use change models (*based on O'Neill et al., 2017*).
Structural measures	Engineering based measures such as dikes and levees.
Sustainable Development Goals (SDG)	The **Sustainable Development Goals (SDGs)**, such as 'climate action', 'No poverty', and 'Sustainable Cities and Communities', is an initiative by the United Nations that raises awareness to end poverty, protect the planet, and ensure that by 2030 all people enjoy peace and prosperity (b*ased on https://www.undp.org/sustainable-development-goals*).

1 Introduction

1.1 Coastal flood risk and adaptation

Coastal floods are one of the deadliest (Callaghan et al., 2014; Creach et al., 2016; CRED, 2015) and costliest (Hinkel et al., 2014; Kron, 2012.; Wahl et al., 2017) of natural hazards, triggering or contributing to economic disruption (Koks et al., 2019; Mandel et al., 2021), displacement (Hauer et al., 2019; Robert McLeman, 2018), (mental) health implications (Olanrewaju et al., 2019; Tong, 2017), environmental disasters (Rakib et al., 2019), poverty traps (Hallegatte & Rozenberg, 2017; Winsemius et al., 2018), and geomorphic change (Phillips, 2018; Vousdoukas et al., 2020). Coastal zones are among the most highly developed areas in the world, containing a multitude of human settlements (Neumann et al., 2015), critical infrastructure (Koks et al., 2019) and ecosystem services (Erwin, 2009). Moreover, coastal zones are attractive areas for human settlement and almost two-thirds of urban settlements with population higher than 5 million are at least partly located in coastal zones (McGranahan et al., 2016). When extreme weather events cause storm surge events, these coastal zones can be threatened. Together, mean sea level variations, tides, waves and storm surges resulting from the passing of low pressure systems and strong winds (Idier et al., 2019; Woodworth et al., 2019) are putting developed areas at risk of flooding.

The risk that human settlements can experience from coastal flooding can be defined as a function of hazard, exposure and vulnerability (Kron, 2005); where physical parameters such as coastal flood depth, duration and extent represent the hazard; exposure is defined as the situation of an element (e.g. people, infrastructure, housing, production capacities and other tangible human assets) subject to and at risk of coastal flooding; and vulnerability is the susceptibility of an individual, a community, assets or systems to the impacts of hazards determined by physical, social, economic and environmental factors (UNDRR, 2016). Together, disaster risk from coastal flooding can be defined as the potential loss of life, injury, or destroyed or damaged assets that could occur to a system, society or a community in a specific period of time (UNDRR, 2016).

In the coming century, coastal communities are projected to face increases in coastal flood risk (Brown et al., 2018; Hallegatte et al., 2013; Hinkel et al., 2014; Jongman et al., 2012; Merkens et al., 2018; Neumann et al., 2015). The Intergovernmental Panel on Climate Change (IPCC) states that it is likely that we will face a global mean sea-level rise by the end of the 21st century in the range of approximately 0.43 – 0.84 meter compared to 1986-2005 and that impacts on society will be vast (Oppenheimer et al., 2019). According to a recent study by Raftery et al. (2017), it is unlikely that the Paris Agreement's aim of keeping global warming below a 2°C increase by the end of the 21st century will be met. This may lead to changes in extreme sea levels (Vousdoukas et al., 2017) due to changes in storm surges (Tebaldi et al., 2012) and tides (Pickering et al., 2012). Together, these increases in sea level and a possible change in storminess

will lead to increased flood hazards, as well as threats to shorelines, wetlands, and coastal development (Ericson et al., 2006; Hinkel et al., 2013; Vousdoukas et al., 2020). Moreover, flood hazard is expected to increase because of subsidence. In many deltas and estuaries, groundwater extraction is a major factor contributing to this subsidence (Hallegatte et al., 2013). During the 20th century, the coasts of Tokyo, Shanghai and Bangkok subsided by several meters (Nicholls et al., 2008) and subsidence is expected to continue to affect coastal flood risk in the future (Dixon et al., 2006). Such climate shocks may exacerbate current poverty levels and catalyse the formation of poverty traps in Low- and Middle-Income Countries (LMICs) (Leichenko & Silva, 2014). Global coastal flood risk is also expected to increase in the future as a result of increasing exposure, due to growth in population and wealth, and economic activities in flood-prone areas (Güneralp et al., 2015; Jongman et al., 2012; Neumann et al., 2015; Pycroft et al., 2016).

To prevent this increase in coastal flood risk, or even reduce risk below today's levels, adaptation strategies are necessary. Given the need for coastal adaptation to tackle the expected increase in coastal flood risk, it is critical to improve our understanding of global coastal flood risk and the effectiveness of adaptation strategies on flood risk benefits. Flood risk can be reduced by implementing adaptation measures, such as structural measures or ecosystem-based adaptation, to either reduce the hazard, exposure, vulnerability, or a combination of these (Schanze, 2006). To do so, it is important to disentangle the drivers of flood risk, the costs and benefits of adaptation strategies at the global scale and improve upon conventional flood risk assessments by including Nature-based Solutions and more holistic hybrid approaches. The importance of climate change adaptation and disaster risk reduction is recognized in several global agreements, such as the Paris Agreement (United Nations Framework Convention on Climate Change, 2015) and the Sendai Framework for Disaster Risk Reduction (United Nations Office for Disaster Risk Reduction, 2015).

Building consensus on the need for change, and the best way to implement adaptation measures, is challenging. Therefore, decision-makers experience difficulties realizing goals aligned with global agreements (Barnett et al., 2014). Moreover, as the Paris Agreement requires the measurement of the progress made on adaptation goals, adaptation policies must include present and future risk drivers to achieve these goals in a sustainable matter (Olazabal et al., 2019). Instead of only focusing on one adaptation measure, policy needs to adopt holistic strategies or adaptation pathways to adapt to climate change, such as hybrid solutions (Barnett et al., 2014; Jongman, 2018). Hybrid solutions combine strategies, such as structural measures and nature-based adaptation, to adapt to climate change or reduce residual risk. Nature-based Solutions such as vegetation and ecological engineering are effective measures to reduce flood risk (Cheong et al., 2013; Du et al., 2020; Sutton-Grier et al., 2015; Wang et al., 2014).

Next to flood protection benefits, Nature-based Solutions provide co-benefits such as improved water quality and recreation opportunities (Barbier et al., 2011); supporting fisheries (Seddon et al., 2020); and enhanced carbon sequestration (Worthington et al., 2018), and including these allows shifting from monetary direct impacts of adaptation measures to including community based adaptation strategies. Furthermore, including poverty in adaptation policies will extend the impact analysis beyond the valuation of reduction in flood risk in monetary terms (Hallegatte & Rozenberg, 2017; Winsemius et al., 2018), and will reveal how equity is integrated into adaptation (Araos et al., 2021).

To implement and raise awareness of climate change adaptation and understand local and global disaster risk reduction strategies, it is important to better understand the effectiveness of coastal flood risk adaptation strategies, such as Nature-based Solutions and hybrid strategies. More specifically, it is essential to improve understanding of coastal flood hazard prediction, and adaptation strategies integrated in a holistic Nature-based and hybrid approaches that include valuation beyond monetary terms. Therefore, the overall aim of this thesis is to disentangle coastal flood risk drivers, costs and benefits of adaptation strategies and making the shift from conventional flood risk assessments to integrated and holistic assessments.

1.2 Research challenges

Several scientific challenges continue to exist in assessing coastal flood risk adaptation strategies and disentangling the drivers, costs and benefits of these measures at the global scale. First, to improve coastal adaptation and management, it is critical to better understand and predict the characteristics of sea levels. Second, to improve global coastal flood risk assessment, the effects of climate change, subsidence, and/or socioeconomic change, need to be integrated to attribute these drivers to adaptation costs and in relation to global flood protection levels. Third, the benefits and costs of coastal flood risk reduction and adaptation strategies, such as grey infrastructure and Nature-based Solutions, need to be determined at a global scale to better understand the effectiveness and drives of such strategies on disaster risk reduction. Fourth, we need to integrate traditional assessment frameworks by looking beyond monetary indicators by including co-benefits of adaptation strategies and assessing the distributional impacts of measures in terms of poverty indicators and how equity is integrated into adaptation.

1.2.1 Improve understanding of coastal flood hazard and predictions

In order to improve coastal adaptation, it is critical to better understand and predict the characteristics of sea levels, such as their temporal variation and magnitude over long time periods, typically multiple decades (Höffken et al., 2020; Katherine A. Serafin et al., 2017). Coastal sea level variability results from a combination of multiple processes,

including mean sea level variations, tides, waves and storm surges resulting from the passing of low pressure systems and strong winds (Idier et al., 2019; Woodworth et al., 2019). At hourly time scales or shorter, temporal variation in surge residuals, i.e. the water level after removal of the tide and mean sea level, depends on the direction and variations in wind and pressure gradients, as well as local topographic characteristics such as the bathymetry and complexity of the coastline (Lewis et al., 2013; McInnes et al., 2016; Wu et al., 2017). Surge levels superimposed on high tides can exceed land thresholds, such as natural and human-made coastal profiles, and contribute to nuisance flooding or extreme impacts when caused by tropical or extratropical cyclones. At the global scale, studies have used hydrodynamic modelling (Muis et al., 2020) or data-driven approaches to reconstruct surge time series (Bruneau et al., 2020; Cid et al., 2018; Tadesse et al., 2020; Tadesse & Wahl, 2021). The advantage of hydrodynamic models is that with adequate model resolution and meteorological forcing, they can resolve physical coastal processes and their interactions. They are also valuable for understanding epistemic uncertainties and the relative contributions of different oceanographic and coastal processes in total water levels. However, these models are computationally demanding and take a long time to set up (Christie et al., 2018; Santiago-Collazo et al., 2019; Teng et al., 2017). This limits their ability to be used in the simulation of large ensembles of events (Colberg & McInnes, 2012; Nuswantoro et al., 2016).

To circumvent these limitations, studies have applied data-driven models to predict surge at gauged locations, such as empirical relationships (van den Brink et al., 2004), unsupervised learning algorithms (Cid et al., 2017; Tadesse et al., 2020) or approaches using artificial intelligence like deep learning (Bruneau et al., 2020; Chen et al., 2020; de Oliviera et al., 2009; Lee, 2008), and found comparable or even better performance compared to hydrodynamic models. For example, Tadesse et al. (2020) found the daily maximum surge levels from their data-driven model to outperform the global hydrodynamic model from Muis et al., (2020). They applied random forests and linear regression, selecting as predictors a range of atmospheric (wind speed, mean sea level pressure, precipitation) and oceanographic (sea surface temperature) variables. These predictor variables were selected with various lag-times in a 10 x 10-degree box around the location of interest from remotely sensed satellite products and climate reanalysis datasets. Among deep learning approaches, Artificial Neural Networks (ANN) have been popular Neural Network (NN) models for operational surge level forecasting (Das et al., 2011; de Oliviera et al., 2009; Kim et al., 2016) or the modelling of stochastic storm surge events (Hashemi et al., 2016; Kim et al., 2015). Although limitations exist when applying NN models, such as capturing long-term processes and predicting surge levels at ungauged locations, applying such methods can lead to similar or better results than local hydrodynamic models. At the global scale, Bruneau et al. (2020) were, to my knowledge, the first to use ANN models to predict hourly non-tidal

residual levels at tide stations. They used as predictor variables wind, mean sea level pressure, accumulated precipitation, and wave height from the climate reanalysis dataset ERA5 (Hersbach et al., 2020). The spatial extent of the predictor variables around each location considered was four times smaller (i.e. 5 x 5 degree box) than used in Tadesse et al. (2020). Due to its refined horizontal resolution, this dataset can better resolve characteristics of climate extremes, such as tropical cyclones (track, intensity, maximum wind speeds) than its predecessor ERA-Interim reanalysis (Malakar et al., 2020) even though some improvements are still needed, for example to properly capture their outer size (Bian et al., 2021).

Notwithstanding the differences between the models applied in Tadesse et al. (2020) and Bruneau et al. (2020), the role of the number of predictor variables considered and the spatial extent around each location in the model's performance and ability to learn remains unclear. Next to ANNs, other NN types could be useful for global scale surge level prediction (Reichstein et al., 2019; Shen, 2018). For example, Convolutional Neural Networks (CNN) can process patterns in spatio-temporal climate data and identify weather features to be used for forecasts (Chattopadhyay et al., 2020; Ham et al., 2019). Recurrent neural networks using Long Short-Term Memory (LSTM) layers have been used in hydrology to capture long-term temporal dependencies, necessary to capture the state of a river basin (Fang et al., 2017; Kratzert et al., 2018). A fully global exploration of the capabilities of deep learning approaches to predict surge levels and thus improving coastal hazard predictions has not been developed yet.

1.2.2 Improving global coastal (future) flood risk assessment

To better understand the expected increase in coastal flood risk it is vital to take into account multiple drivers of change, such as climate change, subsidence and socio-economic change, and attribute the potential future change in risk to these drivers. To do this, the modelling of coastal flood risk requires simulations and projections of hazard, exposure, and vulnerability. Global coastal flood models address the hazard events by simulating physical parameters such as inundation extent and depth. Sea level projections and subsidence rates are used as input to force simulations of future coastal flood hazards. Projections of population and GDP are used as input for global exposure models to address socio-economic development. Next to changes in extreme sea levels, human activities in delta areas at the local or regional scale can perturb the coastal system by extracting gas, oil and groundwater and making deltas more vulnerable (Ericson et al., 2006; Syvitski et al., 2009). This extraction results in sediment compaction and subsidence, and subsequently, deltas are subsiding, which can increase the flood hazard. On top of this, socio-economic development is expected to increase flood risk in the near future (Hallegatte et al., 2013) by increasing the exposure of major coastal cities to flood risk (De Sherbinin et al., 2007; Hanson et al., 2011). Global scale models that project future population and GDP data, such as 2UP

(Van Huijstee et al., 2018) and GISMO/IMAGE (Bouwman et al., 2006), make use of Shared Socio-economic Pathways from the IIASA database, which contain projections of future population and GDP at country level.

To date, a limited number of studies have assessed coastal flood risk at the global scale. These studies can roughly be divided into two groups, namely studies involving the Dynamic Interactive Vulnerability Assessment (DIVA) model and the Joint Research Centre of the European Commission (JRC) studies. The DIVA model is a global database of coastal systems that assesses coastal vulnerability and socio-economic impacts due to sea level rise and socio-economic development (Hinkel & Klein, 2009). The DIVA-based studies use the DIVA model and apply extreme sea levels to estimate global scale coastal flood risk (Brown et al., 2016; Hinkel et al., 2014; Hinkel et al., 2010; Hinkel, et al., 2013a; Hinkel et al., 2013b; Nicholls et al., 2010), together with other impact models (Hallegatte et al., 2013; Muis et al., 2015; Ward et al., 2011). These studies provide important insight in the long term changes in coastal flood risk due to socio-economic development and sea level rise (Hinkel et al., 2014). The JRC studies have mainly focused on the European continent and global scale. They use the large-scale Integrated Sea-level and Coastal Assessment Tool (LISCoAsT) to assess large-scale coastal flood impacts (Vousdoukas et al., 2017). They provide extreme sea level (Vousdoukas et al., 2017; 2016b) and its impact on coastal flood hazard (Vousdoukas et al., 2018a), and large scale flood hazard (Vousdoukas et al., 2016a) and risk assessment (Vousdoukas et al., 2018b; Vousdoukas et al., 2018c) in their tool.

Using the DIVA model, Hallegatte et al. (2013) estimated current flood risk in major coastal cities at US$6 billion per year, with a projected increase in EAD by US$46 Billion by 2050 solely taking socioeconomic change into account. With climate change and subsidence taken into account, they projected an increase in flood risk to US$1 trillion per year if no action is undertaken. Using regional sea level rise projections and socio-economic development, Hinkel et al. (2014) estimated with the DIVA model that without adaptation EAD could increase to 0.3-9.3% of global gross domestic product. Vousdoukas et al. (2018a) estimated with LISCoAsT that coastal flood risk in Europe may increase from US$ 1.25 billion to US$ 93-961 billion by the end of the century, depending on the projection used of socio-economic development and climate change. While these studies assess flood risk at the global scale, they do not account for different adaptation objectives, attributing drivers to adaptation costs, and integrate the analysis with a global modelled database on coastal flood protection levels.

1.2.3 Global coastal flood adaptation strategies and Nature-based Solutions

To prevent or reduce increase in flood risk, adaptation measures are required. One option is to develop methods to reduce the probability or magnitude of the hazard, the

so-called 'protect' approach. This can be achieved through the implementation of grey infrastructure, Nature-based Solutions or hybrid adaptation measures (Cheong et al., 2013; Hinkel et al., 2014; Jongman, 2018). Grey infrastructure, such as dikes and levees, can protect the hinterland from flooding events up to a certain exceedance probability. Nature-based Solutions, such as maintaining or restoring vegetation on the foreshore, breaks waves and therefore decreases the run-up of the surge event (Barbier et al., 2008; Shepard et al., 2011). Exposure can be reduced by relocating people or assets from the most hazard-prone regions, or avoiding new development in flood-prone areas (Cummings et al., 2012). Lastly, vulnerability can be reduced by the implementation of measures such as flood proofing of buildings (Aerts et al., 2014), or early warning and evacuation systems (Pappenberger et al., 2015). To date, only a limited number of studies have addressed the benefits and costs of adaptation measures at the global scale. Lincke & Hinkel (2018) show that adaptation through structural adaptation measures is economically feasible for 13% of the global coastline, which accounts for 90% of the global population living in regions prone to coastal hazard. Hinkel et al. (2014) used the DIVA approach to calculate the benefits and costs of adaptation by raising dikes and found that the total costs of investment and maintenance could reach in the range of 12-71 US$ billion by 2100. However, this is much smaller than the avoided direct damages at the global scale.

Recent studies have shown that adaptation measures hold a large potential for significantly reducing this future flood risk (Diaz, 2016; Hinkel et al., 2014; Lincke & Hinkel, 2018). However, the number of global scale studies in which the benefits and costs of disaster risk reduction and adaptation are explicitly and spatially accounted for remains limited. Existing studies have assessed the effect of climate change, subsidence and/or socioeconomic change (Hallegatte et al., 2013; Hinkel et al., 2014; Vafeidis et al., 2019; Vousdoukas et al., 2016b), but have not included different adaptation objectives taking into account multiple flood risk drives or attributed these drivers to adaptation costs. Moreover, most modelling studies of global scale adaptation to coastal flood risk have focused on static adaptation objectives, i.e., protection against the 1 in 100 years flood. However, a framework based on different adaptation objectives, such as keeping future protection levels fixed or optimising protection levels, has not been developed yet.

Instead of only focusing on structural adaptation measures or Nature-based Solutions, Jongman (2018) argues that flood risk management needs to adopt holistic strategies to adapt to climate change, such as early warning systems, risk perception, or hybrid solutions. Hybrid solutions can combine structural measures with Nature-based Solutions, such as maintaining or restoring foreshore vegetation and foreshore geomorphology on the foreshore. Duarte et al. (2013) show that Nature-based Solutions in coastal areas have the potential to reduce the impacts of climate change.

Moreover, recent studies argue that Nature-based Solutions can provide a more sustainable, cost-effective and ecologically sound alternative to structural measures, such as dikes, sea walls and embankments (Narayan et al., 2016; Temmerman et al., 2013; van Wesenbeeck et al., 2017).

While Nature-based Solutions show potential for broad implementation to reduce coastal flood risk (Duarte et al., 2013; Temmerman et al., 2013; van Zelst et al., 2021; Vuik et al., 2016), an assessment of the effectiveness of conserving foreshore vegetation or mangrove restoration on reducing current and future coastal flood risk at the global scale has yet to be carried out. Furthermore, it is important to shift from conventional adaptation strategies towards Nature-based Solutions and more holistic hybrid approaches. Therefore, it is important to assess and quantify the potential effectiveness of Nature-based Solutions and hybrid measures on the global-scale. Although quantifying nature-based or hybrid adaptation can be challenging, it is critical to document such efforts to better understand their effectiveness.

1.2.4 Flood risk adaptation beyond monetary values

Mangroves and other Nature-based Solutions have been demonstrated to protect against current flood risk and provide other benefits such as improved water quality and recreation opportunities (Barbier et al., 2011), supporting fisheries, and enhanced carbon sequestration. They can also provide a more sustainable, cost-effective and ecologically sound alternative to structural measures in combating future flood risk (Narayan et al., 2016; Temmerman et al., 2013; van Wesenbeeck et al., 2017). For example, mangroves and other foreshore vegetation can keep up with sea level rise by natural accretion of mineral and biogenic sediments (Fagherazzi et al., 2012; Kirwan et al., 2010; Mckee et al., 2007). In other words, Nature-based Solutions in coastal areas can potentially reduce the impacts of climate change (Duarte et al., 2013) if they are protected, restored and maintained properly.

Unfortunately, mangrove forests and other foreshore vegetation have been degraded due to climate change and human development (Ward et al., 2017). Already it is estimated that a total of 6% of mangrove forests have been lost in the last fifty years, with land conversion to agriculture or transport infrastructure being the biggest contributions to these losses (Worthington & Spalding, 2018). Due to future climate change and socioeconomic development, foreshore vegetation is under threat of further degradation (Erwin, 2009). This includes increased threats to shorelines, wetlands, mangrove forests, salt marshes, and coastal development as flood risk increases (Jennerjahn et al., 2017; Mitsch & Hernandez, 2013; Vousdoukas et al., 2020; Ward et al., 2017). It is therefore important to portray the urgency of mangrove restoration at the global scale and discuss the feasibility thereof.

Furthermore, people in poverty are particularly vulnerable to shocks such as coastal flooding. Increases in coastal flood risk due to threats on the foreshore can lead to poverty traps as people in poverty are disproportionally exposed to such shocks (Hallegatte, 2016; Hallegatte & Rozenberg, 2017; Winsemius et al., 2018). As these people in poverty are more vulnerable to natural hazards, such as coastal flood risk, it is important to understand and assess the distributional impacts of flood risk adaptation and mangrove restoration in terms of poverty indicators (Villarreal-Rosas et al., 2021) and how equity is integrated into adaptation (Araos et al., 2021). However, the field still lacks a global-scale study addressing how poverty is linked to adaptation measures.

1.3 Main goal and research questions

To improve global coastal (future) flood risk assessment and understanding of how society can adapt in an integrated manner, the previous section highlighted four important research challenges. First, there is a need to improve coastal flood hazard prediction and rapidly predict surge levels for the development of early warning predictions and increasing resolution of predictions. This can be achieved, for instance, by exploring the full capabilities of deep learning approaches to predict surge levels and thus improving coastal hazard predictions. Second, global coastal flood risk assessments need to be further developed by accounting for current protection levels and multiple drivers, such as climate change, socioeconomic change, and subsidence, into their framework and attributing the costs of coastal flood adaptation to these drivers of change. Third, it is important to assess the feasibility of different adaptation objectives and strategies and improve upon conventional adaptation strategies towards Nature-based Solutions and more holistic hybrid approaches. Fourth, we need to improve flood risk assessments by looking beyond monetary indicators. To implement and raise awareness of climate change adaptation and improve understanding of local and global disaster risk reduction strategies, it is important to advance assessments on the effectiveness of coastal flood risk adaptation strategies, such as Nature-based Solutions and hybrid strategies in monetary terms and indicators beyond valuation in terms of money. Following these scientific challenges, the main research objective of this thesis is set:

Disentangling drivers of coastal flood risk and assess costs and benefits of adaptation measures at the global-scale with a focus on nature-based solutions.

To achieve this goal, the following research questions are addressed:

1. Can we improve surge level predictions by harnessing the capabilities of deep learning approaches at the global scale?
2. What is the attribution of adaptation costs to drivers of coastal flood risk?
3. What are the (future) flood risk benefits of structural measures, Nature-based Solutions, and a combination thereof?

4. How can we include adaptation benefits beyond monetary terms in large scale flood risk assessments?

Table 1.1: Overview of chapters and subjects.

	Coastal flood hazard prediction	(Future) Flood risk assessment	Adaptation strategies	Flood risk beyond monetary values
Chapter 2: Surge level estimations	**X**			
Chapter 3: Framework on coastal flood risk and adaptation		**X**	**X**	
Chapter 4: Flood risk benefits of conserving foreshore vegetation		**X**	**X**	
Chapter 5: Mangrove restoration and flood risk reduction			**X**	**X**
Chapter 6: Hybrid adaptation strategies			**X**	**X**

In the following chapters, these research questions are addressed and are categorized by subjects on hazard prediction, (future) flood risk assessment, adaptation strategies, and flood risk beyond monetary value.

- Chapter 2 addresses the need to develop rapid surge level predictions and explores the capabilities of deep learning approaches to improve our understanding of coastal flood hazard prediction.
- Chapter 3 assesses (future) coastal flood risk, provides an overview of different adaptation objectives through structural measures, and communicates the results in the form of an online tool the Aqueduct Global Flood Analyzer webtool (www.wri.org/floods).
- Chapter 4 assesses the (future) flood risk benefits of conserving foreshore vegetation as adaptation strategy.
- Chapter 5 improves our understanding of mangrove restoration and global-scale flood risk reduction in terms of monetary values and poverty indicators.

- Chapter 6 improves our understanding of hybrid adaptation strategies at the global scale and how these adaptation strategies can contribute to poverty alleviation.

2 Surge predictions in coastal areas

This chapter is published as

Tiggeloven, T., Couasnon, A., van Straaten, C., Muis, S. & Ward, P.J. Exploring deep learning capabilities for surge predictions in coastal areas. Sci Rep 11, 17224 (2021). https://doi.org/10.1038/s41598-021-96674-0

Abstract

To improve coastal adaptation and management, it is critical to better understand and predict the characteristics of sea levels. Here, we explore the capabilities of artificial intelligence, from four deep learning methods to predict the surge component of sea-level variability based on local atmospheric conditions. We use an Artificial Neural Networks (ANN), Convolutional Neural Network (CNN), Long Short-Term Memory layer (LSTM) and a combination of the latter two (ConvLSTM), to construct ensembles of Neural Network (NN) models at 736 tide stations globally. The NN models show similar patterns of performance, with much higher skill in the mid-latitudes. Using our global model settings, the LSTM generally outperforms the other NN models. Furthermore, for 15 stations we assess the influence of adding complexity more predictor variables. This generally improves model performance but leads to substantial increases in computation time. The improvement in performance remains insufficient to fully capture observed dynamics in some regions. For example, in the tropics only modelling surges is insufficient to capture intra-annual sea level variability. While we focus on minimising mean absolute error for the full time series including minima, the NN models presented here could be adapted for use in forecasting extreme sea levels or emergency response.

2.1 Introduction

In order to improve coastal adaptation, it is critical to better understand and predict the characteristics of sea levels, such as their temporal variation and magnitude over long time periods, typically multiple decades (Höffken et al., 2020; Katherine A. Serafin et al., 2017). Coastal sea level variability results from a combination of multiple processes, including mean sea level variations, tides, waves and storm surges resulting from the passing of low pressure systems and strong winds (Idier et al., 2019; Woodworth et al., 2019). We focus here on the non-tidal residual, also referred to as surge or surge residual, i.e., the water level after removal of the tide and mean sea level. At hourly time scales or shorter, temporal variation in surge residuals depends on the direction and variations in wind and pressure gradients, as well as local topographic characteristics such as the bathymetry and complexity of the coastline (Lewis et al., 2013; McInnes et al., 2016; Wu et al., 2017). Surge levels superimposed on high tides can exceed land thresholds and contribute to nuisance flooding or extreme impacts when caused by tropical or extratropical cyclones. At the global scale, studies have used hydrodynamic modelling (Muis et al., 2020) or data-driven approaches to reconstruct surge time series (Bruneau et al., 2020; Cid et al., 2018; Tadesse et al., 2020; Tadesse & Wahl, 2021). The advantage of hydrodynamic models is that with adequate model resolution and meteorological forcing, they can resolve physical coastal processes and their interactions. They are also valuable for understanding epistemic uncertainties and the relative contributions of different oceanographic and coastal processes in total water

levels. However, these models are computationally demanding and take a long time to set up (Christie et al., 2018; Santiago-Collazo et al., 2019; Teng et al., 2017). This limits their ability to be used in the simulation of large ensembles of events (Colberg & McInnes, 2012; Nuswantoro et al., 2016).

To circumvent these limitations, studies have applied data-driven models to predict surge at gauged locations, such as empirical relationships (van den Brink et al., 2004), unsupervised learning algorithms (Cid et al., 2017; Tadesse et al., 2020) or approaches using artificial intelligence like deep learning (Bruneau et al., 2020; Chen et al., 2020; de Oliviera et al., 2009; Lee, 2008), and found comparable or even better performance compared to hydrodynamic models. For example, Tadesse et al.(2020) found the daily maximum surge levels from their data-driven model to outperform the global hydrodynamic model from Muis et al.(2016). They applied random forests and linear regression, selecting as predictors a range of atmospheric (wind speed, mean sea level pressure, precipitation) and oceanographic (sea surface temperature) variables. These predictor variables were selected with various lag-times in a 10 x 10 degree box around the location of interest from remotely sensed satellite products and climate reanalysis datasets. Among deep learning approaches, Artificial Neural Networks (ANN) have been popular Neural Network (NN) models for operational surge level forecasting (Das et al., 2011; de Oliviera et al., 2009; Kim et al., 2016) or the modelling of stochastic storm surge events (Hashemi et al., 2016; Kim et al., 2015). Although limitations exist when applying NN models, such as capturing long term processes and predicting at ungauged locations, applying such methods can lead to similar or better results than local hydrodynamic models. At the global scale, Bruneau et al. (2020) were, to our knowledge, the first to use ANN models to predict hourly non-tidal residual levels at tide stations. They used as predictor variables wind, mean sea level pressure, accumulated precipitation, and wave height from the climate reanalysis dataset ERA5 (Hersbach et al., 2020). The spatial extent of the predictor variables around each location considered was four times smaller (i.e. 5 x 5 degree box) than used in Tadesse et al (2020). Due to its refined horizontal resolution, this dataset can better resolve characteristics of climate extremes, such as tropical cyclones (track, intensity, maximum wind speeds) than its predecessor ERA-Interim reanalysis (Malakar et al., 2020) even though some improvements are still needed, for example to properly capture their outer size (Bian et al., 2021).

Notwithstanding the differences between the models applied in Tadesse et al.(2020) and Bruneau et al.(2020), the role of the number of predictor variables considered and the spatial extent around each location in the model's performance and ability to learn remains unclear. Next to ANNs, other NN types could be useful for global scale surge level prediction (Reichstein et al., 2019; Shen, 2018). For example, Convolutional Neural Networks (CNN) can process patterns in spatio-temporal climate data and

identify weather features to be used for forecasts (Chattopadhyay et al., 2020; Ham et al., 2019). Recurrent neural networks using Long Short-Term Memory (LSTM) layers have been used in hydrology to capture long-term temporal dependencies, necessary to capture the state of a river basin (Fang et al., 2017; Kratzert et al., 2018).

In this paper, we explore the capability of different deep learning approaches to predict surge levels at the global scale. To do so, we predict hourly surge using four types of NN and evaluate their predictive skill. We train, validate, and test a CNN, LSTM, and combined CNN-LSTM (ConvLSTM) model to capture spatial, temporal, and spatio-temporal dependencies for surge level observations from 736 tide stations. We benchmark our NN models with a simple probabilistic reference model based on climatology. Next, for 15 selected locations with diverse surge characteristics, we examine the NN skill gained from increasing the spatial extent considered around each location and the number of different variables used as predictors. Additionally, we show the capability of the four NN types to gain skill when adding complexity to their respective network architecture.

2.2 Methods

We predict hourly surge at tide stations from the Global Extreme Sea-Level Analysis Version 2 database (GESLA-2) (Woodworth et al., 2017) using four different deep learning models following the main steps described in this section. In brief, we extract the predictand from the GESLA tide stations and predictor variables from the atmospheric reanalysis ERA5 from ECMWF (Hersbach et al., 2020). For each station, we construct and run four NN model types and compare their performance with observed surge levels and with a simple probabilistic model as benchmark. Finally, for fifteen stations, we analyse the influence of the number of predictor variables, the spatial extent considered around each location (from hereon called spatial footprint), and the architecture of the NN on its performance.

2.2.1 Data preparation

Predictand variable: surge time series.

We use total water levels from the GESLA-2 dataset, a quasi-global dataset of sea levels at a high temporal frequency (15 minutes or one hour) for 1276 stations. Each time series is resampled to an hourly frequency for consistency. The dataset has already been thoroughly controlled to flag any potential erroneous signal, for example for tsunamis and was thus not further inspected (Woodworth et al., 2017). We do not interpolate between periods with no data. The following steps are applied to extract the surge time series and are illustrated in Figure A-1. Since this study focuses on surge prediction, we remove inter-annual mean sea-level variability by subtracting the annual moving average (365 days) (Fig. A-1a). We decompose the de-trended sea-level time series into the tide and non-tidal residual by applying a harmonic analysis using the UTide (Unified Tidal

Analysis and Prediction Functions) Matlab package (Bevacqua et al., 2019; Codiga, 2011; Hoitink & Jay, 2016; Marcos et al., 2015) (Fig. A-1b). UTide uses an automated decision tree to select the most important constituents from 146 tidal constituents and performs a nodal correction for time series longer than 2 years. A comparison with tidal predictions from NOAA at three stations with contrasting tidal environments indicates differences are mainly within +/- 5 cm (Figure A-2). This is in line with the errors typically found from extracting the tide from observed water level series (Hibbert et al., 2015; Williams et al., 2018). A drawback of a harmonic analysis is that the residual time series often contain a remaining tidal signals due to small phase shifts in the predicted tide (Brown et al., 2012; Horsburgh & Wilson, 2007; Marcos et al., 2015). At a daily time scale, using the skew surge overcomes this problem (Haigh et al., 2016) and at an hourly time scale, low-pass filtering methods, such as the recursive Chebyshev Type II filter, have been recommended to fully remove this component (Brown et al., 2014; Lyddon et al., 2018). Here, we select a simple filter and apply a 12-hour moving average to limit the influence of spurious peaks in the predicted tide (Fig. A-1c). This final time series is considered as the predictand variable, i.e., the surge. We investigate to which extent this filter could impact sea-level extremes at three stations, see Figure A-3. The amount of under of overestimation is highly dependent on the relative contribution of the tides and surge in sea-level extremes. A clear advantage however from using this filtering approach is that extreme value analysis becomes more robust to errors in timing.

To train, validate and test the NN models, we select all stations that have at least seven years of data between 1979 until 2019. Bruneau et al.(2020) found that a minimum of six years of training data is needed to obtain stable NN skill. We select an additional year of data that is neither used in the training nor the validation, to test model performance. Therefore, the seven years of data should at least consist of one consecutive year without gaps for testing, and at least 6 years of consecutive sequences (10 days) without missing data (more details in section 2.2.2) for training and validation. This leads to a set of 736 stations (Figure 2-1). To get more insight into regional performance we have more specifically focused our analysis on 15 stations. This subset is chosen to cover different coastal environments(Rueda et al., 2017) and therefore surge characteristics (as further shown in Figure 2-5).

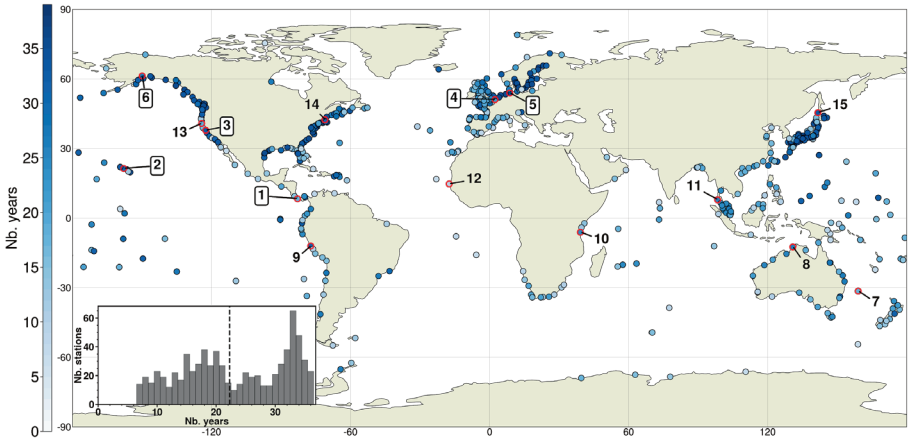

Figure 2-1: Tide stations considered in this study. Inset figure presents the histogram of the length of the data records with the median value shown by a dashed line. The set of 15 stations selected for further analysis is circled in red: 1- Puerto Armuelles (Panama), 2- Honolulu (Hawaii), 3- San Francisco (USA), 4- Dunkerque (France), 5- Cuxhaven (Germany), 6- Anchorage (USA), 7- Lord Howe (Australia), 8- Darwin (Australia) , 9- Callao (Peru), 10-Zanzibar (Tanzania), 11- Ko Taphao (Thailand), 12- Dakar (Senegal), 13- Humboldt Bay (USA), 14- Boston (USA), 15- Wakkanai (Japan). Results for the boxed numbers (1-6) are shown in the main study and the rest (7-15) in Appendix A.

Predictor variables from high resolution climate reanalysis data.

The ERA5 dataset of ECMWF provides a global atmospheric reanalysis with a spatial resolution of 0.25° and an hourly temporal resolution. To predict surges, we extract atmospheric variables at a centred box of 1.25° around the station (i.e., 5 x 5 cells). In total, five variables are used as predictors: the mean sea level pressure (MSLP), the hourly gradient of the MSLP (Δ MSLP) the meridional and zonal wind 10-meter wind components (U and V), and the wind speed magnitude. As with the surge data, the ERA5 data have been detrended by removing the inter-annual mean variability.

2.2.2 Neural network models and skill metrics

Four different types of NN models are set up and trained to predict surges: an Artificial Neural Network (ANN), a Long-Term Short-Term Neural Network (LSTM), a Convolutional Neural Network (CNN), and a Convolutional LSTM (ConvLSTM), which is a combination of the latter two. In this section, we provide an overview of their specific features and selected architecture. For more detailed information, the reader is referred to the accompanying references shown in the following section.

The ANN, the most general form of NN, has been extensively applied in various fields of science to capture nonlinear processes (Shen, 2018). The LSTM is a derivation of the Recurrent Neural Network (RNN) in that it captures sequence-to-sequence patterns in their internal state as memory, but has advantages over the conventional RNN as they can selectively store long term information (Hewamalage et al., 2021; Hochreiter &

Schmidhuber, 1997; Kratzert et al., 2018; Shen, 2018). The CNN is a class of NN models that works well in capturing spatial features, shapes and texture due to its shared weight architecture and is thus often applied for image recognition purposes (Chattopadhyay et al., 2020; Matsugu et al., 2003; Shen, 2018; Sun & Su, 2017). We also apply a ConvLSTM to capture spatiotemporal information. The ConvLSTM combines sequence-to-sequence learning with convolutional layers and emerges in current studies with promising applications in predicting spatiotemporal information (Xingjian et al., 2015).

All the NN model types use the same input data, i.e., the predictor variables, albeit in different formats and their architecture is shown in Figure A-4. They have a similar overall architecture, constructed from a series of layers made of neurons connected to each other. The first layer (called the input layer) contains the input data, i.e., the predictor variables. This input layer is connected to one or multiple hidden layers and finally connected to an output layer, which provides the surge predictions. Information between neurons in consecutive hidden layers is transferred through weighted connections, summed with a bias and scaled using a so-called activation function before being transferred to the neurons of the next layer. All parameters defining the model architecture (e.g. number of neurons, number of hidden layers) and learning process (e.g. choice activation function, subset size of training data (batch size)) are referred to as hyperparameters (Hewamalage et al., 2021). Other important hyperparameters often applied to prevent overfitting are the dropout percentage of the neurons in the last layer (dropout) and layer weights regularizer functions (kernel regularizer) (Cortes et al., 2012).

We use the Python hyperparameter optimization package SHERPA (Hertel et al., 2020) to find the number of neurons, the dropout rate, the regularizer factor l2 in the kernel regularizer function, the number of filters for the CNN/ConvLSTM, and the batch size leading to the lowest mean absolute error (MAE) between predicted and observed surge levels. To do so, we apply a random search optimization with a maximum of 100 trials for each NN at the 15 stations selected (see Figure 2-1). The settings leading to the lowest loss across all 15 stations have been used as default settings for the NN models for all stations. This resulted in the following hyperparameters: 24 filters (for the CNN and ConvLSTM), 48 neurons (for the CNN and ConvLSTM, this applies for the last fully connected layer), a dropout value of 0.1, l2 weight regularizer factor of 0.001 and a batch size of 10 days (240 hourly timesteps).

Depending on the NN model type, the input layer is connected to the following hidden layer:

- ANN: A fully connected layer with an l2 kernel regularizer.

- LSTM: a stateless LSTM layer with a hard sigmoid recurrent activation function.
- CNN: a 2D convolution layer. Each filter has a kernel size of 3 x 3 with same padding and the convolution step is followed by a max-pooling layer with a kernel size of 2 x 2.
- ConvLSTM: a 2D convolution layer following a stateless LSTM layer with a hard sigmoid recurrent activation function. Each filter has a kernel size of 3 x 3 with same padding and the convolution step is followed by a max-pooling layer with a kernel size of 2 x 2.

All of the NN models are activated using the ReLu activation function (Wani et al., 2020). In the cases of the LSTM and ConvLSTM, a hard sigmoid function is used for the recurrent activation (Farzad et al., 2019). The last hidden layer is a fully connected layer with an l2 weight regularizer and a dropout is added. We select the Adam optimizer algorithm (learning rate of 0.001) for the learning rate optimization algorithm and train the NN model to minimise the MAE, the selected loss function, between observed and predicted surge. The output layer, with one node only, represents the predicted surge levels. Because the four NN have different specifications, flattened input data without spatial relationships are fed to the ANN and LSTM. For the CNN and ConvLSTM input dimensions with spatial relationships between grid cells are fed into the NN. Note that for the NN with convolutional layers (CNN and ConvLSTM) the spatial input dimensions are relatively small in relation to the kernel size due to the spatial resolution of the ERA5 data and computational constraints as hourly data is used as temporal resolution in this study. Figure A-4 shows the architecture and input dimensions of the different NN model types used in this study. Additionally, we provide the NN models in the Supplementary Data, whose architecture and hyperparameters can be viewed using a NN visualizer app, such as netron.app.

Figure 2-2 shows an overview of our model chain and ensemble prediction methodology. We partition the predictor and predictand datasets to make the distinction between three phases: training, validation, and testing. Training and validation phases are repeated iteratively to update and tune the model parameters between each iteration, i.e., the so-called epoch. We set the maximum number of epochs to 150 but stop the training phase if no improvement in the loss is detected from the three previous epochs. The testing phase, using data excluded from the training and validation dataset, provides an unbiased evaluation of the model performance for the model parameters selected. We use the most recent year without gaps (365 consecutive days). The rest of the data are allocated into subsets of training data and validation data without gaps. In order to provide probabilistic predictions of surge levels, we use random subsets from this data to fit a model and repeat this operation 20 times to construct an ensemble of 20 models for each NN type similar to Barbarossa et al.(2018)

and Bruneau et al.(2020) as follows. Between the models we use different subsets of the training data while keeping the same model configuration. For each individual model of the ensemble, we randomly sample 50% of the rest of the data and train the model by using 70% of the selected data as training and 30% to validate the model, both randomly selected. For the LSTM and ConvLSTM, the random sampling is performed on batch-sized consecutive sequences without gaps from the time series. Between the epochs, we shuffle the training data (for LSTM and ConvLSTM we shuffle the batch-sized sequences). This ensemble prediction methodology has been set up as a nowcast structure, in which the models are trained on historical data, but can be applied on new data from the same datasets.

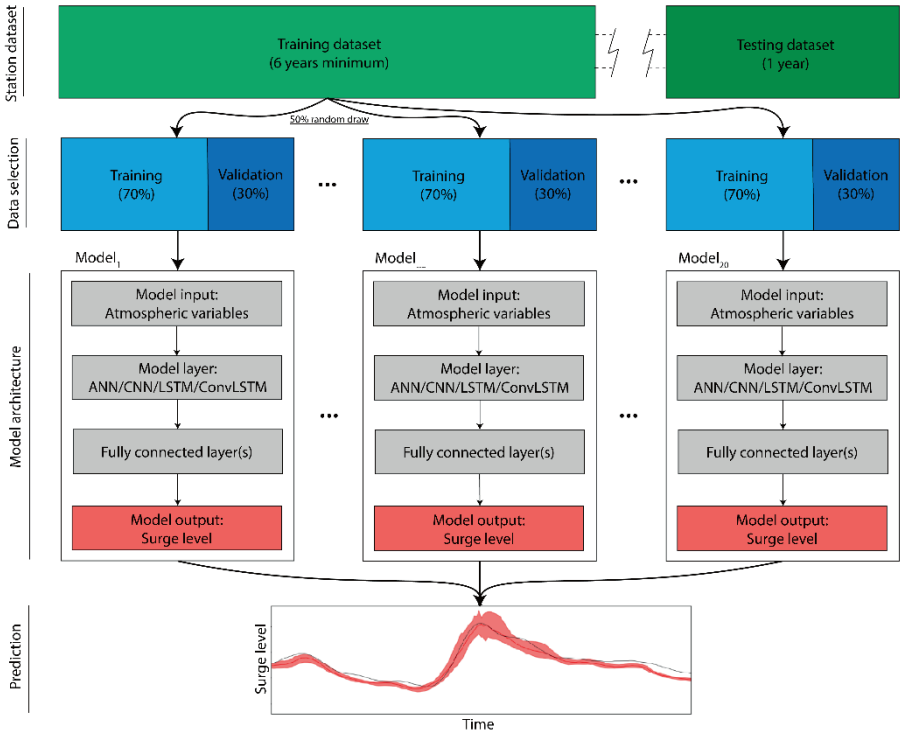

Figure 2-2: Overview of NN model ensemble and selection of data.

The implementation of the NN model types is done with the Python package Keras (Chollet, 2016), which uses Python package Tensorflow as a backend (Abadi et al., 2016). Predictors and predictand data are transformed by subtracting the mean and dividing by the standard deviation based on the training data only and these normalization parameters are stored. The predicted surge levels from the NN models are backtransformed using these parameters. We also tested other transformations for three stations (such as the scaling of each variable based on local maximum and

minimum between 0 and 1 and the Yeo-Johnson transformation), but this did not lead to significant improvements in performance. Data transformation is carried out using the Python package scikit-learn (Pedregosa et al., 2011).

Probabilistic performance and skill metric.

Since the NN models provide an ensemble of surge predictions, we select the Continuous Ranked Probability Score (CRPS) for the NN performance metric, a metric that can account for probabilistic predictions (Hersbach, 2000). Due to the absence of explicit observational uncertainty, the CRPS is more suitable than other metrics such as relative entropy (KL divergence), and is a widely used metric within hydrology and coastal science for probabilistic prediction (Bruneau et al., 2020; Pappenberger et al., 2015; Trinh et al., 2013). The CRPS averages the difference between the observed and predicted cumulative distribution of the surge across all time steps and for deterministic forecasting it reduces to the MAE:

$$\underline{CRPS} = \frac{1}{N}\sum_{t=1}^{N}\int_{-\infty}^{\infty}[P_t(x) - P^o{}_t(x)]^2\,dx \tag{2-1}$$

where N is the number of time steps in the testing year (365 x 24 hours), $P_t(x)$is the predicted stepwise cumulative distribution function (CDF) at time t=i and $P^o{}_t(x)$is the observed CDF at time i of the surge x. Because the observed time series is deterministic, $P^o{}_t(x)$ reduces to the Heaviside function such that $P^o{}_t(x) = 0$ below the observed value and $P^o{}_t(x) = 1$ at the observed surge value and above at time t.

The CRPS is a negatively oriented score and can vary from 0 to ∞, with a value of 0 indicating a perfect deterministic prediction. We report the CRPS in all figures in centimetres. High CRPS scores reflect that the surge distribution is not properly predicted: a wide ensemble spread of predicted surge will capture the observed surge but does not reflect any model skill. On the other hand, a low spread in the model predictions and a model bias will also result in a high CRPS score, as the ensemble will fail to capture the observed surge. In order to better understand the behaviour of the ensemble prediction, the CRPS can be decomposed (Hersbach, 2000) as:

$$\underline{CRPS} = \underline{RELI} + CRPS_{pot} \tag{2-2}$$

where $RELI$ is the reliability component, which indicates whether the distribution of the predicted surge has similar statistical properties to the observed time series, and $CRPS_{pot}$, the potential CRPS, denotes the CRPS when the ensemble forecasts are perfectly reliable ($RELI = 0$, also a negatively oriented metric). In order to decompose the CRPS into the reliability and potential component, we use the crpsDecomposition function from the R package verification (Gilleland, 2015). The potential CRPS is further decomposed into:

$$CRPS_{pot} = \underline{U} - \underline{Resol} \tag{2-3}$$

where the uncertainty component, U, represents the CRPS if only a climatological probabilistic prediction is available, and the resolution component, $Resol$, evaluates the improvement of the NN model ensemble predictions to the average ensemble spread and the observed outliers. A resolution value higher than zero indicates that the model ensemble adds some value compared to the probabilistic climatology distribution. The climatological probabilistic prediction has no model skill and a perfect reliability. We derive the climatological probabilistic prediction using a stratified sampling approach of the observed surge (Hu et al., 2016). We remove noise and spurious effects by calculating a centered moving average with a Gaussian filter and a window size of 30 days (Janoušek, 2011) of the surge used in the training dataset and weighted with the following equation:

$$w = \frac{1}{2\Pi\sigma} \tag{2-4}$$

where σ is the standard deviation expressed in time steps and set to 72 hours. Next, we rank the hourly surge levels for each month of the year and draw 20 equidistant samples to construct the cumulative distribution function of the climatology. These 20 samples represent the predicted ensemble from the probabilistic climatology predictions and are used to calculate the uncertainty component for the CRPS value of the testing year.

Comparing CRPS values between stations can be difficult to interpret because similar CRPS values does not necessarily indicate a similar model skill. In stations with a larger variability, the uncertainty component is larger and the CRPS becomes larger in value and therefore seemingly worse. To correct for this effect, we scale the CRPS value with the uncertainty component (see Eq. 2-3). We select the best NN model type as the one with the lowest CRPS value, $CRPS_{best}$, and calculate the skill gain of each NN model type by normalizing the CRPS value with the CRPS value of the climatological distribution with the following equation:

$$CRPSS = \frac{U - CRPS_{best}}{U} \times 100 \tag{2-5}$$

where CRPSS is now a dimensionless and positively oriented indicator of the skill gain compared to that of the reference ensemble predictions from the probabilistic climatology distribution (Bradley & Schwartz, 2011). The ratio is multiplied by 100 to represent the CRPSS values as a percentage. The CRPSS can vary from -∞ to 100%, with 100% representing a perfect prediction and values higher than 0 indicating a better performance than the probabilistic climatology forecast.

2.2.3 Assessing the influence of NN architecture and predictor variables

The selection of the hyperparameters, predictor variables, and spatial footprint considered around each station have been tuned following an optimization with a simple design rationale for 15 stations, as explained previously. The best settings across the different NN types have been used as default settings for the NN models for all stations. Here, we explore the effect on model performance for the 15 selected stations in response to increasing the spatial footprint of input data, number of predictor variables, and NN design architecture for the four NN types. We use the default settings and perform a sensitivity analysis for each of them. First, we test the influence of the size of the spatial footprint on the performance of the NN models and gradually increase the gridded box centred around the station by 0.5°-degree resolution (0.25°, 0.75°, 1.25°, etc.). Second, we gradually increase the number of predictor variables in the following order: MSLP, wind speed magnitude, U and V, gradient of MSLP, and finally the quadratics of U and V. By doing so, we show the sensitivity of adding more atmospheric predictor variables on model performance. Last, we perform a hyperparameter optimization but focussing on the architecture of the NN model (hidden layers, neurons, and filters). For this optimization we opt for using an optimization algorithm instead of a one-by-one sensitivity analysis, because of the large number of combinations and showing the effects of optimizing on one model for an ensemble. The random search algorithm with a maximum of 100 trials optimizes the number of hidden layers (1, 2, 3, 4, 5), Neurons (24, 48, 96, 192), and filters (8, 16, 24).

2.3 Results

2.3.1 Global performance and skill of the NN models

The CRPSS for each station for the best NN model (i.e., the one with the lowest CRPS) is shown in Figure 2-3. A positive (negative) CRPSS indicates that the NN model has better (worse) predictive skill compared to our reference model, i.e., the probabilistic climatology ensemble. We observe clear spatial patterns in high and low model skill. Stations along the coast of West Europe, eastern Asia, New Zealand, southern Australia, southern Africa, and parts of North and South America generally perform well, with a CRPSS generally higher than 40%. However, stations close to the equator perform poorly, with negative CRPSS scores. These spatial patterns of model skill performance are observed for all NN model types (Figure A-5) and also found in large scale hydrodynamic models (Muis et al., 2020). This indicates that these differences do not necessarily stem from the model type applied but rather point towards more general challenges in capturing surge variability in the tropics.

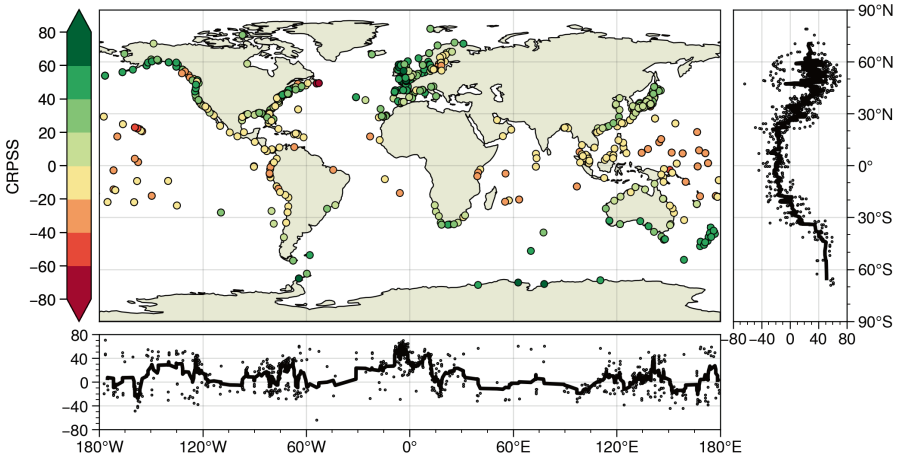

Figure 2-3: Highest CRPSS percentage obtained of all NN models per tide station. Meridional and zonal plots present the CRPSS values with a centred moving average of 10 stations.

We investigate the CRPS decomposition to better understand the NN model performance. Similar spatial patterns are observed for the uncertainty and the resolution component (Figure A-6b and A-6d, respectively), with lowest resolution scores and lowest uncertainty scores at stations near the equator and higher values in mid- to high latitudes. The resolution component of the CRPS, Figure A-6d, is positive for all stations except two locations located southeast of the Newfoundland Island, Canada. The positive resolution values indicate that NN models improve the surge ensemble predictions from our agnostic climatological probabilistic prediction. This does not however guarantee a better model skill. Negative values of the CRPSS can be interpreted as that the overall distribution of observed values is better captured by the distribution of the climatological mean than the NN model predictions. Nonetheless, this shows that there is value, albeit limited, in using a NN and indicates an improvement gained by the NN to better capture the average ensemble spread and behaviour of observed outliers.

The best performing NN model type per station is shown in Figure 2-4. Although the differences between NN model types are marginal (Figure A-5), the LSTM results in the best performance for the majority of the stations (92%). Regions in Europe, Africa, Australia, the Pacific, and the U.S. almost all show the highest CRPSS values for LSTM. The only region that shows a clustering of best performance for the CNN is the southeast of Japan. Convolutional LSTMs show the best performance for a few locations along the east coast of South America and for five islands in the Pacific Ocean. The ANN performs best for only two locations (Atlantic city, USA; and Kuantan, Malaysia). Comparing the CRPS decomposition between the NN model types shows that for almost all stations the reliability score is the lowest for the LSTM. This indicates

that the probabilistic forecast from the LSTM has the closest agreement to the distribution of the observed values (Figure A-7). Similarly, since the uncertainty component of the CRPS is the same for all NN models (by definition), this implies that the resolution is highest for the LSTM at most stations. The LSTM is best in distinguishing types of events and their different distributions of expected surge. In terms of computational time, the LSTM is almost as fast as the ANN, about 1 minute per model on a Bullx system supercomputer, while the CNN and ConvLSTM take on average three and 18 times longer than the ANN, respectively.

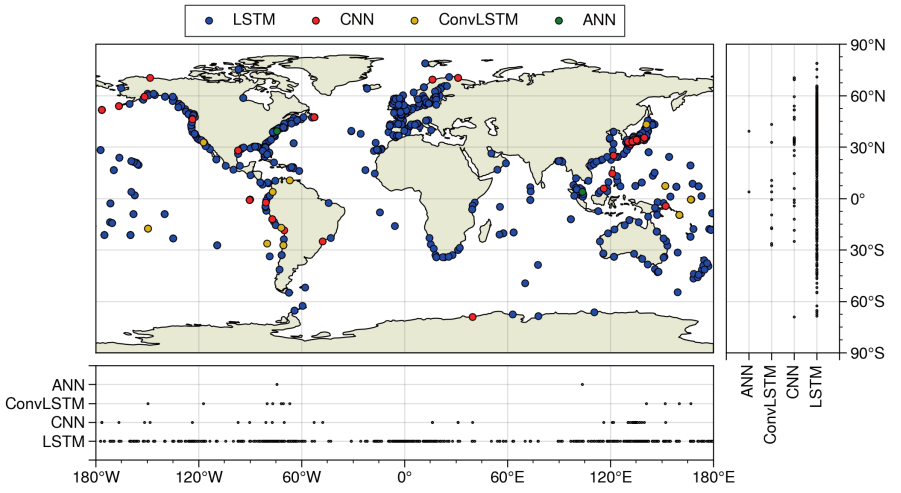

Figure 2-4: NN model type from the highest CRPSS value shown in Figure 2-3. For readability, we display the models in the following order LSTM→CNN→ConvLSTM→ANN.

Local performance at selected tide stations. Figure 2-5 shows the ensemble surge time series predicted from the best NN model type at six of the fifteen selected locations with the observed time series for the testing year. The rest of the stations are shown in Figure A-8 and A-9. For all 15 stations, the LSTM is the best-performing NN model except at Callao, where the CNN model shows the best skill (CRPSS from LSTM: -13.41%; CRPSS from CNN: -13.10%). We note that an inter-station comparison based on the CRPS metric alone would have been misleading and incorrect. As shown in Figure 2-5, stations with the best (highest) CRPSS score do not necessarily have the best (lowest) CRPS score. This is because the uncertainty component of the CRPS, representing a climatological probabilistic prediction, greatly differs per location (as indicated by the difference in the range in scale of the y-axis). Instead, using the CRPSS as our comparison metric normalizes for these differences in climatology.

In Figure 2-5, a positive CRPSS is obtained at four stations, with the highest value of 55% for the Cuxhaven station. At these stations, the general temporal evolution of the

surge is well captured and there is close agreement between observed and predicted time series although extremes are often underestimated. We extract the median from the probabilistic predictions to calculate the coefficient of determination, R^2, with the observed surge levels. R^2 range between 0.57 at Dunkerque up to 0.86 at Cuxhaven. At stations with a negative CRPSS (Honolulu: -40.49%; Puerto Armuelles: -14.44%), we observe that the NN cannot capture low frequency variations of the observed time series that dominate the overall variability. As a result, the lower model skill is lower than ensemble predictions based on the climatology distribution. These low frequencies probably driven by mean sea level variations, independent of atmospheric conditions, and therefore acts here as noise. This effect is also visible for other stations shown in A-8 and A-9 such as Zanzibar (CRPSS: -22.46%), Lord Howe (CRPSS: -14.15%) or Callao (CRPSS: -13.10%).

We compare these predictions with the surge time series obtained from the Global Tide and Surge Model (GTSM), a global hydrodynamic model simulating tides and surge forced with ERA5 (Muis et al., 2020). There is a close agreement between the NN skill, and the results obtained with GTSM. Comparable R^2 values to the NN are found at the stations with a positive CRPSS score and lower R^2 values for negative CRPSS, see Figure 2-5m-r, A-8 and A-9. At the stations of Cuxhaven and Dunkerque, GTSM provides very high agreement with observations, with R^2 of 0.87 and 0.92 respectively compared with 0.86 and 0.57 for the LSTM. Averaged across all the 15 stations, we find an average R^2 value for the LSTM (GTSM) of 0.69 (0.67) for stations with a positive CRPSS stations and 0.08 (-0.16) for negative CRPSS. More generally, the close performance between GTSM and LSTM tends to confirm that poor model skill observed is the result of a lower frequency signal present in the observed time series but not driven by meteorologically driven processes since it is also absent from the GTSM surge time series.

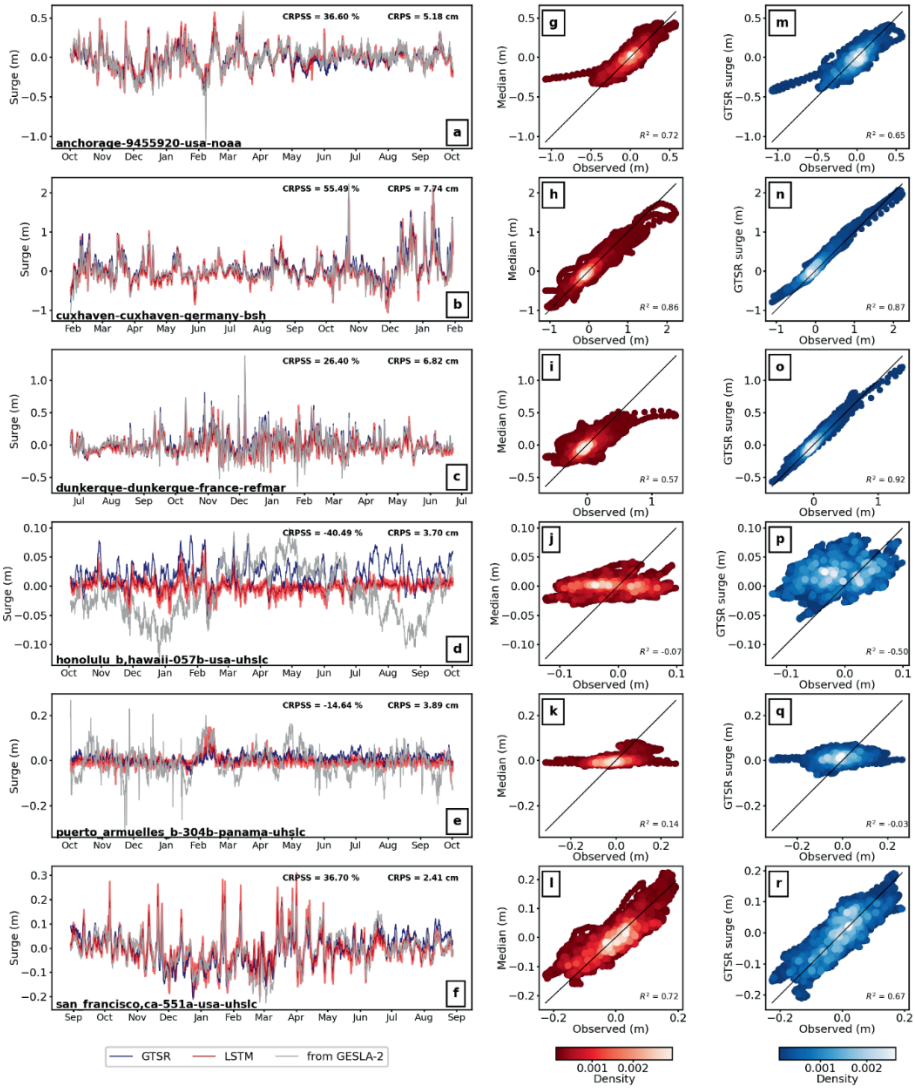

Figure 2-5: a-f) Hourly surge predictions for the testing year from the LSTM model, observed and surge from the Global Tide and Surge Model forced with ERA5 and g-l) scatter plot of the median from the predicted ensemble with the observed surge and m-r) with the GTSM surge.

2.3.2 Assessing the influence of NN architecture and predictor variables

To explore ways to further improve the performance of the ensemble models, we evaluate the skill of the NN model and the complexity of the model input by increasing the number of predictors together with increasing the size of the spatial footprint by 0.5 degree at a time. The spatial footprint is increased from 0.25 degrees (1x1 cells where

the tide station is located) up to 6.25 degrees (13x13 cells) centred box around the station. Furthermore, we perform a hyperparameter optimization allowing more hidden layers (up to 6) in our model architecture together with an optimization of the number of neurons (24, 48, 96, 192) and filters (8, 16, 24).

Influence of predictor variables. Figure 2-6 shows the CRPSS value obtained when increasing the number of predictor variables (y-axis) and the spatial footprint size (x-axis) for the NN for the six locations used throughout this study. Additionally, the same plots for the nine other locations are shown in Figure A-10. The CRPSS improves when enlarging the spatial footprint size for almost all stations and NN types. Moreover, stations that show an increase in CRPSS from a negative to a positive score (from dark red to green) when increasing the number of predictor variables or spatial footprint show the ability to learn of the NN at that location. Increasing the spatial footprint from 0.25-degree resolution to 0.75 degree shows the largest increase in CRPSS value (9.5% on average for all 15 stations). After a spatial footprint of 2.75 degree, the CRPSS improves on average with 0.55% for each 0.25 degree increase of spatial footprint. Between the different NN types, we see that the performance of the CNN and ANN has the largest ability to learn when increasing the spatial footprint as the CRPSS of these NN types improves the most. Furthermore, we see that for stations that have a lower or negative CRPSS like Puerto Armuelles (also Ko Taphao, Lord Howe and Zanzibar in Figure A-8) the learning rate of LSTM increases/decreases sporadically when increasing the spatial footprint. Additionally, the average ensemble model spread increases and leads to a lower CRPSS value. The spread and uncertainty of the ensemble models for the LSTM and ConvLSTM increases when adding complexity to those stations. Due to this larger spread and uncertainty in the predictions, we argue that the LSTM and ConvLSTM do not benefit much from an increase in input or architecture complexity. Next to this, we find no clear difference in learning when increasing the spatial footprint when splitting the stations into stations that are prone to be hit by (extra) tropical cyclones and stations that are not (Figure A-11).

When increasing the number of predictor variables, we see that the best performance is gained when using the 5 (MSLP, gradient of MSLP, U and V, and wind magnitude) or 7 (same as 5 but the quadratic U and V are added; hereafter referred to as U^2 and V^2) predictor variables. Averaged over all 15 stations, we see that when including the wind magnitude predictor to the MSLP in the 2-predictor setup, CRPSS performance increases the most with an average of 5%. For the other predictors (U and V, gradient of MSLP, and U^2 and V^2) performance increases on average of 4.2%, 2.3%, and 0.5% respectively. Highest performance is reached when including the gradient of the MSLP and U^2 and V^2 in the 5 and 7 predictor setups respectively.

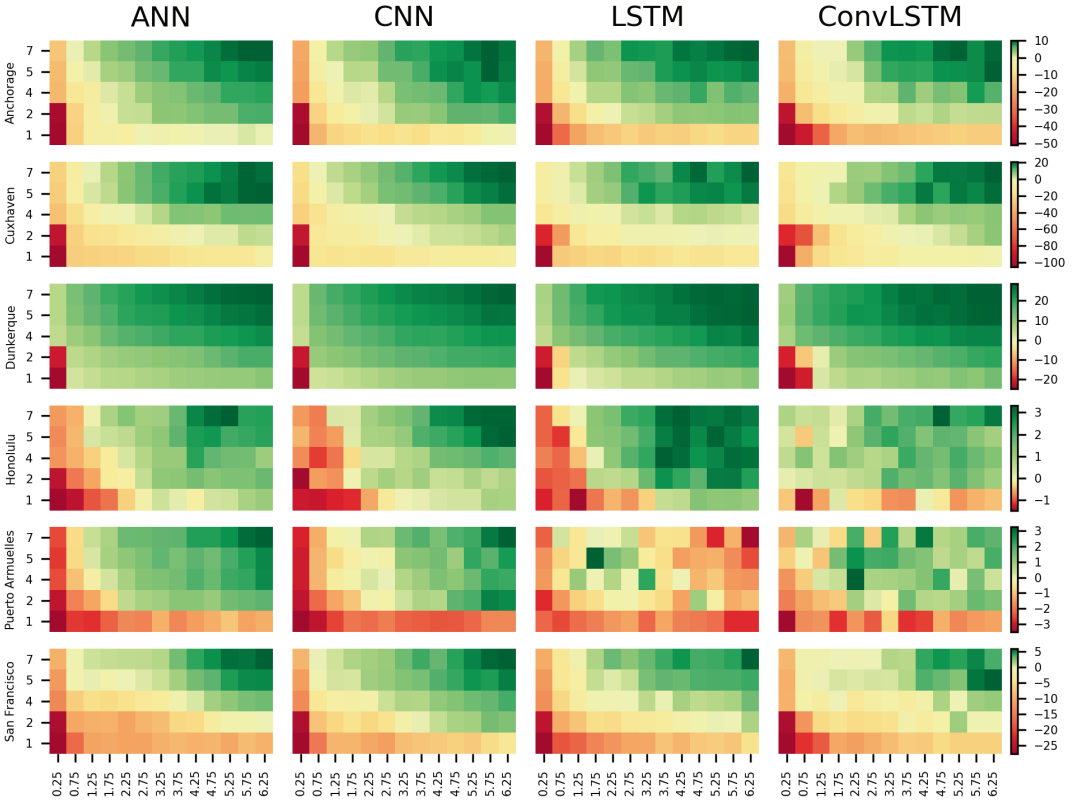

Figure 2-6: CRPSS value of the NN model ensemble for increasing number of predictor variables and spatial footprint size. On the horizontal axis the spatial footprint is depicted and on the vertical axis the number of predictor variables are depicted with cumulatively 1 (MSLP); 2 (wind magnitude); 4 (U and V); 5 (gradient of MSLP); 7 (quadratic of U and V).

Although the CRPSS shows an improvement in model performance for all 15 stations, the computation time increases a lot when enlarging the input dimensions (Figure A-9). Compared to the setup of the global runs and depending on the computation architecture, the computation time, in our case, increases up to 15 times: from 0.3 and 4.8 minutes for the global settings runs to 3.1 and 65 minutes for the fastest and slowest NN which are LSTM and ConvLSTM respectively. Of course, this is just an indication as performance is dependent on layer configurations and hardware. In our case, details of the thin nodes we used can be found here (https://userinfo.surfsara.nl/systems/cartesius/description).

Influence of NN architecture. Next to increasing the number of predictor variables or spatial footprint, we assess the influence of locally optimizing the number of hidden layers, neurons, and filters (for the CNN and ConvLSTM). For the global results, we used a fixed NN design with only one hidden layer of each type and hyperparameters of 48 neurons and 24 filters for the convolutional layers (for the CNN and ConvLSTM only). We compare the performance of the optimized NN models from a local hyperparameter optimization on the number of hidden layers, neurons, and filters with a random search algorithm with that of the models from section 2.3.1. At each of the 15 tide stations, the optimization minimizes the MAE using the whole training dataset.

Table 2-1 shows the results of this hyperparameter optimization for the 15 stations selected. Across all model types, we see that a local optimization leads to a different selection of hyperparameters between stations. In comparison to the CNN and ConvLSTM, we observe a larger spread in the number of optimal hidden layers for the ANN and LSTM ranging between 1 and 5 hidden layers. On average, the CNN requires 3 or more hidden layers (median: 4) and the ConvLSTM centres around 2 or 3 hidden layers (median: 2). The number of filters is preferably 24 for CNN and ConvLSTM, while the latter also sometimes favours a lower number of filters.

In Table 2-1, we also report the CRPSS obtained from the ensemble predictions using these optimized settings and the absolute change in CRPSS, i.e., the difference between the CRPSS obtained here and the CRPSS from the previous NN model applied in section 2.3.1. We see that the change in CRPSS is positive for all stations with the CNN and up to an increase of more than 20% for Dunkerque and Ko Taphao. However, this increase in CRPSS for Ko Taphao does not indicate a meaningful ensemble model improvement as the CRPSS is still negative. For instance, ensemble model predictions for Ko Taphao could become better at generating random predictions that together look like climatology. For these stations, we also see an increase in the hit rate defined as the percentage of hourly time steps the NN ensemble spread captured the observed surge value. This therefore suggests an increase in the ensemble spread that is capturing the signal.

	CRPSS				Change CRPSS				Change hit rate				Hidden layers				Neurons				Filters	
Stations	ANN	CNN	LSTM	ConvLSTM	ANN	CNN	LSTM	ConvLSTM	ANN	CNN	LSTM	ConvLSTM	ANN	CNN	LSTM	ConvLSTM	ANN	CNN	LSTM	ConvLSTM	CNN	ConvLSTM
Anchorage	29.4	40.5	36.8	33.9	0.7	6.2	0.2	-0.2	1.2	17.5	1.9	5.0	3	4	5	2	48	96	48	96	24	16
Boston	31.8	37.7	37.0	33.7	1.7	5.5	-0.9	0.1	2.3	8.9	-2.6	-3.6	4	4	2	2	96	96	24	24	24	16
Callao	-14.5	-3.8	-10.5	-13.2	1.2	9.3	2.9	4.1	3.2	35.4	5.0	3.0	2	4	4	1	24	48	96	24	24	8
Cuxhaven	51.7	56.5	53.2	48.9	3.7	11.7	-0.5	1.5	-1.9	12.0	3.7	-3.9	4	4	4	2	48	24	192	24	24	24
Dakar	-20.6	-6.9	-11.4	-19.6	-0.2	11.2	0.9	-1.0	0.2	19.7	4.0	1.1	1	5	1	5	48	192	192	96	24	16
Darwin	-1.5	5.5	1.5	-7.3	0.7	4.3	-0.6	-6.2	-0.2	11.0	0.3	-2.7	4	5	2	3	96	48	48	96	24	16
Dunkerque	34.4	41.7	40.9	36.2	15.9	21.7	14.5	15.4	0.8	12.1	1.7	2.6	2	3	1	2	24	24	96	192	24	24
Honolulu	-45.4	-40.8	-41.5	-43.0	-0.3	4.5	-1.0	-0.4	-0.3	6.6	0.2	0.0	1	5	3	1	96	192	24	24	24	8
Humboldt	35.0	41.9	41.3	35.9	-0.1	4.9	1.7	-1.2	0.3	17.0	9.0	0.2	2	4	5	2	48	24	192	24	24	24
Ko Taphao	-35.2	-9.9	-26.2	-30.1	-0.4	23.6	-0.1	1.8	0.5	23.1	0.0	0.1	3	5	2	2	24	48	96	48	24	8
Lord Howe	-18.9	-18.3	-14.6	-17.4	-0.4	1.5	-0.4	-1.5	-1.1	4.0	3.4	-0.8	1	4	4	1	24	96	192	48	16	8
Puerto Armuelles	-20.6	-10.7	-21.8	-23.2	0.0	6.2	-7.1	-4.2	0.1	30.4	-5.0	-3.9	3	3	5	3	24	48	192	192	24	16
San Fransisco	30.4	35.6	36.2	34.6	0.3	4.4	-0.4	1.0	-0.7	15.1	-3.4	3.3	2	5	1	3	24	96	192	48	24	24
Wakkanai	33.7	41.0	38.7	34.2	0.6	4.3	-0.8	-1.2	2.3	11.6	-1.8	2.0	2	3	2	4	48	96	96	48	24	16
Zanzibar	-31.9	-22.0	-28.0	-29.0	0.3	6.1	-5.5	-1.1	0.8	14.3	-5.5	-1.5	1	4	5	2	48	24	48	24	24	16
Mean/median	3.9	12.5	8.8	5.0	1.6	8.4	0.2	0.5	0.5	15.9	0.7	0.1	2	4	3	2	48	48	96	48	24	16
Standard deviation	32.2	30.6	32.4	32	4.1	6.4	4.7	4.8	1.3	8.5	4	2.8	-	-	-	-	-	-	-	-	-	-

Table 2-1: Results of the NN architecture hyperparameter optimization. The change in hit rate is expressed in percentages increase of model ensemble ability to capture observed value within the ensemble spread. The summary statistics shown are mean for CRPSS, change in CRPSS and change in hit rate, and the median for the hyperparameters.

For the other NN types, the change in CRPSS is generally smaller, showing a marginal gain from applying more complex NN models. The local optimization even results in a decline in CRPSS value for some NN model types and stations, e.g., the LSTM and ConvLSTM for Puerto Armuelles. This decrease in performance from the local optimization denotes a mismatch between the hyperparameter optimization on the MAE on the *whole* training data and the performance obtained from *ensemble* predictions. This indicates that optimizing for a deterministic prediction does not necessarily lead to a better probabilistic prediction. The change in hit rate frequency indicated in Table 1 shows that NN models that do not improve in CRPSS can improve in hit rate frequency by increasing the spread between members. Each member, however, will be less representative of the others and of the surge progression in reality, leading to a lower CRPSS value than original.

2.4 Discussion

This study provides the first application of four NN model types for hourly surge predictions at the global scale and explores the capabilities of NN models. Unlike previous data-driven studies, we benchmark the performance of the NN models developed in this study against simple probabilistic predictions based on climatology to further understand spatial performance patterns. We also provide, for the first time, a quantitative assessment of the role of the network complexity, the number of predictor variables considered, and the spatial extent considered around each location with respect to the model performance.

Overall, the results found in this study are in line with previous studies from Cid et al.(2017), Tadesse et al.(2020), and Bruneau et al.(2020), which are to our knowledge the only other studies that have looked at either daily or hourly surge predictions from data-driven models at the global scale. Focusing on 15 stations, we found very similar performance between the GTSM hydrodynamic model (Muis et al., 2016), and the LSTM. An important similarity across all these studies is that model skill increases from low to high latitude, where climatology shows that there is more variability in surge levels. This finding is consistent even though model setups and the selection of predictor variables differ across all these studies. This therefore seems to indicate more general challenges in surge predictions, which are summarized next.

In order to predict surges, we selected the predictor variables from atmospheric variables that are known to be the main drivers of surge (Resio & Westerink, 2008; Tadesse et al., 2020). Our analysis of model skill however suggests that other sea level components are still present in the observed time series that cannot be captured by our predictor variables. This effect is particularly visible in the tropics where we find a consistently low model skill, similar to other studies (Cid et al., 2017; Tadesse et al., 2020). Surge variations in tropical regions are often characterized by a small variance, in the order of a few centimetres. In this case, errors in the tidal decomposition can

introduce spurious noise of the same magnitude or more in the non-tidal residual time series that can have a relatively large influence on the time series and the CRPS. In tidally dominated coastal environments, applying a recursive Chebyshev Type II low-pass filter instead of a moving average might better help remove remaining transitory signal in the non-tidal residuals and isolate the high frequency signal in the observed time series (Brown et al., 2012; Lyddon et al., 2018). Moreover, other processes not linked with atmospheric variability can still be present in the observed time series. Steric components (driven by seasonal changes in salinity and thermal expansion), geostrophic currents (due to oceanographic pressure gradients), and river discharge levels in estuaries and deltas can have a similar or larger influence on non-tidal water level variability than surge levels (Cid et al., 2018; Eilander et al., 2020; Idier et al., 2019; Ikeuchi et al., 2017; Ishii & Kimoto, 2009; Miller & Douglas, 2004; Muis et al., 2018; Serafin et al., 2019; Woodworth et al., 2019). Therefore, one could instead add additional predictor variables to cover these different processes. Examples of additional predictor variables available at the global scale that have been applied in other data-driven studies are sea surface temperature, accumulated precipitation, significant wave height, and peak periods (Bruneau et al., 2020; Cid et al., 2018; Tadesse et al., 2020).

The largest anomalies in surge levels are often linked to the passage of low-pressure systems in the mid-latitudes and with tropical cyclones in the tropics. A proper characterization of the moving speed, track, central pressure drops, and size of these atmospheric phenomena is essential to link predicted tropical cyclones to observed surge extremes. Here, we selected the predictor variables from the most recent global reanalysis dataset to ensure a spatially and temporally consistent dataset. While ERA5 can better represent the characteristics of tropical cyclones (position, wind intensity and size) compared to its predecessor product ERA-Interim (Dullaart et al., 2020; Hersbach et al., 2020; Malakar et al., 2020), some regions still exhibit large wind biases (Belmonte Rivas & Stoffelen, 2019; Bian et al., 2021). We expect that these biases do not affect the inter-model comparison because each NN model is independently fit. However, this could affect the spatial patterns of performance. An alternative to reduce this regional bias in future studies could be by including more accurate atmospheric products from local sources such as remote sensing products (Tadesse et al., 2020), even though spatial and temporal data coverage may be limited, or from global forecasting systems (Bloemendaal et al., 2018; Dullaart et al., 2020; Roberts et al., 2018). To improve the representation of tropical cyclones, higher resolution input data could be obtained, for example by applying observed best track data and fitting a parametric wind model (Lin & Chavas, 2012), as done for local(Das et al., 2011; Hashemi et al., 2016). and global studies (Bloemendaal, de Moel, et al., 2020; Marsooli et al., 2019; Muis et al., 2019). To fully harvest the impact of these additional efforts, this should be done in conjunction with a better sampling strategy during training to obtain a more balanced training set (Bruneau et al., 2020).

Our study highlights the complex interplay between hyperparameter optimization, architecture complexity, and the number of predictor variables in model performance. This interplay has not yet been studied in global surge studies using deep learning methods. We show that local model optimization based on deterministic prediction does not necessarily lead to better probabilistic predictions. This means that inter-model comparisons should be carefully interpreted since optimization results can lead to a local optimum in model settings for a few stations rather than a global optimum in model settings for all stations. We found that fitting an ensemble of NN models for each station to provide probabilistic predictions is beneficial to overcome overfitting, unless the ensemble model spread is too large. Nevertheless, the models presented here do not represent a global optimum and further improvements could be made. Because we only carried out the optimization for fifteen stations, optimal settings for other stations or regions could differ from our analysis. Furthermore, using NN instead of hydrodynamic models may lead to several challenges as NN do not help us improve understanding the underlying physical processes of surges, and do not capture long term processes such as sea-level rise or climate variability (Reichstein et al., 2019). In order to face these challenges, future work can make use of physics-informed machine learning to improve the predictive ability and scientific consistency for generalizable NN models (Karpatne et al., 2017; Kashinath et al., 2021; Willard et al., 2020).

Additional efforts should be closely linked to the intended use of the data to evaluate the best NN architecture, hyperparameters and further developments. For example, including longer term temporal dependence could be done by implementing a stateful LSTM instead of the stateless LSTM implemented in this study. Using our global model settings, the input dimensions in relation to the kernel size of the convolutional layers may be small to evaluate the true performance of these NN as edging effects can occur. Decreasing the edging effects while keeping the high temporal resolution can be a challenge for future research (Innamorati et al., 2019; Nasir & Sassani, 2021). Moreover, this study highlighted the potential of convolutional layers when fed with large enough input for surge predictions, an interesting avenue for further research. For applications in coastal flood risk and extreme sea level analysis, the design of the study should be altered to put an explicit emphasis on extremes and consider total water levels instead of focussing on the surge component only. Our analysis on the influence of the pre-processing steps on sea level return periods (Fig. A-3) indicates that errors in the timing of surge residuals can lead to an under or overestimation of extreme sea levels. If compounded with a biased underestimation of extreme surge magnitudes, as observed locally, this could strongly impact reconstructed sea level extremes. A more sophisticated loss function, combining the MAE with other metrics to evaluate extremes, could be implemented to update the layers' weight and better capture extremes. Similarly, our experiment setup focused on predicting surges based on observed time series, and as such, this method cannot be directly applied for predicting

surges at ungauged locations because it requires training data that by definition do not exist. One could circumvent that by applying our approach to modelled data, such as the GTSR dataset (Muis et al., 2016).

2.5 Conclusion and outlook

In this study, we have explored deep learning capabilities to predict surges at the global scale. For 738 tide stations, we developed and applied an ensemble approach for four different types of NN to predict hourly surges. We used surge as the predictand variable extracted from observed sea levels of the GESLA-2 dataset and atmospheric variables as predictor variables from the ERA5 climate reanalysis dataset. To evaluate the NN model performance at each station, we used the CRPS value and benchmarked the results against a simple probabilistic model based on climatology, i.e., the CRPSS. Next, we explored how increasing the NN design complexity affects model performance by adding hidden layers and enlarging the spatial footprint around each station to extract the predictor variables.

Using the same hyperparameter settings across all stations and a spatial footprint of 1.25 degree to extract predictor variables, the LSTM generally outperforms the other NN types. This is because the probabilistic forecast from the LSTM is in closest agreement with the distribution of the observed values, resulting in the best reliability scores in the CRPS. While the LSTM generally performs best globally when considering a spatial footprint of 1.25 degree, we show that the CNN can improve the most when increasing the spatial footprint or number of hidden layers in the model architecture and outperforms the LSTM. This comes, however, at the expense of increasing computational time, up to more than 15 times longer to run.

Our results show that the NN models can capture temporal evolution of surges and outperform large-scale hydrodynamic models. We observe similar performance patterns across all the NN ensemble models, with a performance increasing with latitude and generally high (CRPSS>40%) in mid-latitudes, which is in line with previous studies. Stations around the equator generally do not outperform the simple probabilistic model based on climatology. Additionally, we show that model performance generally improves with increasing the size of the spatial footprint for the selection of the predictor variables, but that increasing the number of hidden layers does not always lead to a better performance.

Finally, we share the surge input and predicted data and the NN models to invite the coastal community to further build on these initial efforts. We foresee that the NN models developed here could be adapted and tailored for specific coastal applications, for example to provide rapid operational forecast of surge levels, for probabilistic coastal flood hazard assessments, or for future predictions of surges.

Data availability

The initial and predicted surge time series at the tide stations analysed, and the NN models at each location in this study are openly available on Zenodo (https://doi.org/10.5281/zenodo.5216849). Easy visualisation of the models including the model hyperparameters and features can be accessed in for example with the netron.app website.

Acknowledgements

The research leading to these results received funding from the Dutch Research Council (NWO) in the form of: a VIDI grant (grant no. 016.161.324); and the MOSAIC project in collaboration with the Netherlands eScience Center (grant no. ASDI.2018.036). The authors would like to thank Job Dullaart for sharing the surge data from the GTSM model forced with ERA5.

Contributions

Author contributions follow the CRediT authorship categories. A.C. and T.T.: Conceptualization, Methodology, Software, Formal analysis, Investigation, Data curation, Writing—original draft, Writing—review and editing, Visualization. C.v.S: Methodology, Writing—original draft, Writing—review and editing,. S.M: Conceptualization, Writing—original draft, Writing—review and editing,. P.J.W: Writing—original draft, Writing—review and editing, Supervision, Funding acquisition.

3 Coastal flood adaptation using structural measures

This chapter is published as

Tiggeloven, T., De Moel, H., Winsemius, H. C., Eilander, D., Erkens, G., Gebremedhin, E., Diaz Loaiza, A., Kuzma, S., Luo, T., Iceland, C., Bouwman, A., Van Huijstee, J., Ligtvoet, W., & Ward, P. J. (2020). Global scale benefit-cost analysis of coastal flood adaptation to different flood risk drivers. Natural Hazards and Earth System Sciences, 20, 1025– 1044. https://doi.org/10.5194/nhess-2019-330

Abstract

Coastal flood hazard and exposure are expected to increase over the course of the 21st century, leading to increased coastal flood risk. To limit the increase in future risk, or even reduce coastal flood risk, adaptation is necessary. Here, we present a framework to evaluate the future benefits and costs of structural protection measures at the global scale, which accounts for the influence of different flood risk drivers (namely: sea-level rise, subsidence, and socioeconomic change). Globally, we find that the estimated expected annual damage (EAD) increases by a factor of 150 between 2010 and 2080, if we assume that no adaptation takes place. We find that 15 countries account for approximately 90% of this increase. We then explore four different adaptation objectives and find that they all show high potential to cost-effectively reduce (future) coastal flood risk at the global scale. Attributing the total costs for optimal protection standards, we find that sea-level rise contributes the most to the total costs of adaptation. However, the other drivers also play an important role. The results of this study can be used to highlight potential savings through adaptation at the global scale.

3.1 Introduction

In recent years, the effects of climate change on coastal flood hazards and its impacts on society have been studied extensively. The Intergovernmental Panel on Climate Change (IPCC) reports that it is likely that we will face a global mean sea-level rise by the end of the 21st century in the range of approximately 0.43 – 0.84 meter compared to 1986-2005 and that impacts on society will be vast (Oppenheimer et al., 2019). According to a recent study by Raftery et al. (2017), it is unlikely that the Paris agreement's aim of keeping global warming below a 2°C increase by the end of the 21st century will be met. This may lead to changes in storm surges (Tebaldi et al., 2012), extreme sea levels (Vousdoukas et al., 2017), and tides (Pickering et al., 2012). Together, these increases in sea-level and a possible change in storminess will lead to increased flood hazards, as well as threats to shorelines, wetlands, and coastal development (Ericson et al. 2006; Hinkel et al., 2013). Moreover, flood hazard is expected to increase as a result of subsidence. In many deltas and estuaries, groundwater extraction is a major factor contributing to this subsidence (Hallegatte et al., 2013). During the 20th century, the coasts of Tokyo, Shanghai and Bangkok subsided by several meters (Nicholls et al., 2008) and subsidence is expected to continue to affect coastal flood risk in the future (Dixon et al., 2006). Global coastal flood risk is also expected to increase in the future as a result of increasing exposure, due to growth in population and wealth, and economic activities in flood-prone areas (Güneralp et al., 2015; Jongman et al., 2012; Neumann et al., 2015; Pycroft et al., 2016).

Today, on average 10% of the world population and 13% of the total urban area in low elevation coastal zones is located less than 10 meters above sea level (McGranahan et al., 2007). In addition, 1.3% of global population is estimated to be exposed to a 1 in

100-year flood (Muis et al., 2016). In the coming century, these people and areas are projected to face increases in coastal flood risk (Brown et al., 2018; Hallegatte et al., 2013; Hinkel et al., 2014; Jongman et al., 2012; Merkens et al., 2018; Neumann et al., 2015).

To prevent this increase in coastal flood risk, or even to reduce risk below today's levels, adaptation measures are necessary. The importance of climate change adaptation and disaster risk reduction is recognized in several global agreements, such as the Paris Agreement (United Nations Framework Convention on Climate Change, 2015) and the Sendai Framework for Disaster Risk Reduction (United Nations Office for Disaster Risk Reduction, 2015). The Sendai Framework sets specific targets for reducing risk by 2030, such as reducing the direct disaster economic loss in relation to GDP and substantially reducing the number of affected people globally.

Recent studies have shown that adaptation measures hold a large potential for significantly reducing this future flood risk (Diaz, 2016; Hinkel et al., 2014; Lincke & Hinkel, 2018). However, the number of global scale studies in which the benefits and costs of disaster risk reduction and adaptation are explicitly and spatially accounted for remains limited. Existing studies have assessed the effect of climate change, subsidence and/or socioeconomic change (Hallegatte et al., 2013; Hinkel et al., 2014; Nicholls et al., 2008; Vousdoukas et al., 2018a), but have not included adaptation objectives or attributed flood risk drivers to adaptation costs. Lincke & Hinkel (2018) assessed the cost-effectiveness of structural protection measures against sea-level rise and population growth using the DIVA model. They found that structural adaptation measures are for 13% of the global coastline feasible to invest in. However, they did not include subsidence and attribution of drivers in their modelling scheme.

In this paper, we develop a model to evaluate the future benefits and costs of structural adaptation measures at the global scale. We use it to address the limitations of current studies addressed above, and thereby extend the current knowledge on the cost-effectiveness of structural adaptation measures in several ways. Firstly, we include human induced subsidence due to groundwater extraction. Secondly, we assess the benefits and costs of several adaptation objectives. Thirdly, we attribute the costs of adaptation to different drivers (namely sea-level rise, subsidence and change in exposure).

3.2 Methods

The overall methodological framework is summarized in Figure 3-1 and consists of the following main steps: (1) flood risk estimation; (2) adaptation costs estimation; (3) benefit-cost analysis for four adaptation objectives; and (4) attribution of the total costs to the different drivers. Each of these steps is described in detail in the following subsections. In brief, flood risk is estimated as a function of hazard, exposure and

vulnerability (United Nations Office for Disaster Risk Reduction, 2016). In the risk model, Expected Annual Damage (EAD) is calculated for different scenarios with and without adaptation, with the difference between these two representing the benefits. The costs are calculated by estimating the dimensions of the required dikes (height and length) and multiplying these by their unit costs. Maintenance costs are also included in the cost model. A benefit-cost analysis is performed for four adaptation objectives, and finally the costs of adaptation are attributed to several risk drivers. The methodological steps takes are explained in detail in Ward et al. (2019), on which the following descriptions are based.

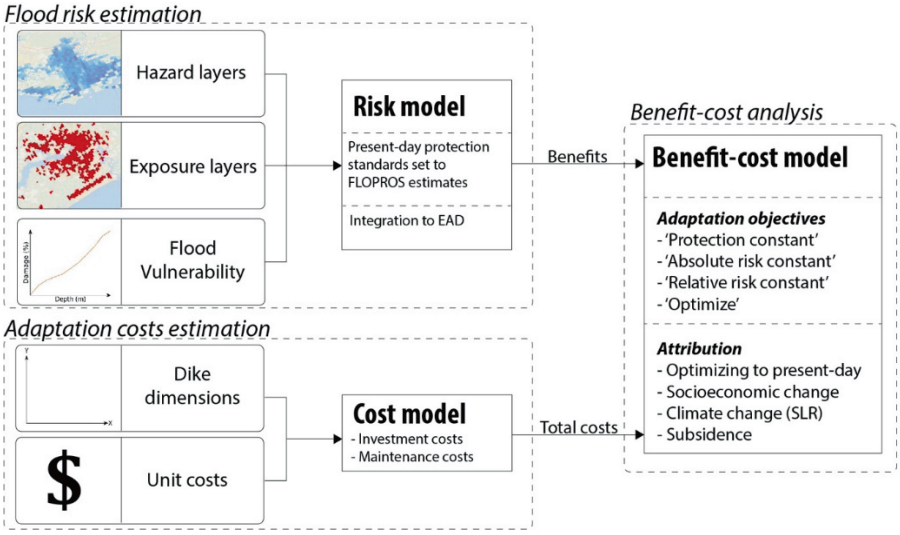

Figure 3-1: Overview of models and data layers for assessing flood risk, costs of adaptation and attribution of different drivers.

3.2.1 Flood risk estimation

We use hydrodynamic simulations of tide and surge, and scenarios of regional sea-level rise, as input to a coastal inundation model, to generate hazard maps for several return periods (2, 5, 10, 25, 50, 100, 250, 500 and 1000 years). These are combined with exposure maps and vulnerability curves (depth-damage functions) in the impact assessment model, using a setup similar to the GLOFRIS impacts module developed by Ward et al. (2013) and extended for future simulations by Winsemius et al. (2016). The global coastal flood impacts are assessed at a horizontal resolution of 30" × 30" and simulated for the different return periods. After calculating the impacts for the different return periods, EAD is calculated by taking the integral of the exceedance probability-impact curve (Meyer et al., 2009). Figure 3-2 shows the different input layers for the flood risk assessment and benefit-cost analyses (note that different sea-level rise and

socioeconomic scenarios are used, and just one is shown in Figure 3-2 as example). The following section describes the flood risk simulations in detail.

Flood hazard

Current flood hazard. In order to simulate coastal inundation hazard, we use extreme sea levels from the Global Tide and Surge Reanalysis (GTSR) dataset by Muis et al. (2016) as input to an inundation model. GTSR has been shown to perform well (Muis et al., 2017) for extratropical regions and contains a database of extreme water levels for different return periods, based on the Global Tide and Surge Model (GTSM). Surge is simulated using wind and pressure fields from the ERA-Interim reanalysis (Dee et al., 2011), and tide is simulated using the Finite Element Solution 2012 (FES2012) model (Carrère & Lyard, 2003). In this modelling scheme, wind (or surface) waves are not included. As tropical cyclones are poorly represented in the input climate dataset, we use a version of GTSR enriched using a historical storm track archive to represent tropical cyclones. These tropical cyclones were simulated using the IBTrACS (International Best Track Archive for Climate Stewardship) archive, which provides a dataset of historical best tracks. All tracks over the period 1979-2004 are used and converted into wind and pressure fields using the parametric Holland model (Delft3D-WES, 2019) in order to simulate alternative water levels using GTSM. These water levels are combined with the time series of GTSR by using the highest water level at each GTSM cell for each time step. Extreme values are estimated using a Gumbel extreme value distribution fit on the annual extremes.

To calculate overland inundation from near-shore tide and surge levels we used a GIS-based inundation routine, similar to Vafeidis et al. (2019). Extreme sea levels from the nearest GTSR location are projected at the coastline. Then, inundation takes place in areas that are hydrologically connected to the sea for that extreme sea level. The model uses the Multi-Error-Removed Improved-Terrain (MERIT) DEM (Yamazaki et al., 2017) at a 30" x 30" resolution as underlying topography. We accommodate three important factors in the inundation routine that are not regularly taken into account in global scale coastal inundation modelling:

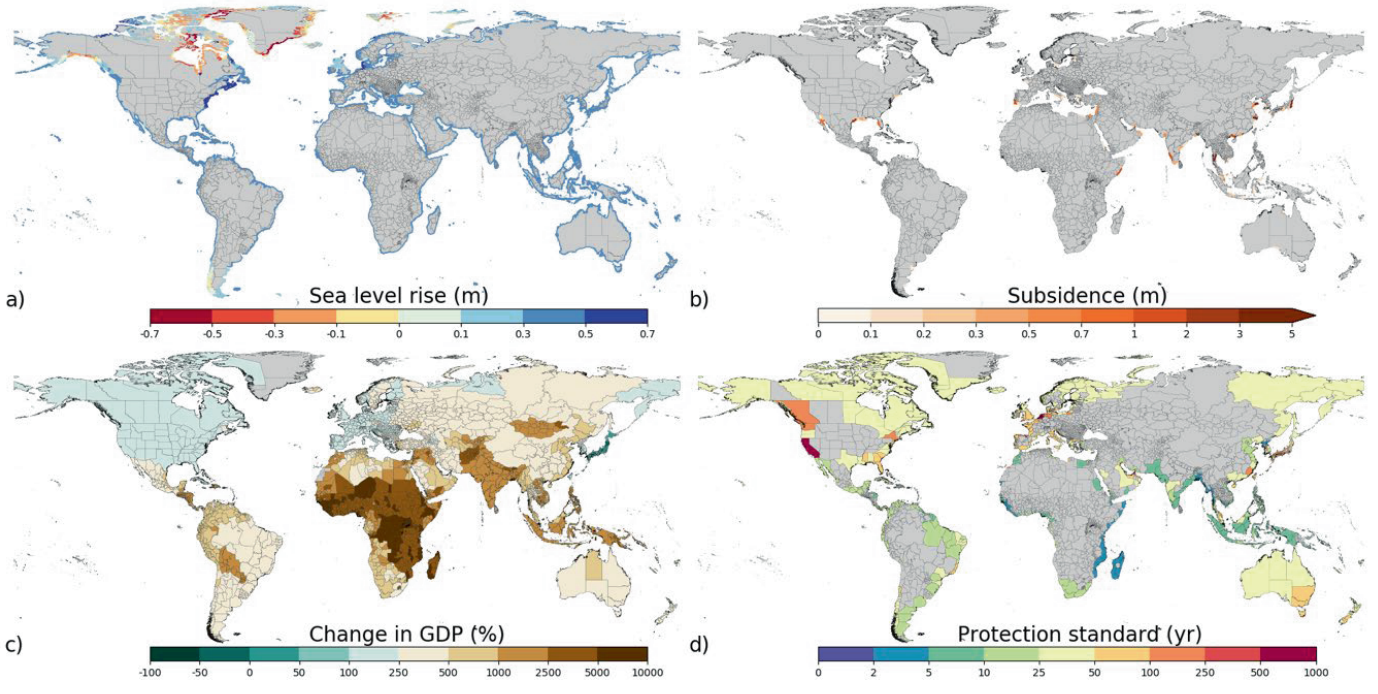

Figure 3-2: Input layers for the benefit-cost analyses: (a) sea level rise for the RCP4.5 scenario in 2080; (b) subsidence in 2080; (c) Change in GDP for the SSP2 scenario in 2080; and (d) current protection standards estimated with the FLOPROS modelling approach.

- We use a resistance factor to simulate the reduction of flooding land inwards as tides and storm surges have a limited time span. We apply this factor over a Euclidean distance from the nearest coastline point. The resistance factor was set to 0.5m/km. Haer et al. (2018) showed the maps to perform well against past flood events in their study in Mexico. Several other studies also use attenuation factors varying between 0.1 and 1.0 m/km (Vafeidis et al., 2019).
- We multiply the resistance factor by a weight, proportional to the amount of permanent water in each cell within the Euclidean pathway towards a land cell under consideration. In this way, grid cells that are marked as land within the terrain model, but in fact represent areas with large amounts of open water are correctly simulated as cells with low resistance. We estimate fractions of permanent water using a 30-year monthly surface water mask dataset at 30 meter resolution, derived from LandSAT archive (Pekel et al., 2016).
- We apply a spatially varying offset between Mean Sea Level according to the FES2012 model, and the datum used by the terrain model MERIT (EGM96) to ensure that the zero datum of our terrain and our extreme sea levels from GTSR are the same.

Future flood hazard. For future hazard simulations we use sea level changes, to simulate future extreme sea levels, and subsidence estimates due to groundwater extraction to estimate how the terrain may change. Global mean sea-level rise projections for RCP4.5 and RCP8.5 are obtained from the RISES-AM project (Jevrejeva et al., 2014). The sea-level rise for this study is simulated as a range of probabilistic outcomes. For this study, we use the 50^{th} percentile, and to assess the sensitivity of the results we also use the 5^{th} and 95^{th} percentiles as input for the inundation model. We use gridded datasets of regional sea-level rise estimates developed by Jackson and Jevrejeva (2016). These data were derived by combining spatial patterns of individual sea-level rise contributions in a probabilistic manner. We include sea-level rise in the inundation routine by adding this additional water level to the extreme sea level. Sea-level rise in 2080 for the RCP4.5 scenario and 50^{th} percentile is shown in Figure 3-2a. In this simulation, most of the regions will face a sea-level rise between the 0.3 and 0.5 meters. Close to the poles, sea level may decrease due to a decline in gravitational forces of the melting ice caps.

Subsidence rates are taken from the SUB-CR model by Kooi et al. (2018), which models subsidence using three existing models, namely the hydrological model PCR-GLOBWB integrated with the global MODFLOW groundwater model (de Graaf et al., 2017; Sutanudjaja et al., 2018), and a land subsidence model (Erkens & Sutanudjaja, 2015), focussing on groundwater levels and resulting subsidence. In this approach, subsidence is modelled due to groundwater extraction, which is the dominant factor of

human-induced subsidence in many coastal areas (Erkens et al., 2015; Galloway et al., 2016). The effects of subsidence, simulated at the resolution of 5' x 5' and spatially interpolated to 30" x 30" resolution, are included in the inundation model by adding the subsidence estimates to the MERIT terrain. Subsidence in 2080 is shown in Figure 3-2b and reaches up to 5-7m in regions in China. Unlike sea level rise, subsidence does not take place along every coastline and is instead projected as a regional phenomenon.

Flood exposure

In our modelling scheme, exposure is represented by maps of built-up area and estimates of maximum damage for three different land use classes in built-up areas. The GLOFRIS model uses current and future built-up area, current and future GDP, and maximum damages on the country level as input. The FLOPROS modelling approach (see section 2.1.5) has current data on built-up area, population, and GDP as input. In the following sections, we describe the exposure data for the current and future simulations.

Current exposure. Current built-up area with a resolution of 5' x 5' are taken from the HYDE database (Klein Goldewijk et al., 2010) and later regridded to the 30" x 30" resolution. Built-up area refers to all kinds of built-up areas and artificial surfaces. Current maximum economic damages are estimated using the methodology of Huizinga et al. (2017). They used a root function to link GDP per capita to construction costs for each country. To convert construction costs to maximum damages, several adjustments are carried out using the suggested factors by Huizinga et al. (2017) for the different occupancy types. Such factors include depreciation and undamageable parts of buildings As a proxy for an approximation of percentage area per occupancy type, we set the urban grid cells of the layers from the HYDE database to 75% residential, 15% commercial and 10% industrial, based on a study by (BPIE, 2011) and a comparison of European cities' share of occupancy type of the CORINE Land Cover data (EEA, 2016). Following Huizinga et al. (2017), the density of buildings per occupancy types are set to 20% for residential and 30% for commercial/industrial.

In order to normalize current risk we use GDP per capita taken from the Shared Socioeconomic Pathways (SSP) database of IIASA, distributed spatially according to the ORNL LandScan 2010 population count map (Bright et al., 2011). As the total population per country in this map is different to the 2010 population stated in the SSP database, we use a correction factor per country to adjust the population per cell.

Future exposure. Future simulations of built-up area are taken from Winsemius et al. (2016) at a resolution of 30" x 30". Using the method described by Jongman et al. (2012), these simulations were computed using changes in gridded population and urban population for different SSPs derived from the GISMO/IMAGE model (Bouwman et al., 2006). These simulations include five narrative descriptions of future

societal development associated with SSP1-5 (O'Neill et al., 2014). Such descriptions include sustainability associated with low challenges (SSP1), middle of the road associated with intermediate challenges (SSP2), regional rivalry associated with high challenges (SSP3), inequality associated with dominance of adaptation challenges (SSP4) and Fossil-fueled development where the mitigation challenges are dominating (SSP5) (O'Neill et al., 2017).

To estimate future maximum damages, we scale the current values with the GDP per capita per country from the SSP database. Boundaries of countries are derived from the Global Administrative areas dataset (GADM, 2012). In order to calculate future risk relative to GDP, future gridded GDP values are taken from Van Huijstee et al. (2018), which uses the national GDP per capita from the SSP database as input.

Flood vulnerability

Vulnerability to flood depth of urban areas is estimated by using different global flood depth-damage functions for each occupancy type and are taken from Huizinga et al. (2017). The resulting damages are represented as percentage of the maximum damage, reaching maximum damages at a water level depth of 6 meters.

Integration to EAD

With the urban damages, calculated for the different return periods, risk is computed and expressed in terms of expected annual damages (EAD). We use a commonly used method in risk assessment to calculate EAD by taking the integral of the exceedance probability-impact (risk) curve (Meyer et al., 2009) and can be written as

$$D = \int_{p=0}^{1} I_\theta(p)dp \tag{3-1}$$

where EAD is 'risk' per year, D is the urban damage (or impact), θ the vulnerability, and p denotes the annual probability of non-exceedance (protection standard divided into 1). To fit a protection standard of a coastal region in the risk computation, the risk curve is truncated at the exceedance probability of the protection standard (expressed as a return period). To estimate the definite integral, we use the trapezoidal approximation. As data on protection standards of coastal regions are not available for many regions, we estimate current protection standards for coastal regions using the FLOPROS modelling approach (Scussolini et al., 2016), as is described in the next section.

FLOPROS modelling approach

To assess the benefits and costs of adaptation objectives, information on current protection standards is needed. We use the FLOPROS modelling approach (Scussolini

et al., 2016) to estimate these protection standards using current exposure data and EAD data from the GLOFRIS model as input. Figure 3-2d shows the estimated FLOPROS flood protection standards for each coastal sub-national unit. Further information about the FLOPOS estimates together with a validation of the results can be found in the Appendix B.

Estimating the benefits of adaptation

To calculate the benefits of adaptation, EAD is calculated for every year of the lifetime of the dike for a certain return period and subtracted from the EAD for every year without adaptation. The lifetime of the dike is set to expire in 2100 and the building period is set to 20 years. During this period EAD is assumed to increase linearly. The results are summed to get the total benefits of adaptation.

3.2.2 Cost estimation

To estimate the costs associated with the different adaptation objectives, we use the same methodology as Ward et al. (2017), which calculates the costs of flood protection by summing the maintenance and investment costs over time for raising dikes to prevent flooding. The following section describes the calculation of costs of adaptation and the adaptation objectives in more detail.

To calculate the costs of adaptation, first dike heights need to be calculated. The current dike height calculations are taken from a recent study by van Zelst et al. (2019). Their methodology is to first derive coastal segments and perpendicular coast-normal transects (766,034 transects in total). For each transect, bed levels are constructed and subsequently, hydrodynamic conditions and wave attenuation are derived. Lastly, the resulting sea water levels are translated into dike heights. The coastlines are derived from OpenStreetMap (OSM) and moved 100 m land inwards to smoothen the coast lines and to position the lines at a likely place to establish a dike system. Transects are derived perpendicular to the coastlines for each 1' x 1'-cell that has a coastline segment. Each transect is described by its slope, ocean bathymetry, foreshore, elevation, and surge levels among other things. To capture most foreshores, the transects are stretched 4 km land inward and seaward. The main source of bed level data is the Earth Observation (USGS Landsat and Copernicus Sentinel 2) based high resolution intertidal elevation map (20 m horizontal and 30-50 cm vertical accuracy) of Calero et al. (2017). As this dataset does not contain data for all bed levels along the transects, the gaps are filled by ocean bathymetry data from GEBCO (30", 10 m vertically) and topography data from MERIT (3", 2 m vertically). The water levels are derived from the GTSR dataset (Muis et al., 2016) and corresponding wave conditions at different return periods from the ERA-Interim reanalysis (Dee et al., 2011). With a lookup-table, consisting of numerical modelling results, the wave attenuation over the foreshore is determined. Due to the unknown direction, incoming waves are assumed to run perpendicular to the coast. Finally, current dike heights in respect to the surge level are

calculated with the empirical EuroTop formulations (Pullen et al., 2007) and are based on a standard 1:3 dike profile without berms and with a maximum allowed overtopping discharge of 1 L/m²/s. This is representative for a low-cost dike. We exclude coastlines where there is no built-up area, or no inundation is simulated.

In order to calculate future dike heights, sea-level rise from the RISES-AM project (Jackson & Jevrejeva, 2016) is used in the calculation of the crest heights for different return periods. This is done by adding sea level rise directly to the crest height. Next to sea level rise, future dike heights are calculated with subsidence levels (see section 3.2.1.). Subsidence is assumed to take place directly on the dike and therefore computed on the crest height, which is similar for sea level rise calculations.

The costs of raising dikes are estimated by calculating the total length of dike heightening per grid cell and multiplying by a unit cost set to USD 7 million km·m based on reported costs in New Orleans (Bos, 2008). This value of US$ 7 million km·m is within a reasonable range when compared to various studies (JC Aerts et al., 2013; Jonkman et al., 2013; Stephan Lenk et al., 2017). This includes investment cost, groundwork-, construction- and engineering costs, property or land acquisition, environmental compensation, and project management. Subsequently, the costs are converted to US$2005 Power Purchasing Parity (PPP) using GDP deflators from the World Bank and average annual market exchange rates from the European Central Bank for each country. Construction index multipliers, based on civil engineering construction costs, adjust the construction costs to account for differences between countries (Ward et al., 2010). The lengths of the dikes are estimated using the 766,034 coastline transects. Maintenance costs are represented as percentages of investment costs and are set to 1% per year.

3.2.3 Benefit-cost analysis

Finally, a benefit-cost analysis is performed by calculating the benefits and costs for adaptation until 2100 for sub-national regions. These regions are defined as the next administrative unit below national scale in the Global Administrative Areas Database (GADM). The benefits and costs are discounted with a discount rate of 5% until 2100 (lifespan of investment) and with Operation and Maintenance (O&M) costs of 1%. It is assumed that investments are made in 2020 and construction is finished in 2050. During this time period, benefits and costs for investment are assumed to increase linearly. We use Net Present Value (NPV) shown in Eq. (3-2) and Benefit-Cost Ratios (BCR) shown in Eq. (3-3) as indicators of economic efficiency.

$$R_C^B = \left. \sum_{t=1}^{n} \frac{B_t}{(1+r)^t} \middle/ \left(\sum_{t=1}^{n} \frac{C_t}{(1+r)^t} \right) \right. \tag{3-2}$$

$$V = \sum_{t=1}^{n} \frac{B_t - C_t}{(1+r)^t} \tag{3-3}$$

where t denotes the time in years, n the lifespan of the investment, r the discount rate, B_t the benefits per year, C_t costs per year expressed as maintenance costs, and C_0 the initial investment costs.

The Benefit-cost analysis is carried out for two different sea-level rise scenarios (RCPs) and five different socioeconomic scenarios (SSPs). All the results are shown for two scenario combinations (van Vuuren et al., 2014), namely RCP4.5/SSP2 and RCP8.5/SSP5. The former is used for a 'middle of the road' scenario with medium challenges for mitigation and adaptation (Riahi et al., 2017) that can broadly be aligned with the Paris agreement targets (Tribett et al., 2017), while the latter is used as a 'fossil-fuel development' world (Kriegler et al., 2017).

Adaptation objectives

For the benefit-cost analysis, four future investment objectives are explored: (1) 'Protection constant', which keeps protection levels in the future the same as current protection levels; (2) 'Absolute risk constant', which calculates future protection standards when the absolute value for EAD is kept the same as current; (3) 'Relative risk constant', which calculates future protection standards when EAD as a percentage of GDP is kept the same as current; and (4) 'Optimize', which calculates future protection standards by maximizing NPV. The future protection standards for the four adaptation objectives are estimated at discrete intervals (2, 5, 10, 25, 50, 100, 250, 500 and 1000 years). The future protection standards when no adaptation takes place are calculated by assuming that dikes are maintained at the current height, but with no additional heightening. In the 'optimize' adaptation objective, only regions with BCR greater than 1 are included; no adaptation takes place for regions with BCR less than 1.

Attribution of costs

To attribute costs to different drivers, the following method is used. For the 'optimize' adaptation objective, the costs are attributed to four terms: (1) optimization under current conditions (CUR); (2) socioeconomic change (SEC); (3) sea level rise driven by climate change (SLR); and (4) subsidence driven by groundwater depletion (SUB). The following conceptual equations illustrate the attribution methodology:

$$A_{CUR} = NPV_{CUR}/NPV_{ALL} \tag{3-4}$$

$$A_{SEC} = (NPV_{SEC} - NPV_{CUR})/NPV_{ALL} \quad (3\text{-}5)$$

$$A_{SLR} = NPV_{SLR\ (baseline\ protection\ SEC)}/NPV_{ALL} \quad (3\text{-}6)$$

$$A_{SUB} = NPV_{SUB\ (baseline\ protection\ SEC)}/NPV_{ALL} \quad (3\text{-}7)$$

Equation (4-7) show the attribution calculation with A the attribution and NPV the net present value calculated with Eq. (3-4) The subscripts denote the attribution terms: CUR refers to optimizing in current conditions; SEC refers to socioeconomic change; SLR refers to sea-level rise; and SUB refers to subsidence. ALL refers to when all risk drivers are taken into account. In the subscript between brackets, the baseline protection standard used during the calculation of NPV is indicated. Because the 'optimize' adaptation objective is an optimization and not all regions have optimized their protection standards for the current climate, this last term must be accounted for. The optimization term is the costs of maximizing NPV with current conditions (NPV_{CUR}). Subsequently, the costs for socioeconomic change are computed by taking the difference in costs between NPV_{CUR} and maximizing NPV when only socioeconomic change is considered (NPV_{SEC}). To determine the attribution of costs for climate change, the baseline protection is set to the protection standards associated with the NPV_{SEC} term. Subsequently, the costs are estimated by maximizing NPV when both sea-level rise and socioeconomic change are considered (NPV_{SLR}). The attribution of subsidence is the same procedure as with NPV_{SLR}, by swapping the sea-level rise driver with the subsidence driver (NPV_{SUB}). All attributions of costs are expressed in percentages with reference to maximizing NPV for future conditions (NPV_{ALL}), which is the same as the 'optimize' adaptation objective.

In some cases, the percentages of the different drivers do not add up to 100%. This is the case when absolute dike heights associated with NPV_{SEC} are higher than NPV_{ALL} (in other words: adding climate change and subsidence would result in lower optimal dike heights in the benefit-cost analysis). In these cases, we set attribution for ATR_{SEC} to 100%, and ATR_{SLR} and ATR_{SUB} to 0%. Another exception is when optimal protection standards for NPV_{SEC} are higher than NPV_{SLR} or NPV_{SUB}. This occurs when the increase in absolute dike height in the optimization is lower than the effect of sea-level rise or subsidence, and results in a lower protection standard. For all other cases, except the two mentioned above, the sum adds to 100%.

3.3 Results and Discussion

In this section, we first present an assessment of current and future risk without adaptation. Next, we present global benefit-cost analyses for the different adaptation objectives. Then, we present the results of the benefit-cost analyses and the attribution of costs to different drivers at the regional scale. Finally, we assess the sensitivity of the results to changes in various parameters.

3.3.1 Overview of future flood risk assuming no adaptation.

Globally, the estimated EAD increases by a factor of 150 between 2010 and 2080, if we assume that no adaptation takes place in the middle of the road scenario RCP4.5/SSP2. Figure 3-3 shows the top 15 countries that contribute to this coastal flood risk, in 2010 (Figure 3-3a) and 2080 (Figure 3-3b) – note the different scales on the x-axis. China, Bangladesh, and India have the highest flood risk in absolute terms in 2010. In 2080, these three countries remain in the top four if no adaptation takes place and are joined by the Netherlands. The 15 countries shown account for 89% of coastal flood risk worldwide in 2010 (US$19.6 billion per year globally). Although the countries in the top 15 change between current and future assuming no adaptation, the total share of EAD residing in the top 15 countries remains approximately the same: 87% of global flood risk in 2080 if no adaptation takes place (US$3 trillion per year globally for RCP4.5/SSP2 and US$6.8 trillion for RCP8.5/SSP5).

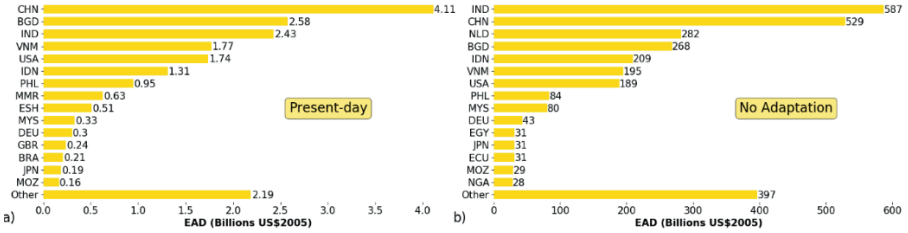

Figure 3-3: Top 15 countries with coastal flood risk in (a) current conditions; and (b) 2080 if no adaptation takes place for the scenario RCP4.5/SSP2. Note that the countries and value on the x-axis change for each graph. The countries are denoted by ISO 3166-1 alpha-3 codes.

3.3.2 Global scale assessment of flood risk under the different adaptation objectives.

For all four adaptation objectives, a globally aggregated overview of the benefits, costs, BCR, and NPV is provided in Table 3.1. All objectives have a positive NPV and BCR higher than 1, indicating that globally the benefits in terms of reduced risk would exceed the investment and maintenance costs. Note that only regions with positive NPV are included for the 'optimize' adaptation objective. The 'absolute risk constant' adaptation objective has the lowest BCR, while the 'optimize' adaptation objective has, by definition, the highest BCR. Higher costs and benefits are found for the RCP8.5/SSP5

scenario compared to the RCP4.5/SSP2 scenario, as a result of the larger EAD (and therefore avoided EAD) under this scenario. On average, the costs are ca. 25% larger in the former, and the benefits roughly double.

Table 3-1: Global overview of benefit-cost analysis for the different adaptation objectives (benefits, costs, and NPV are in billion US$2005).

		Benefits	Costs	BCR	NPV
Protection constant	RCP4.5–SSP2	9,706	359	27	9,347
	RCP8.5–SSP5	18,730	445	42	18,285
Absolute-risk constant	RCP4.5–SSP2	11,550	820	14	10,730
	RCP8.5–SSP5	23,020	999	23	22,021
Relative-risk constant	RCP4.5–SSP2	11,019	498	22	10,521
	RCP8.5–SSP5	22,095	606	36	21,489
Optimize	RCP4.5–SSP2	11,468	459	25	11,008

The top 15 countries that contribute the most to coastal flood risk for the four adaptation objectives for RCP4.5/SSP2 in 2080 are shows in Figure 3-4. The total share of EAD residing in the top 15 countries remains approximately the same: 94% of global flood risk in the 'protection constant' adaptation objective (US$ 767 billion per year globally); 93% in the 'absolute risk constant' adaptation objective (US$238 billion per year); 90% in the 'relative risk constant' adaptation objective (US$421 billion per year); and 91% in the 'optimize' adaptation objective (US$242 billion per year globally). Note that EAD can increase in the future for the 'absolute risk constant' adaptation objective in certain regions as we cap protection standards at 1000. The simulated optimal protection standards of the Netherlands are lower than in the 'protection constant' adaptation objective, resulting in a high future EAD of US$60.9 billion per year. This is because the simulated marginal costs of dike heightening up to a protection standard of 1000 years outweigh the marginal benefits. However, it should be noted that the benefits do exceed the costs up to a 1000-year protection standard, and that if this were implemented, the future EAD for the Netherlands in the 'optimize' adaptation objective would therefore be much lower than shown in Figure 3-4. Figure B-2 shows the top 15 countries for RCP8.5/SSP5.

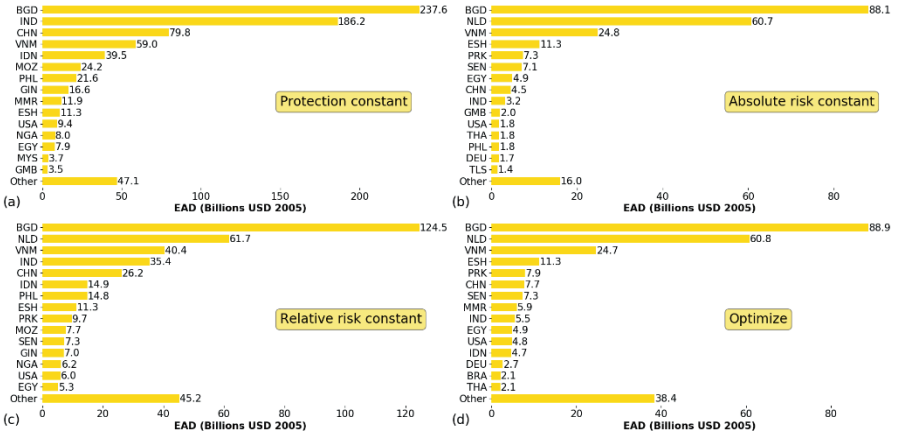

Figure 3-4: Top 15 countries with coastal flood risk in (a) 2080 if protection standards are kept constant; (b) 2080 if absolute risk is kept constant; (c) 2080 if relative risk is kept constant; and (d) 2080 if protection standards are optimized for the scenario RCP4.5/SSP2. Note that the countries and value on the x-axis change for each graph. The countries are denoted by ISO 3166-1 alpha-3 codes.

3.3.3 Regional scale assessment of flood risk under the different adaptation objectives.

To show spatial patterns of the four adaptation objectives, the following results are shown at the sub-national scale in Figures 5-8. Here, results are shown for RCP4.5/SSP2 only. The same results for RCP8.5/SSP5 can be found in Figures B-2 - B-5, and the data for all scenario combinations can be found in Supplementary Data. Although there are some differences between the results for RCP4.5/SSP2 and RCP8.5/SSP5, the overall patterns are very similar.

In the **'protection constant'** adaptation objective, the benefits outweigh the costs for the majority of the regions (78%; 612 of the 784 sub-national regions assessed). Nevertheless, this would still lead to an increase in relative risk (i.e., EAD as a percentage of GDP) in the future for 82% (641) of the regions assessed. Therefore, only raising dikes to keep up with the current protection standard would lead to a substantial increase in future risk in the majority of the world's regions for scenario RCP4.5/SSP2. Sub-national regions in southern Asia, southeastern Asia, eastern Australia, the east and west coast of North America, and parts of Europe have the highest BCR and NPV (Figure 3-5). Note that the protection standards (Figure 3-5a) are the same as the current protection standards (Figure 3-2d).

In the **'absolute risk constant'** adaptation objective (Figure 3-6), dikes would need to be upgraded to have high protection standards (usually between 100 and 1000 years) to keep risk constant at current levels. The costs to achieve this are high (globally, more than twice as high as under the 'protection constant' adaptation objective) and therefore

a lower number of sub-national regions (71%; 557) have a positive BCR, although this is still very high. In most sub-national regions, the risk relative to GDP decreases in the future if this adaptation objective is implemented, although 5% (38) of the sub-national regions show an increase in risk relative to GDP.

In the **'relative risk constant'** adaptation objective (Figure 3-7), the protection standards required are generally lower than in the 'absolute risk constant' adaptation objective. The highest protection standards required are found in eastern Asia and parts of North America. A similar number of sub-national regions have a BCR higher than 1 as is the case for 'absolute risk constant', namely 71% of the sub-national regions assessed. To keep relative risk constant or absolute risk constant some sub-national regions need to have a future protection standard that is higher than 1000-year (the highest return period assessed in this study). Because of this, the relative change in risk in the 'Relative risk constant' adaptation objective increases for 5% (36) of the regions assessed.

In the **'optimize'** adaptation objective (Figure 3-8), the highest optimal protection standards are generally found in eastern Asia, southeastern Asia, southern Asia, and the Gulf coast of the USA. High protection standards are also found in parts of Europe and other parts of the USA, parts of western and eastern Africa, some parts of South America, and southeastern Australia. The highest change in protection standards compared to current are found in southern Asia and southeastern Asia. In most sub-national regions, the benefits exceed the costs when upgrading protection standards (78%). However, in some sub-national regions the BCR is less than 1 (indicated with hatched lines). The highest values of NPV (Figure 3-8c) are found in parts of southern and southeastern Asia, North America, and northwest Europe. While most sub-national regions show a positive return on investment, there is still an increase in relative risk in 36% of the sub-national regions assessed, under the 'optimize' adaptation objective. In these cases, it is economically efficient to implement protection measures up to a certain level, yet the economic costs of keeping EAD as a percentage of GDP constant would exceed the avoided damages. Regions where this is especially the case include: Europe, North America, South America, Japan, and Australia, as shown in Figure 3-8d.

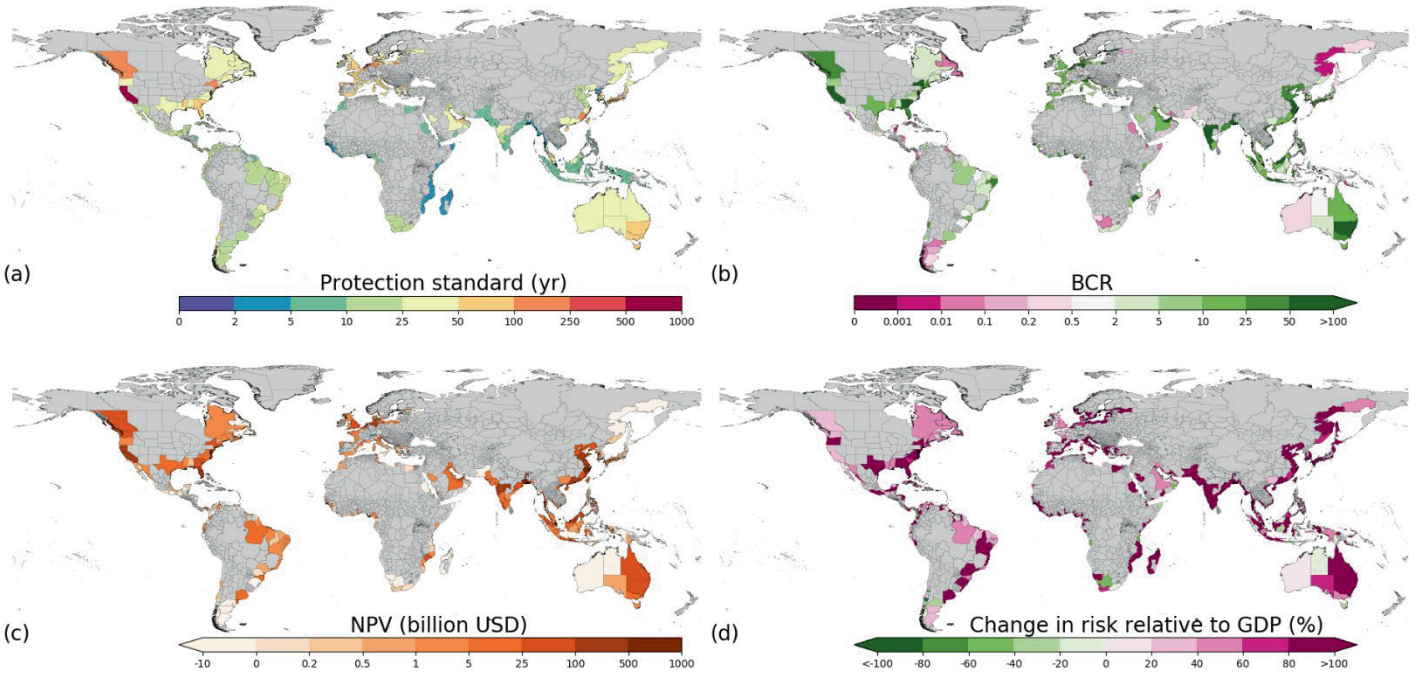

Figure 3-5: 'Protection constant' adaptation objective results of (a) protection standards; (b) BCRs; (c) total NPV; and (d) change in risk relative to GDP for RCP4.5/SSP2. Note that the protection standards (a) are the same as FLOPROS estimates. Regions with no data are indicated with grey colour.

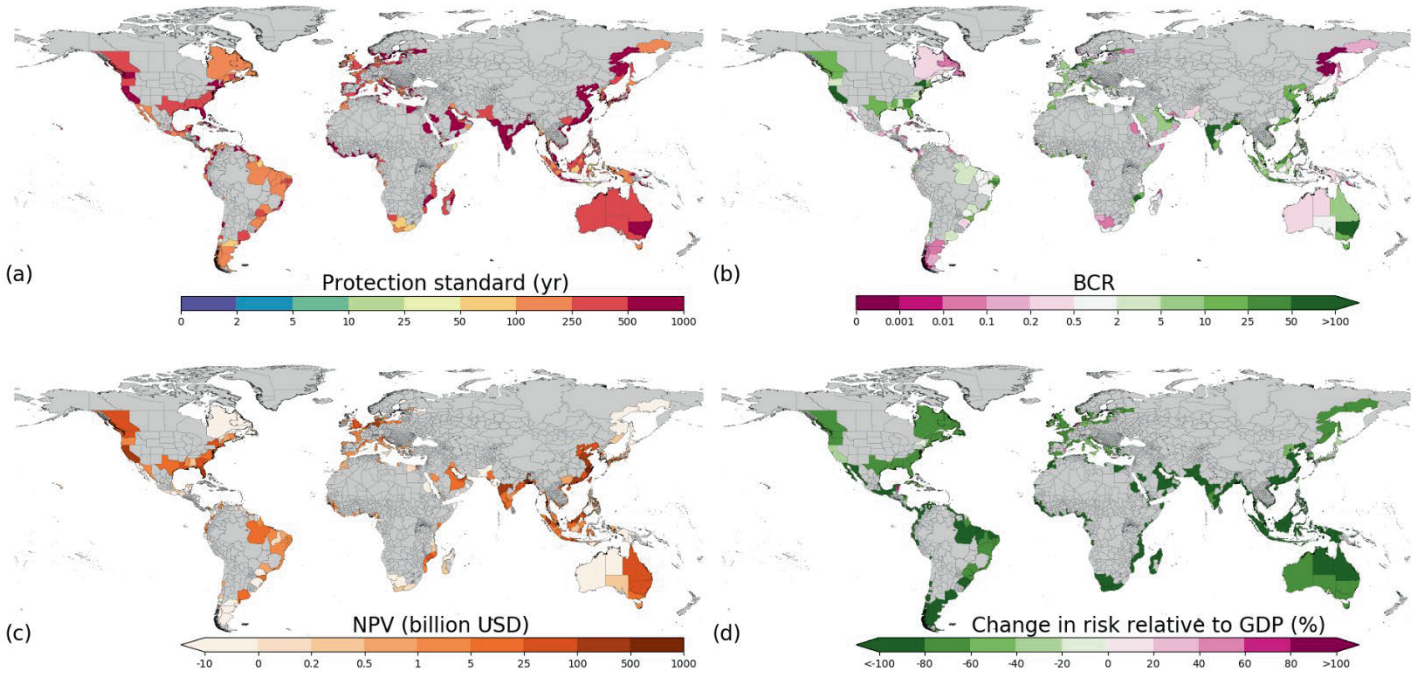

Figure 3-6: 'Absolute risk constant' adaptation objective results of (a) protection standards; (b) BCRs; (c) total NPV; and (d) change in risk relative to GDP for RCP4.5/SSP2. Regions with no data are indicated with grey colour.

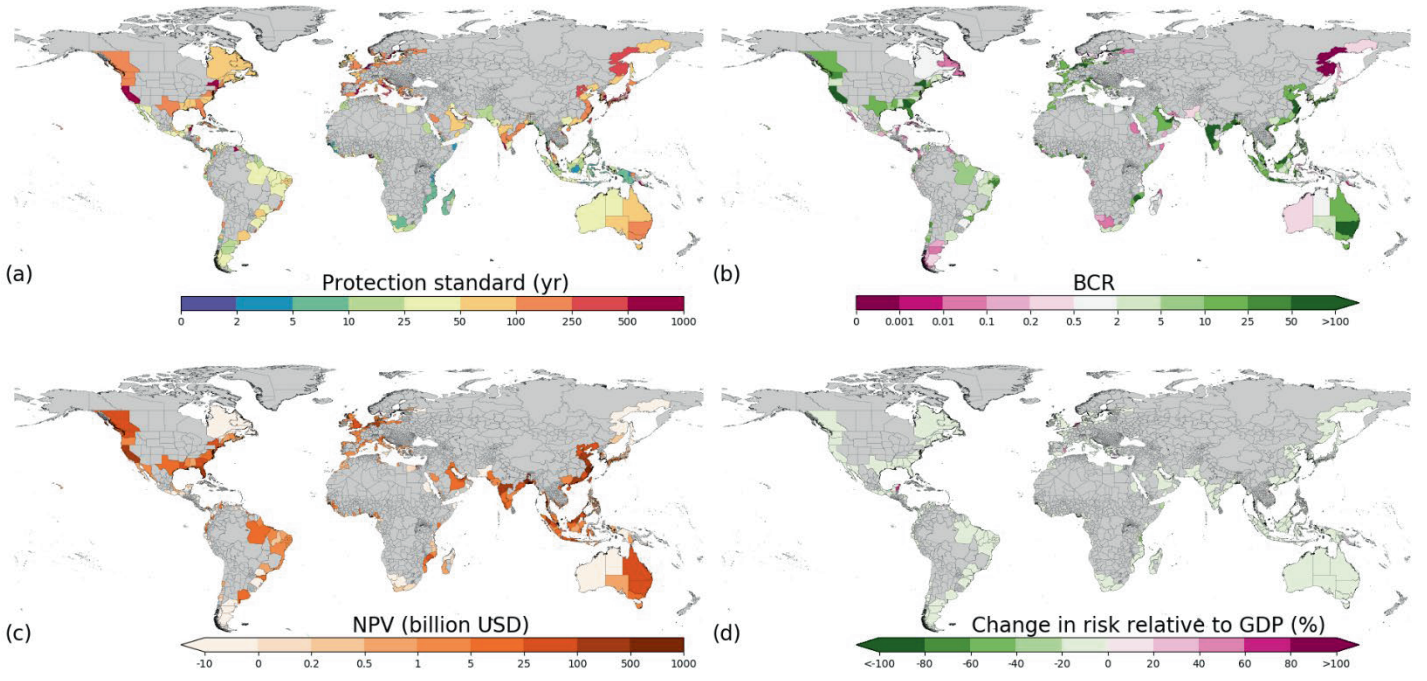

Figure 3-7: 'Relative risk constant' adaptation objective results of (a) protection standards; (b) BCRs; (c) total NPV; and (d) change in risk relative to GDP for RCP4.5/SSP2. Regions with no data are indicated with grey colour.

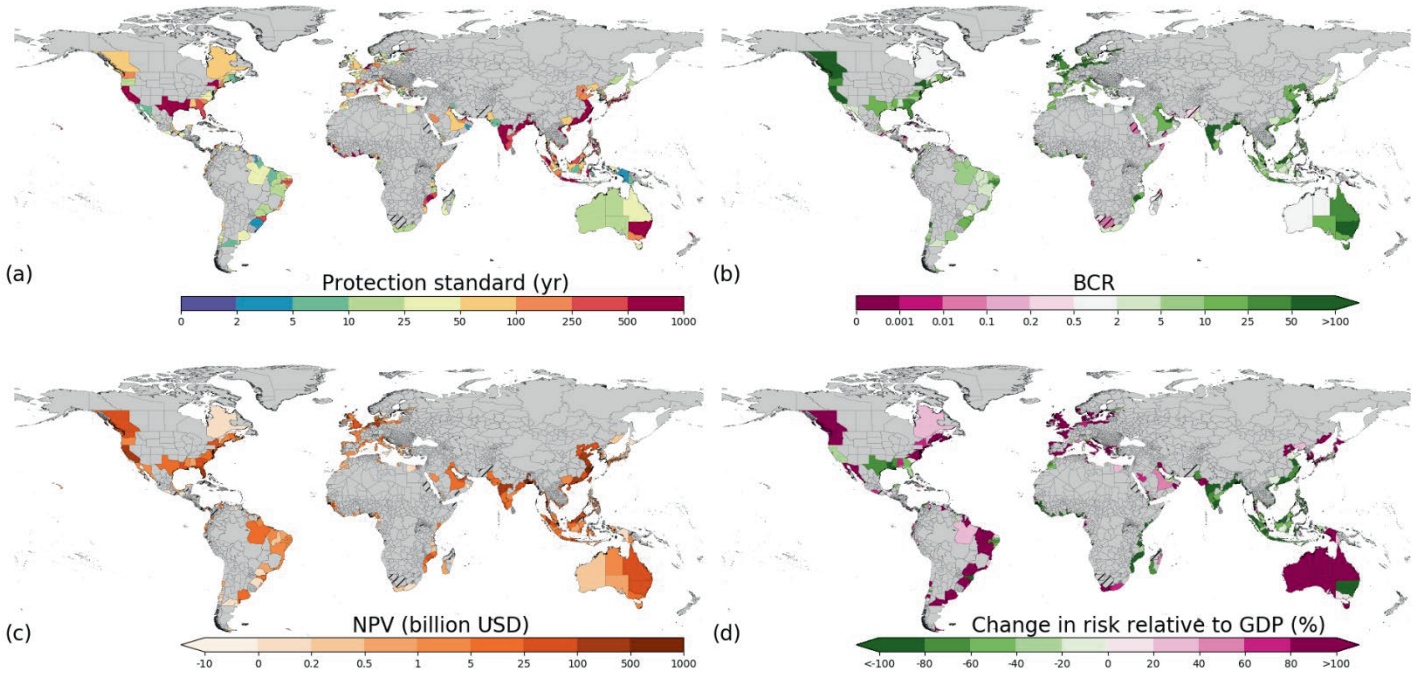

Figure 3-8: 'Optimize' adaptation objective results of (a) optimal protection standards; (b) BCRs; (c) total NPV; and (d) change in risk relative to GDP for RCP4.5/SSP2. Regions where no optimal protection standards are found are indicated with hatched lines and regions with no data are indicated with grey colour.

Many sub-national regions with decreases in relative risk can be found in southern Asia, southeastern Asia, parts of the Gulf coast of the USA, New South Wales in Australia, several sub-national regions in Africa, and some parts of South America, among others. In these regions, the increase in risk is generally very high, which means that the costs of investment in protection are lower than the avoided damages relative to GDP. Generally, in these regions, protection standards and/or absolute dike heights increase the most.

In the middle of the road scenario of RCP4.5/SSP2, where the world will face intermediate adaptation and mitigation challenges, we see that most of the sub-national regions assessed would economically benefit from adaptation. We further see that the adaptation objectives differ in changes in relative risk and the level of adaptation that would take place. For instance, in the 'protection constant' adaptation objective we see that although the protection standards stay the same, the relative risk increases for most sub-national regions. This can be explained by the increase of the severity and frequency of the flood hazard due to sea-level rise and subsidence, and the increase of exposure of assets due to socioeconomic change. Compared to the 'optimize' adaptation objective, the 'protection constant' adaptation objective under-protects in most sub-national regions. In the 'absolute risk constant' adaptation objective we see that relative risk decreases in most sub-national regions while protection standards increase greatly. Due to climate change, socioeconomic change, and subsidence, we see an increase in GDP exposed to flooding. Therefore, protection standards must increase vastly to meet the same level of absolute risk. In this adaptation objective, most sub-national regions are over-protected compared to the 'optimize' adaptation objective. In the 'relative risk constant' adaptation objective, we see that some sub-national regions are over-protected while other sub-national regions, for instance in southeastern Asia are under-protected. The 'optimize' adaptation objective shows the most economically feasible results in terms of maximizing NPV and has the highest BCR in most regions. In the 'fossil-fuel development' scenario of RCP8.5/SSP5, where mitigation will face high and adaptation low challenges (van Vuuren et al., 2014), we see that higher protection standards are required in order to keep risk constant and to maximize NPV (see Figures B-3 – B-6). The results of the adaptation objectives can be used as a first proxy to indicate in which sub-national regions adaptation through structural measures may be economically feasible. Moreover, the results indicate regions where adaptation is needed to maximize NPV and which objectives are under or over protecting sub-national regions compared to the 'optimize' adaptation objectives. Due to the scope of this study, local scale models and assessments should be used for the design and implementation of individual adaptation measures.

3.3.4 Attribution of costs to different drivers of risk

In Figure 3-9, we show the percentage of the total costs of the 'optimize' adaptation objective (Figure 3-9a) that can be attributed to each of the following risk drivers: climate change (in this case sea-level rise) (Figure 3-9b); optimizing current protection standards (Figure 3-9c); socioeconomic change (Figure 3-9d); and subsidence (Figure 3-9e). The results are shown for the RCP4.5/SSP2 scenario and only for sub-national regions that have a BCR higher than 1 in the 'optimize' adaptation objective.

The total costs exceed US$1 billion for 10% of the sub-national regions assessed and exceed US$1 million for 63%. For most parts of the globe, climate change (in this case sea level rise) contributes the most to the costs of adaptation, exceeding 50% of the total costs in 98% of the sub-national regions (Figure 3-9a), and exceeding 90% of the total costs in 58% of the sub-national regions. However, the other drivers can also play an important role, but are dwarfed in absolute terms by the costs related to sea-level rise. For example, in southern Asia, southeastern Asia, and eastern Africa optimizing to current conditions and socioeconomic change are important drivers and, in some cases, the most important driver. There are some other regional exceptions where climate change is not the most dominant driver of adaptation costs. Moreover, locally land subsidence due to groundwater extraction can cause huge flood problems and bring large costs in some areas (Dixon et al., 2006; Yin et al., 2013), but are not seen when aggregated to the sub-national regions of this study. However, there are a few regions where subsidence is a more dominant driver (i.e., parts of India, China, Japan, and Taiwan). The results show that climate change is not the most dominant driver in 4 of the 5 countries that have the highest share of future EAD if no adaptation takes place (i.e., China, Bangladesh, India, and Indonesia). Generally, the same patterns are found in the attribution results for the RCP8.5/SSP5 scenario, which can be found in the Figure A-7.

Figure 3-10 shows the attribution of the costs for the same scenario and adaptation objective, aggregated to the World Bank regions. In all the regions (except southern Asia), sea-level rise is the most dominant driver, accounting for between 26% (southern Asia) and 86% (Latin America and Caribbean) of the costs of adaptation. The costs of increasing dike height to achieve optimal protection under current conditions are highest in the Low- and Middle-Income Countries. This is especially the case for the Northern America and Pacific and Southern Asia regions, with values of 17% and 12% respectively. The relative contribution of socioeconomic change is largest in eastern Asia & Pacific, southern Asia, and Sub-Saharan Africa, with values of 34%, 49% and 24% respectively. Of all drivers, subsidence is the least dominant with values up to 11% (eastern Asia & Pacific) and 14% (southern Asia). Figure A-8 shows the attribution aggregated to the World Bank regions for RCP8.5/SSP5.

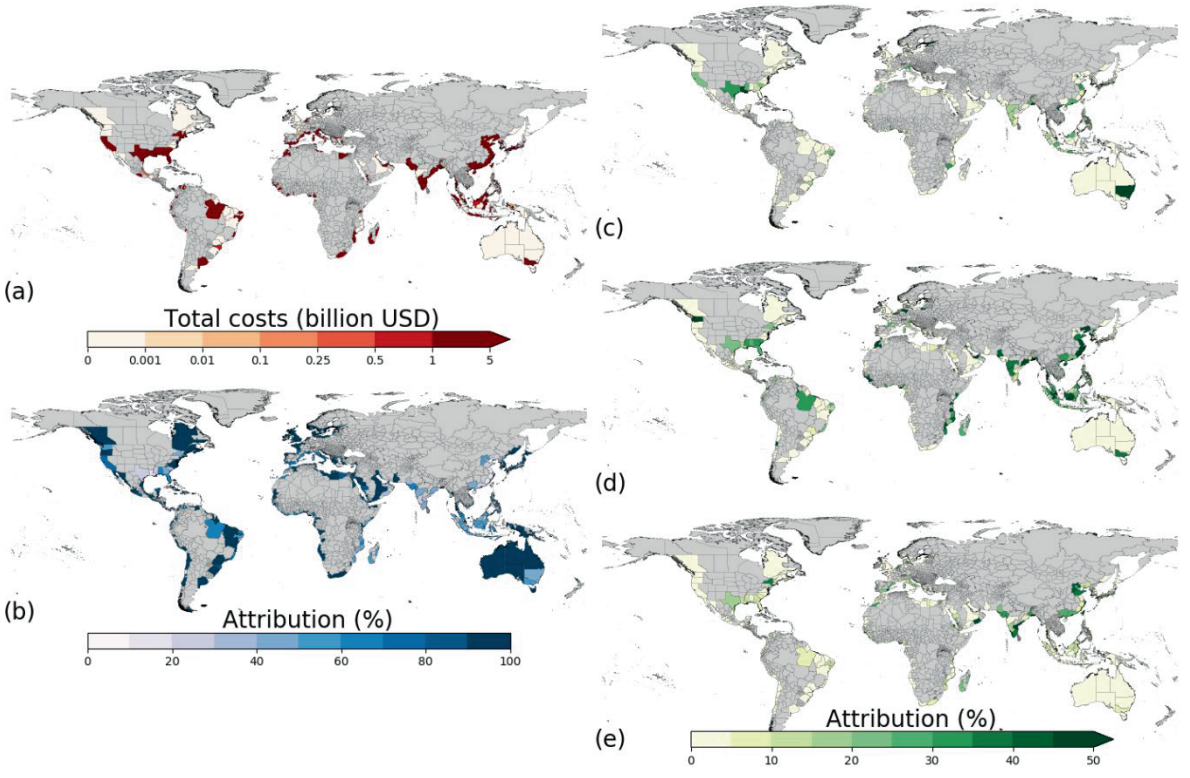

Figure 3-9: Attribution of costs overview for RCP4.5/SSP2 with (a) total costs; (b) attribution of sea-level rise ($\boldsymbol{ATR_{SLR}}$); (c) attribution of current optimizing ($\boldsymbol{ATR_{CUR}}$); (d) attribution of socioeconomic change ($\boldsymbol{ATR_{SEC}}$); and (e) subsidence ($\boldsymbol{ATR_{SUB}}$). Note that the attribution of SLR is on a different scale and regions with no data are indicated with grey colour.

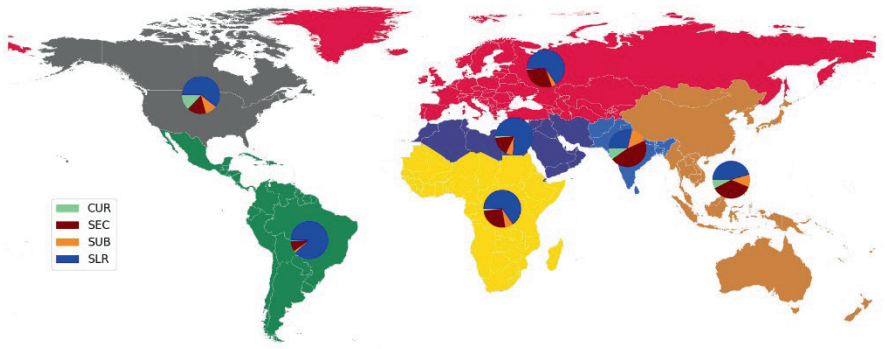

Figure 3-10: Attribution of costs of adaptation for World Bank regions under the 'optimize' adaptation objective and RCP4.5/SSP2 for optimizing to current conditions (CUR), socio-economic change (SEC) subsidence (SUB), and sea-level rise (SLR).

3.3.5 Sensitivity analysis

In this section, we show the sensitivity of the results to the use of different: SSPs, sea-level rise projections, discount rates, and operation and maintenance (O&M) costs. In Table 3-2, we show results (of BCR) standardized to a baseline scenario with the following assumptions: RCP4.5, SSP2 (middle of the road), discount rate of 5%, and O&M of 1%. We employed a one-at-a-time sensitivity analysis, so for each row in the table only one parameter has changed, and the values shown are standardized by calculating the relative change. All associated BCRs for the standardized values shown in Table 3-2 are still higher than 1. Globally, BCRs range between 6 and 116 for the different model runs (25 for the reference). At the global scale the BCRs are most sensitive to the use of the different SSPs and discount rates. They cause the largest changes in BCR, with standardized values of 0.45 and 2.13 found in southern Asia and Sub-Saharan Africa. Differences in SLR input affect the BCR by a factor of up to 0.35. Europe & Central Asia and North America are the least sensitive to the changes in input parameters. The O&M costs show BCRs that are more in line with the reference model run, higher or lower values up to 0.16.

Table 3-2: Sensitivity analysis of model runs with different input parameters. BCRs are standardized to the model run with RCP4.5/SSP2, discount rate of 5%, and O&M costs of 1%. SLR low refers to sea-level rise using the 5th percentile and SLR high to the 95th percentile.

	Eastern Asia and Pacific	Europe and central Asia	Latin America and Caribbean	Middle East and northern Africa	North America	Southern Asia	Sub-Saharan Africa	Global
Reference BCR	23	116	6	34	32	28	8	25
Sensitivity to SSP projection								
SSP1	1.32	1.01	1.17	1.06	0.95	1.51	1.61	1.28
SSP3	0.74	0.82	0.76	0.82	0.87	0.50	0.45	0.70
SSP4	1.11	0.97	0.94	0.88	1.02	0.95	0.47	1.02
SSP5	1.68	0.97	1.44	1.17	1.16	2.00	2.13	1.62
Sensitivity to SLR projection								
SLR low	1.07	1.08	1.17	1.19	1.17	1.02	1.16	1.09
SLR high	0.97	0.65	0.80	0.70	0.86	0.94	0.89	0.89
Sensitivity to discount rate								
r 3 %	1.53	1.06	1.48	1.30	1.35	1.69	1.72	1.51
r 8 %	0.68	0.72	0.62	0.74	0.77	0.54	0.49	0.65
Sensitivity to O&M rate								
O&M 0.1 %	1.16	1.12	1.12	1.08	1.13	1.13	1.14	1.14
O&M 2 %	0.88	0.88	0.86	0.88	0.93	0.88	0.87	0.88

3.3.6 Comparison to previous studies

Hallegatte et al. (2013) performed a study on future flood risk for 136 major coastal cities. They estimated an EAD of US$6 billion for current conditions, while in our study we find an EAD of US$19.6 billion. Our estimates of EAD is higher, which is to be expected given the difference in extent of the studies where we estimate risk for all global coastlines as opposed to 136 major coastal cities in their study. Hallegatte et al. (2013) projected future risk increasing up to US$60-63 billion if protection standards are kept constant by 2050. In our study we find an EAD of US$84 billion by 2050 when keeping protection standards constant (RCP4.5/SSP2 scenario). If no adaptation is implemented in 2050, Hallegatte et al. (2013) estimate EAD over US$1 trillion, where we find US$1.1 trillion.

Hinkel et al. (2010) attributed adaptation costs to sea-level rise using dikes for the European Union. They estimated this to be between US$2.6-3.5 billion. In our results we find values between US$10.1 billion and US$16.5 billion for the European Union for the scenarios RCP4.5 and RCP8.5 respectively. In a follow-up study, Hinkel et al. (2014) estimate global costs of protecting the coast with dikes. They estimate a range of US$12-71 billion, while our study estimates the global costs of adaptation for the 'optimize' adaptation objective between US$459 billion and US$603 billion for the RCP4.5/SSP2 and RCP8.5/SSP5 respectively. It should be noted that Hinkel et al. (2010) and Hinkel et al. (2014) use a demand function for safety where dikes are raised following relative sea-level rise and socioeconomic development, while we don't use that function and optimize protection standards by maximizing NPV. This adaptation

objective allows dynamic optimization per sub-national region and can result in higher adaptation costs if the net benefits increase. Additionally, we use different scenarios than those used in Hinkel et al. (2010) and Hinkel et al. (2014).

Lastly, we compare our results of economic feasibility for sub-national regions and coastlines to the findings of Lincke & Hinkel (2018), in which they found that it is economically feasible to invest in protection for 13% of the coast globally. Using their method they found a lower share of protected coastline compared to previous studies (Nicholls et al., 2008; Tol, 2002). In our study, we found that for the 'optimize' adaptation objective that 78% of the sub-national regions have a BCR higher than 1, indicating that it is economically feasible to implement adaptation in many regions through raising dikes. In our study, the benefit-cost analysis is carried out at the sub-national scale, whereby dikes are only raised on coastal reaches where our transects show there to be potential hazard (inundation) and urban exposure. If we calculate the percentage of the entire global coastline for which this leads to dike heightening in our model with a BCR higher than 1, it amounts to 3.3% of the global coastline. This is lower than the value in Lincke & Hinkel (2018), but we reason that this difference is a result of the difference in spatial aggregation, where the distance between our transects is 1 kilometre horizontal resolution at the equator, whilst Lincke & Hinkel (2018) raise dikes along the coast of entire coastal segments, which have lengths ranging from 0.009 to 5213 kilometre, with a mean of 85 kilometre. This can explain why we have lower percentage of coast that is feasible to protect than Lincke & Hinkel (2018).

3.3.7 Limitations and future research

While our model scheme does not include dynamic inundation modelling, it does include resistance factors similar to those used by Vafeidis et al. (2019), in order to account for water-level attenuation. It therefore represents an advance on previous studies that have used planar inundation modelling methods (i.e., bathtub models). An improvement could be made by using a dynamic inundation modelling scheme (Vousdoukas et al., 2016a), but at the cost of increased computing time. Another improvement can be made by including waves in our inundation modelling, which is found to be an important component in inundation modelling (Vousdoukas et al., 2017). The inundation modelling scheme can be further improved by increasing the resolution from 30" to a higher resolution in order to better understand local scale signals and patterns, since the scale of assessment and resolution of input data has a significant implication on flood risk model results (Wolff et al., 2016). However, we stress that this study aims to understand global flood risk and general patterns on the sub-national scale, and this study can be used as a first proxy indicating feasibility of adaptation through structural measures, such as dikes.

For this study, results are shown for the scenario RCP4.5/SSP2 and RCP8.5/SSP5 in Appendix B. The range of sea-level rise input values (between the 5th percentile of

RCP4.5 and the 95th percentile of RCP8.5) cover a wide range of sea-level rise uncertainty (approximately 0.3 – 0.7m at the equator in the Atlantic Ocean). While in reality the effects of climate change will continue to rise beyond 2100 even if Paris Agreement is met (Clark et al., 2016), our study examines adaptation objectives until 2100. Results for all combinations of these two RCPs together with all five SSPs can be found in the supplementary data.

Several uncertainties exist on the cost calculation side. The first is the monetary value we assumed for the costs of dike heightening. Although we account for differences in costs between countries by using different construction factors and market exchange rates, in reality the costs might differ between regions and may be higher due to local conditions (both physical and socioeconomic). We also use a linear cost function for dike heightening. Using this linear cost function for large scale studies has been found a reasonable assumption according to (Stephan Lenk et al., 2017).

Another important uncertainty in this study is the current protection standards estimated with the FLOPROS modelling approach, as data on flood protection along the global coastlines are not available. These only provide a first order estimate of current protection standards per sub-national region. In the Figure B-1, a validation of the coastal protection standards estimated with the FLOPROS modelling approach is provided. Values are shown for several locations for which reliable reported estimates of protection standards are available. These reported values are either shown as a range (minimum and maximum reported values) or a single value. Overall, the model performs well. The only location for which the reported values provide a range, and the FLOPROS model lies outside this range, is Durban. However, note that reported values are for the city of Durban, whilst the FLOPROS model value is for the state in which it is located. An improvement to this study could be made by, for instance, mapping flood protections globally by using Earth Observation-based methods.

In this study, several uncertainties exist with assumptions on expected damages per occupancy type. First, we assumed the percentage of occupancy type per grid cell to be the same for all locations, whilst it is spatially heterogeneous, and secondly, we assumed the building density per occupancy type. An improvement could be made by using Machine Learning to improve accuracy of urban land cover and building types (Hecht et al., 2015; Huang et al., 2018). We also used depth-damage curves per occupancy type, but these curves also differ between buildings in these occupancy types. To further improve the exposure data of our framework, the Global Human Settlement layer (Pesaresi et al., 2016) can be used for high-resolution population mapping.

The sub-national regions where no adaptation objective shows a positive BCR, should not be interpreted that no adaptation to coastal flood risk should take place. In fact, other adaptation measures (or a combination of multiple measures) besides raising

dikes might be more economically feasible in any regions studied, including those with BCRs higher than 1. In this study we only assumed grey infrastructure as adaptation measures, but there are also other measures to reduce flood risk. For instance, the vulnerability can be improved by wet or dry proofing buildings (J. C. J. H. Aerts et al., 2014) or people and assets can be moved to less flood prone areas in order to reduce the exposure to floods (R. McLeman & Smit, 2006). Lastly, several local studies show the benefits of nature-based or hybrid adaptation measures (Cheong et al., 2013; Jongman, 2018; Temmerman et al., 2013). Vegetation on the foreshore has a significant role in the breaking of waves (Shepard et al., 2011) and attenuates storm water levels (Zhang et al., 2012). An improvement could be made by including other adaptation measures besides grey infrastructure as adaptation measures.

3.4 Conclusion

In this study, four adaptation objectives for reducing (future) coastal flood risk through structural measures have been explored and a benefit-cost analysis has been performed on the sub-national scale for the entire globe. Furthermore, the costs of adaptation have been attributed to different drivers of flood risk: sea-level rise, socio-economic change, subsidence, and optimizing to current conditions. Globally, we find that EAD increases by a factor of 150 between 2010 and 2080, if we assume that no adaptation takes place, and find that 15 countries account for approximately 90% of this increase.

We find that all four adaptation objectives show high potential to reduce (future) coastal flood risk at the global scale in a cost-effective manner. The 'optimize' adaptation objective shows the highest NPV (more than US$11 trillion) with a BCR of 25, while the 'protection constant' adaptation objective shows the lowest NPV (US$9.3 trillion) with a BCR of 27 for the RCP4.5/SSP2 scenario.

At the regional scale, we show that the adaptation objectives can be achieved with a BCR more than 1 for most of the sub-national regions. This ranges from 78% for the 'optimize' adaptation objective to 71% for the 'absolute risk constant' adaptation objective. However, we also show that under the 'optimize' adaptation objective, relative risk would still increase compared to current values in 36% of the sub-national regions assessed.

We assess the sensitivity of the results by performing a one-at-a-time sensitivity analysis to various assumptions and find that, given the uncertainties, implementing structural adaptation measures is a feasible solution to reduce (future) coastal flood risk. Although differences in BCR exist, we show that changes in parameters still result in positive BCRs (between 6 and 116 globally) for the 'optimize' adaptation objective.

Attributing the total costs for the 'optimize' adaptation objective, we find that sea-level rise contributes the most and exceeds 50% of the total costs in 98% of the sub-national

regions assessed and exceeds 90% of the total costs in 63% of the sub-national regions. However, the other drivers also play an important role, but are dwarfed in absolute terms by the total costs related to the attribution.

The results of this study can be used to highlight potential savings through adaptation at the sub-national scale. Clearly, local scale models and assessments should be used for the design and implementation of individual adaptation measures, but our results can be used as a first proxy indicating regions where adaptation through structural measures may be economically feasible. To increase the accessibility of the results to the risk community, results of this study will be integrated into the Aqueduct Global Flood Analyzer webtool (www.wri.org/floods).

Supplementary data availability.

The results of this study for all RCP and SSP combinations for protection standards, change in risk relative to GDP, B:C ratio and NPV for all four adaptation objectives are available at: https://doi.org/10.5281/zenodo.3475120.

Acknowledgement.

The research leading to these results received funding from: The Netherlands Organisation for Scientific Research (NWO) in the form of a VIDI grant (grant no. 016.161.324); the Aqueduct Global Flood Analyzer project, via subsidy 5000002722 from the Netherlands Ministry of Infrastructure and Water Management - the latter project is convened by the World Resources Institute; the Future Water Challenges 2 project, funded by the Netherlands Ministry of infrastructure and Water Management; and La Fondation d'Enterprise SCOR pour la science under the project COASTRISK.

Author contributions

TT, PJW, HdM, and HCW conceived the study. All co-authors contributed to the development and design of the methodology. HCW and DE provided coastal inundation layers, and GE provided subsidence rates. AB, JvH, and WL provided data on urban land use and GDP projections. TT analysed the data, with contributions from PJW, HdM, HCW, EG, ADL, SK, and TL. TT prepared the paper, with contributions from all co-authors.

4 Benefits of conserving foreshore vegetation

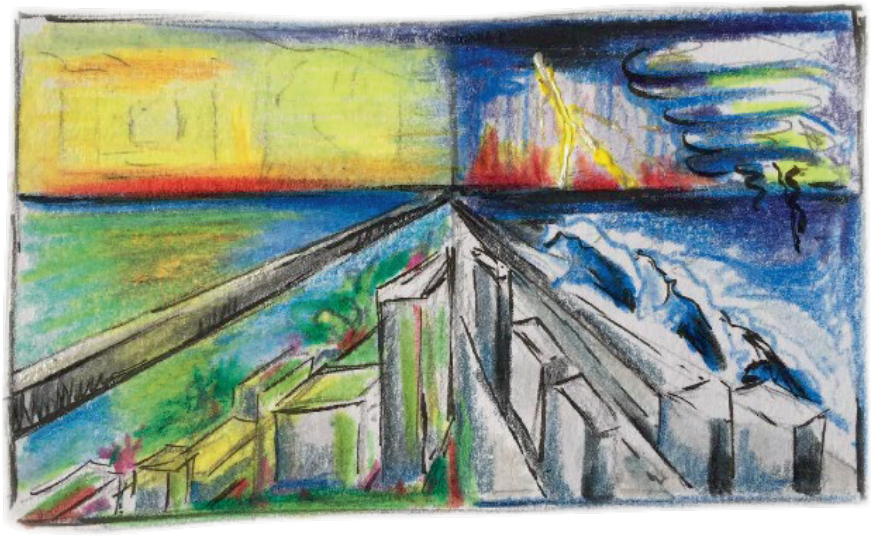

This chapter is published as

Tiggeloven, T., de Moel, H., van Zelst, V. T., van Wesenbeeck, B. K., Winsemius, H. C., Eilander, D., & Ward, P. J. (2022). The benefits of coastal adaptation through conservation of foreshore vegetation. Journal of Flood Risk Management, e12790.

Abstract

Due to rising sea levels and projected socio-economic change, global coastal flood risk is expected to increase in the future. To reduce this increase in risk, one option is to reduce the probability or magnitude of the hazard through the implementation of structural, Nature-based or hybrid adaptation measures. Nature-based Solutions in coastal areas has the potential to reduce impacts of climate change and can provide a more sustainable and cost-effective alternative to structural measures. In this paper, we present the first global scale assessment of the benefits of conserving foreshore vegetation as a means of adaptation to future projections of change in coastal flood risk. In doing so, we extend the current knowledge on the economic feasibility of implementing global scale Nature-based Solutions. We show that globally foreshore vegetation can contribute to a large decrease in both absolute and relative flood risk (13% of present-day, and 8.5% of future conditions in 2080 of global flood risk). Although this study gives a first proxy of the flood risk reduction benefits of conserving foreshore vegetation at the global scale, it shows promising results for including nature-based and hybrid adaptation measures in coastal adaptation schemes.

4.1 Introduction

Coastal zones are attractive areas for human settlement and have three times higher population density than the global average (Small & Nicholls, 2003). Recent research shows that 1.3% of the global population lives in coastal zones that are exposed to a 1 in 100-year flooding event (Muis et al., 2016) and future population in coastal zones is expected to grow, increasing the exposure to coastal flooding (Neumann et al., 2015). Next to this increase in exposure, coastal flood hazard will change through climate change and subsidence (Nicholls & Cazenave, 2010; Vousdoukas et al., 2018a). Due to rising global temperatures, sea-level rise is projected to accelerate during the 21st century (Oppenheimer et al., 2019), leading to an increase in coastal flood hazard (Vitousek et al., 2017). Next to sea-level rise, climate change is projected to lead to changes in flood hazard through changes in tides (Idier et al., 2017), surge levels (Little et al., 2015), extreme sea levels (Vousdoukas et al., 2017) and wind-wave climate (Hemer et al., 2013). These changes of flood hazard and exposure will lead to increases in global coastal flood risk (Hallegatte et al., 2013; Hinkel et al., 2014; Neumann et al., 2015; Tiggeloven et al., 2020; Vousdoukas et al., 2018a).

To prevent or reduce this increase in flood risk, adaptation measures are required. One option is to develop methods to reduce the probability or magnitude of the hazard, the so-called 'protect' approach. This can be achieved through the implementation of structural, Nature-based Solutions or hybrid adaptation measures. Lincke & Hinkel (2018) show that adaptation through structural adaptation measures is economically feasible for 13% of the global coastline, which accounts for 90% of the

global population living in regions prone to coastal hazard. In addition, Hinkel et al. (2014) show that the avoided damages of adaptation are much higher than the costs of adaptation and Tiggeloven et al. (2020) show that adaptation through structural measures shows high potential to reduce (future) coastal flood risk. Instead of only focusing on structural adaptation measures, Jongman (2018) argues that flood risk management needs to adopt holistic strategies to adapt to climate change, such as early warning systems, risk perception, Nature-based or hybrid solutions. Hybrid solutions combine structural measures with Nature-based Solutions, such as maintaining or restoring foreshore vegetation and foreshore geomorphology on the foreshore. Duarte et al. (2013) show that Nature-based Solutions in coastal areas has potential to reduce the impacts of climate change. Moreover, recent studies argue that Nature-based Solutions can provide a more sustainable, cost-effective and ecologically sound alternative to structural measures, such as dikes, sea walls and embankments (Siddharth Narayan et al., 2016; Temmerman et al., 2013; van Wesenbeeck et al., 2017).

Foreshore vegetation plays a significant role in dissipating wave energy (Barbier et al., 2008; Shepard et al., 2011), attenuating storm surges (Wamsley et al., 2010; Zhang et al., 2012), and providing economic benefits through coastal flood protection (Menéndez et al., 2020a). Structural measures alone can have negative effects as they have a costly maintenance, and need continual heightening and widening to keep up with sea-level rise (Temmerman et al., 2013). On the other hand, ecosystems can respond to sea level rise by natural accretion of mineral and biogenic sediments (Fagherazzi et al., 2012; Kirwan et al., 2010; Mckee et al., 2007). By providing additional benefits, such as improving water quality and recreation (Barbier et al., 2011), ecosystems could be more cost-effective in the long term than structural measures under similar scenarios (Broekx et al., 2011; Turner et al., 2007). However, the reduction of flood risk through the presence of foreshore vegetation under future change, and the benefits of using foreshore vegetation as future adaptation measures, have not been assessed at the global scale.

This paper aims to address this gap by providing a first proxy assessment on the benefits of conserving foreshore vegetation as a means of adaptation to future projections of change in coastal flood risk. We approach this aim in two ways. First, we show the reduction of coastal flood risk that could be attained by conserving foreshore vegetation under various combinations of future climate and socioeconomic scenarios. Here, we include foreshore dynamics (wave attenuation) through foreshore vegetation to assess flood risk reduction in terms of expected annual damage and expected annual population exposed. Secondly, we provide the first global scale study on the benefits of implementing adaptation measures using a combination of structural adaptation measures and conserving foreshore vegetation for future flood risk scenario projections.

4.2 Methods

This study extends the coastal flood risk assessment framework developed by Tiggeloven et al. (2020) to also include the effects of foreshore vegetation on global flood risk reduction. The latter is achieved using the approach of van Zelst et al. (2021). The main steps of this study are: (1) flood risk estimation; (2) wave attenuation estimation; and (3) estimating the benefits of adaptation measures. In brief, flood risk is estimated as a function of hazard, exposure and vulnerability (United Nations Office for Disaster Risk Reduction, 2016). Flood risk, expressed in terms of both Expected Annual Damages (EAD) and Expected Annual Population Exposed (EAPE), is calculated over time for scenarios with and without adaptation measures. The benefits are calculated as the reduction in EAD with and without adaptation measures. These benefits for conserving foreshore vegetation are estimated in the adaptation objective 'Protection constant', in which it is assumed that present-day protection standards are kept the same in the future as the current protection standards. This section contains a brief description of the methods involved with the setup of the modelling framework, and is based on detailed descriptions by Tiggeloven et al. (2020) and Ward et al. (2020) for the modelling framework, and van Zelst et al. (2021) for details on global wave attenuation by mangroves and salt marshes in coastal areas.

4.2.1 Flood risk estimation

We estimated coastal flood impacts using the GLOFRIS risk assessment framework of Ward et al. (2013) to combine data on flood hazard (inundation maps), exposure (current and future built-up exposure maps with associated maximum damage values), and vulnerability (depth-damage curves). The flood impacts are assessed at a horizontal resolution of 30" x 30" and simulated for several return periods (2, 5, 10, 25, 50, 100, 250, 500, 1000 years). This section contains an overview of the methods used to estimate flood hazard, exposure, vulnerability, and risk.

Flood hazard is represented by maps of inundation depth for several return periods (2, 5, 10, 25, 50, 100, 250, 500 and 1000 years). These are simulated using a 2D topographic inundation modelling routine that accounts for water level attenuation. As underlying topography, we use the Multi-Error-Removed Improved-Terrain (MERIT) DEM (Yamazaki et al., 2017) at a 30" x 30" resolution. In order to simulate the reduction of flooding land inwards due to the limited time span of tides and storm surges, we included a resistance factor in the inundation routine similar to Vafeidis et al. (2019). As input for the inundation model, we use extreme sea level values from the Global Tide and Surge Reanalysis (GTSR) dataset by Muis et al. (2016) enriched with simulated tropical cyclones using the IBTrACS (International Best Track Archive for Climate Stewardship) archive, as described by Tiggeloven et al. (2020). Future inundation is simulated using sea-level rise to simulate future extreme sea levels and subsidence rates through groundwater extraction to estimate how the terrain may

change. We use gridded projections of sea-level rise from the RISES-AM project, in which sea-level rise rates are regionalized using spatial variability associated with gravitational-rotational fingerprints (Jackson & Jevrejeva, 2016). For this study we use a range of probabilistic outcomes (5th, 50th and 95th percentiles) for two Representative Concentration Pathways (RCP), i.e. RCP4.5 and RCP8.5. Subsidence is modelled through groundwater extraction and rates are taken from the SUB-CR model (Kooi et al., 2018).The flood hazard maps are available through Ward et al. (2020).

Exposure data used in this study consists of current gridded built-up area taken from the HYDE database (Klein Goldewijk et al., 2011) and future built-up area from Winsemius et al. (2016) both at a resolution of 30" x 30". Current maximum economic damages are estimated using the methodology of Huizinga et al. (2017) and future estimates are scaled with the GDP per capita per country from the Shared Socioeconomic Pathway (SSP) database. Based on a study by BPIE (2011) and EEA (2016), we set the area of occupancy type per grid cell to 75% residential, 15% commercial, and 10% industrial. Following Huizinga et al. (2017), the density of buildings per occupancy types are set to 20% for residential and 30% for commercial/industrial. In order to calculate future risk relative to GDP per region, future gridded GDP values are taken from Van Huijstee et al. (2018), which uses the national GDP per capita from the SSP database as input.

Vulnerability to flooding is estimated by using different global flood depth-damage functions for each occupancy type and are taken from Huizinga et al. (2017). The resulting damages are represented as a percentage of the maximum damage. Subsequently, flood impacts per cell are calculated by estimating the percentage of maximum damage per occupancy type at the inundation depth in each cell, and are expressed in the following equation:

$$I_\theta(p) = \theta_r(p)M_r + \theta_c(p)M_c + \theta_i(p)M_i \quad (4\text{-}1)$$

where I_θ is the flood impact at the inundation depth associated with the annual probability of non-exceedance p (1 divided by the return period), θ is the vulnerability, and M is the maximum damage assigned for residential (r), commercial (c) and industrial (i) occupancy types. To estimate flood risk in terms of EAD, we first estimate these flood impacts per return period at the resolution of 30" x 30". Subsequently, EAD can be estimated by taking the integral of the exceedance probability-impact (risk) curve (Meyer et al., 2009) and is shown in the following equation:

$$D = \int_{p=0}^{1} I_\theta(p)dp \tag{4-2}$$

where D is EAD. To fit a protection standard of a coastal region in the risk computation, the risk curve is truncated at the exceedance probability of the protection standard (expressed as a return period). To estimate the area under the curve, we use the trapezoidal approximation. Under the same conditions, higher protection standards indicate that EAD would decrease as the hinterland is protected for storms up to the corresponding protection standard. Similar to the EAD estimation, EAPE is estimated by taking the integral of exposed population associated with the recurrence intervals assessed. As data on protection standards of coastal regions are not available for many regions, we estimate current protection standards for coastal regions using the FLOPROS modelling approach (Scussolini et al., 2016). The resulting coastal protection standards are described and validated in Tiggeloven et al. (2020).

4.2.2 Wave attenuation and crest height estimation

This study estimates the effects of wave attenuation through foreshore vegetation globally. In order to estimate these effects of foreshore vegetation on wave attenuation and required crest height estimation, we use the following procedure of van Zelst et al. (2021): (1) derive coastal segments and corresponding coast-normal transects; (2) construct bed-level profiles and vegetation cover; (3) derive representative hydrodynamic conditions and wave attenuation under these conditions; and (4) estimate required crest heights under current and future conditions. We use OpenStreetMap (OSM, 2015) to derive the coastlines and move them 100 m land inwards in order to find a likely position to establish a dike system. Detection of already established dike systems is not explicitly taking into account here. However, large geomorphological features as present in MERIT DEM are included and we use a baseline protection standard for each region using the FLOPROS database. For every cell containing a coastline segment at 1' x 1' resolution, its coastline length and a transect perpendicular to the coast are derived at the centre of the segment resulting in 495,361 transects that are on average 1.1 km apart. For each transect, the foreshore width and slope and the vegetation width and type within the foreshore are derived along the same coast-normal transect. The following sections contain an overview of the methods involved for estimating the required crest heights; for details we refer to van Zelst et al. (2021).

The bed-level data consists of three datasets where the main source is derived from the FAST inter-tidal elevation product at 20 m horizontal resolution and 30-50 m vertical resolution (Calero et al., 2017). Bathymetry data are derived from GEBCO at 30" x 30" horizontal resolution and tens of meters vertically, and topography data are derived

from the MERIT DEM at 3" x 3" horizontal resolution and 2 m vertically. Vegetation presence at 10 m resolution is derived from the FAST coastal vegetation map, which is based on Landsat-8 and Sentinel-2 satellite images. To determine the type of vegetation we use global salt marsh (Mcowen et al., 2017) and mangrove (Giri et al., 2011) maps, complemented with Corine Land Cover (CLC, Europe only) and GlobCover v2.2 maps where the former lack coverage. The properties of the vegetation relevant for wave attenuation (spatial density, height, diameter and drag coefficient) have been determined in the FAST project based on field measurements and literature. In this study, salt marshes in the temperate zone are represented by a parameterization that is typical for North Western Europe winter state salt marshes. Mangroves are represented as (young) pioneering mangroves. Details on the representation of vegetation in the numerical modelling activities can be found in van Zelst et al. (2021). Figure 4-1 displays an overview of the present-day foreshore vegetation (salt marshes and mangroves) used in this methodology. Countries that have the largest areal extent (km2) of vegetation are Australia, Indonesia, United States and Brazil. Figure 4-1 shows that mangroves are most dominant between the 30°N and 30°S latitude, and salt marshes are largely present in the northern hemisphere above the 30°N latitude. Note that data on foreshore vegetation are lacking in a lot of regions in the Mediterranean Sea, which indicates that results in those regions should be interpreted with caution.

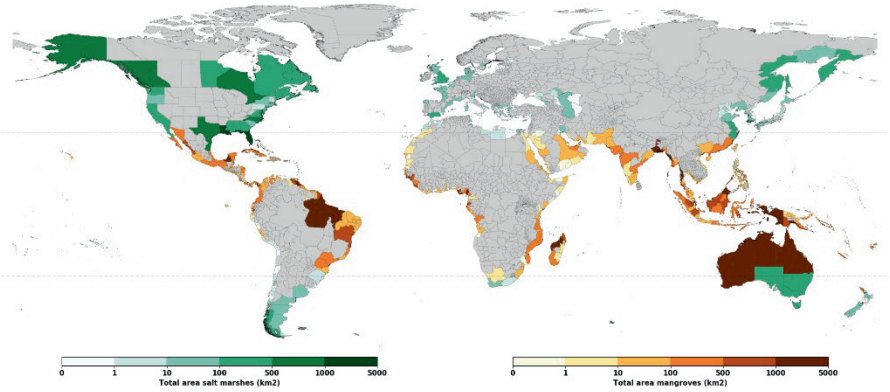

Figure 4-11: Total area of foreshore vegetation displayed for the most dominant type of the sub-national region (salt marshes and mangroves) assessed in wave attenuation calculations. The auxiliary lines of 30°N and 30°S latitude is added to show loosely the boundary of dominant foreshore vegetation type. Sub-national regions with no data are indicated with grey colour.

Wave conditions have been derived from the ERA-Interim (Dee et al., 2011) reanalysis using a peak-over-threshold approach. Offshore significant wave heights for the same range of return periods are transformed to a nearshore wave height that is limited by depth-induced breaking. To determine the wave attenuation over a foreshore and the

resulting significant wave height relevant for the flood defence on a transect, we use a lookup-table by combing 668,304 XBeach (van Rooijen et al., 2016) hydrodynamic numerical modelling results for combinations of foreshore slopes, vegetation covers, and hydrodynamic conditions (van Zelst et al., 2021). The values for these input conditions are based on the expected range of conditions, i.e., the distribution functions of these parameters globally. This table contains wave heights modelled by XBeach (van Rooijen et al., 2016) at regular intervals along a steady slope, both with and without salt marsh or mangrove vegetation. Wave angle of incidence is assumed coast normal to represent a worst-case scenario. Wave attenuation along the vegetated coastlines is determined based on the closest match between the derived transects characteristics and look-up table results.

Subsequently, required crest heights are estimated with the empirical EuroTop formulations (Pullen et al., 2007) with respect to the surge level for a standard 1:3 dike profile without berms and an allowed overtopping discharge of 1 l/s/m. The reduction in required crest height is calculated by subtracting dike crest height for the scenarios with foreshore vegetation and all foreshore vegetation removed. We assume the same coastal profile with and without coastal vegetation, which is a conservative approach. We hereby cancel out the effect of the coastal profile and solely focus on the contribution of foreshore vegetation. Future crest heights are estimated using regional sea-level rise from Jackson and Jevrejeva (2016) and subsidence rates from Kooi et al. (2018). This is carried out by adding subsidence and sea-level rise rates directly on the crest heights. Thus, natural accretion on vegetated foreshores and changing foreshore hydrodynamics due to relative sea-level rise is not included in this study.

4.2.3 Benefits of conserving foreshore vegetation and adaptation costs

We perform an analysis on the benefits of conserving foreshore vegetation to simulate the effects of foreshore vegetation on coastal flood protection. We first estimate the costs of structural adaptation measures and the benefits of foreshore vegetation in the adaptation objective 'Protection constant', where the present-day protection standards are kept the same in the future through structural adaptation measures. Then, to estimate the contribution of conserving foreshore geomorphology and vegetation as an adaptation measure (hereafter referred to as 'Conserving foreshore vegetation'), we estimate the benefits of conserving foreshore vegetation relative to the total benefits of the adaptation objective 'Protection constant'.

To calculate the investment costs associated with the dike dimensions we use the estimated required dike heights and the dike lengths from the coastlines from the OpenStreetMap. We then estimate the investment costs of structural measures by multiplying by a unit cost set to USD 7 million km dike length·m dike heightening

based on reported costs in New Orleans (Bos, 2008). This value of US$ 7 million km·m is within a reasonable range when compared to various studies (Aerts et al., 2013; Jonkman et al., 2013; Lenk et al., 2017), and is used in this study for both building a new dike system and heightening an already existing one. This includes investment costs, groundwork-, construction- and engineering costs, property or land acquisition, environmental compensation, and project management. Subsequently, the costs are converted to US$2005 Power Purchasing Parity (PPP) by first adjusting to US$2005 values using GDP deflators from the World Bank Open Data website (https://data.worldbank.org/) and then using PPP to market exchange rates from OECD, taken from the IIASA SSP database (Riahi et al., 2017). Construction index multipliers, based on civil engineering construction costs, adjust the implementation costs of structural measures to account for differences between countries (Ward et al., 2010).

The benefits of the adaptation measures are expressed as flood risk reduction and estimated by computing the difference in EAD without the adaptation measure or foreshore vegetation and EAD with the adaptation measure, see Eq. 4-3.

$$B_t = \int_{p=0}^{p=p_n} I_\theta(p)dp - \int_{p=0}^{p=p_a} I_\theta(p)dp \tag{4-3}$$

, where B_t is the benefit of adaptation at time step t, p_n is the non-exceedance probability with no adaptation and p_a the non-exceedance probability with adaptation. We estimate flood risk reduction by taking the difference between flood risk estimated with the scenario where foreshore vegetation is present and the scenario where foreshore vegetation is completely removed. We do this under present-day conditions and future conditions. To do so, we calculate the crest heights of all populated coastlines prone to flooding associated with FLOPROS protection standards with vegetation and project these crest heights on protection standards when no foreshore vegetation is assumed, in order to estimate the difference in protection standards. Subsequently, we use Eq. 3 to estimate the present-day and future flood risk reduction through foreshore vegetation by filling in the different protection standards with and without foreshore vegetation. We estimate flood risk reduction relative to the flood risk in the scenario without foreshore vegetation presence. In these estimations we take into account the current protection standards estimated with the FLOPROS modelling approach described earlier. Furthermore, we estimate the total benefits by summing the reduction in EAD up to 2100.

In this study, we use two scenario combinations in order to address future projections (van Vuuren et al., 2014), namely RCP4.5-SSP2 and RCP8.5-SSP5. The RCP4.5-SSP2

scenario combination can be linked to a 'middle of the road scenario' with medium challenges and adaptation (Riahi et al., 2017), which can be broadly aligned with the Paris agreement targets (Hope et al., 2017). The RCP8.5-SSP5 scenario combination addresses a 'fossil-fuel development' world (Kriegler et al., 2017), in which the world faces high mitigation and low adaptation challenges. For uncertainty analysis within these scenario combinations, we use a probability range of sea-level rise.

4.3 Results

In this section, we present the results of the current risk reduction performance of the foreshore vegetation present, as well as the benefits of conserving foreshore vegetation in the future under the 'Protection constant' adaptation objective. Firstly, we show the present-day reduction in flood risk, expressed in both EAD and EAPE. Additionally, we show the increase in protection standards that can be attributed to the foreshore vegetation that is currently present, indicating their current value in terms of flood protection. Then, we show the future reduction in flood risk and EAPE for different scenario combinations. Lastly, we show the benefits of conserving foreshore vegetation and the contribution to the total benefits of adaptation with uncertainty for sea-level rise projections. Table 4-1 provides a global overview of the results discussed for the reduction in EAD and EAPE under current conditions and for future scenarios in 2080. Next to this, the table shows the total benefits of conserving foreshore vegetation for the scenarios of RCP4.5/SSP2 and RCP8.5/SSP5.

Table 4-3: Global overview of the results discussed in this study for both absolute and relative reduction in EAD, reduction in EAPE, and total benefits. EAD and EAPE values for both scenarios are estimated for the year 2080. Note that no value is given for total benefits under current conditions as this value is only calculated for RCP/SSP scenarios.

Scenario	Reduction in EAD (US$ B)	Reduction in EAAP (# people K)	Total benefits (US$ B)
Present-day	2.5 (12.4%)	342 (5.9%)	-
RCP4.5/SSP2	71 (8.5%)	995 (5.7%)	280 (3.0%)
RCP8.5/SSP5	164 (8.0%)	902 (6.0%)	532 (2.9%)

4.3.1 Present-day and future risk reduction through foreshore vegetation

Present-day coastal flood protection standards are affected by the effects of wave attenuation through foreshore vegetation. Globally, the total reduction in EAD provided by present-day foreshore vegetation is estimated at US$2.5 billion, which amounts to 13% of global EAD and 0.4% of total GDP exposed. Figure 4-2 shows the present-day relative reduction in EAD and EAPE, increase in protection standards, and absolute reduction in EAD in the horizontal bar plot through foreshore vegetation for continental regions. The absolute reduction in EAD provided by present-day

foreshore vegetation is especially strong in the continental regions of southeastern Asia, eastern Asia, southern Asia, and northern America. We also find that, globally, EAPE is reduced by 6% through wave attenuation by foreshore vegetation. Relative reduction through foreshore vegetation is found to be highest in the Caribbean, Western Asia, and Australia and New Zealand. Additionally, we find that the absolute reduction in EAD provided by present-day foreshore vegetation for sub-national regions with high density of salt marshes in the United States and parts of Europe also contributes to a large share of present-day risk reduction (see Figure C-1 and Figure C-2). We see that the relative increase in protection standards provided by foreshore vegetation is up to 25% in continental regions of Caribbean, Central America, and Australia. The estimated relative increase of protection standards for sub-national regions are shown in Figure C-3, which shows that the increase in protection standards provided by present-day foreshore vegetation is especially strong in regions in Northern America, Australia, South-eastern Asia, and South America.

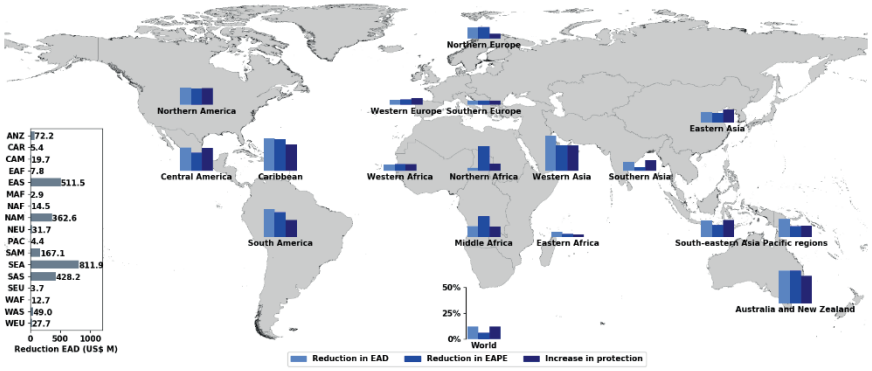

Figure 4-2: Present-day relative reduction to risk without foreshore vegetation of EAD and EAPE, and increase in protection standards through foreshore vegetation. ANZ, Australia and New Zealand; CAR, Caribbean; CAM, Central America; EAF, Eastern Africa; EAS, Eastern Asia; MAF, Middle Africa; NAF, Northern Africa; NEU, Northern Europe; PAC, Pacific regions that include Melanesia, Polynesia, and Micronesia; SAM, South America; SEA, South-eastern Asia; SAS, Southern Asia; WAF, Western Africa; WAS, Western Asia; WEU, Western Europe.

With sea-level rise, subsidence and socio-economic change, future flood risk increases. We find that by conserving present-day foreshore vegetation, EAD in 2080 could be reduced by 71 US$ billion, which amounts to 8.5% of total EAD globally under the scenario combination RCP4.5-SSP2. For the scenario combination RCP8.5-SSP5, we find values of 168US$ billion and 8% of global EAD. We further estimate that the risk reduction relative to total exposed GDP is doubled to 0.8% for both scenario combinations compared to present-day estimates. The results of estimated future reduction in EAD and EAPE through foreshore vegetation for sub-national regions for the scenario combinations RCP4.5-SSP2 and RCP8.5-SSP4 is shown in Figure 4-3.

The largest future flood risk reduction is found in sub-national regions of West Bengal (India; from current to US$243 million to future US$24.9 billion) which is located in the Sundarbans, Maharashtra (India; from current US$158 million to future US$4.7 billion) which is one of the sub-national regions in India with the largest share of mangroves; Guangdong (China; from current US$266 million to future US$4.2 billion) which has one of the largest shares of mangroves in all of China (B. Chen et al., 2017); Louisiana (USA; from current US$216 million to future US$1.2 billion) which contains a large share of wetlands of the United States; and Sarawak (Malaysia; from current US$105 million to future US$969 million) for the scenario combination RCP4.5-SSP2 (see Figure C-1 for results on present-day flood risk reduction provided by foreshore vegetation for sub-national regions).

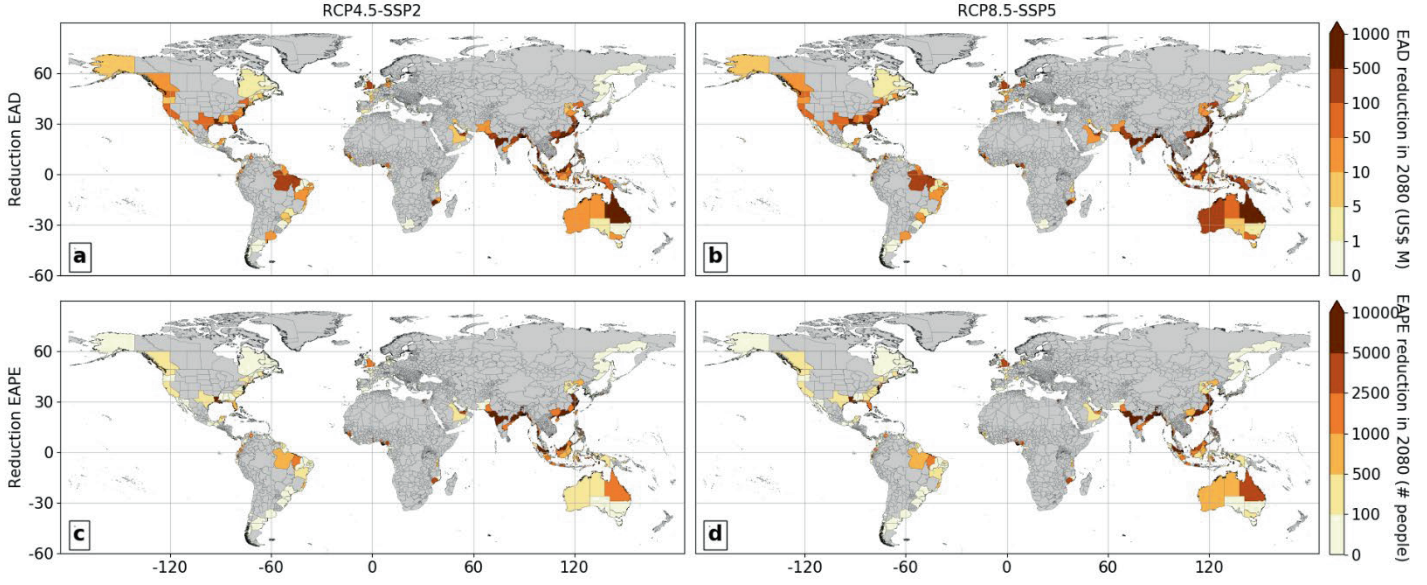

Figure 4-3: Relative reduction in EAD and EAPE through wave attenuation of foreshore vegetation in 2080 for the scenario combinations RCP4.5-SSP2 and RCP8.5-SSP5. Sub-national regions with no data are indicated with grey colour.

Globally, we see a reduction in EAPE of 6%, with the largest share in the sub-national regions of West Bengal (India; from current 98 thousand to future 310 thousand population exposed), Khulna (Bangladesh; from current 21 thousand to future 58 thousand population), and Camarines Sur (Philippines; from current 13 thousand to future 46 thousand population exposed) for the scenario combination RCP4.5-SSP2. We see that compared to present-day relative risk reduction, future relative risk reduction will for most sub-national regions be in the same order of magnitude for most sub-national regions, with some sub-national regions having a lower relative reduction.

We find that although relative risk reduction does not change much, absolute risk reduction through foreshore vegetation increases for most sub-national regions due to an increase in future flood hazard and exposure. We show that flood risk reduction is highest for sub-national regions in Northern America, Brazil, Western Europe, Southern Asia, China, Southeastern Asia and Australia due to high exposure to flood risk and/or large areas of foreshore vegetation. We see that sub-national regions with a lower share in risk reduction have high absolute values for flood risk reduction due to a high value of exposed assets in deltas (e.g., sub-national regions in China, Southern Asia, and Louisiana).

4.3.2 Benefits and reduction in adaptation costs of conserving foreshore vegetation

In this section, the results are shown for the total discounted benefits of conserving foreshore vegetation with the adaptation objective 'Protection constant'. The total global discounted benefits of conserving foreshore vegetation up to 2100 are estimated at US$274 billion for the scenario combination RCP4.5-SSP2, which amounts to 2.9% of the total benefits for keeping protection standards the same. The highest values of foreshore vegetation benefits relative to total benefits are found in sub-national regions in Southern Asia, South-eastern Asia, Eastern Asia, South America, and Australia (see Figure 4-4). The error bars show the sensitivity of the results to the different sea-level rise probabilistic projections within the RCP scenario while using the same coastal profile, which is found to be within a couple of percentage points. For the scenario combination RCP8.5-SSP5, we find that the global total discounted benefits are twice the amount of the value for RCP4.5-SSP2 and estimated at US$533 billion, which also amounts to approximately 2.9% of total benefits of adaptation (see Figure C-5). We find that, due to a higher rate of sea-level rise, the total benefits will increase for most sub-national regions and that the sensitivity of the results to the different sea-level rise probabilistic projections within the RCP scenario are smaller.

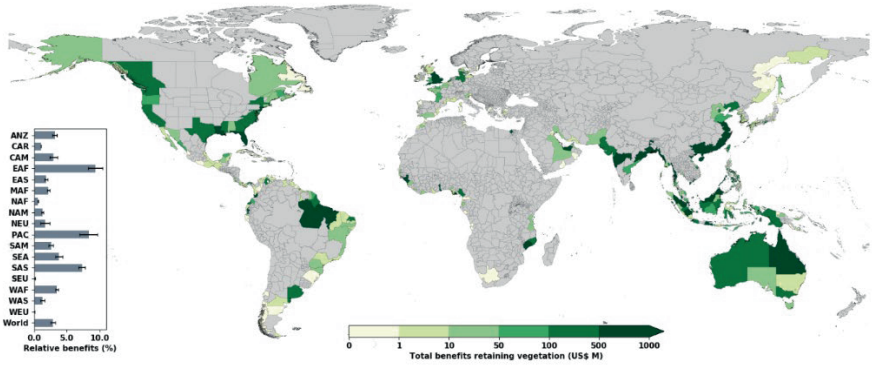

Figure 4-4: Total discounted benefits of conserving foreshore vegetation in the adaptation objective 'Protection constant' for the scenario combination RCP4.5/SSP2. Sub-national regions with no data are indicated with grey colour. The error bars in the horizontal bar plot indicate the uncertainty range for the probabilistic sea-level rise projections of the 5th and 95th percentile. ANZ, Australia and New Zealand; CAR, Caribbean; CAM, Central America; EAF, Eastern Africa; EAS, Eastern Asia; MAF, Middle Africa; NAF, Northern Africa; NEU, Northern Europe; PAC, Pacific regions that include Melanesia, Polynesia, and Micronesia; SAM, South America; SEA, South-eastern Asia; SAS, Southern Asia; WAF, Western Africa; WAS, Western Asia; WEU, Western Europe.

To keep current protection standards constant with rising sea-level, adaptation is necessary. We show that through conserving foreshore vegetation, a reduction in required dike heights can be achieved. In Figure 4-5, we show the reduction of adaptation costs of structural adaptation measures through conserving foreshore vegetation, as well as the remaining costs required for structural adaptation measures (leftover structural adaptation costs). We find that globally the total adaptation costs of structural measures are reduced by US$34 billion if foreshore vegetation is conserved. The highest reductions of adaptation costs through conserving foreshore vegetation, both in absolute and relative terms, are found in Australia. We further estimate savings in adaptation costs through conserving foreshore vegetation of higher than US$4 billion in Northern America, South-eastern Asia, Southern America, and Eastern Asia.

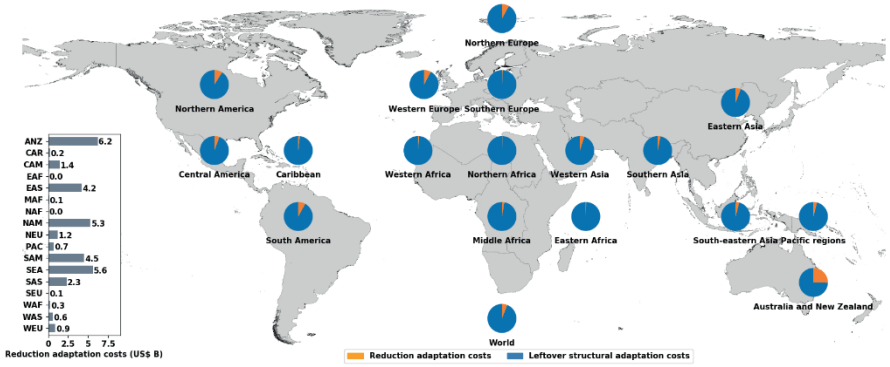

Figure 4-5: Reduction in adaptation costs of conserving foreshore vegetation and leftover structural adaptation costs in the adaptation objective 'Protection constant' for the scenario combination RCP4.5/SSP2. ANZ, Australia and New Zealand; CAR, Caribbean; CAM, Central America; EAF, Eastern Africa; EAS, Eastern Asia; MAF, Middle Africa; NAF, Northern Africa; NEU, Northern Europe; PAC, Pacific regions that include Melanesia, Polynesia, and Micronesia; SAM, South America; SEA, South-eastern Asia; SAS, Southern Asia; WAF, Western Africa; WAS, Western Asia; WEU, Western Europe.

4.4 Discussion

We present the first global scale assessment of future flood risk reduction through conserving foreshore vegetation and the benefits of conserving foreshore vegetation under future scenarios and adaptation objective 'Protection constant'. We show that foreshore vegetation contributes a large share of flood risk reduction and that absolute EAD reduction is estimated to increase if foreshore vegetation is conserved under future projections of sea-level rise and socioeconomic change. Our estimates point out that conserving foreshore vegetation is an effective measure to reduce future flood risk. We further show that the benefits of conserving foreshore vegetation for flood risk reduction are estimated at approximately US$274 billion, which can account for up to 20% of the total benefits in the protection constant adaptation objective for some sub-national regions. This indicates that ecosystem-based flood protection and Nature-based Solutions constitute promising alternatives or complementary measures to other adaptation measures (e.g. structural measures), which is in line with recent studies on Nature-based Solutions (Borsje et al., 2011; Duarte et al., 2013; Shepard et al., 2011; Spalding et al., 2014; Temmerman et al., 2013; van Zelst et al., 2021; Vuik et al., 2016).

Assessing the present-day global coastal flood protection of foreshore vegetation in economic terms, we estimated avoided damages of US$2.5 Billion per year, which amounts to 13% of global coastal flood risk in terms of EAD. Menéndez et al. (2020) assessed the benefits of present-day global coastal flood protection of mangroves and found that mangroves provide flood protection benefits exceeding US$65 Billion per year, which is 9% of their estimated global EAD. We see that their estimated global EAD is more than 40 times higher than our estimate, and also higher than values

reported in other studies (Stephane Hallegatte et al., 2013; Hinkel et al., 2014; Tiggeloven et al., 2020). Moreover, it is more than twice as high as reported values for all natural catastrophes in the Munich Reinsurance for the period 1980-2017 (Löw, 2018). This can be accounted for as they do not use present-day protection standards in their analysis. In relative terms of flood risk reduction relative to GDP, we find that mangroves reduce 9.8% of global EAD, which is in the same magnitude as estimates found by Menéndez et al. (2020). In a study reporting the value of coastal wetlands on flood risk reduction, Narayan et al. (2017) estimated flood risk reduction through salt marshes on average to be 18% and up to 70% in some regions within the Ocean County in the US, while we show for the whole state of New Jersey that flood losses could be reduced by 35.6%. While local scale studies show potential benefits of foreshore vegetation on wave load reduction (Horstman et al., 2014; Vuik et al., 2016), it is difficult to compare their results to our study on extreme events as those measurements are often done under daily conditions.

This study only shows the benefits of conserving foreshore vegetation in terms of flood risk reduction, while in reality foreshore vegetation also provides other ecosystem services as co-benefits such as fishery, recreation (Barbier et al., 2011; Cheong et al., 2013), carbon storage (Mitsch et al., 2015) and climate change mitigation (Duarte et al., 2013), e.g. by accumulation of sediments (Kirwan et al., 2010). Next to this, adaptation using a range of different measures might be more feasible in the long run (Jongman, 2018; Sutton-Grier et al., 2015). In this study, we only assume conserving present-day vegetation and structural measures as adaptation measures to reduce flood risk while there are also other adaptation measures. For instance, such adaptation measures include dry and wet proofing (Aerts et al., 2014), migration to less flood prone areas (R. McLeman & Smit, 2006), or a combination of adaptation through pathways (de Ruig et al., 2019).

The values found in this study for the effects of conserving foreshore vegetation under future change are estimated by assuming that all foreshore vegetation is conserved compared to when all foreshore vegetation is lost due to sea-level rise. In reality, foreshore vegetation will not be lost completely when no human maintenance is carried out, but only a part of the vegetation may disappear due to sea-level rise, erosion and conversion to urban or agricultural land-use (Blankespoor et al., 2014; Schuerch et al., 2018; Vousdoukas et al., 2020). Therefore, the values found in this study need to be interpreted as the maximum added value of foreshore vegetation for flood risk reduction and adaptation costs reduction. For instance, if all foreshore vegetation is lost then flood risk would be estimated to increase with the values found in this study. Furthermore, we assume the same coastal profile for all scenarios in this study so the results solely focus on the effects of foreshore vegetation, while in reality the coastal profile is governed by hydrodynamics (e.g. wave heights and currents) and

geomorphology (e.g. sediment availability) (Winterwerp et al., 2013). Next to this, this study does not take into account the costs of conserving foreshore vegetation and future work could include an assessment of feasibility of conservation costs under climate change.

Several more limitations and uncertainties exist in this study and are discussed in more detail in Tiggeloven et al. (2020) and van Zelst et al. (2021) such as wave dampening effects and required crest heights estimation methodology. Firstly, several uncertainties exist on the cost calculation and the flood risk calculation. In this study, we use linear costs for structural measures, since according to Lenk et al. (2017), using a linear cost function for large scale assessments is a reasonable assumption. Although we include construction costs and market exchange rates, locally the costs might differ due to both physical and socioeconomic local conditions. Secondly, we estimate flood hazard (inundation) using a GIS-based approach rather than a fully dynamic inundation model (Vousdoukas et al., 2018a), but we do account for water-level attenuation similar to Vafeidis et al. (2019). Moreover, we estimate flood risk using a number of assumptions on the share of building occupancy and present-day protection standards using the FLOPROS modelling approach (Scussolini et al., 2016). Next to this, because this study uses extreme storm surges, the effects of wave load reduction for extreme events are uncertain and less known as most case studies focus on daily conditions (Horstman et al., 2014; Vuik et al., 2016; Vuik et al., 2018).

The results of this study can be used to highlight flood risk reduction through foreshore vegetation at the sub-national scale and the importance of conserving foreshore vegetation under future change. However, we stress that this study aims to give a first proxy on the benefits of conserving foreshore vegetation through flood risk reduction. Local assessments should be used for the design and implementation of individual adaptation measures. At the sub-national and global scale, this study provides insights in Nature-based Solutions by showing the potential of flood risk reduction through foreshore vegetation. Even though the results can only be seen as indicative, we believe that it is valuable to gain insight into the effects of conserving foreshore vegetation on the global scale and support the need to include this more in both global assessments and detailed assessments at the regional scale. Going further, this study can be improved by including other Nature-based Solutions strategies, such as restoring wetlands or mangroves, and including an uncertainty analysis of future responses of global coastal wetlands to sea-level rise. Furthermore, an improvement can be made by including a global scale study on the benefits and costs of nature-based, hybrid and structural adaptation measures.

4.5 Conclusion

We present the first global scale assessment of reducing future flood risk through conserving foreshore vegetation. We find that globally the reduction in flood risk through conserving foreshore vegetation is estimated to increase in the range of 28 up to 67-fold compared to present-day conditions, which amounts to US$71 billion for RCP4.5-SSP2 and US$168 billion for RCP8.5-SSP5 in terms of EAD in 2080. We further find that the relative reduction in flood risk through foreshore vegetation is estimated at 8.5% globally, compared to 13% under current conditions. For individual sub-national regions risk reduction can reach up to 50% of the total estimated future flood risk. Assessing the benefits of hybrid adaptation measures in the adaptation objective to keep protection standards constant with hybrid adaptation measures, we find that the benefits of conserving foreshore vegetation can reach up to US$1 billion for sub-national regions in South-eastern Asia, Southern Asia, China, Australia, and Brazil. Globally, the total benefits of conserving vegetation in the adaptation objective are estimated at US$274 billion. We further show that the relative benefits of conserving foreshore vegetation are estimated at 2.9% of the total benefits of flood protection for keeping protection standard constant under the RCP4.5/SSP2 scenario combination and reach more than 20% for some sub-national regions. Therefore, the results of this study show that Nature-based Solutions can be effective adaptation measures. Although this study only provides a first proxy of the flood risk reduction benefits of conserving foreshore vegetation at the global scale, it shows promising results for including nature-based and hybrid adaptation measures in coastal adaptation schemes.

Acknowledgements

The research leading to these results received funding from the Dutch Research Council (NWO) in the form of a VIDI grant (grant no. 016.161.324) and the Future Water Challenges 2 project, funded by the Netherlands Ministry of Infrastructure and Water Management. We acknowledge funding from the SCOR Corporate Foundation for Science under the project COASTRISK.

Data availability

The results of this study for all RCP and SSP combinations are available at Zenodo DOI: 10.5281/zenodo.5878864. Figures of the results of RCP8.5–SSP5 combination are show in Appendix C.

5 Benefits of Mangrove Restoration

This chapter is based on

Tiggeloven, T., Mortensen, E.S., de Moel, H., van Zelst, V. T., van Wesenbeeck, B. K., Worthington, T., Spalding, M. & Ward, P. J. (2022). T Mangrove restoration and coastal flood adaptation: a global perspective. *In review*

Abstract

To reduce current and future coastal flood risk, it is critical to better understand how adaptation measures, including Nature-based Solutions, can reduce that risk. Here, we present the first global-scale assessment of the potential risk reduction that could be achieved by mangrove restoration under scenarios of climate and socioeconomic change. Unlike previous studies of Nature-based Solutions, we provide a quantitative assessment of the benefits of mangrove restoration in terms of reduced economic damage, exposed population, and poverty. We find that mangrove restoration could reduce a large share of future flood risk, namely a US$40-90 billion reduction (or ~11% of the total) of expected annual damage, and a 740,000-820,000 reduction (or ~10% of the total) of expected annual affected population. By carrying out a Benefit Cost Analysis we find that mangrove restoration is economically viable for the majority of the sub-national regions assessed (i.e., 173 out of 250 regions). At the global scale, the Benefit-Cost Ratio for mangrove restoration under future conditions ranges between 33 and 70, with a Net Present Value between US$135 billion and US$294 billion. Because absolute risk values and/or Benefit Cost Analysis do not differentiate between the relative wealth impacts on people, we also estimated the impact of mangrove restoration on poverty. We show that restoring mangroves benefits people living in poverty more than other people, because the former group are often more prone to coastal flooding. As such, mangrove restoration in Low- and Middle-Income Countries (LMICs) could contribute to the resilience of people in poverty.

5.1 Introduction

In the coming century, coastal areas and their populations are projected to face increases in coastal flood risk driven by socioeconomic and climate change (Hallegatte et al., 2013; Hinkel et al., 2014; Nicholls & Cazenave, 2010; Tiggeloven et al., 2020; Vousdoukas et al., 2018a). Such climate shocks may exacerbate current poverty levels and catalyse the formation of poverty traps in LMICs (Hallegatte, 2016; Leichenko & Silva, 2014), with global flood risk at the forefront of the potential impacts. To mitigate the expected increase in coastal flood risk it is critical to better understand both risks and the effects of different adaptation measures. Foreshore vegetation plays a significant role in protecting coastal areas from current flood risk because it dissipates wave energy (Phan et al., 2019) and storm surge attenuation (Vuik et al., 2016). For instance, during Hurricane Irma, mangroves are estimated to have averted US$1.5 billion in flood surge-related property damages. Annually, mangroves are estimated to reduce flood damages by up to 25% in Florida, USA (Narayan et al., 2019). Menéndez et al. (2020) estimate the global flood protection benefits of mangrove forest to exceed US$65 billion per year, while research shows that local scale management of mangroves can be used as climate adaptation and provide livelihood for local communities (del Valle et al., 2020; Schmitt et al., 2013). Moreover, in a study on foreshore vegetation and adaptation, van

Zelst et al. (2021) show that incorporating foreshore vegetation in flood protection results in a more sustainable and financially attractive adaptation strategy compared to grey infrastructure only.

In the last decades, large areas of mangrove forests and other foreshore vegetation degraded rapidly due to climate change and human development (Alongi, 2008; Gedan et al., 2010; Goldberg et al., 2020; Ward et al., 2017). Over 4.3% of mangrove forests were lost in the 20 years to 2016 (Spalding & Leal, 2021) with considerably higher losses prior to that (e.g. FAO, 2007), with conversion to agriculture or aquaculture as the main drivers of direct human loss (Goldberg et al., 2020). Due to future climate change and socioeconomic development, foreshore vegetation is under threat of further degradation (Friess et al., 2019; Jennerjahn et al., 2017; Mitsch & Hernandez, 2013; Saintilan et al., 2019). The loss of these ecosystems disproportionally affects vulnerable groups and communities that live close to the coast, especially local fishermen, and often heavily depend on natural resources (Barbier, 2015; Daw et al., 2011). Especially, local fishermen, who often belong to the poorest groups in development countries, depend on coastal resources and access to the sea (Lawson et al., 2012; Solaymani & Kari, 2014). Hard infrastructure often disconnects these groups from their main source of income and makes it difficult for them to keep a close watch on their boats, which often is their most valuable asset. Increases in coastal flood risk due to sea level rise, increased storminess and removal of coastal ecosystems can lead to poverty traps as people in poverty are disproportionally impacted (Hallegatte, 2016; Hallegatte & Rozenberg, 2017; Winsemius et al., 2018). As we expect that people in poverty are more vulnerable to ecosystem loss, the restoration may actually have added benefits in terms of poverty indicators (Villarreal-Rosas et al., 2021) and integrating this into adaptation (Araos et al., 2021) can help in directing investments to areas which specifically benefit vulnerable groups.

Besides reducing current flood risk, Nature-based Solutions such as mangroves have been estimated to be effective in combating future flood risk (Narayan et al., 2016; Temmerman et al., 2013; van Wesenbeeck et al., 2017). For example, when not constrained by development, mangroves and other foreshore vegetation have the potential to keep pace with sea level rise by natural accretion of mineral and biogenic sediments (Fagherazzi et al., 2012; Kirwan et al., 2010; Mckee et al., 2007). In other words, Nature-based Solutions in coastal areas can potentially reduce the impacts of climate change (Duarte et al., 2013) if they are restored, protected and managed properly. While Nature-based Solutions show potential for broad implementation to reduce coastal flood risk (Duarte et al., 2013; Temmerman et al., 2013; van Zelst et al., 2021; Vuik et al., 2016), no studies have been carried out to assess the effectiveness of mangrove restoration on reducing current and future coastal flood risk for the socially vulnerable at the global scale. This study aims to bridge this gap and provide a global-

scale assessment of the potential benefits (in terms of flood risk reduction) and costs of mangrove restoration, including future conditions of climate and socioeconomic development. This effort highlights regions where mangrove restoration shows potential for success and where these adaptation measures might benefit from further targeted research.

5.2 Global scale flood risk benefits of mangrove restoration

We find that annual global flood risk under present-day conditions could potentially be reduced by US$1.5 billion per year, which is 11% of global Expected Annual Damages (EAD) if all restorable mangrove areas are restored (Table 1). Moreover, the Expected Annual Affected Population (EAAP) can be reduced by 300,000 people (~8%). Under future projections, potential risk reduction increases considerably in absolute terms for both EAD (~28-65 times) and EAAP (~2.6-~2.8 times). The potential reduction in relative terms in the future is 9-11% for EAD and 8-10 for EAAP for the scenario combinations of RCP4.5/SSP2 and RCP8.5/SSP5. Overall, mangrove restoration is estimated to be an economically feasible adaptation measure, as the BCR is far above one (33-70), resulting in NPV between US$135 billion and US$294 billion (Table 1) for the scenario combinations of RCP4.5/SSP2 and RCP8.5/SSP5.

Table 5-1: Global-scale overview of the benefits of mangrove restoration in terms of potential flood risk reduction under present-day conditions and future scenarios. EAD and NPV values are displayed in US$ billion and EAAP in thousands. In brackets, we show the percentages of reduction in EAD/EAAP relative to the total values. Note that no value is given for total benefits under current conditions as this value is only calculated for the RCP/SSP scenarios.

Scenario	Reduction in EAD (US$ B)	Reduction in EAAP (# people K)	NPV (US$ B)	Benefit-Cost Ratio
Present-day	1.5 (10.8%)	289 (7.9%)	-	-
RCP4.5/SSP2	42 (8.9%)	823 (9.7%)	135	33
RCP8.5/SSP5	98 (8.6%)	738 (10.3%)	294	70

5.3 Regional scale flood risk benefits of mangrove restoration

We show that South-eastern Asia (SEA) has the highest potential absolute risk reduction, with more than two-thirds of the global potential risk reduction in terms of both EAD (>US$1 billion) and EAAP (218 thousand) (Figure 5-1). Other regions that show high potential absolute risk reduction in EAD are Southern Asia (SAS; US$120 million) and Eastern Asia (EAS; US$146 million). The highest potential relative risk reduction per sub-continental region is found in Western Africa (WAF) for both EAD (24%) and EAAP (28%), with the largest contribution from Nigeria. We find the highest increases in protection levels in South-eastern Asia (16%) and Australia & New Zealand (17%). A country scale ranking (top 15) and corresponding benefits of mangrove restoration can be found in Table D-1. The countries with the highest potential absolute

risk reduction in terms of EAD are Vietnam, Philippines, Indonesia, and China (US$0.45, US$0.24, US$0.22, and US$0.15 billion respectively), and the countries with the highest potential absolute risk reduction in terms of EAAP are Vietnam, Indonesia, India, and Nigeria (171,000, 29,000, 26,000, and 23,000 respectively). At the sub-national scale, the largest potential risk reduction in EAD is found in Thái Bình (Vietnam; US$355 million), Guangdong (China; US$127 million), and Cebu (Philippines; US$121 million) and the largest potential risk reduction in EAAP is found in Thái Bình (Vietnam; 135,000), West Bengal (India; 22,000), and Cà Mau (Vietnam; 19,000). Although a substantial amount of flood risk can be reduced, the residual risk remains high (approximately 90%).

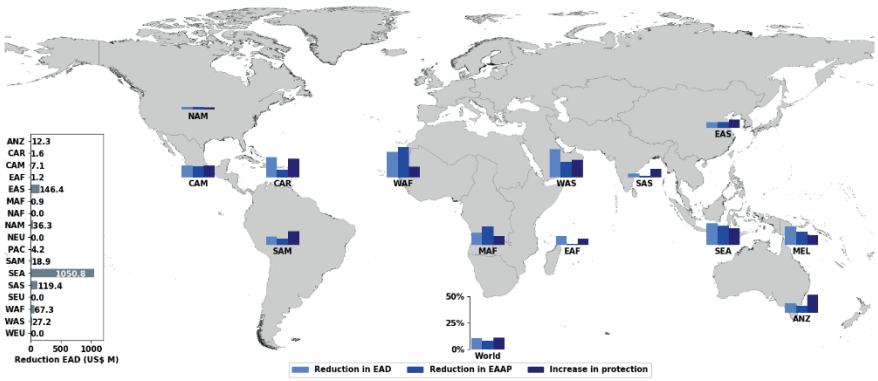

Figure 5-1: Flood risk reduction benefits of mangrove restoration under present-day conditions in terms of potential risk reduction in EAD, potential risk reduction in EAAP, and increase in protection levels. Relative risk reduction values are displayed in the world plot and absolute reduction in EAD is shown in US$ Millions in the subplot. ANZ, Australia and New Zealand; CAR, Caribbean; CAM, Central America; EAF, Eastern Africa; EAS, Eastern Asia; MAF, Middle Africa; NAF, Northern Africa; NEU, Northern Europe; PAC, Pacific regions that include Melanesia, Polynesia, and Micronesia; SAM, South America; SEA, South-eastern Asia; SAS, Southern Asia; WAF, Western Africa; WAS, Western Asia; WEU, Western Europe.

The highest potential reduction in future flood risk can be found in southeastern Asia, Southern Asia, and eastern Asia (Figure 5-2). Regionally, the largest share of potential risk reduction in EAD (Figure 5-2a-b) is found in: Thái Bình (Vietnam; US$9 billion in RCP4.5/SSP2 and US$20 billion in RCP8.5/SSP5), which has seen numerous restoration projects in recent years; West Bengal (India; US$5 billion in RCP4.5/SSP2 and US$13 billion in RCP8.5/SSP5), where mangrove areas are located in the Sundarbans; and Rivers State (Nigeria; US$4 billion in RCP4.5/SSP2 and US$11 billion in RCP8.5/SSP5), which has the largest mangrove forests of Africa. Sub-national regions with the highest potential risk reduction in EAAP are Rivers State (Nigeria, 267 thousand), Thái Bình (Vietnam, 165 thousand), and West Bengal (India, 68 thousand). The countries with the highest future potential risk reduction in EAD are Vietnam (US$12 billion), Indonesia (US$8 billion), India (US$6 billion) and the Philippines

(US$5 billion), and those with the highest future potential risk reduction in EAAP are Nigeria (294 thousand), Vietnam (223 thousand), Indonesia (106 thousand) and the Philippines (70 thousand). This indicates that mangrove restoration potential is high in areas with high population growth, but potential flood damage rises even more in other areas.

To show the regional effectiveness of mangrove restoration per areal extent, Figure D-3 shows the reduction in EAD and EAAP per km^2 of mangrove restoration extent in 2080. Hotspots of EAD reduction relative to restorable mangrove extent are found in Southern Asia, Eastern Asia, and South-eastern Asia, with the highest values in three sub-national regions of Vietnam: Thái Bình, Ninh Bình, and Hai Phong City. While some sub-national regions do not show high effectiveness in terms of EAD relative to restorable extent, they do show higher effectiveness in terms of EAAP (for instance regions in the Americas).

5.4 Benefit and cost analysis of mangrove restoration

Globally, mangrove restoration shows a positive return on investment (i.e., BCR exceeds 1) in the majority of sub-national regions assessed (70%; 173 out of 250). We see the highest Benefit-Cost Ratios (BCRs) for regions in Western Africa, Southern Asia, South-eastern Asia, and Eastern Asia. For sub-national regions, the highest BCRs are found in Thái Bình (Vietnam), East Region (Singapore), Ninh Banh (Vietnam), and Tainan (Taiwan); the latter has a relatively small extent in mangrove forest (Figure 5-3). Total NPV is highest for the sub-national regions of Thái Bình (Vietnam; US$43 billion), West Bengal (India; US$ 14 billion), and Rivers State (Nigeria; US$10 billion) (Table D-1). Most of the sub-national regions that show negative return on investments are in Central America and the Caribbean, where total NPV is negative. South-eastern Asia (US$90 billion), Southern Asia (US$21 billion), and Western Africa (US$13 billion) are the sub-continental regions where highest total NPV are estimated. Although a large share of restorable mangrove is in Australia (more than 5% of global total), we see positive BCRs for east and southern states of Australia but a BCR around 1 for the other states. Countries with the highest BCRs are Taiwan, Singapore, and China (Table D-1).

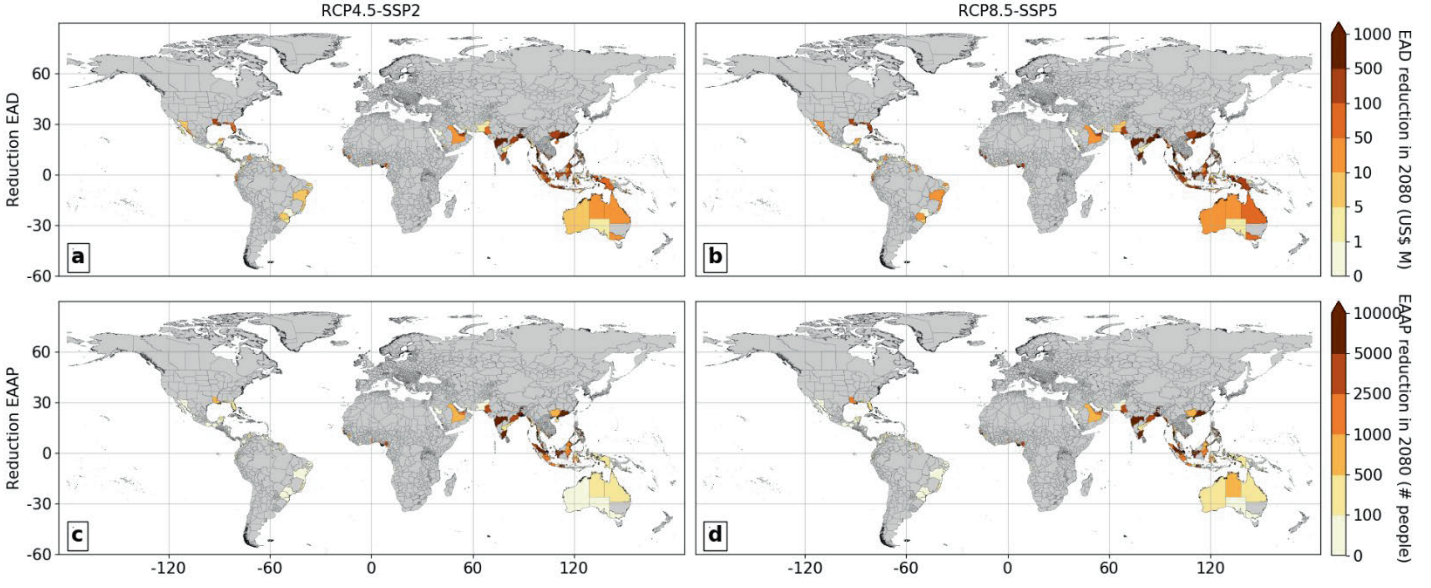

Figure 5-2: Future (2080) potential risk reduction in EAD (4a and 4b) and EAAP (4c and 4d) for sub-national regions under the scenarios RCP4.5/SSP2 (4a and 4c) and RCP8.5/SSP5 (4b and 4d).

Figure D-4 shows the total discounted benefits of mangrove restoration for sub-national regions for RCP4.5/SSP2. Most of the areas that show BCRs lower than or close to 1 have relatively low total discounted benefits. Other sub-national regions with relatively high total discounted benefits (high percentage of assets), but low BCRs are mostly located in high-income countries such as Australia or the United States (Florida), as adaptation measures in these regions are more expensive due to higher prices for resources and labour. BCRs for the RCP8.5/SSP5 scenario show similar patterns, albeit with higher B:C ratios, and are found in Figure D-5.

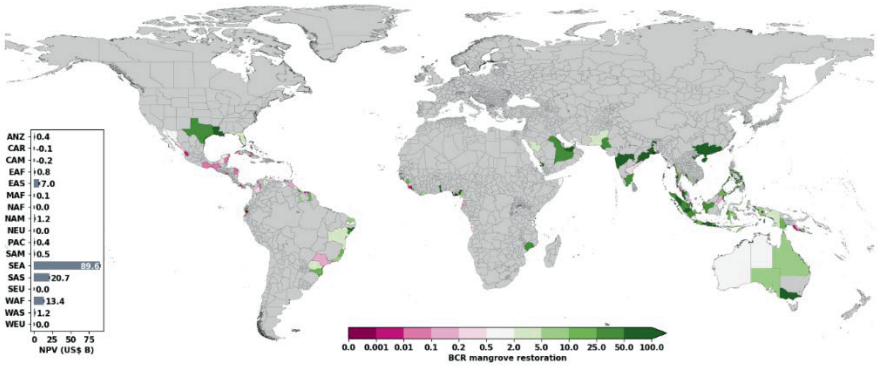

Figure 5-3: Benefit-Cost Ratios of mangrove restoration under the future scenario of RCP4.5/SSP2 shown for sub-national regions in the world plot and sub-continental regions in the subplot. Regions that show up in grey are indicated to have no intersection of mangrove restoration, coastal flooding and/or exposure. ANZ, Australia and New Zealand; CAR, Caribbean; CAM, Central America; EAF, Eastern Africa; EAS, Eastern Asia; MAF, Middle Africa; NAF, Northern Africa; NEU, Northern Europe; PAC, Pacific regions that include Melanesia, Polynesia, and Micronesia; SAM, South America; SEA, South-eastern Asia; SAS, Southern Asia; WAF, Western Africa; WAS, Western Asia; WEU, Western Europe.

5.5 Poverty analysis of mangrove restoration

We find that people living in poverty constitute a large proportion of the population living in flood prone areas: 75% (25 million people) in Bangladesh; 67% (300 thousand people) in Nigeria; and 87% (80 thousand people) in Pakistan. In Bangladesh this is a similar ratio as the whole of the country, but in Nigeria it is lower than in the whole of the country (67% vs 74%), whilst in Pakistan it is higher (87% vs 51%) as Nigeria has most of the assets located at the coast. People living in poverty is expected to increase by the year 2050, however the people living in flood prone areas relative to country totals stay approximately the same.

Table 5-2: Population living in poverty for country statistics, population living in flood prone areas and population living in areas where Nature-based Solutions (NbS) are possible.

		Country population		Flood prone population		Population with NbS	
Country	Time	**In poverty**	**Total**	**In poverty**	**Total**	**In poverty**	**Total**
Bangladesh	**Present-day**	114 (76%)	149	26 (75%)	34	11 (75%)	15
	2050	196 (76%)	150	41 (74%)	56	14 (75%)	19
Nigeria	**Present-day**	117 (74%)	158	0.3 (67%)	0.4	0.3 (67%)	0.4
	2050	277 (75%)	370	1.6 (66%)	2.5	1.6 (66%)	2.5
Pakistan	**Present-day**	88 (51%)	173	0.08 (87%)	0.1	0.08 (88%)	0.09
	2050	151 (52%)	292	0.16 (81%)	0.2	0.16 (81%)	0.2

When looking at the wealth distribution of the population in areas of potential mangrove restoration and the population outside these areas, we find that wealth is unevenly distributed for several countries. Figure 5-4 shows this difference as shifts in distributional population curves between people living outside flood prone areas (red), people living inside flood prone areas (blue), and people living inside flood prone areas with mangrove restoration benefits (green). We find that the population distributions of regional wealth index for people living in flood prone areas with mangrove benefits are more likely to have a lower wealth index than the people outside flood prone areas. This is significantly different in Bangladesh, El Salvador, Mexico, Indonesia, and the Philippines. Looking at the distributional curves of for instance Bangladesh and Cameroon, we observe that people with higher wealth index (>0) are almost exclusively found in regions where no mangrove restoration is possible. Furthermore, we show that people with a higher wealth index (0 and higher), are more likely to be living outside flood prone areas as is clearly shown for example for Cameroon, Colombia, El Salvador, India, Mexico, Nigeria, and Vietnam. Mangrove restoration for El Salvador is estimated to be not feasible in economic terms, although when looking into equity aspects of adaptation strategies it is apparent that people with a lower wealth index in that country would benefit from mangrove restoration. Taken together, these findings show that, in some countries, mangrove restoration as an adaptation measure favours population with lower wealth levels, and as such could contribute to reducing inequality.

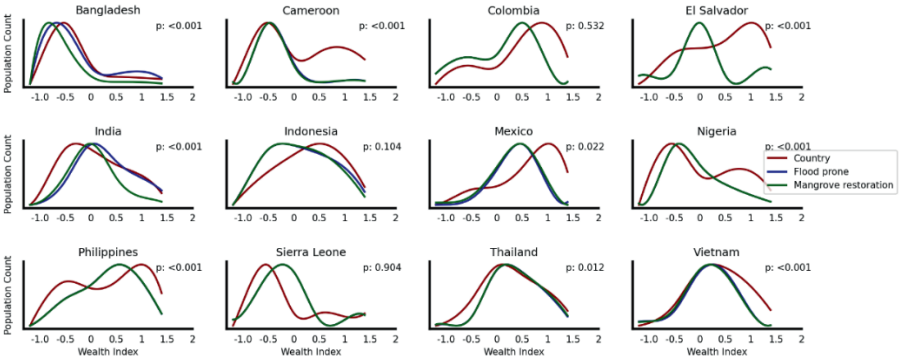

Figure 5-4: Normalized distribution of the wealth index for people living outside flood prone, inside flood prone and mangrove restoration areas. Note the order of lines is red → blue → green.

5.6 Discussion

We present the first global-scale assessment of mangrove restoration and its impact on current and future potential flood risk reduction and the benefits of mangrove restoration as adaptation measure under scenarios of socioeconomic and climate change. The results of the study show that mangrove restoration is an effective measure to contribute to future flood risk mitigation and indicates that future benefits of mangrove restoration can be assessed using existing flood risk assessment frameworks. Overall, this study indicates that mangroves can be efficient and cost-effective in reducing risk in many regions. These findings are in line with other studies on risk reduction by present ecosystems, such as Beck et al., 2018; Menéndez et al., 2020; Tiggeloven et al., 2021; and van Zelst et al., 2020. In a study on the global flood protection benefits of present-day mangroves, Menéndez et al. (2020) estimated a potetnial reduction in present-day EAD of 9% of the total. Tiggeloven et al. (2021) estimated the same reduction in EAD of US$2.5 billion, or 13% of global EAD. By implementing mangrove restoration, we estimate an additional US$1.5 billion, or 10% of global EAD, additional reduction in EAD. Previous research identified potential extent of mangroves to be restored (Worthington et al., 2018) and their potential storm-protection benefits (Barbier, 2017). For example, a meta-analysis of potential benefits of mangrove restoration by Su et al. (2021) suggests that mangrove restoration is a cost-effective measure that offers positive benefit-cost ratios between 6 and 10. In our assessment, we estimate benefit-cost ratios of mangrove restoration at the global scale is 33-70 for RCP4.5/SSP2. However, most of the individual regions have benefit-cost ratios between 2 and 10, with a maximum reach of a benefit-cost ratio of 100.

While most of the sub-national regions indicate positive return on investments, certain regions (for example, areas of the Caribbean and South America) have benefit-cost ratios below 1. However, mangrove restoration can still be valuable to communities on a smaller scale as potential flood risk reduction can still be realized. Such numbers are based on full mangrove restoration; however, they do not account for the many other benefits that are provided by mangroves, which will, in turn generate considerable additional value. We also show the importance of looking beyond absolute risk values in order to assess the benefits of measures. Here, we use poverty indicators to understand the range of impacts of adaptation on different people. We show that the effects of restoring mangroves are unevenly distributed across the population in terms of poverty, and that only looking into property damages and people exposed is not enough to understand the range of impacts of adaptation on people on the ground.

While this study focusses solely on flood protection benefits of mangrove restoration, other co-benefits of Nature Contributions to People (NCP), such as fishery, carbon

storage and tourism (Spalding & Parrett, 2019; Zeng et al., 2021; zu Ermgassen et al., 2020), are not included. These NCPs can consist of provisions (e.g., timber and charcoal), regulation (e.g., erosion control and saltwater intrusion), habitat (e.g., fishery and biodiversity), and cultural services (e.g., recreation) (Akber et al., 2018). Including the value of these and other NCPs could increase the economical feasibility of mangrove restoration (Dahdouh-Guebas & Cannicci, 2021). For Example, Worthington et al. (2018) show that the global restoration of mangroves could contribute to the sequestration of 69 million tons of carbon in above-ground biomass and 269 million tons of soil carbon. It could also provide habitat for trillions of finfish, crabs and shrimps, among other species. Also Education and training of practitioners and scientists in public and private sectors is vital to enhance understanding on the protection and management of (restored) mangroves (Erwin, 2009). Particularly as Rahman & Mahmud (2018) note that without strong will of these sectors and local people, restoration efforts are challenging and likely to fail.

While we focus on the global scale, it is critical to reassess the findings of this study on the regional and local scale in order to correctly interpret the feasibility of mangrove restoration at smaller scales as uncertainties and biases exists in global flood risk models (Hinkel et al., 2021). Given this global scale, this study made several assumptions. Firstly, it is based on a simplified premise that all potential restoration areas are restored and so provides an upper limit on possible benefits as of several other drivers may reduce the efficacy of restoration, such as seedling failure, the planting of monospecific stands, and the poor choice of planting sites in tidal zones. In general, local site assessment and community knowledge are critical to successfully start and continue mangrove restoration projects (Frantzeskaki, 2019; Nguyen et al., 2016; Valenzuela et al., 2020). Moreover, the effects of spatial and temporal variations of the vegetated foreshore and stability of vegetation during extreme conditions is not included in this study, which can contribute to uncertainty in mangrove effectiveness to coastal protection (Vuik et al., 2018). In reality, restoration is restricted by social, cultural or economic barriers, as well as biophysical restrictions (Lovelock & Brown, 2019). Even considering that benefits may only be a proportion of those described here, it should also be noted that partial restoration may not yield directly proportional benefits. Also, our models assume a mature forest, where in reality it can take some years for a restored mangrove to deliver such benefits. Next to this, the potential role of mangroves to maintain surface elevation through vertical accreation with sea level rise is not taken into account here (Lovelock et al., 2015; Saintilan et al., 2020). Several other limitations exist and are discussed in Tiggeloven et al. (2020) for calculations on (future) flood risk and assessment on economic feasibility of adaptation, in van Zelst et al. (2021) for wave propagation and role of foreshore vegetation, and in Tiggeloven et al. (2021) for benefits of foreshore vegetation in terms of potential flood risk reduction.

Our analysis strengthens the body of evidence that mangrove restoration may be critical in climate adaptation. As a Nature-based Solution, mangrove restoration overcomes long-term forecast uncertainty without the risk of under or overprotecting (e.g. with dikes), and enables the continuation of natural coastal dynamics as they provide additional benefits. Risk reduction in coastal areas comes from a combination of factors, including engineering and societal change and adaptation. In future it might be possible to enhance work such as this, for example by incorporating hybrid adaptation strategies that use both grey and green infrastructure are showing potential to further optimise flood risk strategies (Du et al., 2020; van Zelst et al., 2021). While the economic estimates can be powerful means to influence policy they show some weighting towards wealthy nations with high GDP while EEAP statistics highlight the particular benefits that would accrue to LIMCs, notably in Asia and Africa. Implementation of Nature-based Solutions can be used as integral component of design policies, strategies and action, and can be implemented in an integrated manner to tackle global societal challenges (Cohen-Shacham et al., 2016; Maes & Jacobs, 2017; Seddon et al., 2020).

Although a proxy analysis, we believe that this study provides valuable insight into the feasibility of mangrove restoration at the global scale, and support the need for sustainable adaptation and large-scale implementation of Nature based Solutions. Furthermore, implementing adaptation measures, such as mangrove restoration, in LMICs can contribute to the resilience of people in poverty, driving poverty alleviation and helping to tackle poverty traps.

5.7 Methods

This study estimates global-scale (future) flood protection benefits of mangrove restoration under scenarios of socioeconomic and climate change. We extend on the methodology to assess reduction in coastal flood risk by implementing Nature-based Solutions described in Tiggeloven et al. (2022) by including areas of potential mangrove restoration in the modelling scheme. Generally, we take the following main steps: (1) Coastal foreshore setup and protection level estimation; (2) Flood risk modelling; (3) benefit-cost analysis for scenario combinations of RCP4.5/SSP2 and RCP8.5/SSP5; and (4) poverty analysis. In brief, we use the wave attenuation model of van Zelst et al. (2021) and mangrove restoration tool by Worthington & Spalding (2018) in order to estimate current and future protection levels (see Figure 5-5). Flood risk is estimated as a function of hazard, exposure and vulnerability (United Nations Office for Disaster Risk Reduction, 2016). Expected Annual Damages (EAD) are calculated over time for scenarios with and without mangrove restoration, where the difference between those two scenarios represents the benefits of restoration. A benefit-cost analysis is performed for mangrove restoration under climate change and socioeconomic change at the global scale, and finally a poverty analysis is assessed for three LMICs with mangrove restoration potential.

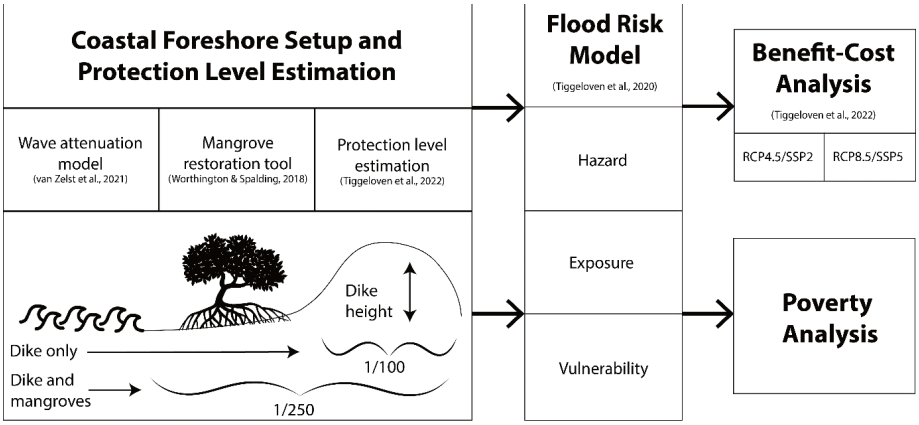

Figure 5-5: Flowchart of the methodology used in this study with an illustration of protection level estimation.

5.7.1 Coastal foreshore setup and protection level estimation

The following section contains a short overview of the coastal properties and wave attenuation model to account for the wave-vegetation interaction as implemented by van Zelst et al. (2021). In brief, cross-shore transects are derived with water level, elevation, wave data and vegetation. Wave attenuation is estimated with the following computational steps: offshore wave propagation, nearshore wave propagation, wave energy dissipation and levee overtopping estimates.

Current dike heights required to prevent inland flooding per return period are estimated by assessing bed levels, hydrodynamic conditions, and wave attenuation for each derived coast-normal transect (495,361 transects in total). These transects are derived from OpenStreetMap and each transect is described by its coastal profile (e.g., slope, ocean bathymetry, foreshore, elevation, length, and surge levels among other things). Wave conditions per foreshore transect from the ERA-Interim dataset (Dee et al., 2011) are obtained by using a peak-over-threshold approach for multiple return periods. Offshore significant wave heights are transformed to a nearshore wave height limited by depth-induced breaking. Water levels are derived from the GTSR dataset (Muis et al., 2016) and corresponding wave conditions at different return periods from the ERA-Interim reanalysis (Dee et al., 2011). A lookup-table is used to determine wave attenuation over a foreshore and the resulting significant wave height relevant for the flood defence. This has been done by combining 668,304 XBeach (van Rooijen et al., 2016) hydrodynamic numerical modelling results for combinations of foreshore slopes, vegetation covers, and hydrodynamic conditions (van Zelst et al., 2021). This table contains wave heights at regular intervals along a steady slope, both with and without mangrove vegetation as modelled by XBeach. To represent a worst-case scenario, wave angle of incidence is assumed to be coast normal. Coastlines where there is no urban area or where there is no simulated inundation are excluded.

Mangrove restoration is assessed under different scenarios of socioeconomic and climate change. In brief, we assess mangrove restoration using the mangrove restoration potential map derived from Worthington & Spalding (2018) and estimate the (future) benefits of this strategy. To assess the effectiveness of this adaptation measure, we perform a benefit-cost analysis and estimate flood protection benefits under climate change and socioeconomic change. The Mangrove Restoration Potential Map shows areas of recent (1996-2016) mangrove loss and identifies, within these locations, those areas where mangroves show potential to be restored. In total it identifies over 800,000 ha of restorable mangrove areas, which amounts to nearly 6% of the total global extent of mangrove area. This map is spatially intersected with the transects use in the wave attenuation model. Potential effects of mangrove restoration on flood risk reduction are estimated through difference in protection levels of foreshores with and without mangrove restoration. Present-day coastal flood protection levels including current mangroves are taken from Tiggeloven et al. (2020). The wave attenuation effects of mangrove restoration are calculated using the same foreshore set-up, resulting in the increase in protection levels due to the increase in wave-vegetation interaction of the restored mangroves. Countries that show the highest percentage of mangrove loss are the USA, Mexico, and Vietnam. southeastern Asia has the largest extent of potentially restorable mangrove areas, with approximately 50% of the global restorable mangrove extent (Worthington & Spalding, 2018). To estimate mangrove restoration benefits for flood protection, we spatially analysed the area of mangroves to be restored per transect that is prone to flood risk. Figure 5-6 shows mangrove locations with restoration potential, aggregated to sub-national regions. Among these regions we see that sub-national regions in Nigeria, Brazil, Bangladesh, and Indonesia have the highest restorable density of regions that are prone to flood risk.

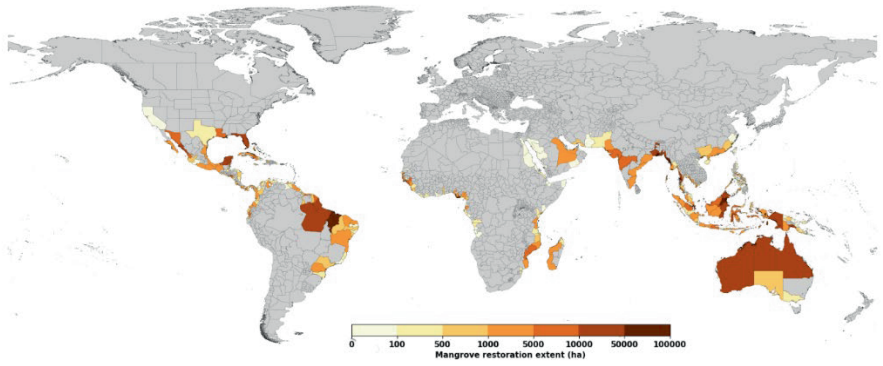

Figure 5.6: Total extent of mangrove forests in hectares potential to be restored, aggregated to the sub-national level.

5.7.2 Flood risk estimation

We combine coastal flood hazard layers with exposure data and vulnerability curves to estimate the flood impacts by using the GLOFRIS impacts module developed by Ward et al. (2013), extended for future simulations by Winsemius et al. (2016), and extended to coastal flood risk assessment by Tiggeloven et al. (2020). The flood impacts are assessed at a horizontal resolution of 30" × 30" and simulated for several return periods.

Flood hazard: We simulate coastal water levels using hydrodynamic simulations of tide and surge, and scenarios of regional sea-level rise. We use these data to generate sea levels for nine different return periods (2, 5, 10, 25, 50, 100, 250, 500, and 1000 years), which are in turn used to force a planar inundation model that accounts for attenuation similar to Vafeidis et al. (2019), and is described in detail by Tiggeloven et al. (2020). Extreme sea level values from the Global Tide and Surge Reanalysis (GTSR) dataset by Muis et al. (2016) are taken to calculate inundation depths using the Multi-Error-Removed Improved-Terrain (MERIT) DEM (Yamazaki et al., 2017) at a 30" x 30" resolution as underlying topography. Because tropical cyclones are poorly represented in the climate input data of GTSR, we use an enriched version of GTSR that includes simulated tropical cyclones using the IBTrACS (International Best Track Archive for Climate Stewardship) archive, as described by Tiggeloven et al. (2020). We apply a resistance factor to simulate the reduction of flooding land inwards as tides and storm surges have a limited time span.

In our flood hazard simulations, we use projected sea-level rise to simulate future extreme sea levels and land subsidence rates to estimate how the terrain may change. Global mean sea-level rise projections are obtained from the RISES-AM project (Jevrejeva et al., 2014) and regionalized using spatial variability associated with gravitational-rotational fingerprints (Jackson & Jevrejeva, 2016). We use sea-level rise for two Representative Concentration Pathways (RCPs), namely RCP4.5 and RCP8.5, and include a range of probabilistic outcomes (5^{th}, 50^{th} and 95^{th} percentiles). Subsidence rates are more regionally distributed, at some regions higher than sea-level rise rates, and are taken from the SUB-CR model by Kooi et al. (2018). In this approach, subsidence is modelled due to groundwater extraction, which is the dominant factor of human-induced subsidence in many coastal areas (Erkens et al., 2015; Galloway et al., 2016).

Flood exposure: The methodology to derive flood exposure in terms of built-up area, population and GDP are described in Tiggeloven et al. (2020). Built-up area refers to all urban areas and artificial surfaces. Current maximum economic damages are estimated using the methodology of Huizinga et al. (2017). As an approximation of percentage area per occupancy type, we set the urban grid cells to 75% residential, 15% commercial and 10% industrial, based on a study by the Buildings Performance Institute Europe (BPIE, 2011) and a comparison of European cities' share of occupancy

type of the CORINE Land Cover data (EEA, 2016). Following Huizinga et al. (2017), the density of buildings per occupancy type are set to 20% for residential and 30% for commercial/industrial. Future simulations of built-up area are taken from Winsemius et al. (2016) at a resolution of 30" x 30". To estimate future maximum damages, we scale the current values with growth in GDP per capita per country from the SSP database. Boundaries of countries are derived from the Global Administrative areas dataset (GADM, 2012). To calculate future risk relative to GDP and population exposed, future gridded population and GDP values are taken from Van Huijstee et al. (2018), which uses the national GDP per capita from the SSP database as input.

Flood vulnerability: By using different global flood depth-damage functions vulnerability to flood water of urban areas is estimated for each occupancy type and are taken from Huizinga et al. (2017). The resulting damages are represented as a percentage of the maximum damage, reaching maximum damages at an inundation depth of 6 meters. Subsequently, flood impacts are calculated by estimating the percentage of maximum damage per occupancy type at the required inundation depth and is expressed in the following equation:

$$I_\theta(w) = \theta_r(w)M_r + \theta_c(w)M_c + \theta_i(w)M_i \tag{5-1}$$

where I_θ is the flood impact at inundation depth of w, θ is the vulnerability at a certain inundation depth, and M is the maximum damage assigned for residential (r), commercial (c) and industrial (i) occupancy types.

Flood risk: Through assessing flood impacts per return period flood risk in terms of EAD is estimated at the resolution of 30" x 30". EAD can be estimated by taking the integral of the exceedance probability-impact (risk) curve (Meyer et al., 2009) and is shown in the following equation:

$$D = \int_{p=0}^{1} I_\theta(p)dp \tag{5-2}$$

where D is EAD, I is the urban damage (or impact) with θ representing the vulnerability, and p denotes the annual probability of non-exceedance. To fit a protection level of a coastal region in the risk computation, the risk curve is truncated at the exceedance probability of the protection level (expressed as a return period). To estimate the definite integral, we use the trapezoidal approximation. As data on protection levels of coastal regions are not available for many regions, we estimate current protection levels for coastal regions using the FLOPROS modelling approach (Scussolini et al., 2016),

which is described and validated for the coastal flood protection by Tiggeloven et al. (2020). Using the same approach, Expected Annual Affected Population (EAAP) is estimated by replacing the damage with population exposed to a flood hazard. EAD and EAAP are estimated with and without mangrove restoration.

5.7.3 Benefit-cost analysis

We perform a benefit-cost analysis and estimate the feasibility of an investment with two indicators, namely Net Present Value (NPV), which is the net return on investment discounted to present value, and the Benefit-Cost Ratio (BCR), which is the ratio between discounted benefits and discounted costs. The benefit of the investment in adaptation is the avoided damages expressed as the difference between EAD with and EAD without mangrove restoration (equation 3).

$$B = \int_{p=0}^{p=p_n} I_\theta(p)dp - \int_{p=0}^{p=p_a} I_\theta(p)dp \tag{5-3}$$

where B is the benefit of investment, p_n is the annual probability of non-exceedance when no adaptation is implemented, and p_a is the annual probability of non-exceedance when adaptation is implemented. The costs of mangrove restoration are set to US$2000 per hectare of mangroves and maintenance costs are set to US$50 per hectare per year based on the following studies (J. C. J. H. Aerts, 2018; Bayraktarov et al., 2016; Marchand, 2008; Siddharth Narayan et al., 2016). Subsequently, the costs are converted to US$2005 Power Purchasing Parity (PPP) by first adjusting to US$2005 values using GDP deflators from the World Bank Open Data website (https://data.worldbank.org/) and then using PPP to market exchange rates from OECD, taken from the IIASA SSP database (Riahi et al., 2017).

To calculate the total benefits and costs of mangrove restoration at present value, they are calculated for each time step set to years (until 2100), summed, and discounted over time. BCR are estimated by dividing the total discounted benefits by the total discounted costs, following equation 4 and NPV following equation 5.

$$R_C^B = \left. \sum_{t=1}^{n} \frac{B_t}{(1+r)^t} \middle/ \left(\sum_{t=1}^{n} \frac{C_t}{(1+r)^t} \right) \right. \tag{5-4}$$

$$V = \sum_{t=1}^{n} \frac{B_t - C_t}{(1+r)^t} \tag{5-5}$$

Where R_C^B is the benefit-cost ratio, C_t the costs at time t, V the net present value, and r is the discount rate. The benefit-cost analysis is performed by calculating the benefits and costs for adaptation for sub-national regions. These regions are defined as the next administrative unit below national scale in the Global Administrative Areas Database (GADM). The benefits and costs are discounted with a discount rate of 5%.

The analysis is carried out for two different sea-level rise scenarios (using RCPs) and five different socioeconomic scenarios (using SSPs). All the results are shown for two scenario combinations (van Vuuren et al., 2014), namely RCP4.5/SSP2 and RCP8.5/SSP5. The former is used for a 'middle of the road' scenario with medium challenges and adaptation (Riahi et al., 2017) that can broadly be aligned with the Paris agreement targets (Tribett et al., 2017), while the latter is used as a 'fossil-fuel development' world (Kriegler et al., 2017). Results of the other combinations can be found in the supplementary data.

5.7.4 Poverty analysis

In this study we provide an assessment of the distributional impacts of mangrove restoration for two poverty indicators: people living below a poverty line (Tatem et al., 2013) and regional wealth index (Chi et al., 2021). We estimate these effects on poverty indicators for three population groups, namely: (1) population living outside flood prone areas; (2) population living in flood prone areas; and (3) population living in flood prone areas who may benefit from mangrove restoration. For the first indicator, people living under a poverty line, three countries were selected where mangrove restoration is possible and gridded data of people living under a poverty line are available, namely Bangladesh, Nigeria, and Pakistan. For Bangladesh we use the Bayesian-based geostatistics map from Steele et al. (2017), using US$2.5 per day as poverty line. For Nigeria and Pakistan, the mean likelihood of people living in poverty from Tatem et al. (2013) is used. Furthermore, the distributional impacts of mangrove restoration on population dynamics are assessed with the regional wealth index to estimate differences in population distributions per population group. Distributional curves of population frequency and wealth index for the three population groups are assessed with the dataset of micro estimates of population regional wealth index by Chi et al. (2022) for 2018 at the resolution of 2.4km. For the Kuhlna region in Bangladesh, we use the regional wealth index estimates from Steele et al. (2017) because of better coverage. We assess the effects on both indicators by using an overlay of the population living in the three areas with the likelihood of people living in poverty and the wealth index for each of the three countries. To test for differences between populations in the different areas, the Mann-Whitney U test is selected, as distributions were not found to be Gaussian.

6 Hybrid Solutions

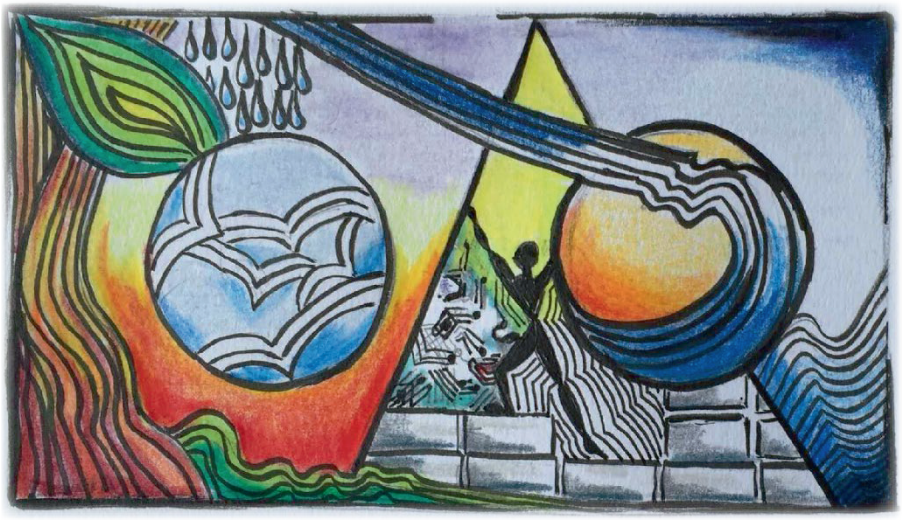

This chapter is based on

Tiggeloven, T., de Moel, H.. & Ward, P. J. (2022). Hybrid solutions and global coastal flood risk management. *In review*

Abstract

To implement and raise awareness of coastal climate change adaptation, it is important to better understand the effectiveness of coastal flood risk adaptation strategies, such as Nature-based Solutions and hybrid strategies. In this study, we use a modelling approach to assess costs and benefits of such adaptation strategies. Additionally, we explore the impact of adopting Nature-based Solutions in coastal areas in relation to the alleviation of poverty conditions. Our analysis shows that Nature-based Solutions increase the cost-effectiveness of adaptation strategies for two-thirds (68%) of the regions assessed. Globally, we estimate a total reduction in the cost of structural adaptation measures of 8% by implementing two types of Nature-based Solutions (restoration 2% and conservation 6%), and that regionally the highest Net Present Value can reach almost US$1 trillion for sub-national units. Furthermore, we find that populations living in flood-prone areas where nature-based solutions are possible have a relatively low wealth index. Implementing such adaptation measures, such as mangrove restoration and conserving foreshore vegetation, in Low- and Middle-Income Countries (LMICs) can contribute to the resilience of people living in poverty, driving poverty alleviation, and helping to tackle poverty traps.

6.1 Introduction

Coastal floods are one of the deadliest (Callaghan et al., 2014; Creach et al., 2016; CRED, 2015) and costliest (Hinkel et al., 2014; Kron, 2012.; Wahl et al., 2017) natural hazards, triggering or contributing to economic disruption (Koks et al., 2019; Mandel et al., 2021), displacement (Hauer et al., 2019; Robert McLeman, 2018), and poverty traps (Hallegatte & Rozenberg, 2017; Winsemius et al., 2018). In the coming century, coastal communities are projected to face increases in coastal flood risk (Brown et al., 2018; Hallegatte et al., 2013; Hinkel et al., 2014; Jongman et al., 2012; Merkens et al., 2018; Neumann et al., 2015) as coastal areas are experiencing increases in urban development, sea-level rise, and degradation of foreshore vegetation (Brown et al., 2018; Deb & Ferreira, 2017; Neumann et al., 2015). Next to sea-level rise, climate change may lead to increase in extreme sea levels (Vousdoukas et al., 2017) due to increases in storm surges (Tebaldi et al., 2012) and tides (Pickering et al., 2012). Coastal zones are among the most highly developed areas in the world, containing a multitude of human settlements (Neumann et al., 2015), critical infrastructure (Koks et al., 2019) and ecosystem services (Erwin, 2009). Moreover, coastal zones are attractive locations for human settlement: between 1990 and 2000 almost two-thirds of urban settlements with population higher than 5 million were at least partly located in coastal zones (McGranahan et al., 2007). Furthermore, people living in poverty are particularly vulnerable to shocks such as coastal flooding. Increases in coastal flood risk due to sea level rise, increased storminess and removal of coastal ecosystems can lead to self-

reinforcing mechanisms that ''trap'' people in poverty (i.e., poverty traps; Dasgupta, 2007; Hallegatte, 2016; Hallegatte & Rozenberg, 2017; Winsemius et al., 2018).

Generally, flood risk can be reduced by implementing adaptation measures such as structural measures (e.g., dikes and levees) and Nature-based solutions (Cheong et al., 2013; Hinkel et al., 2014; Jongman, 2018). Nature-based Solutions for coastal protection consists of maintaining or restoring vegetation on the foreshore, reducing wave intensity and therefore decreasing the run-up of surge events (Barbier et al., 2008; Shepard et al., 2011). Nature-based Solutions not only protect against coastal flood risks, but also provide other benefits, such as improved water quality, recreational opportunities, fisheries support and enhanced carbon sequestration (Barbier et al., 2011).

Instead of solely focusing on either structural measures or Nature-based Solutions, Jongman (2018) argues that flood risk management needs to adopt holistic strategies to adapt to climate change, such as hybrid strategies. Hybrid strategies can combine structural measures with Nature-based Solutions, such as dikes and levees in combination with maintaining or restoring foreshore vegetation. For example, Du et al. (2020) show for a case study in Shanghai that hybrid strategies that include both structural measures and Nature-based Solutions will reduce future flood risk more than structural measures only, while having higher return on investments.

Given the expected increase in coastal flood risk, it is critical to improve our understanding of global coastal flood risk and the effectiveness of adaptation strategies to reduce those risk. The importance of climate change adaptation and disaster risk reduction is recognized in several global agreements, such as the Paris Agreement (United Nations Framework Convention on Climate Change, 2015) and the Sendai Framework for Disaster Risk Reduction (United Nations Office for Disaster Risk Reduction, 2015). However, decision makers face difficulties in aligning with these global agreements, partly due to a poor understanding of the effectiveness of potential adaptation measures. Cost-benefit analyses can provide insights on the efficacy of certain adaptation measures on reducing coastal flood risk. Further, the impact of coastal flood adaptation measures needs to be evaluated also beyond monetary terms. Including poverty in adaptation policies will extend the impact analysis beyond the valuation of reduction in flood risk in monetary terms (Hallegatte & Rozenberg, 2017; Winsemius et al., 2018), and will reveal how poverty is integrated into adaptation (Araos et al., 2021).

So far, no studies have provided a global scale analysis on the feasibility of implementing hybrid strategies to reduce the expected increase in future coastal flood risk. To better understand the impacts of hybrid strategies on coastal flood risk reduction, we assess the effects and feasibility of structural measures and Nature-based

Solutions in the form of conserving foreshore vegetation, mangrove restoration, and a combination of those. Further, we assess the spatial pattern of vulnerability indicators (poverty and regional wealth index) to assess where the benefits of Nature-based Solutions could potentially amplify when looking into non-monetary indicators.

6.2 Methods

Without adaptation, future protection levels will likely decline due to sea-level rise and subsidence. This can be compensated by adding new measures or increasing the standard of existing measures (structural Nature-based Solutions, or a combination thereof). In this study, we assess the effectiveness of these different coastal flood adaptation strategies at the global scale under scenarios of socioeconomic and climate change. We extend on the methodology described in Tiggeloven et al. (2022), which describes a method to assess the flood risk benefits of Nature-based Solutions, by including hybrid strategies in the modelling scheme. In summary, we take the following main steps: (1) Selection of **adaptation measures and protection level** estimation using the wave attenuation model by van Zelst et al. (2021), coastal FLOPROS protection estimates by Tiggeloven et al. (2020) and mangrove restoration tool by Worthington & Spalding (2018); (2) **Flood risk estimation** by combining data of hazard, exposure, vulnerability and protection levels; (3) **benefit-cost analysis** using the future scenarios of RCP4.5/SSP2 and RCP8.5/SSP5; and (4) **vulnerability indicator analysis** using the regional wealth index by Chi et al. (2021). A detailed description of the methods used for estimating the protection levels and for the cost-benefit analysis can be found in Tiggeloven et al. (2022). A detailed description on the coastal flood risk model used in this study can be found in Tiggeloven et al. (2020).

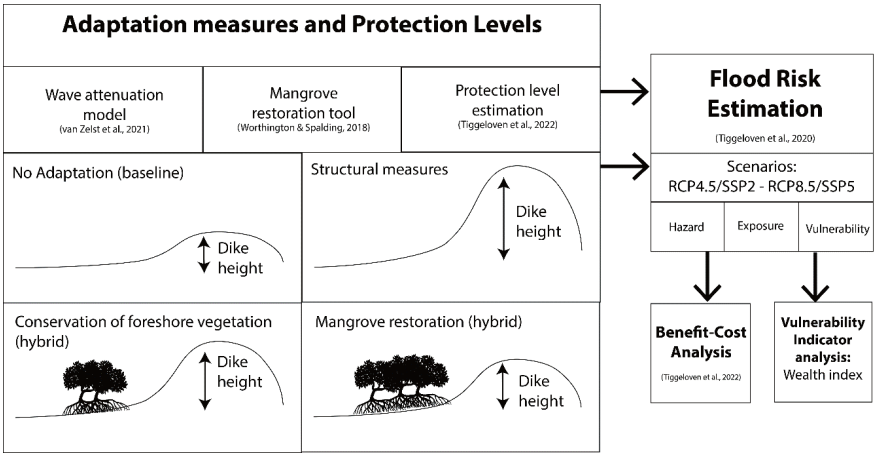

Figure 6-1: Flowchart of the methodology used in this study with illustrations of protection level estimation for the four different adaptation strategy scenarios.

6.2.1 Adaptation measures under scenarios of change

The following adaptation measures are assessed for scenarios of socioeconomic and climate change: no adaptation, structural measures (dikes/levees), and two hybrid strategies with a combination with dikes and Nature-based Solutions. The first of these hybrid strategies is a combination between dikes and conservation of foreshore vegetation, and the latter extends on this this by also including mangrove restoration. For each of these adaptation measures, the objective is set to keep current protection levels constant in the future. We also simulate a baseline scenario in which no adaptation is implemented, meaning that current protection is maintained at its current height. For a detailed description on global coastal adaptation strategies, we refer the reader to Tiggeloven et al. (2020) for structural measures and Tiggeloven et al. (2021) for future benefits of conserving foreshore vegetation.

No adaptation (baseline)

The no adaptation strategy serves as the baseline strategy throughout this paper. Here, dike heights are maintained and kept at their present-day heights. Without adaptation measures, the future protection levels will decline due to sea-level rise and degradation of foreshore vegetation, and risk will increase because of this and socio-economic change. The benefits of adaptation measures will be estimated by the reduction in risk compared to this baseline strategy.

Structural measures

The height of dikes required to keep current protection levels constant are estimated with the wave attenuation model by van Zelst et al. (2021), which uses empirical EuroTop formulations (Pullen et al., 2007) and are based on a standard 1:3 dike profile without berms and with a maximum allowed overtopping discharge of 1 L/m^2/s given foreshore condition and extreme sea levels. Water levels are derived from the GTSR dataset (Muis et al., 2016) and corresponding wave conditions at different return periods from the ERA-Interim reanalysis (Dee et al., 2011). We exclude coastlines where there is no built-up area, or no inundation is simulated. To estimate future dike heights, we also use regional sea-level rise from Jackson and Jevrejeva (2016) for the RCP4.5 and RCP8.5 scenarios.

Conservation of foreshore vegetation (hybrid)

The conservation approach includes keeping foreshore vegetation extent and dimensions for the future the same as they are now. This approach will focus on the flood protection benefits where foreshore vegetation is conserved and safeguarded so that no more areas will be degraded. The wave attenuation model for present-day foreshore conditions is complemented with areas where foreshore vegetation, such as salt marshes and mangroves, are present. This allows us to account for the wave-vegetation interaction and to estimate the effects of foreshore vegetation on wave

damping. Maps of salt marshes are derived from Mcowen et al. (2017) and mangroves from Giri et al. (2011), complemented with Corine Land Cover (CLC, Europe only) and GlobCover v2.2 maps where the former lack coverage.

Mangrove restoration (hybrid)

The second Nature-based Solution is mangrove restoration, which will focus on restoring mangrove forests globally in areas that show potential for mangrove forests to be restored. To identify these areas, we use the Mangrove Restoration Potential Map of Worthington & Spalding (2018), which maps areas where mangroves show potential to be restored (estimated a total of 800,000 ha). As with the current foreshore vegetation, the mangrove restoration is added to the wave attenuation model to estimate the effects of wave dampening.

6.2.2 Flood risk model

Flood risk is estimated as a function of hazard, exposure and vulnerability (UNDRR, 2016). To estimate the flood hazard, we use the approach described in Tiggeloven et al. (2020). Here we summarise the main points and refer the reader to the paper for further details.

Hazard: We use coastal water levels using hydrodynamic simulations of tide and surge of the GTSR model (Muis et al., 2016c), and scenarios of regional sea-level rise for the RCP4.5 and RCP8.5 scenarios. Flood hazard is represented by maps of inundation depth for several return periods of sea levels taken from GTSR (2, 5, 10, 25, 50, 100, 250, 500 and 1000 years) and are used to force a planar inundation model that accounts for attenuation, similar to Vafeidis et al. (2019). As underlying topography, we use the Multi-Error-Removed Improved-Terrain (MERIT) DEM (Yamazaki et al., 2017) at a 30" x 30" resolution.

Exposure: We represent exposure using maps of urban density, population, and GDP at a resolution of 30" x 30". The maps for the current situations are taken from Van Huijstee et al. (2018). For the future, we use maps from the 2UP model (Van Huijstee et al., 2018), using SSP1-5, for time-periods 2010-2080. Future simulations of built-up area are taken from Winsemius et al. (2016) at a resolution of 30" x 30". To estimate future maximum damages, we scale the current values with growth in GDP per capita per country from the SSP database. We set the area of occupancy type per grid cell to 75% residential, 15% commercial, and 10% industrial, similar to Tiggeloven et al. (2020).

Vulnerability: we estimate vulnerability to flooding using different global flood depth-damage functions for each occupancy type, taken from Huizinga et al. (2017). The resulting damages are represented as a percentage of the maximum damage, reaching maximum damages at an inundation depth of 6 meters. Subsequently, flood impacts

are calculated by estimating the percentage of maximum damage per occupancy type at the required inundation depth and is expressed in the following equation:

$$I_\theta(w) = \theta_r(w)M_r + \theta_c(w)M_c + \theta_i(w)M_i \quad (6\text{-}1)$$

where I_θ is the flood impact at inundation depth of w, θ is the vulnerability at a certain inundation depth, and M is the maximum damage assigned for residential (r), commercial (c) and industrial (i) occupancy types.

Risk: Flood risk in terms of Expected Annual Damages (EAD) is estimated through assessing flood impacts per return period at the resolution of 30" x 30". EAD can be estimated by taking the integral of the exceedance probability-impact (risk) curve (Meyer et al., 2009) and is shown in the following equation:

$$D = \int_{p=0}^{1} I_\theta(p)dp \quad (6\text{-}2)$$

where D is EAD, I is the urban damage (or impact) with θ representing the vulnerability, and p denotes the annual probability of non-exceedance. To fit a protection standard of a coastal region in the risk computation, the risk curve is truncated at the exceedance probability of the protection standard (expressed as a return period). To estimate the definite integral, we use the trapezoidal approximation. As data on protection standards of coastal regions are not available for many regions, we estimate current protection standards for coastal regions using the FLOPROS modelling approach (Scussolini et al., 2016), which is described and validated for coastal flood protection by Tiggeloven et al. (2020). Using the same approach, Expected Annual Affected Population (EAAP) is estimated by replacing the impacts with population exposed to a flood hazard.

The analysis is carried out for two different sea-level rise scenarios (using RCPs) and five different socioeconomic scenarios (using SSPs). All the results are shown for two scenario combinations (van Vuuren et al., 2014), namely RCP4.5/SSP2 and RCP8.5/SSP5. The former is used for a 'middle of the road' scenario with medium challenges and adaptation (Riahi et al., 2017) that can broadly be aligned with the Paris agreement targets (Tribett et al., 2017), while the latter is used as a 'fossil-fuel development' world (Kriegler et al., 2017).

Benefit-Cost Analysis

EAD is estimated over time for scenarios with and without adaptation, where the difference between those two scenarios represents the benefits of adaptation. A benefit-cost analysis is performed for the different adaptation strategies under climate change and socioeconomic change at the global scale. The benefits and costs are assessed using

a discount rate of 5% until the lifespan of the structural measures investment and with Operation and Maintenance (O&M) costs of 1%. It is assumed that investments begin in $t = 0$ years and construction is finished in $t = 30$ years, and increasing linearly between, following Equation 6-3.

$$C_t = \{I(u,W)/c, I(u,W) * m, \quad \frac{if\ t < c}{if\ t \geq c} \tag{6-3}$$

, where C_t are the costs at time t in years, m the maintenance costs in percentages, and c is the duration of the construction in years. During this period the benefits will linearly increase.

To assess benefit-cost analyses of adaptation, we use the adaptation objective of keeping future protection levels constant. We estimate the costs of flood protection by summing the maintenance and investment costs over time for raising dikes to prevent flooding, following the methodology described by Ward et al. (2017). To estimate the costs associated with the different adaptation objectives, we estimate the dike dimensions using the same approach described by Tiggeloven et al. (2020). The benefits and costs of adaptation at present value, are calculated for each time step (set to years) until 2100, discounted over time, and summed. Benefit-Cost Ratios (BCR) are estimated by dividing the total discounted benefits by the total discounted costs, following Equation 6-4 and NPV following Equation 6-5.

$$R_C^B = \sum_{t=1}^{n} \frac{B_t}{(1+r)^t} \Bigg/ \left(\sum_{t=1}^{n} \frac{C_t}{(1+r)^t} \right) \tag{6-4}$$

$$V = \sum_{t=1}^{n} \frac{B_t - C_t}{(1+r)^t} \tag{6-5}$$

Where R_C^B is the benefit-cost ratio, C_t the costs at time t, V the net present value, and r is the discount rate. The benefit-cost analysis is performed by calculating the benefits and costs for adaptation for sub-national regions. These regions are defined as the next administrative unit below national scale in the Global Administrative Areas Database (GADM).

Social vulnerability indicator: wealth index

In this study we provide an initial assessment of the distributional impacts of the modelled hybrid strategies for the social vulnerability indicator of regional wealth index. We estimate the coastal flood adaptation effects on these indicators for three

population groups, namely: (1) population living outside flood prone areas; (2) population living in flood prone areas; and (3) population living in flood prone areas that may benefit from Nature-based Solutions, and thus where hybrid strategies are possible. Distributional curves of population frequency and wealth index for the three population groups are assessed with the dataset of micro estimates of population regional wealth index of Chi et al. (2022). We assess the effects on the social vulnerability indicator by using an overlay of the different population groups with population dynamics and regional wealth indices, displacement, and age structures. To test if the population distribution of regional wealth index for people outside flood prone areas and people affected by mangrove restoration are significantly different, the Mann-Whitney U test is selected, as distributions were not found to be Gaussian.

6.3 Results

6.3.1 Hybrid strategies for global coastal flood risk assessment

Our findings show that hybrid strategies often outweigh structural measures in terms of cost-effectiveness when looking at direct flood risk benefits of adaptation measures at the global scale. Our analysis shows that there is value gained in using hybrid strategies compared to structural measures only for two-thirds (68%) of the regions assessed for the scenario RCP4.5/SSP2 as is shown in the left panel of Figure 6-2. Our results (inset bar chart Figure 6-2) show that hybrid strategies have larger BCR than structural measures in 100% of the sub-national unites in Northern America, 82% in Western Europe, and 75% Australia and New Zealand. 85% of the sub-national unit assessed in Western Africa, 85% in Eastern Africa, and 70% in Central America show a favour for using structural measures only.

To show the effectiveness of combining measures, we estimate the increase or decrease in cost-effectiveness in terms of change in BCR between structural measures only and hybrid strategies (Fig 6-2, main map). For some regions in which the BCR of a hybrid strategy exceeds that of the structural measures strategy, the difference in BCR between the two exceeds 50%, such as in Quebec (Canada), Picardie (France), Thái Bình (Vietnam), East (Singapore), Yuen Long (Hong Kong), Aysén (Chili), and Northern Territory (Australia). On the other hand, there is only one sub-national region where the structural measures strategy is showing an increase higher than 25% and that is Nayarit (37%, Mexico). In other words, although some regions have a higher BCR for structural measures in some regions, the difference is generally less pronounced.

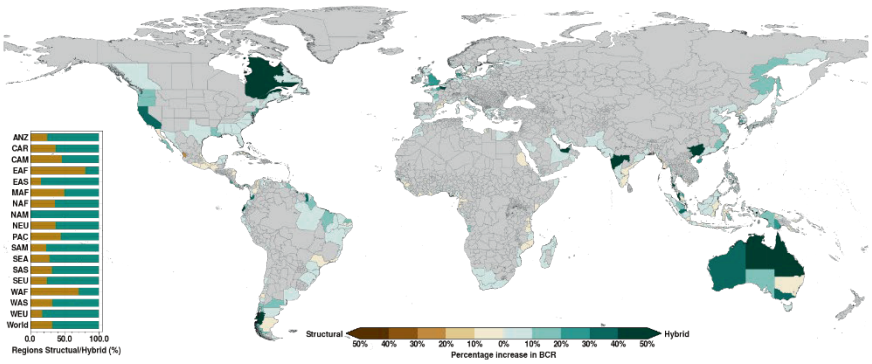

Figure 6-2: Percentage increase in BCR for implementing structural measures versus hybrid strategies. Percentage sub-national regions favouring structural/hybrid strategies per sub-continental regions are shown in the inserted panel on the left side.

Looking into the regional differences in BCR between structural measurs and hybrid strategies for the scenario of RCP4.5/SSP2 (Fig. 6-3), we observe that both Nature-based Solutions oftentimes are in the same range of ratios as each other, except for East (Signapore) and Thái Bình (Vietnam). Moreover, we find that usually both Nature-based Solutions are more cost-effective than structural measures or both are less cost-effective in most of the sub-national units assessed. Next to this, we find that structural measures are more feasible in regions where a lot of coastal wetlands and foreshore vegetation are situated and relatively few people are exposed to coastal flooding as the costs of conserving large areas of foreshore vegetation outpace the benefits (e.g., Sundarbans in India/Bangladesh, New South Wales in Australia, and Guerrero in Mexico). This is because, in these regions it is not or slightly feasible to implement adaptation and as we set structural measures dynamically, these regions favour a slight increase in dike height. Furthermore, hotspots of sub-national regions show favouring both hybrid strategies (e.g., northern America, eastern Asia, and western Europe) or structural measures (e.g., Central America and Africa) Breaking down the BCR further into best strategies per region, we show that conservation of foreshore vegetation is an important hybrid strategies and oftentimes most beneficial strategy.

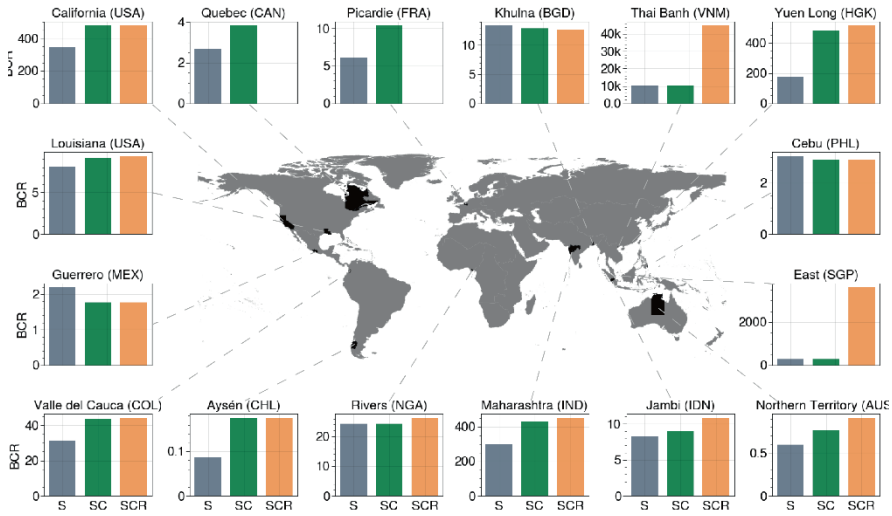

Figure 6-3: Benefit-Cost Analysis of different adaptation strategies for selected sub-national regions with the possibility on Nature-based Solutions.

The effects of hybrid strategies on the reduction of adaptation costs in the future are shown in Figure 4 for RCP4.5/SSP2 at the sub-continental scale (Fig. 6-4). Globally, we estimate a total reduction in adaptation costs compared to structural measures of 8% by implementing two types of Nature-based Solutions (restoration 2% and conservation 6%). The highest reduction is found in the sub-continental regions of Southeastern Asia (US$10 billion), Australia and New Zealand (US$8.6 billion), Northern America (US$5.4 billion), and Eastern Asia (US$5.3 billion). This shows that while a large reduction can be achieved by implementing Nature-based Solutions, still a lot of adaptation costs remain. Furthermore, we show the effectiveness of adaptation measures by estimating the NPV of the adaptation strategies with the highest NPV adaptation strategies in Fig. E-1, showing that highest NPV values are estimated for the sub-continental regions of Eastern Asia (US$2.4 trillion), Southeastern Asia (US$ 1.9 trillion), Southern Asia (US$1.6 trillion), and Western Europe (US$41.5 trillion). Highest NPV for individual sub-national regions are found in West Bengal (US$950 billion, India), Zheijang (US$849 billion, China), and Zuid-Holland (US$556 billion, the Netherlands).

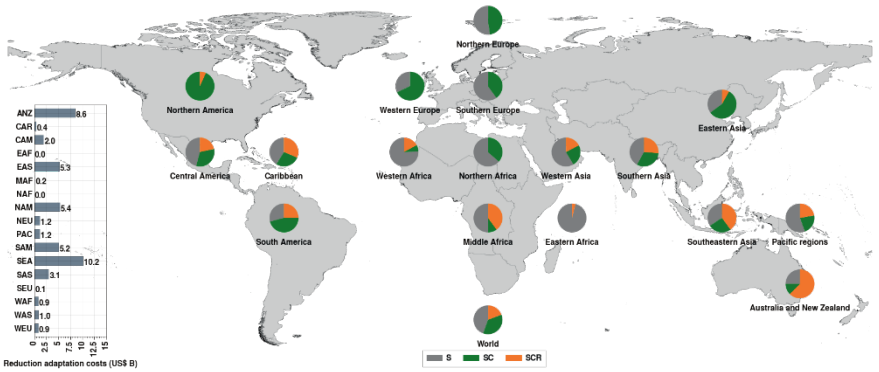

Figure 6-4: The adaptation strategies with the highest NPV per sub-continental region for structural measures (S), structural measures and conservation of foreshore vegetation (SC) and SC together with mangrove restoration (SCR).

6.3.2 Nature-based Solutions through a poverty perspective

For several countries we find that the wealth index is unevenly distributed between people living outside coastal flood hazard areas and people living within them. The population distribution curves in Figure 6-5 show these differences in the wealth index between people living outside flood prone areas (red), people living inside flood prone areas (blue), and people living inside flood prone areas where Nature-based Solutions could be implemented (green). The results show that in many places people living in flood prone areas are more likely to have a lower wealth index than people living outside flood prone areas. Countries where the distributions are significantly different (p-value < 0.05) are Guyana, Liberia, Kenya, Vietnam, Philippines, Timor-Leste, Sri-Lanka, and Bangladesh. Additionally, the wealth index distribution curves of people living in flood prone areas where Nature-based Solutions can be implemented are the same as those of people living in flood prone areas generally (e.g., Vietnam, Thailand, Kenya, Suriname, and Liberia). This is not the case for Guyana, Peru, Sri Lanka, and Bangladesh, where the wealth index is even lower for people living inside flood prone areas who experience benefits from Nature-based Solutions areas. Altogether, we find that in most countries people living in flood prone areas where Nature-based Solutions can be implemented tend to have low values of the wealth index, indicating that if these measures would be implemented, they could contribute to the reduction of climate shocks to people with low wealth index.

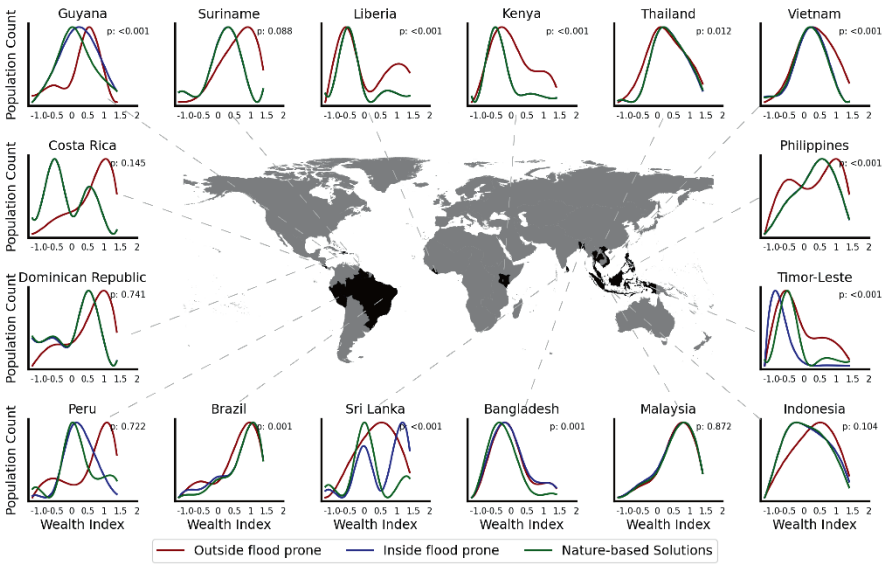

Figure 6-5: Population distributions of regional wealth index for people living outside flood prone areas (red), inside flood prone areas (blue) and areas where hybrid strategies are implemented in the study (green). Note the order of curves is red → blue → green, and that for all cases where the blue curve is not visible, it is overlapping with the green curve.

6.4 Outlook

We present a global-scale assessment of hybrid solutions and (future) potential flood risk reduction and the benefits of a combination of adaptation measures under scenarios of socioeconomic and climate change. Unlike previous studies on Nature-based and hybrid solutions, we provide a quantitative assessment on the benefits in terms of monetary flood risk reduction on a global scale, including a benefit-cost analysis, and provide social vulnerability analysis in the form of population distributions using wealth indexes. Our analysis shows that there is value gained in adding Nature-based Solutions to the portfolio of adaptation strategies, and that doing so could increase the cost-effectiveness of adaptation strategies for two-thirds (68%) of the regions assessed. Globally, we estimate a total reduction in adaptation costs compared to structural measures of 8% by implementing two types of Nature-based Solutions (restoration 2% and conservation 6%). Regionally the highest Net Present Value can reach almost US$1 trillion for sub-national units. The results of the study show that Nature-based Solutions are an effective measure in combination with structural measures to contribute to future flood risk mitigation. a Further, future benefits from implementing Nature-based Solutions will amplify when looking into non-monetary indicators.

As people in poverty are more vulnerable to climatic shocks and stresses (Hallegatte, 2016), it is important to understand the impact of mangrove restoration on the proportion of the population living in poverty. Unlike previous Nature-based Solutions studies, we provide a quantitative assessment of the benefits of Nature-based Solutions in terms of reduced economic damage. While this study focusses solely on flood protection benefits of mangrove restoration, there are other Nature Contributions to People (NCP), such as fishery, carbon storage and tourism (Spalding & Parrett, 2019; Zeng et al., 2021; zu Ermgassen et al., 2020). These NCPs provide provisions (e.g., timber and charcoal), regulation (e.g., erosion control and saltwater intrusion), habitat (e.g., fishery and biodiversity), and cultural services (e.g., recreation) (Akber et al., 2018). Including the value of these and other NCPs could increase the economical feasibility of mangrove restoration (Dahdouh-Guebas & Cannicci, 2021).

Although this study is a proxy analysis, we believe that it is valuable to gain more insight into the feasibility of mangrove restoration at the global scale. The implementation of Nature-based Solutions can be used as an integral component of policies, strategies and actions to risk reduction. Nature-based Solutions can be implemented in an integrated manner to tackle global societal challenges (Cohen-Shacham et al., 2016; Maes & Jacobs, 2017; Seddon et al., 2020). Furthermore, implementing adaptation measures, such as mangrove restoration and conserving foreshore vegetation, in LMICs can contribute to the resilience of people in poverty, driving poverty alleviation and helping to tackle poverty traps.

7 Synthesis

In the 21st century, coastal areas and their populations are projected to face increases in coastal flood risk due to socioeconomic and climate change. Climate shocks may exacerbate current poverty levels and catalyse the formation of poverty traps in Low- and Middle-Income Countries (LMICs), with global flood risk at the forefront of the potential impacts. To mitigate or prevent the expected increase in coastal flood risk it is critical to improve our understanding of global coastal flood risk and the effectiveness of adaptation strategies on flood risk benefits. Following this need, this thesis aims to disentangle drivers of coastal flood risk and assess costs and benefits of adaptation measures at the global scale with a focus on Nature-based Solutions. These issues were addressed in chapters 2 to 6 by assessing the following research questions:

- Can we improve surge level predictions by harnessing the capabilities of deep learning approaches at the global scale?
- What is the attribution of adaptation costs to drivers of coastal flood risk?
- What are the (future) flood risk benefits of structural measures, Nature-based Solutions, and a combination thereof?
- How can we include adaptation benefits beyond monetary terms in large scale flood risk assessments?

This chapter summarises the main findings regarding each research question. Furthermore, the remaining scientific challenges and the way forward are discussed. Finally, this chapter concludes with a discussion of the societal context and policy implications of this thesis.

7.1 Key research questions

Question 1 | Can we improve surge level predictions by harnessing the capabilities of deep learning approaches at the global scale?

In chapter 2 (Tiggeloven et al., 2021), deep learning approaches are explored for predicting surge levels at the global scale. For 738 tide stations, we developed and applied an approach to predict hourly surges using four different types of Neural Networks (NN). For this, surge levels are extracted using observed sea levels from the GESLA-2 dataset, which serve as the predictand variable. Various atmospheric variables from the ERA5 climate reanalysis dataset serve as predictor variables. To evaluate the NN model performance at each station, the results are benchmarked against a simple probabilistic model based on climatology. To explore how increasing the NN design complexity affects model performance, hidden layers are added, and the spatial footprint used around each station to extract the predictor variables is enlarged.

Using the same hyperparameter settings across all stations and a spatial footprint of 1.25 degree to extract predictor variables, chapter 2 shows that the Long Short-Term

Memory (LSTM) generally outperforms the other NN types. This is because the probabilistic forecast from the LSTM is in closest agreement with the distribution of the observed values, resulting in the best reliability scores in the Continuous Ranked Probability Score (CRPS). However, we show that the Convolutional Neural Network (CNN) can improve on performance the most when increasing the spatial footprint or number of hidden layers in the model architecture and outperforms the LSTM. Increasing complexity comes, however, at the expense of increasing computational time, up to more than 15 times longer to run compared to simpler setup of the NN model.

My results show that the NN models can capture temporal evolution of surges, and that they are sometimes capable of outperforming large-scale hydrodynamic models. I observe similar performance patterns across all the NN ensemble models. The performance generally increases with latitude and is generally high (CRPSS>40%) in mid-latitudes (30-60 degrees), which is in line with previous studies. Stations around the equator (0-30 degrees) generally do not outperform the simple probabilistic model based on climatology and show that other variables such as Sea Surface Temperature, steric components or geostrophic currents might also need to be explored to improve on performance. Additionally, I show that model performance generally improves with an increasing size of the spatial footprint used for the selection of the predictor variables, but that increasing the number of hidden layers does not always lead to a better performance. In order to allow the coastal modelling community to further build on these initial efforts, I have made all of the detrended and decomposed surge signal and predicted surge level data, as well as the NN models, openly available (Tiggeloven et al., 2021). Moreover, a better understanding and prediction of the characteristics of sea levels will contribute to improving coastal adaptation and management.

Question 2 | What is the attribution of adaptation costs to drivers of coastal flood risk?

Chapter 3 assesses different coastal flood adaptation objectives and corresponding risk levels at the global scale and performs a benefit-cost analysis of those objectives. Furthermore, the costs of adaptation have been attributed to different drivers of flood risk: sea-level rise, socio-economic change, subsidence, and optimizing to current conditions.

A methodological framework is created to assess the following steps: (1) flood risk estimation; (2) adaptation costs estimation; (3) benefit-cost analysis for four adaptation objectives; and (4) attribution of the total costs to the different drivers. In the risk model, Expected Annual Damage (EAD) is calculated for different scenarios with and without adaptation. The costs are calculated by estimating the dimensions of the required dikes (height and length) and multiplying these by their unit costs. A benefit-cost analysis is

performed for four adaptation objectives, namely: (1) 'Protection constant'; (2) 'Absolute risk constant'; (3) 'Relative risk constant'; and (4) 'Optimize', which calculates future protection standards by maximizing Net Present Value (NPV). To better understand the drivers of flood risk change and adaptation costs, these costs of adaptation are attributed to several risk drivers, namely (1) optimization under current conditions (CUR); (2) socioeconomic change (SEC); (3) sea level rise driven by climate change (SLR); and (4) subsidence driven by groundwater depletion (SUB). Finally, present-day protection levels are needed to better estimate flood risk, and chapter 3 produced the first global scale estimates of coastal flood protection levels.

The results of chapter 3 show that EAD increases by a factor of 150 between 2010 and 2080, if no adaptation were to take place, and that 15 countries account for approximately 90% of this increase. All four adaptation objectives show high potential to reduce (future) coastal flood risk at the global scale in a cost-effective manner. When future protection standards are optimized for highest NPV, we find a Benefit-Cost Ratio (BCR) of 76 with NPV of more than US$11 trillion, while the 'protection constant' adaptation objective showed the lowest NPV (US$9.5 trillion) with a BCR of 67 for the RCP4.5/SSP2 scenario. At the regional scale, the results show that the adaptation objectives could be achieved with a BCR more than 1 for most of the sub-national regions. This ranges from 89% for the 'optimize' adaptation objective to 79% for the 'absolute risk constant' adaptation objective. However, under the 'optimize' adaptation objective, relative risk is still projected to increase compared to current values in 32% of the sub-national regions assessed. Attributing the total costs for the 'optimize' adaptation objective, sea-level rise contributes the most and exceeds 50% of the total costs in 98% of the sub-national regions assessed and exceeds 90% of the total costs in 58% of the sub-national regions. However, the other drivers also play an important role, but are dwarfed in absolute terms.

Question 3 | What are the (future) flood risk benefits of structural measures, Nature-based Solutions, and a combination thereof?

To reduce current and future coastal flood risk, it is critical to better understand how adaptation measures, including Nature-based Solutions, can reduce that risk. This is addressed in chapters 4-6, which present the first global scale assessment of reducing future flood risk through Nature-based Solutions and hybrid strategies. These studies extend on the coastal flood risk assessment framework developed in chapter 3 by assessing the effects of foreshore vegetation and structural measures on global flood risk reduction under socioeconomic and climate change. The main steps of our study are: (1) flood risk estimation; (2) wave attenuation estimation; and (3) estimating the benefits of adaptation measures. The wave attenuation model for present-day foreshore conditions is complemented with areas that show potential to restore mangroves as

identified by the mangrove restoration tool, to account for the wave-vegetation interaction and estimate the effects of mangrove restoration on wave damping.

In chapter 4, we show that foreshore vegetation contributes a large share of flood risk reduction and that absolute EAD reduction is estimated to increase if foreshore vegetation is conserved under future projections of sea-level rise and socioeconomic change. Our results show that conserving foreshore vegetation is an effective measure to reduce future flood risk. We further show that the benefits of conserving foreshore vegetation for flood risk reduction are estimated at approximately US$274 billion, which can account for up to 20% of the total benefits in the protection constant adaptation objective for some sub-national regions. We found that globally the reduction in flood risk through conserving foreshore vegetation is estimated to increase in the range of 28 up to 67-fold compared to present-day conditions, which amounts to US$71 billion for RCP4.5-SSP2 and US$168 billion for RCP8.5-SSP5 in terms of EAD in 2080. We further found that the relative reduction in flood risk through foreshore vegetation is estimated at 8.5% globally, compared to 13% under current conditions.

Chapter 5 presents the first global-scale assessment of mangrove restoration and (future) potential flood risk reduction and the benefits of mangrove restoration as adaptation measure under scenarios of socioeconomic and climate change. The results of the study show that mangrove restoration is an effective measure to contribute to future flood risk mitigation and indicates that future benefits of mangrove restoration can be assessed using existing flood risk assessment frameworks. We show that a large share of future flood risk of US$40-90 billion (~9% of total EAD for both scenarios assessed) may be reduced by implementing mangrove restoration. Next to reducing property damages, we show that restoring mangroves could place up to 820,000 people at a lower risk of coastal flooding under future conditions compared to not restoring mangroves.

Chapter 6 combines previous chapters into an assessment of hybrid adaptation strategies at the global scale. Implementing Nature-based Solutions will increase the feasibility of adaptation strategies for two-thirds (68%) of the regions assessed. Globally, we estimate a total reduction in adaptation costs of 8% by implementing Nature-based Solutions, compared to using grey infrastructure only.

Therefore, the results of these studies indicated that Nature-based Solutions constitute promising alternatives or complementary measures to other adaptation measures (e.g. structural measures).

Question 4 | How can we include adaptation benefits beyond monetary terms in large scale flood risk assessments?

In chapter 5 and 6, we show the importance of using more indicators than economic ones alone, in order to assess the benefits of measures. Here, we use poverty indicators to better understand the distribution of adaptation benefits on the population affected. We show that the effects of Nature-based Solutions and flood hazards are unevenly distributed across the population in terms of poverty, and that people with a lower wealth index could benefit more from Nature-based Solutions. We argue that only looking into property damages and people exposed is not enough to understand the range of impacts of adaptation on population distributions. Furthermore, implementing adaptation measures, such as mangrove restoration, in LMICs can contribute to the resilience of people in poverty, poverty alleviation and help tackle poverty traps.

We furthermore show that people living under the poverty line in Bangladesh are dispoportionally more affected by coastal flood risk and would thus particulary benefit from adaptation measures, such as mangrove restoration. Moreover, mangroves contribute to the safeguarding of communities by providing coastal flood protection benefits, as people in poverty are more vulnerable to such hazards (Adhikari et al., 2010; Mirza, 2011; Salik et al., 2015). We also find that among those populations who will be exposed to coastal flooding in the near future, there is a disproportionate increase in people affected towards the poorer sections of society. Therefore, implementing adaptation in low-income countries could contribute to the resilience of people in poverty, poverty alleviation and help tackle poverty traps (Hallegatte, 2016; Leichenko & Silva, 2014; Winsemius et al., 2018).

7.2 Remaining scientific challenges and the way forward

In this thesis, the need for coastal adaptation to tackle the expected increase in coastal flood risk was assessed by disentangling drivers of coastal flood risk and assessing costs and benefits of adaptation measures at the global scale with a focus on Nature-based Solutions. In doing so, this thesis suggests that it is important improve on traditional large-scale flood risk assessments by including Nature-based Solutions and more holistic hybrid approaches. Although this thesis includes limited aspects of Nature-based and hybrid solutions, and valuation of adaptation strategies beyond monetary terms, it is important for future research to continue developing towards more holistic hybrid approaches. Some of the remaining scientific challenges include: (1) enhanced hazard prediction by improving flood inundation models, paving the way towards improved early warning systems; (2) refining flood risk assessment by using object-based assessments instead of aggregation methods for protection levels and exposure information; (3) improving the simulation of adaptation strategies by including a myriad

of adaptation measures and expanding on this by using dynamic approaches; and (4) next to including poverty analysis, incorporate further co-benefits of adaptation measures into flood risk assessments, such as ecosystems services related to Nature-based Solutions. Possible ways to address these four challenges are discussed in the following paragraphs.

Firstly, an improvement could be made in future research by improving on the flood inundation modelling scheme. This can be done by using a hydro-dynamic inundation modelling scheme (e.g. Vousdoukas et al., 2016a). While the research in this thesis does not include dynamic inundation modelling, it does include resistance factors similar to those used by Vafeidis et al. (2019), in order to account for water-level attenuation. It therefore represents an advance on previous studies that have used planar inundation modelling methods (i.e., bathtub models). However, this comes at the cost of increased computing time and studies on future climate change and inundation have yet to implement such hydro-dynamic modelling scheme at the global-scale. A workaround would be to use so-called nested models that look into regions of interest but are globally applicable. Another improvement of using hydro-dynamic modelling schemes over traditional bathtub models, is that it includes a temporal component of coastal flooding. However, to implement this for current and future research, more research is needed on the evolution of surge levels, or so-called hydrographs. Another improvement can be made by including waves in inundation modelling, which is found to be an important component in inundation modelling (Vousdoukas et al., 2017). The inundation modelling scheme can be further improved by increasing the resolution from 30" to a higher resolution in order to better understand local scale signals and patterns, since the scale of assessment and resolution of input data has a significant implication on flood risk model results (Wolff et al., 2016). Moreover, building on the NN models developed in chapter 2 that can rapidly predict the temporal evolution of surge levels, and feeding those results into hydro-dynamic models, would pave the way for rapid inundation forecasts. This can be done by developing regional NN models in which each coastline is represented by a NN model as opposed to have a model for each gauge station. Moreover, developing regional models will allow to better assess temporal input for coastal inundation schemes and early warning systems. Furthermore, by including climate change projection on future surge level evolutions, we can improve our understanding of surge level prediction and the temporal evolution thereof.

Secondly, an important improvement can be made by using object-based information instead of aggregated data for representing flood protection levels and exposure. An uncertainty in this thesis is the current flood protection level, which is estimated using the FLOPROS modelling approach, as high-resolution data on flood protection along the global coastlines are not available. An improvement could be made, for instance,

by mapping object-based flood protection globally by using Earth Observation-based methods (Wing et al., 2019), or using widespread surveys and local expertise to better understand current protection levels (Hallegatte et al., 2013). Furthermore, several uncertainties exist with assumptions on aggregation of exposure information. We assume the percentage of occupancy type per grid cell to be the same for all locations, whilst in reality it is spatially heterogeneous, and next to this, we assumed the building density per occupancy type. An improvement could be made by using Earth Observation-based methods to detect object-based elements, or Machine Learning to improve the accuracy of urban land cover and building types (Hecht et al., 2015; Huang et al., 2018).

Thirdly, the results in this thesis can be enhanced by including and combining more adaptation measures in order to give a more comprehensive overview of potential flood risk reduction. For example, hybrid adaptation strategies that use grey and green infrastructure are showing potential to further optimise flood risk strategies (Du et al., 2020; van Zelst et al., 2021), but can be even further expanded by inlcuding migration (Hauer et al., 2019; Lincke & Hinkel, 2021), flood proofing (de Ruig et al., 2019) or other Nature-based Solutions such as restoration of salt marshes or coral reefs (Beck et al., 2018). Furthermore, an improvement can be made by including dynamic adaptation pathways in the adaptation modelling scheme used in this thesis (Haasnoot et al., 2013). Next to this, adaptation using a range of different measures might be more feasible in the long run (Jongman, 2018; Sutton-Grier et al., 2015).

Finally, while this thesis focusses on the flood protection benefits of mangrove restoration, other co-benefits of Nature Contributions to People (NCP), such as fishery and carbon storage, are not included. These NCPs can consist of provisions (e.g., timber and charcoal), regulation (e.g., erosion control and saltwater intrusion), habitat (e.g., fishery and biodiversity), and cultural services (e.g., recreation) (Akber et al., 2018). Including the value of these and other NCPs could increase the economic feasibility of mangrove restoration (Dahdouh-Guebas & Cannicci, 2021). For example, Soanes et al. (2021) indicate the effectiveness of reducing flood exposure by mangrove restoration in the Caribbean, and Barros et al. (2021) argue that NbS requires local scale knowledge to benefit from social, environmental, and economic benefits simultaneously. Our model results suggest that mangrove restoration is not feasible for many regions in the Caribbean. However, by including NCPs or looking into the increase in resilience of coastal communities in the Caribbean a more comprehensive assessment of mangrove restoration feasability for this region can be made (Soanes et al., 2021; Su et al., 2021; Ward et al., 2017). For instance, Worthington et al. (2018) show that the global restoration of mangroves could contribute to the sequestration of 69 million tons of carbon in above-ground biomass and 269 million tons of soil carbon. It could also provide habitat for trillions of finfish, crabs and shrimps, among other

species. These benefits will become more vital in the future due to climate change, when the role of wetlands becomes more important (Erwin, 2009; Jennerjahn et al., 2017; IPCC, 2019; Powell et al., 2011). Furthermore, implementing adaptation measures, such as mangrove restoration, in LMICs will contribute to the resilience of people in poverty, help with poverty alleviation and tackle poverty traps.

7.3 Societal context and policy implications

The results presented in this thesis contribute to the ongoing efforts of academia, the risk management community, and policy makers to better understand coastal flood risk reduction and adaptation. In this section, we outline the importance of this thesis from a policy and decision making perspective to the ongoing efforts of international organisations to reduce disaster risk. Furthermore, we note the contribution of this thesis to: decision making in a societal context; human development efforts; and risk communication.

In the last decade, one in five persons of the global population was affected by disasters and this is expected to increase in the future due to climate change and socioeconomic development (UNDRR, 2015). The increase in disaster risk and the need for action have been acknowledged by several international organisations within the effort of reducing disaster risk and loss of lives, livelihoods and health. During the third UN World conference on disaster risk reduction, the Sendai Framework for Disaster Risk Reduction was developed, and calls for improved risk assessments and achieving substantial reduction in diasaster risk between the period 2015-2030 (UNDRR, 2015). Another example is the Paris Agreement of the Conference of Parties (COP), which aims to take decisions and enhance collective efforts to limit average global temperature increase well below 2 degrees (UNFCCC, 2021). This thesis contributes to Priority for Action 1 for the Sendai Framework, i.e. understanding disaster risk, by providing global maps of hotspots of disaster risk under current and future conditions, and global maps indicating potential ways to reduce this risk. Moreover, linking the need to limit climate change impacts and the Sustainable Development Goals (SDG) (https://sdgs.un.org/goals), this thesis contributes to the SDG of climate action, and sustainable cities and communities. By improving upon current understanding of (future) coastal flood risk, adaptation and Nature-based Solutions, and community resilience with a focus on poverty, we have increased the understanding of the impacts of adaptation measures beyond monetary terms.

Schulte et al. (2021) argue that succesful adaptation measures should include a range of different strategies and local scale factors, as climate change is taking place in diverse social, economic, political, institutional, financial, technical, and biophysical contexts. While the scope of this thesis is aimed at the global scale, the results can be used to inform policy makers on the regional scale or city-level. In recent years, several global

flood risk models have been developed and are being in use by a wide range of users and practitioners with applications in disaster risk management activities, international development organizations, the reinsurance industry, and flood forecasting and early warning. For example, the results of chapter 2 can be further developed into forecasting models and can contribute to ongoing efforts of the risk community to better map surge level predictions during (extra) tropical storms, as the approach used allows for rapid forecasting and advances our collective efforts to better understand coastal flood risk and adaptation. Doing so, an early warning system can be developed and used to prevent or mitigate coastal flood risk at the regional scale or city-level. To take urgent action to confront the climate crisis, a global network of mayors initiated the C40 Cities organisation (c40.org). To inform a new project of the C40 network (Water Safe Cities), the results of chapter 3 of this thesis are being used with the aim to increase understanding of the impacts of floods and drought at the city level globally.

In order to bridge the gap between academia and the risk management community, we integrated the data processed in chapter 3 into the Aqueduct Global Floods webtool (www.wri.org/floods). This webtool allows any user to examine current and future risk, as well as the benefits of strucutral flood protection at the sub-national scale. Clearly, local scale models and assessments should be used for the design and implementation of individual adaptation measures, but our results can be used as a first proxy for indicating regions where adaptation through structural measures may be economically feasible. Potential next steps could be to integrate Nature-based Solutions and hybrid adaptation strategies in the webtool, to better inform policy makers and provide results of chapter 4 to 6 in an accessible way.

Engagement with local communities is an important driver for adaptation implementation of Nature-based Solutions (Schulte et al., 2021). Additionally, focusing on a single function of mangrove restoration (in this case flood protection benefits) can result in unwarrented consequences for biodiversity (Seddon et al., 2020) and can make success more unpredictable (Powell et al., 2011). Therefore, a holistic and integrated approach to mangrove restoration should be followed in practice, using avaialable ecological knowledge on good restoration practices (Lewis, 2005). Education and training of practitioners and scientists in public and private sectors are vital to enhance understanding on the protection and management of (restored) mangroves (Erwin, 2009). As NbS enables the so-called option value it overcomes long-term forecast uncertainty without the risk of under or overprotecting (e.g. with dikes). Implementation of Nature-based Solutions can be used as integral component of design policies, strategies and action, and can be implemented in an integrated manner to tackle global societal challenges (Cohen-Shacham et al., 2016; Maes & Jacobs, 2017; Seddon et al., 2020).

Implementing adaptation measures, such as mangrove restoration, in LMICs could contribute to the resilience of people in poverty, help with poverty alleviation, decrease the risk of displacement and migration, and tackle poverty traps. The loss of these ecosystems disproportionally affects vulnerable groups and communities that live close to the coast and often heavily depend on natural resources (Barbier, 2015; Daw et al., 2011). Especially, local fishermen, who often belong to the poorest groups in development countries, depend on coastal resources and access to the sea. Hard infrastructure often disconnects these groups from their main source of income and makes it difficult for them to keep a close watch on their boats, which often is their most valuable asset. Increases in coastal flood risk due to sea level rise, increased storminess and removal of coastal ecosystems can lead to poverty traps as people in poverty are disproportionally exposed to such shocks (Hallegatte, 2016; Hallegatte & Rozenberg, 2017; Winsemius et al., 2018). As we expect that people in poverty are more vulnerable to ecosystem loss, which increases their exposure to natural hazards, understanding distributional impacts of mangrove restoration in terms of poverty indicators (Villarreal-Rosas et al., 2021) and how poverty is integrated into adaptation (Araos et al., 2021) can help in selection of investment hotspots that specifically benefit socially vulnerable groups. The results found in this thesis can help policymakers to assess the threat of coastal flooding and design sustainable adaptation measures taking into account poverty dynamics.

Appendices

Appendix A

Supplementary Figures A

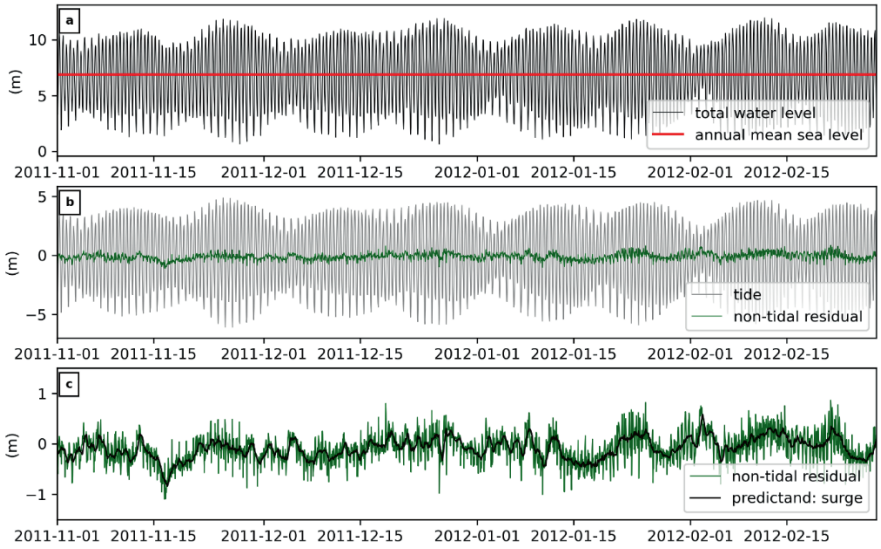

Figure A-1: Pre-processing steps applied to the time series of total water level to obtain the surge predictand variable used for this study. a) The annual mean sea level from the total water level from GESLA-2 is subtracted to remove annual mean sea-level variability. b) The detrended total water level is decomposed to obtain the tide and non-tidal residual. c) To limit the impact of harmonic prediction and timing errors, a 12-hour moving average is applied to obtain the surge variable used in this study. The time series shown in from the tidal station Anchorage (location 6 in Figure 2-1).

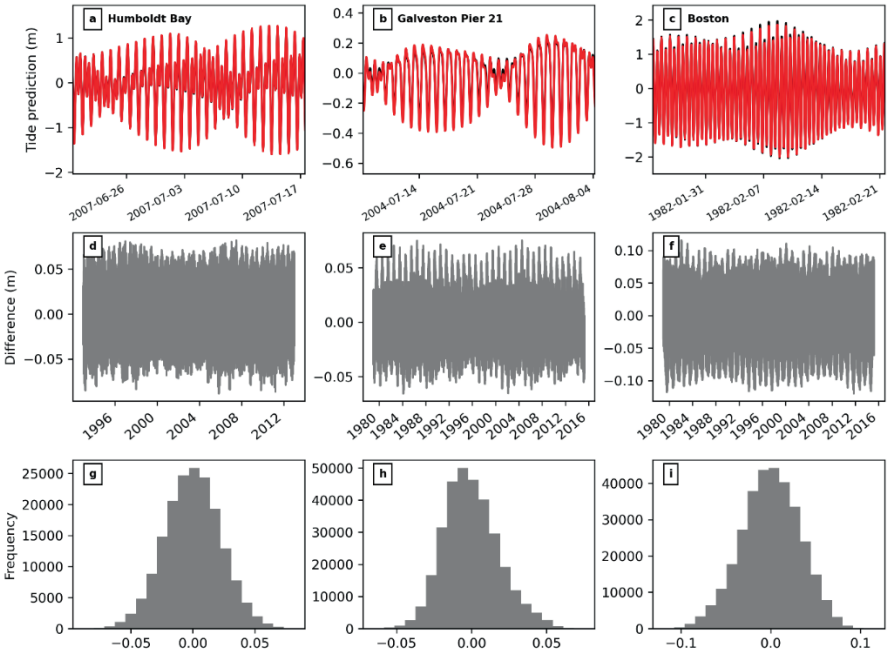

Figure A-2: (a-c) Tidal predictions obtained from the UTide package (in black) and NOAA tidal predictions (in red) for a) Humboldt bay (mean tidal range (MTR): 1.49 m), b) Galveston Pier 21 (MTR: 0.31 m) and c) Boston (MTR: 2.89 m). The time span shows the highest differences obtained between both tidal predictions. (d-f) Absolute difference between the two timeseries. (g-i) Histograms from the absolute differences. NOAA tidal predictions were obtained from https://tidesandcurrents.noaa.gov/.

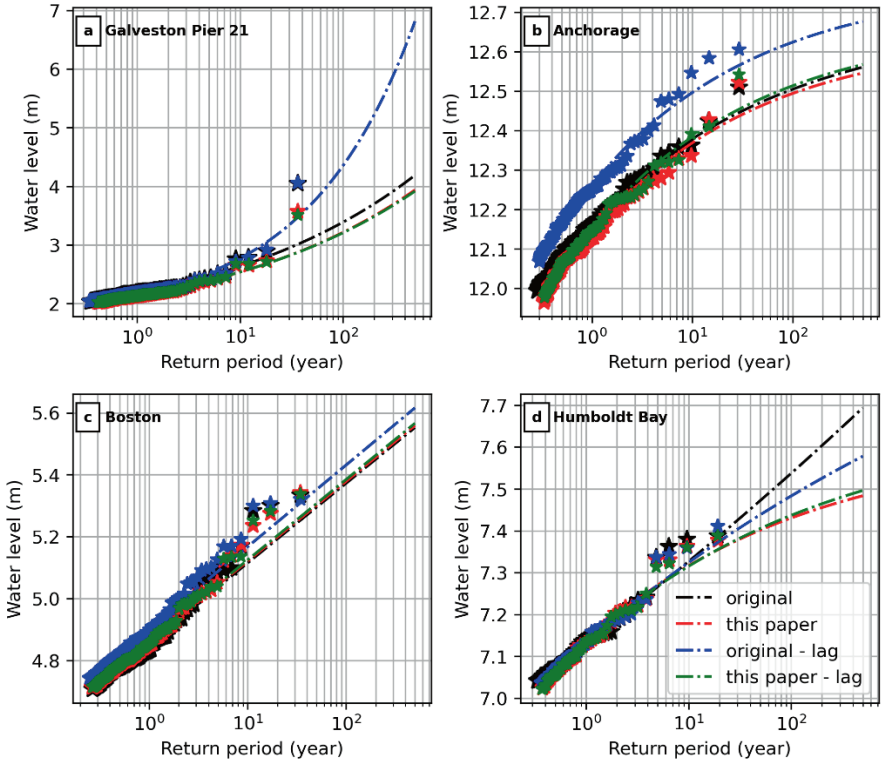

Figure A-3: Exceedance frequency and extreme value distribution for the de-trended water level (original, in black), the sum of the tide and non-tidal residual with a lag of 1 hour (original - lag, in blue), the sum of the tide and surge residual derived in this paper (this paper, in red) and the sum of the tide and surge residual with a lag of 1 hour (this paper - lag) for a) Galveston Pier 21, b) Anchorage, c) Boston and d) Humboldt bay.

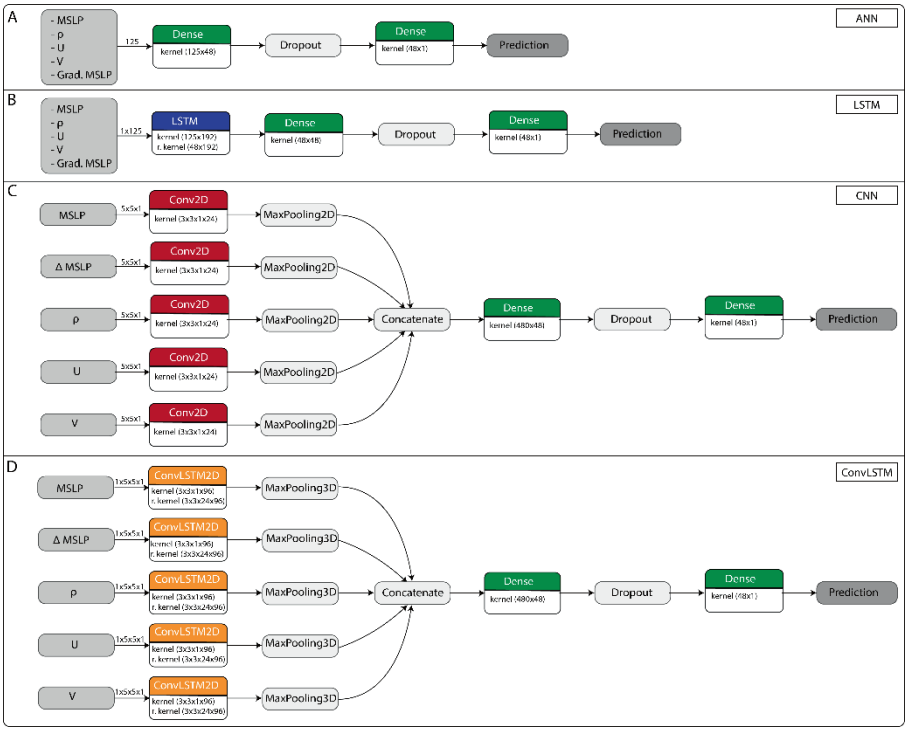

Figure A-4: NN architecture for ANN (a), LSTM (b), CNN (c), and ConvLSTM (d) with predictor variable MSLP, gradient of MSLP (Grad. MSLP), wind magnitude (ρ), and U and V. The regular densely connected layers are denoted in green, LSTM layer in blue, convolutional 2D layer for the CNN in red, and the convolutional LSTM 2D layer in orange for the ConvLSTM. For every NN layer the kernel dimensions are shown and for the LSTM and ConvLSTM also the recurrent kernel dimensions are displayed. After the convolutional layers there is a max pooling layer (2D for CNN; 3D for ConvLSTM) to downsample the input and after which input is flattened and concatenated before fed into the densely connected layer. Note that each NN type ends with the same sequence of densely connected layer → dropout → densely connected layer → prediction.

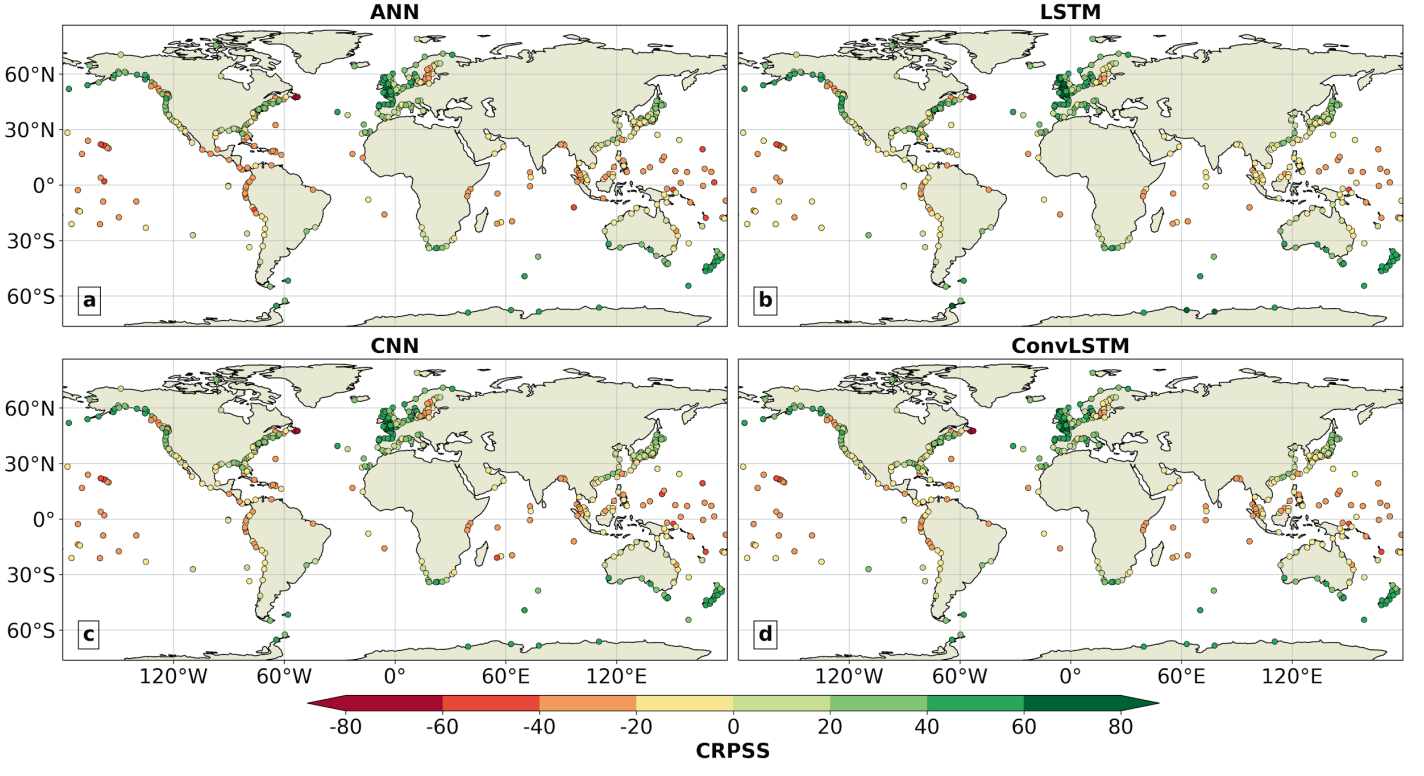

Figure A-5: CRPSS of the ensemble run for the four NN.

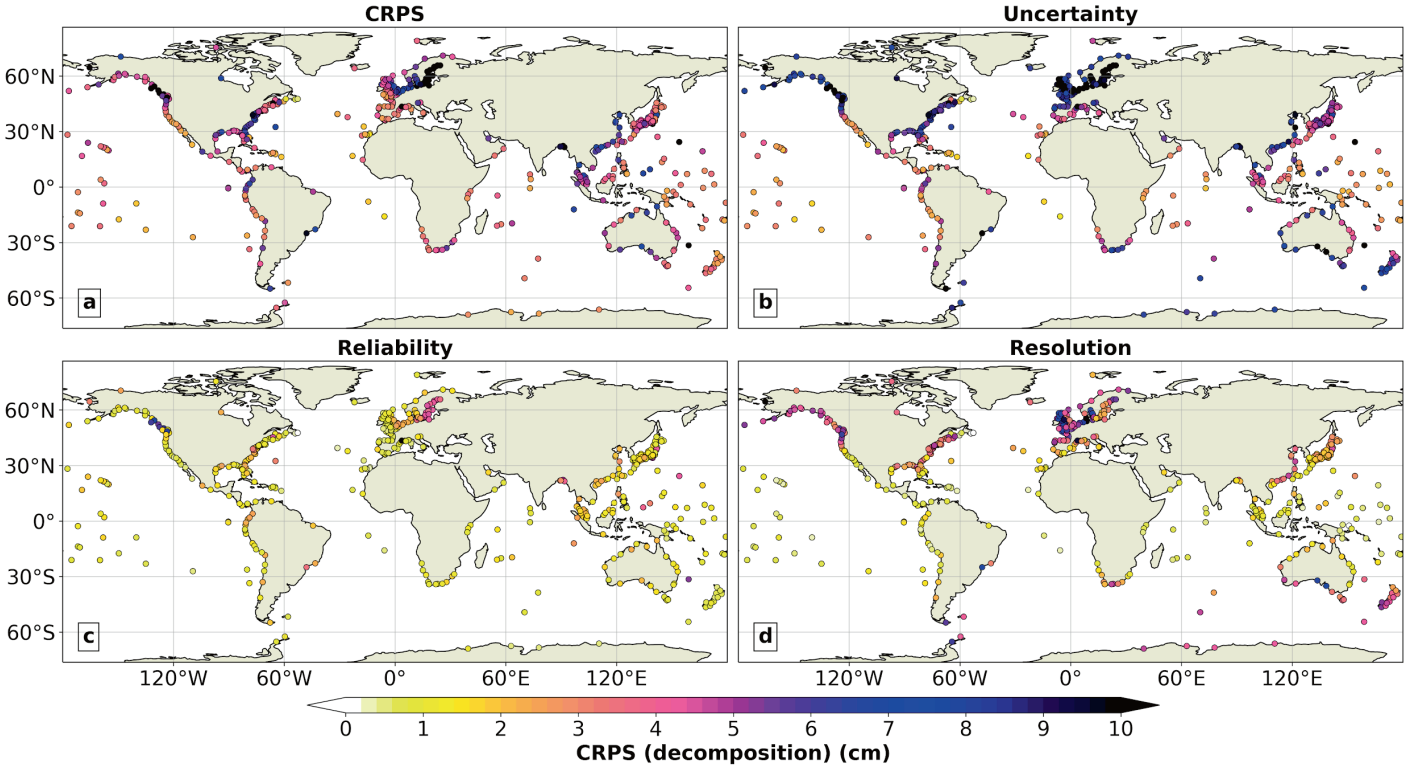

Figure A-6: CRPS decomposition for the best NN per tide station. The CRPS value of the climatological reference distribution is expressed as the uncertainty component of the CRPS.

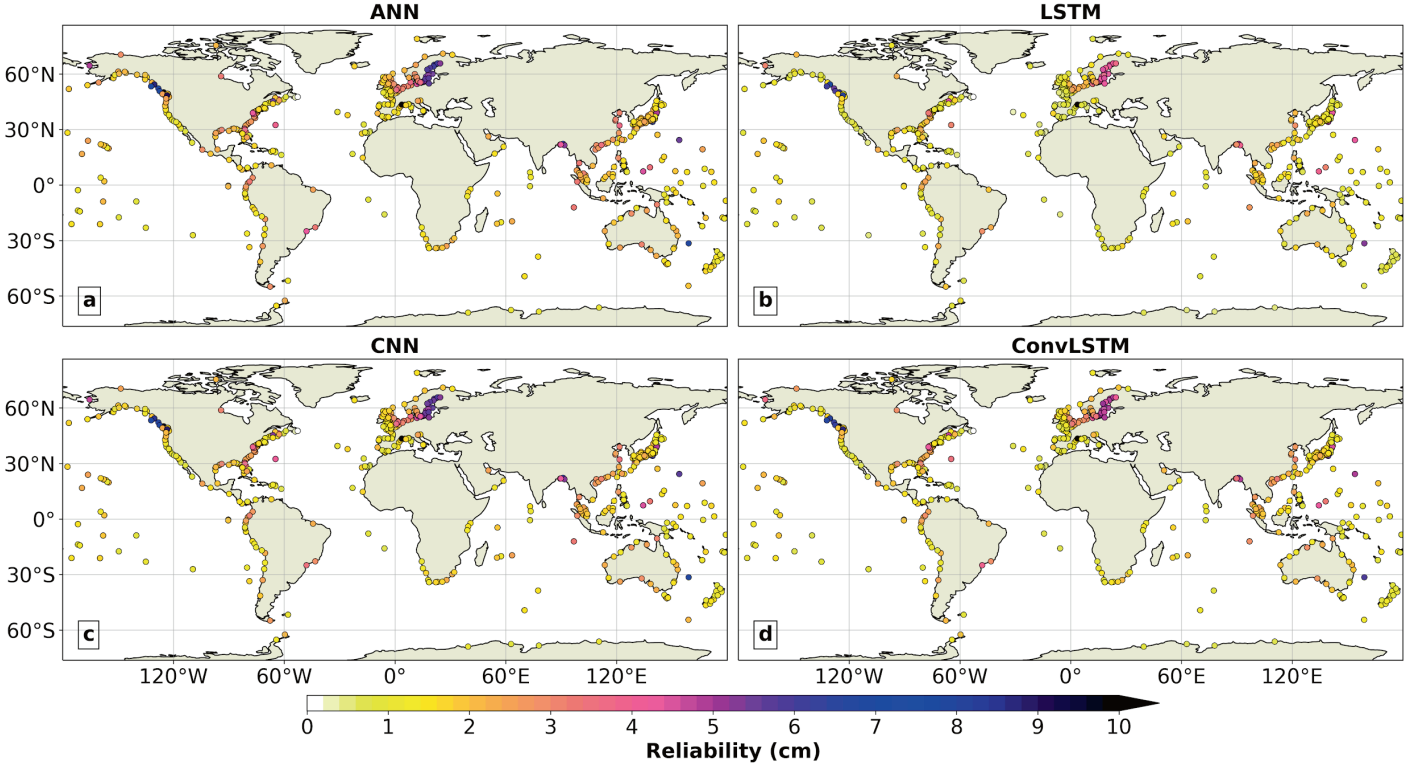

Figure A-7: Reliability component of the CRPS for the four NN.

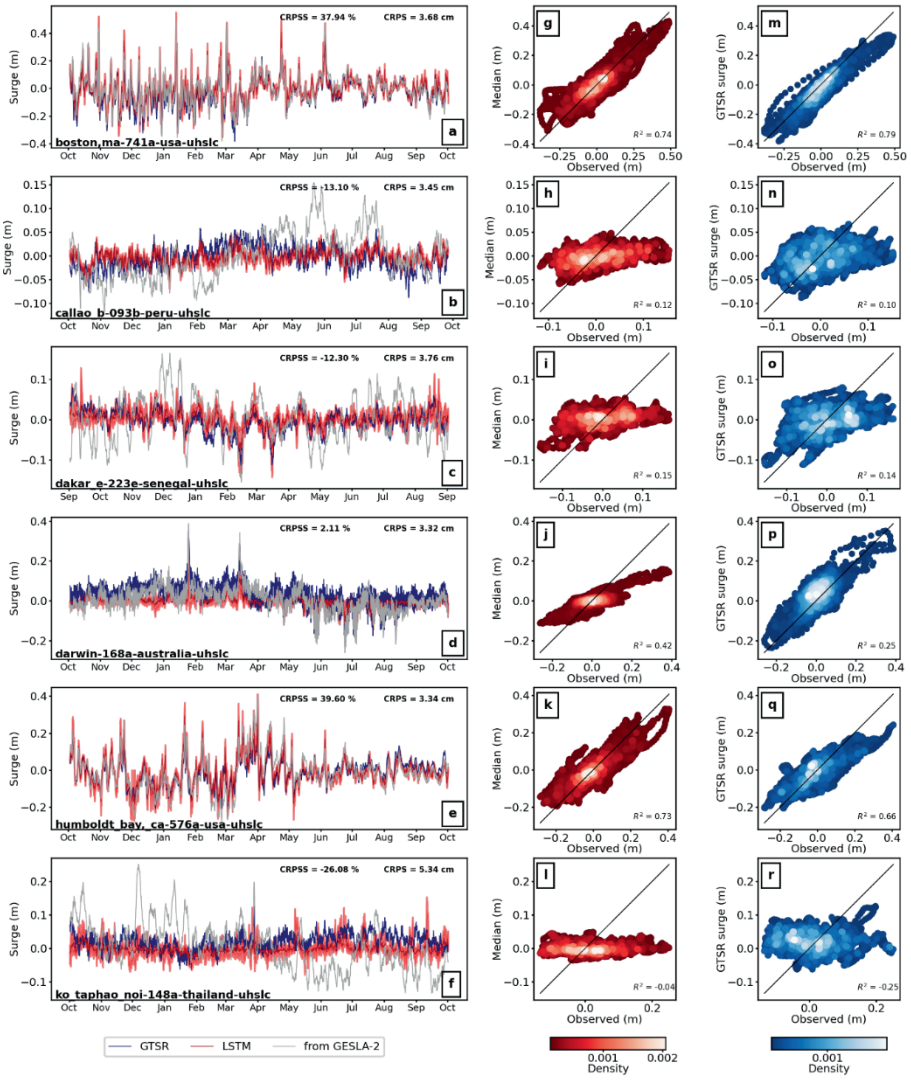

Figure A-8: a-f) Hourly surge predictions for the testing year from the LSTM/CNN model, observed and surge from the Global Tide and Surge Model and g-l) scatter plot of the median from the predicted ensemble with the observed surge and m-r) with the GTSM surge.

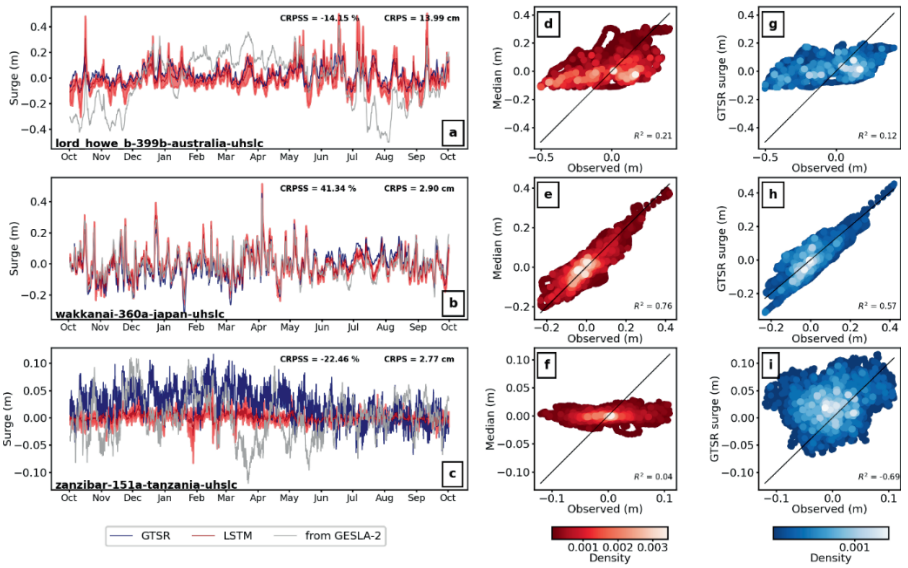

Figure A-9: a-c) Hourly surge predictions for the testing year from the LSTM model, observed and surge from the Global Tide and Surge Model and d-f) scatter plot of the median from the predicted ensemble with the observed surge and g-i) with the GTSM surge

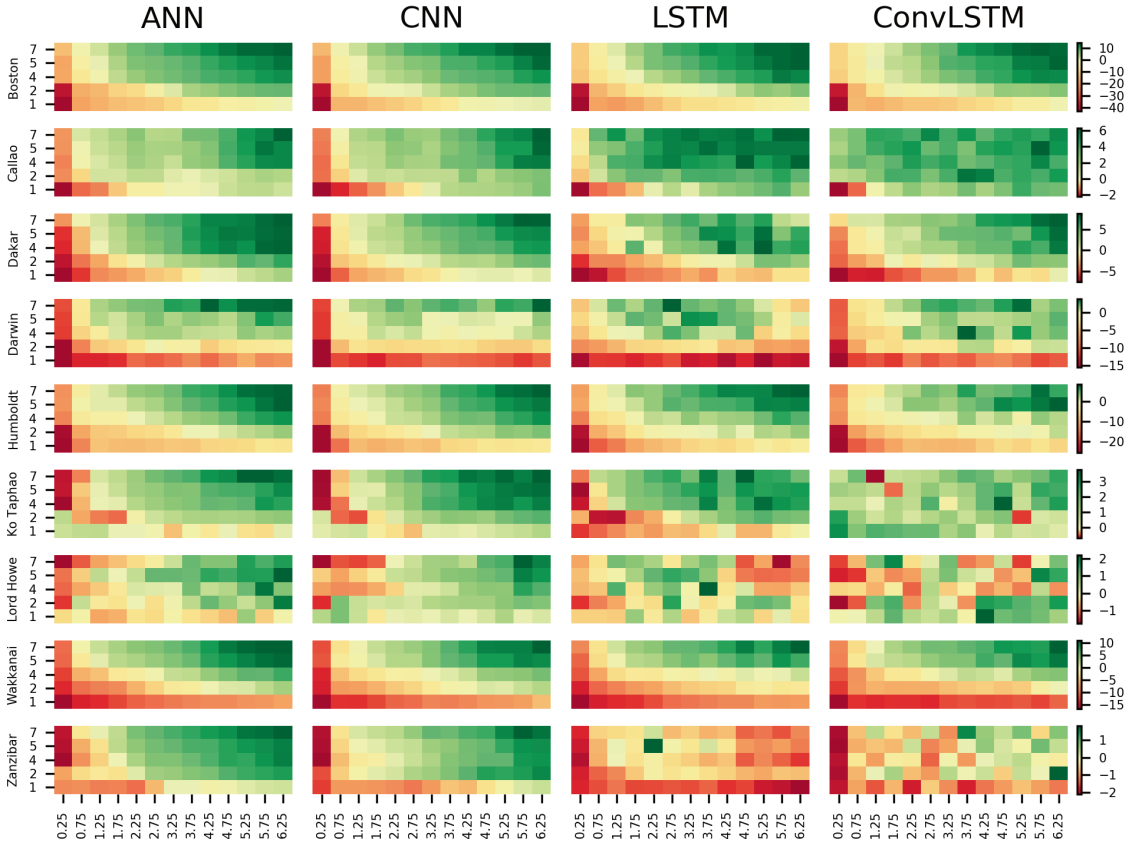

Figure A-10: CRPSS value of the NN model ensemble for increasing number predictor variables and spatial footprint size.

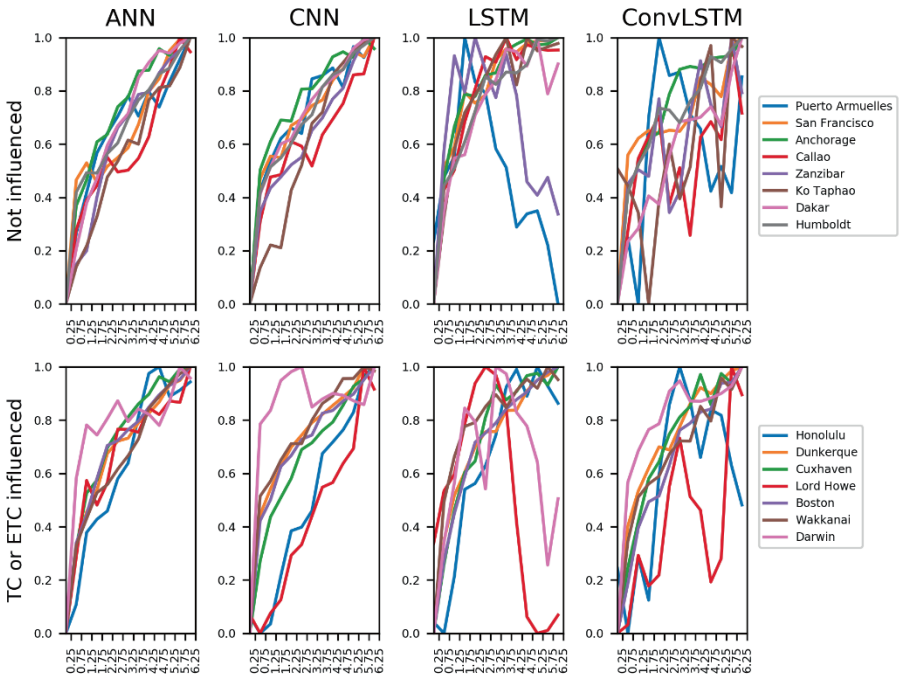

Figure A-11: Normalized learning rate of increasing spatial footprint for the four different NN ensembles. The stations have been split into groups of prone to Tropical cyclones (TC) or ExtraTropical Cyclones (ETC) and not influenced by (E)TC based on the IBTrACS dataset, as done in (Bloemendaal, Haigh, et al., 2020). Darwin is the only station which was classified as prone to TCs.

Appendix B

Supplementary Notes B

This section contains a brief description of the coastal protection standards estimated with the FLOPROS modelling approach. Higher protection standards can be found at regions with high economic activity and high asset exposure. Regions with low risk have lower estimated protection standards. Regions without modelled risk in the GLOFRIS model are excluded. This occurs in regions where we have no data on exposure or no coastal inundation is simulated. These protection standards are used in our paper as the current protection, on top of which the future costs of dike heightening are calculated. The protection standards for The Netherlands are manually set to 1000-year return period. This is because, for whole of The Netherlands protection standards are known to be higher than 1000-year return period.

Supplementary Figures B

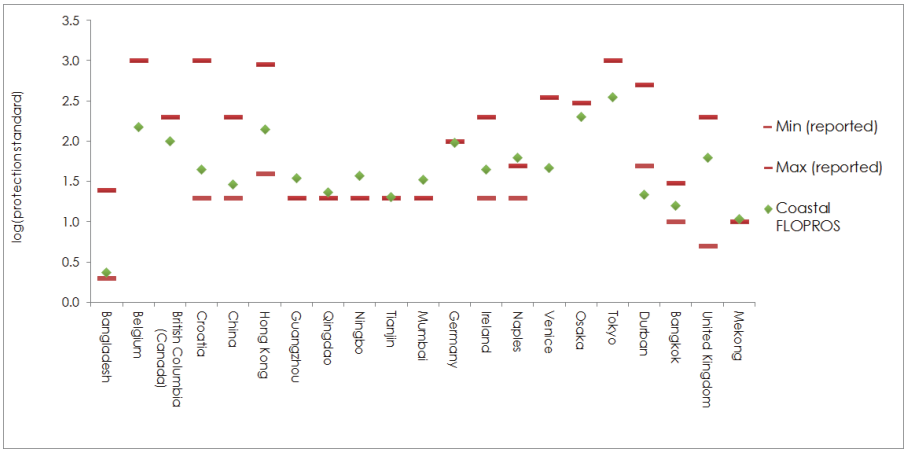

Figure B-1: Validation of the coastal protection standards estimated using the FLOPROS modelling approach against reported protection standards.

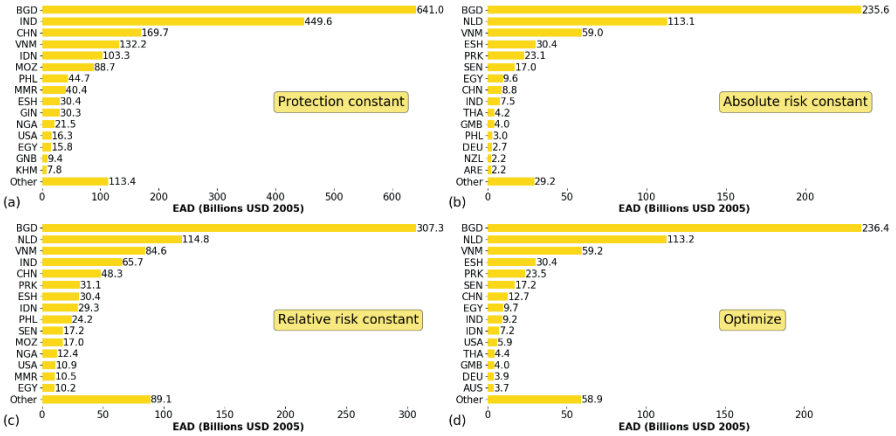

Figure B-2: Top 15 countries with coastal flood risk in (a) 2080 if protection standards are kept constant, (b) 2080 if absolute risk is kept constant, (c) 2080 if relative risk is kept constant, and (d) 2080 if protection standards are optimized for the scenario RCP8.5–SSP5. Note that the countries and value on the x axis change for each graph. The countries are denoted by ISO 3166-1 alpha-3 codes

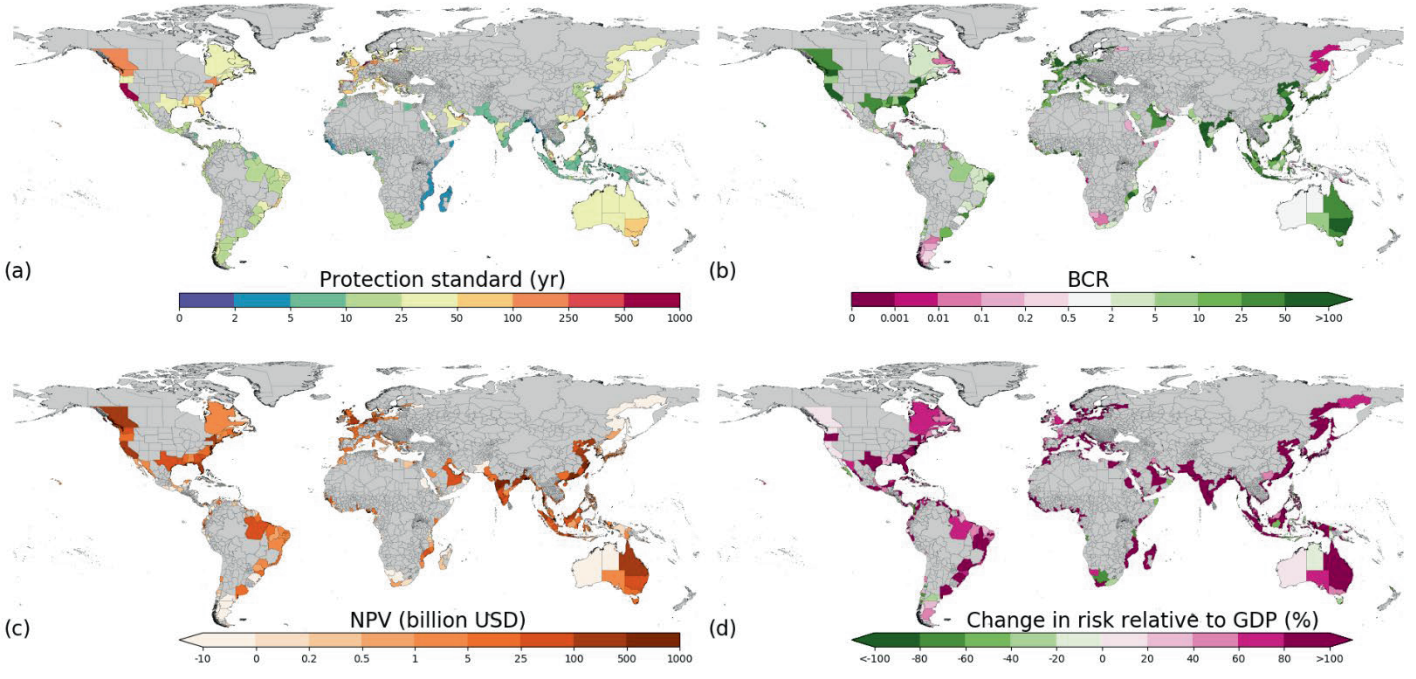

Figure B-3: Protection constant adaptation objective results of (a) protection standards, (b) BCRs, (c) total NPV, and (d) change in risk relative to GDP for RCP8.5–SSP5. Note that the protection standards (a) are the same as FLOPROS estimates. Regions with no data are indicated in grey.

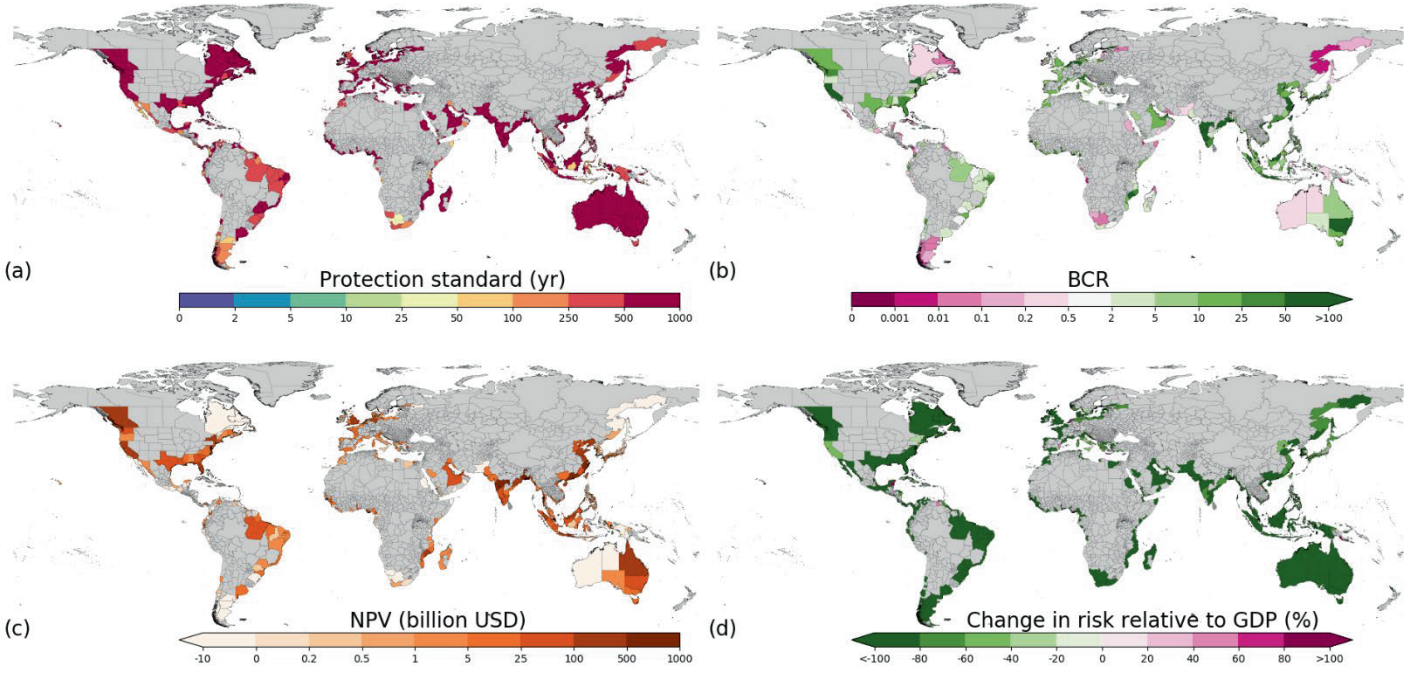

Figure B-4: Absolute-risk-constant adaptation objective results of (a) protection standards, (b) BCRs, (c) total NPV, and (d) change in risk relative to GDP for RCP8.5-SSP5. Regions with no data are indicated in grey.

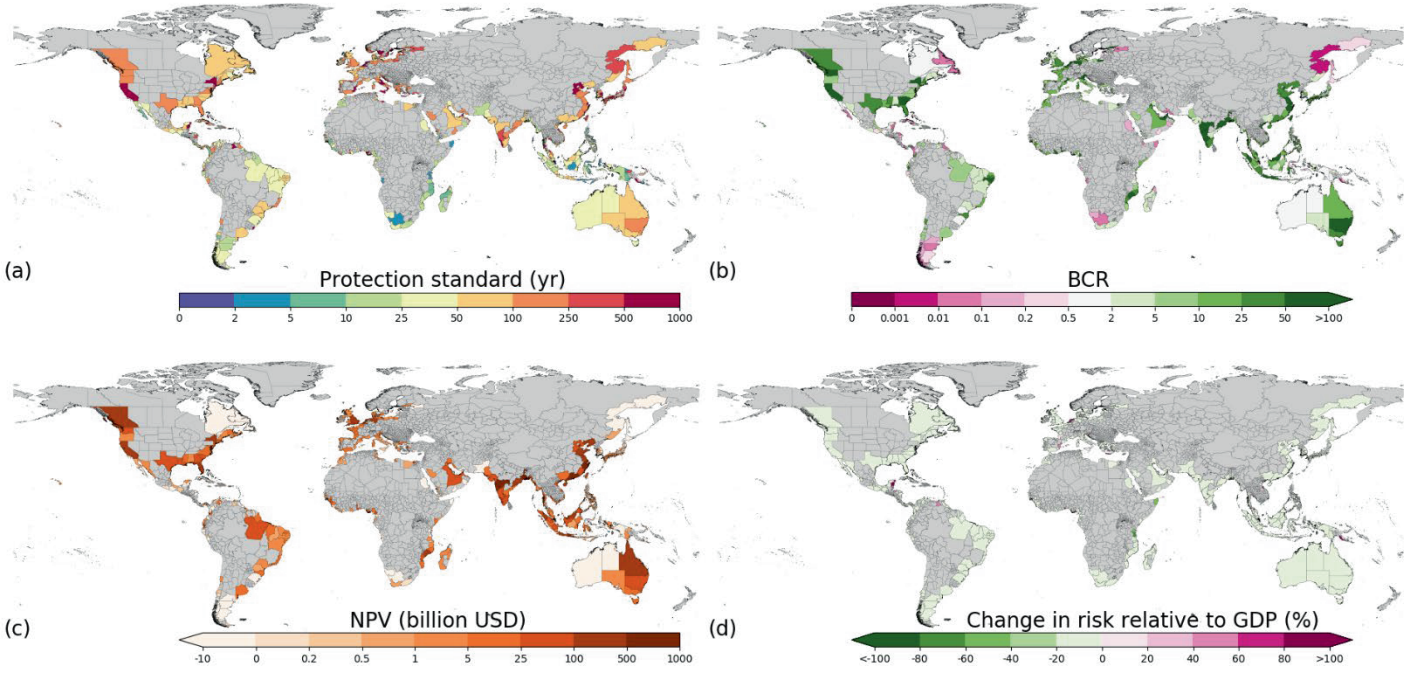

Figure B-5: Relative-risk-constant adaptation objective results of (a) protection standards, (b) BCRs, (c) total NPV, and (d) change in risk relative to GDP for RCP8.5–SSP5. Regions with no data are indicated in grey

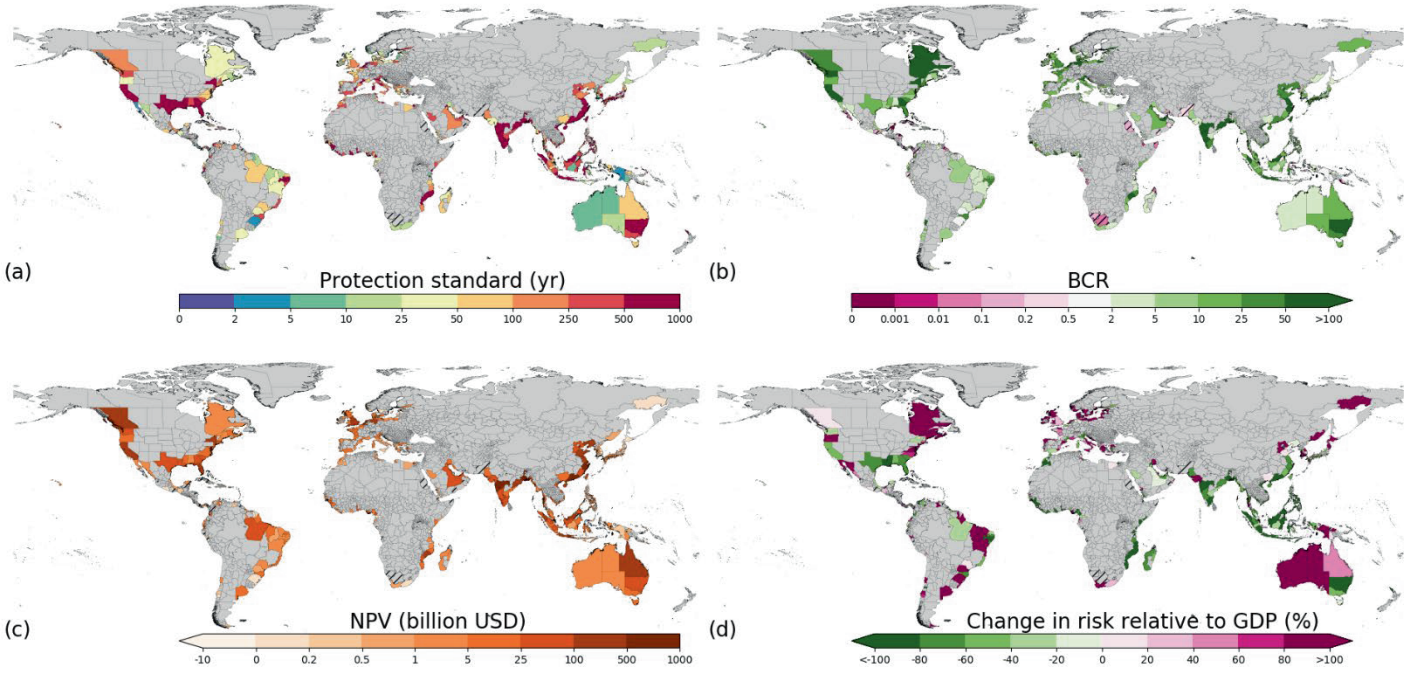

Figure B-6: Optimize adaptation objective results of (a) optimal protection standards, (b) BCRs, (c) total NPV, and (d) change in risk relative to GDP for RCP8.5–SSP5. Regions where no optimal protection standards are found are indicated with hatched lines, and regions with no data are indicated in grey.

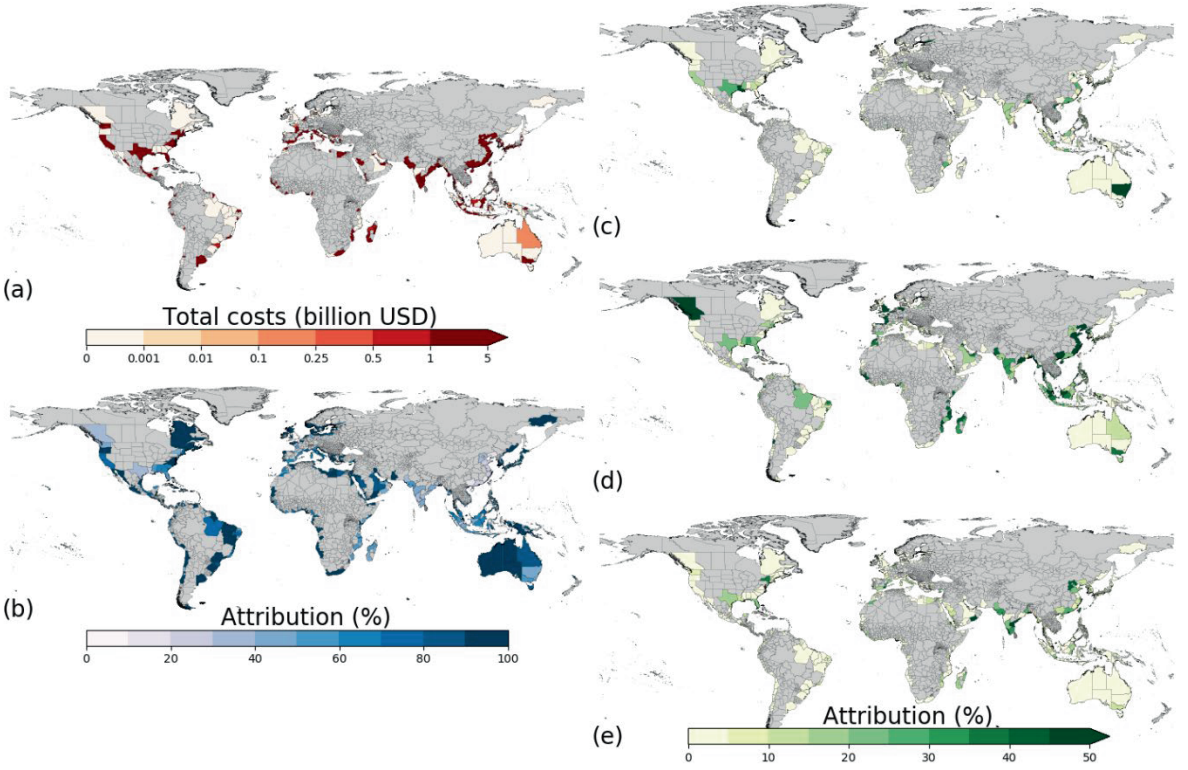

Figure B-7: Attribution of costs overview for RCP8.5–SSP5, with (a) total costs, (b) attribution of sea-level rise (ATR_{SLR}), (c) attribution of current optimizing (ATR_{CUR}), (d) attribution of socioeconomic change (ATR_{SEC}), and (e) subsidence (ATR_{SUB}). Note that the attribution of SLR is on a different scale, and regions with no data are indicated in grey.

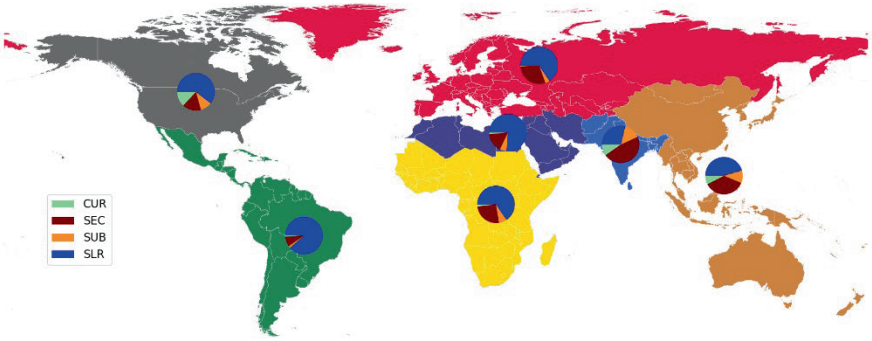

Figure B-8: Attribution of costs of adaptation for World Bank regions under the optimize adaptation objective and RCP8.5–SSP5 for optimizing to current conditions (CUR), socioeconomic change (SEC), subsidence (SUB), and sea-level rise (SLR).

Appendix C
Supplementary Figures C

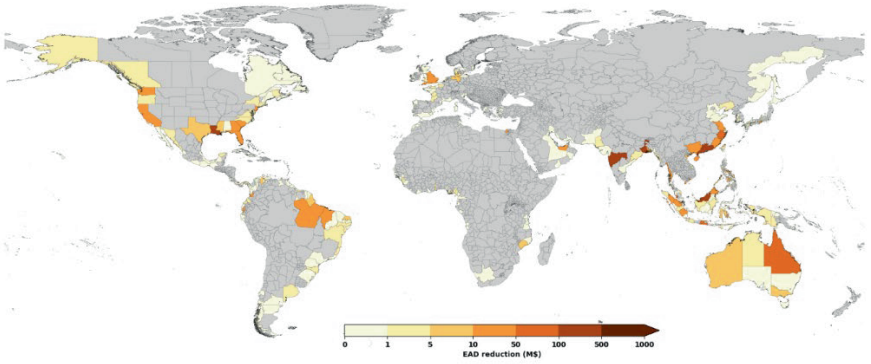

Figure C-12: Present-day absolute reduction of EAD though wave attenuation of foreshore vegetation. Sub-national regions with no data are indicated with grey colour.

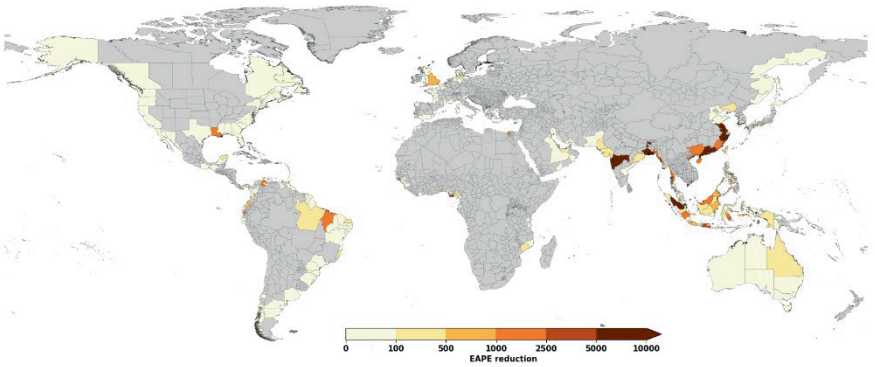

Figure C-13: Present-day absolute reduction of EAPE though wave attenuation of foreshore vegetation. Sub-national regions with no data are indicated with grey colour.

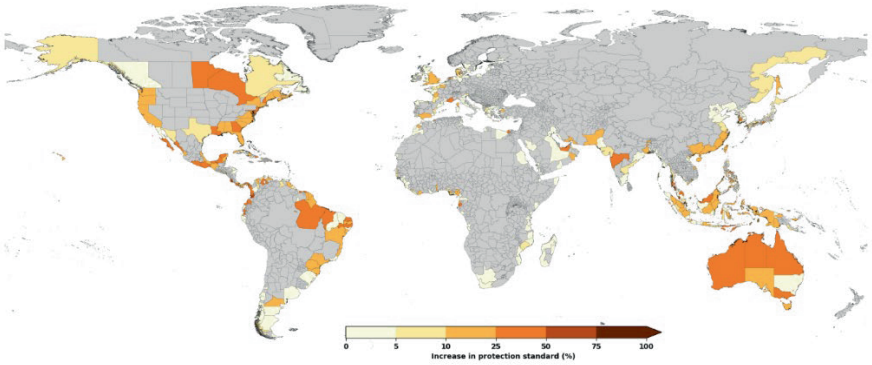

Figure C-14: Present-day increase in protection standards through the presence of foreshore vegetation. Sub-national regions with no data are indicated with grey colour.

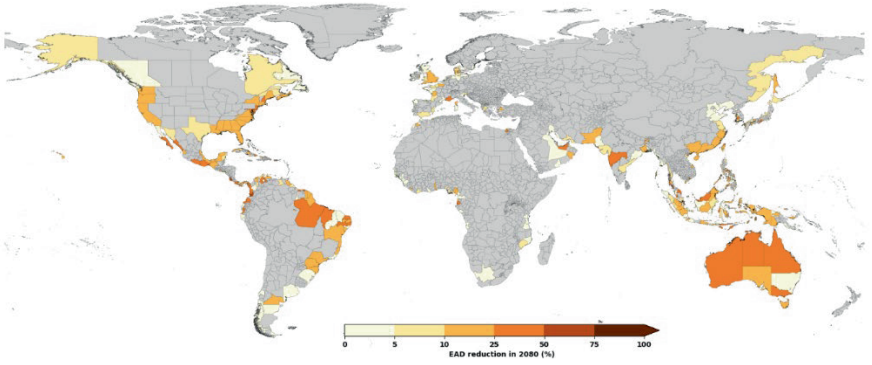

Figure C-15: Future relative reduction of EAD though wave attenuation of foreshore vegetation in 2080 under the RCP4.5/SSP2 scenario combination. Sub-national regions with no data are indicated with grey colour.

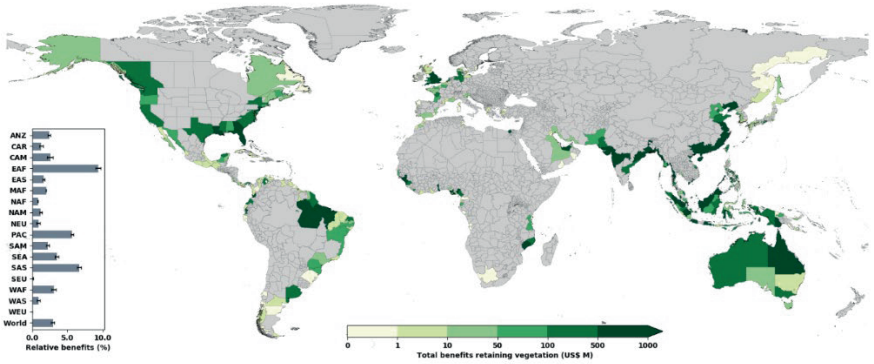

Figure C-16: Total discounted benefits of retaining vegetation in the adaptation objective 'keeping protection standards constant' for the scenario combination RCP8.5/SSP5. Sub-national regions with no data are indicated with grey colour. ANZ, Australia and New Zealand; CAR, Caribbean; CAM, Central America; EAF, Eastern Africa; EAS, Eastern Asia; MAF, Middle Africa; NAF, Northern Africa; NEU, Northern Europe; PAC, Pacific regions that include Melanesia, Polynesia, and Micronesia; SAM, South America; SEA, South-eastern Asia; SAS, Southern Asia; WAF, Western Africa; WAS, Western Asia; WEU, Western Europe.

Appendix D

Supplementary Figures and Tables D

Figure D-1: Mangrove extent per transect in hectares.

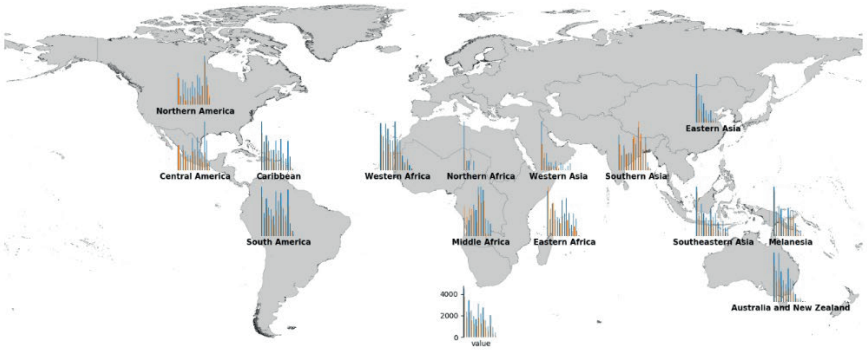

Figure D-2: Distribution of restorable mangrove forest width per urban/rural transects.

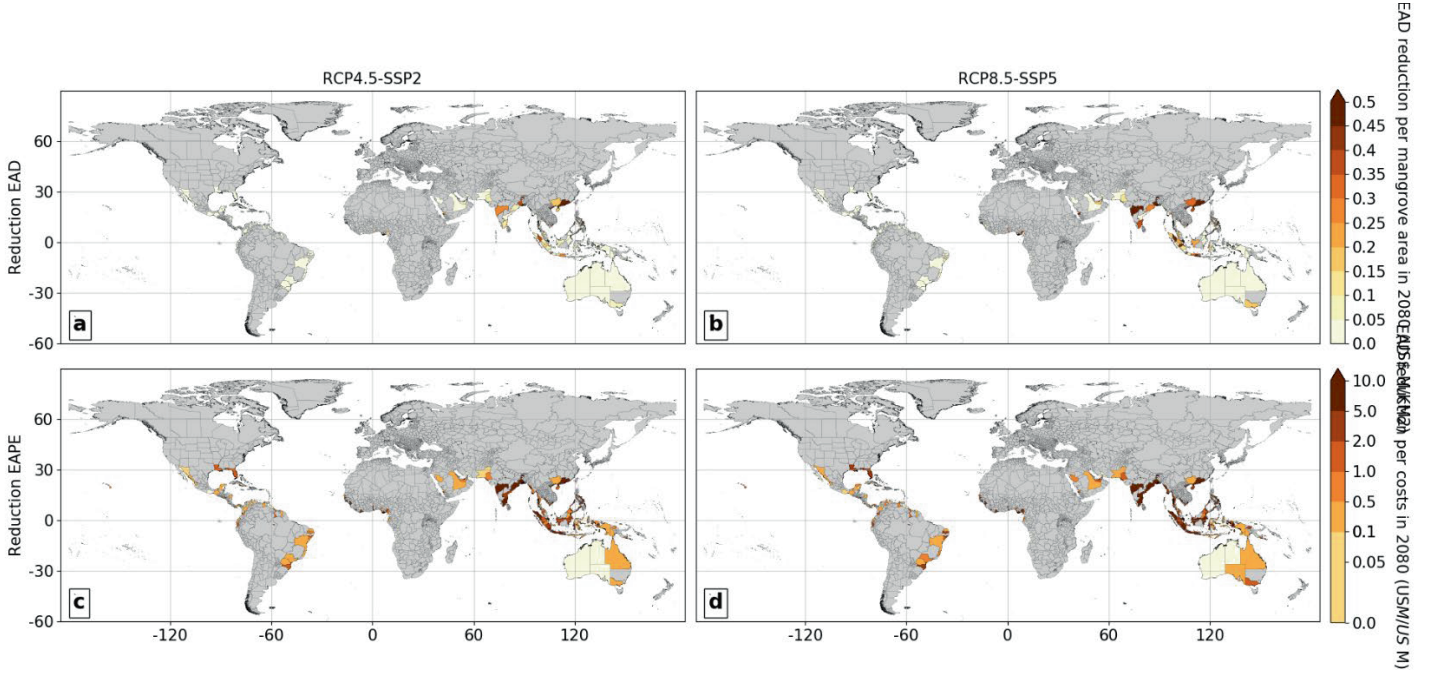

Figure D-3: Reduction of EAD and EAPE normalized to restorable mangrove extent.

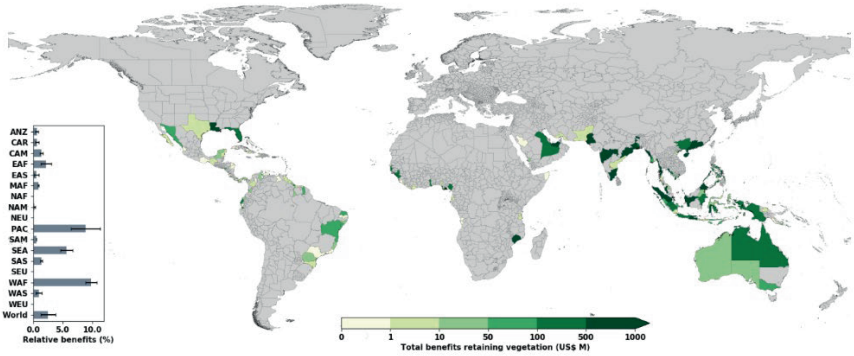

Figure D-4: Total benefits of mangrove restoration for the scenario of RCP4.5/SSP2.

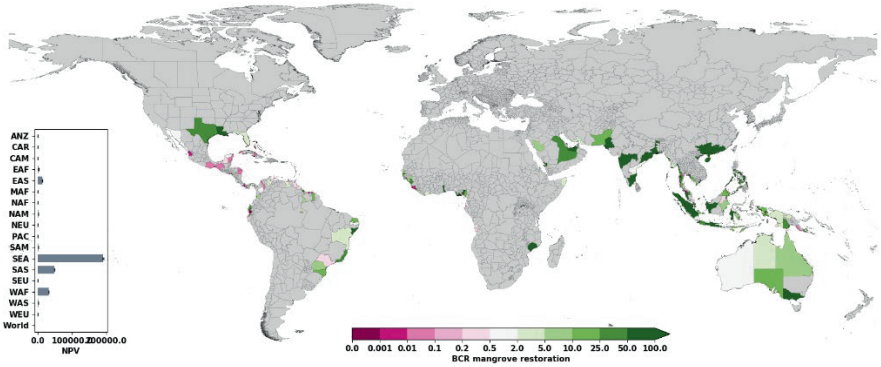

Figure D-5: Benefit-Cost Ratios of mangrove restoration under the future scenario of RCP8.5/SSP5 shown for sub-national regions in the world plot and sub-continental regions in the subplot. ANZ, Australia and New Zealand; CAR, Caribbean; CAM, Central America; EAF, Eastern Africa; EAS, Eastern Asia; MAF, Middle Africa; NAF, Northern Africa; NEU, Northern Europe; PAC, Pacific regions that include Melanesia, Polynesia, and Micronesia; SAM, South America; SEA, South-eastern Asia; SAS, Southern Asia; WAF, Western Africa; WAS, Western Asia; WEU, Western Europe.

Table D-1: Country scale ranking of the (future) benefits of mangrove restoration in terms of flood risk reduction under present-day conditions and future scenarios. EAD and NPV values are displayed in US$ billion and EAPE in thousands.

Present-day				**RCP4.5/SSP2**								**RCP8.5/SSP5**							
EAD		**EAPE**		**EAD**		**EAPE**		**NPV**		**BCR**		**EAD**		**EAPE**		**NPV**		**BCR**	
ISO	**Value**	**ISO**	**Value**	**ISO**	**Value**	**ISO**	**Value**	**ISO**	**Value**	**ISO**	**Value**	**ISO**	**Value**	**ISO**	**Value**	**ISO**	**Value**	**ISO**	**Value**
VNM	0.445	VNM	171.1	VNM	12.1	NGA	293.6	VNM	50.9	TWN	11246.6	VNM	26.3	NGA	271.8	VNM	103.9	TWN	14302.4
PHL	0.243	IDN	29.1	IND	7.7	VNM	223.1	IND	20.1	SGP	875.9	IND	18.6	VNM	193.0	IND	47.6	CHN	1055.2
IDN	0.217	IND	25.5	IDN	5.8	IND	106.3	IDN	15.4	CHN	541.3	IDN	15.0	IND	94.4	IDN	38.4	VNM	947.2
CHN	0.146	NGA	22.7	PHL	5.4	PHL	69.8	PHL	14.5	VNM	464.8	PHL	12.2	PHL	63.1	PHL	30.9	SGP	832.6
IND	0.113	CHN	14.3	NGA	4.5	IDN	52.7	NGA	10.8	BHR	441.0	NGA	11.4	IDN	50.5	NGA	26.8	BHR	582.0
MYS	0.089	PHL	11.6	CHN	2.2	CHN	15.8	CHN	7.0	GMB	222.0	CHN	4.4	CHN	16.9	CHN	13.6	GMB	426.6
NGA	0.062	BGD	5.7	MYS	1.0	BGD	15.2	THA	3.1	ARE	196.2	THA	1.8	BGD	11.8	MMR	6.7	NGA	406.5
USA	0.036	MMR	2.8	THA	0.8	MYS	10.8	MYS	3.0	NGA	164.8	MYS	1.7	MYS	8.2	THA	6.3	GNB	291.9
THA	0.032	MYS	2.6	BGD	0.5	GIN	10.1	MMR	2.3	PHL	134.0	BGD	1.3	GIN	4.3	MYS	4.5	PHL	284.7
ARE	0.025	THA	0.8	GIN	0.4	PAK	3.3	GIN	1.5	MTQ	108.9	MMR	1.2	THA	3.2	GIN	3.0	IND	234.6
MMR	0.021	PAK	0.7	MMR	0.4	MMR	3.3	USA	1.2	IND	99.8	GIN	0.8	PAK	3.1	MOZ	1.9	ARE	234.5
AUS	0.012	SEN	0.5	USA	0.2	SEN	3.1	ARE	1.0	GNB	92.3	USA	0.4	MMR	2.7	USA	1.7	MTQ	224.1
ECU	0.009	BRA	0.3	ARE	0.2	CMR	3.0	MOZ	0.6	GHA	84.6	GHA	0.3	CMR	2.7	PAK	1.2	GHA	199.0
BRA	0.005	USA	0.3	ECU	0.1	THA	2.5	PAK	0.6	THA	45.3	ARE	0.3	USA	1.6	ARE	1.2	PAK	91.5
MEX	0.005	CMR	0.3	GHA	0.1	GHA	1.7	GMB	0.5	PAK	42.0	ECU	0.3	SEN	1.6	GMB	0.9	THA	86.7

Appendix E

Supplementary Figure E

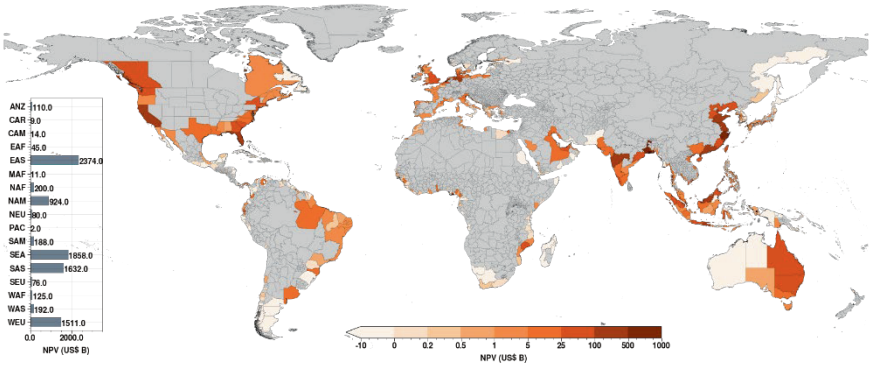

Figure E-1: The NPV of the adaptation strategies with the highest cost-effectiveness for the scenario of RCP4.5/SSP2

References

Abadi, M., Agarwal, A., Barham, P., Brevdo, E., Chen, Z., Citro, C., Corrado, G. S., Davis, A., Dean, J., Devin, M., Ghemawat, S., Goodfellow, I., Harp, A., Irving, G., Isard, M., Jia, Y., Jozefowicz, R., Kaiser, L., Kudlur, M., ... Zheng, X. (2016). *TensorFlow: Large-Scale Machine Learning on Heterogeneous Distributed Systems*. http://arxiv.org/abs/1603.04467

Adhikari, B., Baig, S. P., & Iftikhar, U. A. (2010). The Use and Management of Mangrove Ecosystems in Pakistan: *Http://Dx.Doi.Org/10.1177/1070496510384392*, *19*(4), 446–467. https://doi.org/10.1177/1070496510384392

Aerts, J. C. J. H. (2018). A Review of Cost Estimates for Flood Adaptation. *Water 2018, Vol. 10, Page 1646*, *10*(11), 1646. https://doi.org/10.3390/W10111646

Aerts, J. C. J. H., Botzen, W. J. W., Emanuel, K., Lin, N., de Moel, H., & Michel-Kerjan, E. O. (2014). Evaluating flood resilience strategies for coastal megacities. *Science (New York, N.Y.)*, *344*(6183), 473–475. https://doi.org/10.1126/science.1248222

Aerts, JC, Botzen, W., & De Moel, H. (2013). Cost estimates of flood protection and resilience measures. *Annals of the New York Academy of Sciences*, *1294*(39–48).

Akber, M. A., Patwary, M. M., Islam, M. A., & Rahman, M. R. (2018). Storm protection service of the Sundarbans mangrove forest, Bangladesh. *Natural Hazards*, *94*(1), 405–418. https://doi.org/10.1007/S11069-018-3395-8/TABLES/4

Alongi, D. M. (2008). Mangrove forests: Resilience, protection from tsunamis, and responses to global climate change. *Estuarine, Coastal and Shelf Science*, *76*(1), 1–13. https://doi.org/10.1016/J.ECSS.2007.08.024

Araos, M., Jagannathan, K., Shukla, R., Ajibade, I., Coughlan de Perez, E., Davis, K., Ford, J. D., Galappaththi, E. K., Grady, C., Hudson, A. J., Joe, E. T., Kirchhoff, C. J., Lesnikowski, A., Alverio, G. N., Nielsen, M., Orlove, B., Pentz, B., Reckien, D., Siders, A. R., ... Turek-Hankins, L. L. (2021). Equity in human adaptation-related responses: A systematic global review. *One Earth*, *4*(10), 1454–1467. https://doi.org/10.1016/J.ONEEAR.2021.09.001

Barbarossa, V., Huijbregts, M. A. J., Beusen, A. H. W., Beck, H. E., King, H., & Schipper, A. M. (2018). FLO1K, global maps of mean, maximum and minimum annual streamflow at 1 km resolution from 1960 through 2015. *Scientific Data*, *5*(1), 180052. https://doi.org/10.1038/sdata.2018.52

Barbier, E. B. (2015). Climate change impacts on rural poverty in low-elevation coastal zones. *Estuarine, Coastal and Shelf Science*, *165*, A1–A13. https://doi.org/10.1016/J.ECSS.2015.05.035

Barbier, E. B. (2017). Valuation of Mangrove Restoration. *Oxford Research Encyclopedia of Environmental Science*. https://doi.org/10.1093/ACREFORE/9780199389414.013.458

Barbier, E. B., Hacker, S. D., Kennedy, C., Koch, E. W., Stier, A. C., & Silliman, B. R. (2011). The value of estuarine and coastal ecosystem services. *Ecological Monographs*, *81*(2), 169–193. https://doi.org/10.1890/10-1510.1

Barbier, E. B., Koch, E. W., Silliman, B. R., Hacker, S. D., Wolanski, E., Primavera, J., Granek, E. F., Polasky, S., Aswani, S., Cramer, L. A., Stoms, D. M., Kennedy, C. J., Bael, D., Kappel, C. V, Perillo, G. M. E., & Reed, D. J. (2008). Coastal ecosystem-based management with nonlinear ecological functions and values. *Science (New York, N.Y.)*, *319*(5861), 321–323. https://doi.org/10.1126/science.1150349

Barnett, J., Graham, S., Mortreux, C., Fincher, R., Waters, E., & Hurlimann, A. (2014). A local coastal adaptation pathway. *Nature Climate Change 2014 4:12*, *4*(12), 1103–1108. https://doi.org/10.1038/nclimate2383

Barros, P., Alves, R., Djordjevicá, S., Djordjevicá, D., & Javadi, A. A. (2021). Understanding the NEEDS for ACTING: An integrated framework for applying nature-based solutions in Brazil. *Water Science and Technology*. https://doi.org/10.2166/WST.2021.513

Bayraktarov, E., Saunders, M. I., Abdullah, S., Mills, M., Beher, J., Possingham, H. P., Mumby, P. J., & Lovelock, C. E. (2016). The cost and feasibility of marine coastal restoration. *Ecological Applications*, *26*(4), 1055–1074. https://doi.org/10.1890/15-1077

Beck, M. W., Losada, I. J., Menéndez, P., Reguero, B. G., Díaz-Simal, P., & Fernández, F. (2018). The global flood protection savings provided by coral reefs. *Nature Communications*, *9*(1), 2186. https://doi.org/10.1038/s41467-018-04568-z

Belmonte Rivas, M., & Stoffelen, A. (2019). Characterizing ERA-Interim and ERA5 surface wind biases using ASCAT. *Ocean Science*, *15*(3), 831–852. https://doi.org/10.5194/os-15-831-2019

Bevacqua, E., Maraun, D., Vousdoukas, M. I., Voukouvalas, E., Vrac, M., Mentaschi, L., & Widmann, M. (2019). Higher probability of compound flooding from precipitation and storm surge in Europe under anthropogenic climate change. *Science Advances*, *5*(9), eaaw5531. https://doi.org/10.1126/sciadv.aaw5531

Bian, G., Nie, G., & Qiu, X. (2021). How well is outer tropical cyclone size represented in the ERA5 reanalysis dataset ? *Atmospheric Research*, *249*, 105339. https://doi.org/10.1016/j.atmosres.2020.105339

Blankespoor, B., Dasgupta, S., & Laplante, B. (2014). Sea-Level Rise and Coastal Wetlands. *Ambio*, *43*(8), 996–1005. https://doi.org/10.1007/s13280-014-0500-4

Bloemendaal, N., de Moel, H., Muis, S., Haigh, I. D., & Aerts, J. C. J. H. (2020). Estimation of global tropical cyclone wind speed probabilities using the STORM dataset. *Scientific Data*, *7*(1), 1–11. https://doi.org/10.1038/s41597-020-00720-x

Bloemendaal, N., Haigh, I. D., de Moel, H., Muis, S., Haarsma, R. J., & Aerts, J. C. J. H. (2020). Generation of a global synthetic tropical cyclone hazard dataset using STORM. *Scientific Data*, *7*(1), 40. https://doi.org/10.1038/s41597-020-0381-2

Bloemendaal, N., Muis, S., Haarsma, R. J., Verlaan, M., Irazoqui Apecechea, M., de Moel, H., Ward, P. J., & Aerts, J. C. J. H. (2018). Global modeling of tropical cyclone storm surges using high resolution forecasts. *Climate Dynamics*, *in prep.*(0), 0. https://doi.org/10.1007/s00382-018-4430-x

Borsje, B. W., van Wesenbeeck, B. K., Dekker, F., Paalvast, P., Bouma, T. J., van Katwijk, M. M., & de Vries, M. B. (2011). How ecological engineering can serve in coastal protection. *Ecological Engineering*, *37*(2), 113–122. https://doi.org/10.1016/J.ECOLENG.2010.11.027

Bos, A. J. (2008). *Optimal safety level for the New Orleans East polder; A preliminary risk analysis*.

Bouwman, A. F., Kram, T., & Klein Goldewijk, K. (2006). *Integrated modelling of global environmental change: an overview of Image 2.4*.

BPIE. (2011). *Europe's Buildings under the Microscope - a country by country review of the energy performance of buildings*.

Bradley, A. A., & Schwartz, S. S. (2011). Summary verification measures and their interpretation for ensemble forecasts. *Monthly Weather Review*, *139*(9), 3075–3089. https://doi.org/10.1175/2010MWR3305.1

Bright, E.A., Coleman, P.R., Rose, A.N., Urban, M. L. (2011). *LandScan 2010 High Resolution Global Population Data Set [dataset]*.

Broekx, S., Smets, S., Liekens, I., Bulckaen, D., & De Nocker, L. (2011). Designing a long-term flood risk management plan for the Scheldt estuary using a risk-based approach. *Natural Hazards*, *57*(2), 245–

266. https://doi.org/10.1007/s11069-010-9610-x

Brown, J. M., Bolanos, R., Howarth, M. J., & Souza, A. J. (2012). Extracting sea level residual in tidally dominated estuarine environments. *Ocean Dynamics*, *62*(7), 969–982. https://doi.org/10.1007/s10236-012-0543-7

Brown, J. M., Bolaños, R., & Souza, A. J. (2014). Process Contribution to the Time-Varying Residual Circulation in Tidally Dominated Estuarine Environments. *Estuaries and Coasts*, *37*(5), 1041–1057. https://doi.org/10.1007/s12237-013-9745-6

Brown, S., Nicholls, R. J., Goodwin, P., Haigh, I. D., Lincke, D., Vafeidis, A. T., & Hinkel, J. (2018). Quantifying Land and People Exposed to Sea-Level Rise with No Mitigation and 1.5°C and 2.0°C Rise in Global Temperatures to Year 2300. *Earth's Future*, *6*(3), 583–600. https://doi.org/10.1002/2017EF000738

Brown, Sally, Nicholls, R. J., Lowe, J. A., & Hinkel, J. (2016). Spatial variations of sea-level rise and impacts: An application of DIVA. *Climatic Change*, *134*(3), 403–416. https://doi.org/10.1007/s10584-013-0925-y

Bruneau, N., Polton, J., Williams, J., & Holt, J. (2020). Estimation of global coastal sea level extremes using neural networks. *Environmental Research Letters*, *15*(7). https://doi.org/10.1088/1748-9326/ab89d6

Calero, J., Hendriksen, G., Dijkstra, J., & Lelij, A. van der. (2017). *FAST MI-SAFE platform: Foreshore assessment using space technology*.

Callaghan, J., and, S. P.-A. M., & 2014, undefined. (2014). Major coastal flooding in southeastern Australia 1860–2012, associated deaths and weather systems. *Researchgate.Net*. https://doi.org/10.22499/2.6403.002

Carrère, L., & Lyard, F. (2003). Modeling the barotropic response of the global ocean to atmospheric wind and pressure forcing - comparisons with observations. *Geophysical Research Letters*, *30*(6). https://doi.org/10.1029/2002GL016473

Chattopadhyay, A., Hassanzadeh, P., & Pasha, S. (2020). Predicting clustered weather patterns: A test case for applications of convolutional neural networks to spatio-temporal climate data. *Scientific Reports*, *10*(1), 1–13. https://doi.org/10.1038/s41598-020-57897-9

Chen, B., Xiao, X., Li, X., Pan, L., Doughty, R., Ma, J., Dong, J., Qin, Y., Zhao, B., Wu, Z., Sun, R., Lan, G., Xie, G., Clinton, N., & Giri, C. (2017). A mangrove forest map of China in 2015: Analysis of time series Landsat 7/8 and Sentinel-1A imagery in Google Earth Engine cloud computing platform. *ISPRS Journal of Photogrammetry and Remote Sensing*, *131*, 104–120. https://doi.org/10.1016/j.isprsjprs.2017.07.011

Chen, R., Zhang, W., & Wang, X. (2020). Machine learning in tropical cyclone forecast modeling: A review. *Atmosphere*, *11*(7), 1–29. https://doi.org/10.3390/atmos11070676

Cheong, S.-M., Silliman, B., Wong, P. P., van Wesenbeeck, B., Kim, C.-K., & Guannel, G. (2013). Coastal adaptation with ecological engineering. *Nature Climate Change*, *3*(9), 787–791. https://doi.org/10.1038/nclimate1854

Chi, G., Fang, H., Chatterjee, S., & Blumenstock, J. E. (2021). Micro-Estimates of Wealth for all Low- and Middle-Income Countries. *Proceedings of the National Academy of Sciences*, *119*(3). https://doi.org/10.1073/PNAS.2113658119/-/DCSUPPLEMENTAL

Chollet, F. (2016). *Keras*.

Christie, E. K., Spencer, T., Owen, D., McIvor, A. L., Möller, I., & Viavattene, C. (2018). Regional coastal flood risk assessment for a tidally dominant, natural coastal setting: North Norfolk, southern North Sea. *Coastal Engineering*, *134*(January 2017), 177–190. https://doi.org/10.1016/j.coastaleng.2017.05.003

Cid, A., Camus, P., Castanedo, S., Méndez, F. J., & Medina, R. (2017). Global reconstructed daily surge levels from the 20th Century Reanalysis (1871–2010). *Global and Planetary Change*, *148*(November), 9–21. https://doi.org/10.1016/j.gloplacha.2016.11.006

Cid, A., Wahl, T., Chambers, D. P., & Muis, S. (2018). Storm Surge Reconstruction and Return Water Level Estimation in Southeast Asia for the 20th Century. *Journal of Geophysical Research: Oceans*, *123*(1), 437–451. https://doi.org/10.1002/2017JC013143

Clark, P. U., Shakun, J. D., Marcott, S. A., Mix, A. C., Eby, M., Kulp, S., Levermann, A., Milne, G. A., Pfister, P. L., Santer, B. D., Schrag, D. P., Solomon, S., Stocker, T. F., Strauss, B. H., Weaver, A. J., Winkelmann, R., Archer, D., Bard, E., Goldner, A., ... Plattner, G.-K. (2016). Consequences of twenty-first-century policy for multi-millennial climate and sea-level change. *Nature Climate Change*, *6*(4), 360–369. https://doi.org/10.1038/nclimate2923

Codiga, D. (2011). *Unified tidal analysis and prediction using the UTide Matlab functions*. https://scholar.google.com/ftp://po.gso.uri.edu/pub/downloads/codiga/pubs/2011Codiga-UTide-Report.pdf

Cohen-Shacham, E., Walters, G., ... C. J.-I. G., & 2016, undefined. (2016). Nature-based solutions to address global societal challenges. *Serval.Unil.Ch*. https://doi.org/10.2305/IUCN.CH.2016.13.en

Colberg, F., & McInnes, K. L. (2012). The impact of future changes in weather patterns on extreme sea levels over southern Australia. *Journal of Geophysical Research: Oceans*, *117*(C8), n/a-n/a. https://doi.org/10.1029/2012JC007919

Cortes, C., Mohri, M., & Rostamizadeh, A. (2012). L2 Regularization for Learning Kernels. *Proceedings of the 25th Conference on Uncertainty in Artificial Intelligence, UAI 2009*, 109–116. http://arxiv.org/abs/1205.2653

Creach, A., Chevillot-miot, E., Mercier, D., & Pourinet, L. (2016). Vulnerability to coastal flood hazard of residential buildings on Noirmoutier Island (France). *Journal of Maps*, *12*(2), 371–381. https://doi.org/10.1080/17445647.2015.1027041/SUPPL_FILE/TJOM_A_1027041_SM3056.PDF

Cummings, C. A., Todhunter, P. E., & Rundquist, B. C. (2012). Using the Hazus-MH flood model to evaluate community relocation as a flood mitigation response to terminal lake flooding: The case of Minnewaukan, North Dakota, USA. *Applied Geography*, *32*(2), 889–895. https://doi.org/10.1016/J.APGEOG.2011.08.016

Dahdouh-Guebas, F., & Cannicci, S. (2021). Mangrove Restoration Under Shifted Baselines and Future Uncertainty. *Frontiers in Marine Science*, *0*(December), 1864. https://doi.org/10.3389/FMARS.2021.799543

Das, H. S., Jung, H., Ebersole, B., Wamsley, T., & Whalin, R. W. (2011). an Efficient Storm Surge Forecasting Tool for Coastal Mississippi. *Coastal Engineering Proceedings*, *1*(32), 21. https://doi.org/10.9753/icce.v32.currents.21

Daw, T., Brown, K., Rosendo, S., & Pomeroy, R. (2011). Applying the ecosystem services concept to poverty alleviation: the need to disaggregate human well-being. *Environmental Conservation*, *38*(4), 370–379. https://doi.org/10.1017/S0376892911000506

de Graaf, I. E. M., van Beek, R. L. P. H., Gleeson, T., Moosdorf, N., Schmitz, O., Sutanudjaja, E. H., & Bierkens, M. F. P. (2017). A global-scale two-layer transient groundwater model: Development and application to groundwater depletion. *Advances in Water Resources*, *102*, 53–67. https://doi.org/10.1016/J.ADVWATRES.2017.01.011

de Oliviera, M. M. F., Ebecken, F. F., de Oliviera, J. L. F., & de Azevedo Santos, I. (2009). Neural network model to predict a storm surge. *Journal of Applied Meteorology and Climatology*, *48*(1), 143–155. https://doi.org/10.1175/2008JAMC1907.1

de Ruig, L. T., Barnard, P. L., Botzen, W. J. W., Grifman, P., Hart, J. F., de Moel, H., Sadrpour, N., & Aerts, J. C. J. H. (2019). An economic evaluation of adaptation pathways in coastal mega cities: An illustration for Los Angeles. *Science of the Total Environment*, *678*, 647–659. https://doi.org/10.1016/j.scitotenv.2019.04.308

De Sherbinin, A., Schiller, A., & Pulsipher, A. (2007). The vulnerability of global cities to climate hazards. *Environment and Urbanization*, *19*(1), 39–64. https://doi.org/10.1177/0956247807076725

Dee, D. P., Uppala, S. M., Simmons, A. J., Berrisford, P., Poli, P., Kobayashi, S., Andrae, U., Balmaseda, M. A., Balsamo, G., Bauer, P., Bechtold, P., Beljaars, A. C. M., van de Berg, L., Bidlot, J., Bormann, N., Delsol, C., Dragani, R., Fuentes, M., Geer, A. J., ... Vitart, F. (2011). The ERA-Interim reanalysis: configuration and performance of the data assimilation system. *Quarterly Journal of the Royal Meteorological Society*, *137*(656), 553–597. https://doi.org/10.1002/qj.828

del Valle, A., Eriksson, M., Ishizawa, O. A., & Miranda, J. J. (2020). Mangroves protect coastal economic activity from hurricanes. *Proceedings of the National Academy of Sciences of the United States of America*, *117*(1), 265–270. https://doi.org/10.1073/PNAS.1911617116/-/DCSUPPLEMENTAL

Delft3D-WES. (2019). *Delft3D-WES User Manual*. (3.01; p. 46). Deltares.

Diaz, D. B. (2016). Estimating global damages from sea level rise with the Coastal Impact and Adaptation Model (CIAM). *Climatic Change*, *137*(1–2), 143–156. https://doi.org/10.1007/S10584-016-1675-4/FIGURES/3

Díaz, S., Pascual, U., Stenseke, M., Martín-López, B., Watson, R. T., Molnár, Z., Hill, R., Chan, K. M. A., Baste, I. A., Brauman, K. A., Polasky, S., Church, A., Lonsdale, M., Larigauderie, A., Leadley, P. W., Van Oudenhoven, A. P. E., Van Der Plaat, F., Schröter, M., Lavorel, S., ... Shirayama, Y. (2018). Assessing nature's contributions to people: Recognizing culture, and diverse sources of knowledge, can improve assessments. *Science*, *359*(6373), 270–272. https://doi.org/10.1126/SCIENCE.AAP8826/SUPPL_FILE/AAP8826-DIAZ-SM.PDF

Disaster(CRED), C. for R. on the E. of. (2015). *The Human Cost Of Natural Disasters: A global perspective*. http://repo.floodalliance.net/jspui/handle/44111/1165

Dixon, T. H., Amelung, F., Ferretti, A., Novali, F., Rocca, F., Dokka, R., Sella, G., Kim, S.-W., Wdowinski, S., & Whitman, D. (2006). Subsidence and flooding in New Orleans. *Nature*, *441*(7093), 587–588. https://doi.org/10.1038/441587a

Du, S., Scussolini, P., Ward, P. J., Zhang, M., Wen, J., Wang, L., Koks, E., Diaz-Loaiza, A., Gao, J., Ke, Q., & Aerts, J. C. J. H. (2020). Hard or soft flood adaptation? Advantages of a hybrid strategy for Shanghai. *Global Environmental Change*, *61*, 102037. https://doi.org/10.1016/J.GLOENVCHA.2020.102037

Duarte, C. M., Losada, I. J., Hendriks, I. E., Mazarrasa, I., & Marbà, N. (2013). The role of coastal plant communities for climate change mitigation and adaptation. In *Nature Climate Change* (Vol. 3, Issue 11, pp. 961–968). https://doi.org/10.1038/nclimate1970

Dullaart, J. C. M., Muis, S., Bloemendaal, N., & Aerts, J. C. J. H. (2020). Advancing global storm surge modelling using the new ERA5 climate reanalysis. *Climate Dynamics*, *54*(1–2), 1007–1021. https://doi.org/10.1007/s00382-019-05044-0

EEA. (2016). *Corine Land Cover 2012 seamless 100m raster database (Version 18.5)*.

Eilander, D., Couasnon, A., Ikeuchi, H., Muis, S., Yamazaki, D., Winsemius, H. C., & Ward, P. J. (2020). The effect of surge on riverine flood hazard and impact in deltas globally. *Environmental Research Letters*, *15*(10), 104007. https://doi.org/10.1088/1748-9326/ab8ca6

Ericson, J. P., Vörösmarty, C. J., Dingman, S. L., Ward, L. G., & Meybeck, M. (2006). Effective sea-level rise and deltas: Causes of change and human dimension implications. *Global and Planetary Change*, *50*(1–2), 63–82. https://doi.org/10.1016/J.GLOPLACHA.2005.07.004

Erkens, G., Bucx, T., Dam, R., De Lange, G., & Lambert, J. (2015). Sinking coastal cities. *Proceedings of the International Association of Hydrological Sciences*, *372*, 189–198. https://doi.org/10.5194/piahs-372-189-2015

Erkens, G., & Sutanudjaja, E. H. (2015). Towards a global land subsidence map. *Proceedings of the International Association of Hydrological Sciences*, *372*, 83–87. https://doi.org/10.5194/piahs-372-83-2015

Erwin, K. L. (2009). Wetlands and global climate change: The role of wetland restoration in a changing world. *Wetlands Ecology and Management*, *17*(1), 71–84. https://doi.org/10.1007/S11273-008-9119-1/TABLES/1

Fagherazzi, S., Kirwan, M. L., Mudd, S. M., Guntenspergen, G. R., Temmerman, S., D'Alpaos, A., van de Koppel, J., Rybczyk, J. M., Reyes, E., Craft, C., & Clough, J. (2012). Numerical models of salt marsh evolution: Ecological, geomorphic, and climatic factors. *Reviews of Geophysics*, *50*(1), RG1002. https://doi.org/10.1029/2011RG000359

Fang, K., Shen, C., Kifer, D., & Yang, X. (2017). Prolongation of SMAP to Spatiotemporally Seamless Coverage of Continental U.S. Using a Deep Learning Neural Network. *Geophysical Research Letters*, *44*(21), 11,030-11,039. https://doi.org/10.1002/2017GL075619

FAO. (n.d.). The state of food and agriculture, 2007: paying farmers for environmental services. In *2007*. Retrieved February 22, 2022, from https://scholar.google.com/scholar?hl=en&as_sdt=0%2C5&q=The+state+of+food+and+agriculture%2C+2007%3A+paying+farmers+for+environmental+services&btnG=

Farzad, A., Mashayekhi, H., & Hassanpour, H. (2019). A comparative performance analysis of different activation functions in LSTM networks for classification. *Neural Computing and Applications*, *31*(7), 2507–2521. https://doi.org/10.1007/s00521-017-3210-6

Frantzeskaki, N. (2019). Seven lessons for planning nature-based solutions in cities. *Environmental Science & Policy*, *93*, 101–111. https://doi.org/10.1016/J.ENVSCI.2018.12.033

Friess, D. A., Rogers, K., Lovelock, C. E., Krauss, K. W., Hamilton, S. E., Lee, S. Y., Lucas, R., Primavera, J., Rajkaran, A., & Shi, S. (2019). The State of the World's Mangrove Forests: Past, Present, and Future. *Annual Review of Environment and Resources*, *44*, 89–115. https://doi.org/10.1146/ANNUREV-ENVIRON-101718-033302

GADM. (2012). *GADM database of Global Administrative Areas*.

Galloway, D. L., Erkens, G., Kuniansky, E. L., & Rowland, J. C. (2016). Preface: Land subsidence processes. *Hydrogeology Journal*, *24*(3), 547–550. https://doi.org/10.1007/s10040-016-1386-y

Gedan, K. B., Kirwan, M. L., Wolanski, E., Barbier, E. B., Silliman, B. R., Gedan, K. B., Kirwan, M. L., Wolanski, E., Barbier, E. B., & Silliman, B. R. (2010). The present and future role of coastal wetland vegetation in protecting shorelines: answering recent challenges to the paradigm. *Climatic Change 2010 106:1*, *106*(1), 7–29. https://doi.org/10.1007/S10584-010-0003-7

Gilleland, M. (2015). *Package "verification."* https://cran.microsoft.com/snapshot/2018-04-09/web/packages/verification/verification.pdf

Giri, C., Ochieng, E., Tieszen, L. L., Zhu, Z., Singh, A., Loveland, T., Masek, J., & Duke, N. (2011). Status and distribution of mangrove forests of the world using earth observation satellite data. *Global Ecology and Biogeography*, *20*(1), 154–159. https://doi.org/10.1111/j.1466-8238.2010.00584.x

Goldberg, L., Lagomasino, D., Thomas, N., & Fatoyinbo, T. (2020). Global declines in human-driven mangrove loss. *Global Change Biology*, *26*(10), 5844–5855. https://doi.org/10.1111/GCB.15275

Güneralp, B., Güneralp, İ., & Liu, Y. (2015). Changing global patterns of urban exposure to flood and drought hazards. *Global Environmental Change*, *31*, 217–225.

https://doi.org/10.1016/J.GLOENVCHA.2015.01.002

Haasnoot, M., Kwakkel, J. H., Walker, W. E., & ter Maat, J. (2013). Dynamic adaptive policy pathways: A method for crafting robust decisions for a deeply uncertain world. *Global Environmental Change*, *23*(2), 485–498. https://doi.org/10.1016/J.GLOENVCHA.2012.12.006

Haer, T., Botzen, W. J. W., van Roomen, V., Connor, H., Zavala-Hidalgo, J., Eilander, D. M., & Ward, P. J. (2018). Coastal and river flood risk analyses for guiding economically optimal flood adaptation policies: a country-scale study for Mexico. *Philosophical Transactions of the Royal Society A: Mathematical, Physical and Engineering Sciences*, *376*(2121), 20170329. https://doi.org/10.1098/rsta.2017.0329

Haigh, I. D., Wadey, M. P., Wahl, T., Ozsoy, O., Nicholls, R. J., Brown, J. M., Horsburgh, K., & Gouldby, B. (2016). Analysis : Spatial and temporal analysis of extreme sea level and storm surge events around the coastline of the UK. *Nature Scientific Data*, *3*, 1–14. https://doi.org/10.1038/sdata.2016.107

Hallegatte, S. (2016). *Shock waves: managing the impacts of climate change on poverty*. https://books.google.com/books?hl=en&lr=&id=H1IUCwAAQBAJ&oi=fnd&pg=PP1&dq=Shock+waves:+managing+the+impacts+of+climate+change+on+poverty&ots=pJ__gFDTKD&sig=nqRda4KN7HbLQTLt4NVTUlOYt_g

Hallegatte, Stephane, Green, C., Nicholls, R. J., & Corfee-Morlot, J. (2013). Future flood losses in major coastal cities. *Nature Climate Change*, *3*(9), 802–806. https://doi.org/10.1038/nclimate1979

Hallegatte, Stephane, & Rozenberg, J. (2017). Climate change through a poverty lens. *Nature Climate Change 2017 7:4*, *7*(4), 250–256. https://doi.org/10.1038/nclimate3253

Ham, Y. G., Kim, J. H., & Luo, J. J. (2019). Deep learning for multi-year ENSO forecasts. *Nature*, *573*(7775), 568–572. https://doi.org/10.1038/s41586-019-1559-7

Hanson, S., Nicholls, R., Ranger, N., Hallegatte, S., Corfee-Morlot, J., Herweijer, C., & Chateau, J. (2011). A global ranking of port cities with high exposure to climate extremes. *Climatic Change*, *104*(1), 89–111. https://doi.org/10.1007/s10584-010-9977-4

Hashemi, M. R., Spaulding, M. L., Shaw, A., Farhadi, H., & Lewis, M. (2016). An efficient artificial intelligence model for prediction of tropical storm surge. *Natural Hazards*, *82*(1), 471–491. https://doi.org/10.1007/s11069-016-2193-4

Hauer, M. E., Fussell, E., Mueller, V., Burkett, M., Call, M., Abel, K., McLeman, R., & Wrathall, D. (2019). Sea-level rise and human migration. *Nature Reviews Earth & Environment 2019 1:1*, *1*(1), 28–39. https://doi.org/10.1038/s43017-019-0002-9

Hecht, R., Meinel, G., & Buchroithner, M. (2015). Automatic identification of building types based on topographic databases – a comparison of different data sources. *International Journal of Cartography*, *1*(1), 18–31. https://doi.org/10.1080/23729333.2015.1055644

Hemer, M. A., Fan, Y., Mori, N., Semedo, A., & Wang, X. L. (2013). Projected changes in wave climate from a multi-model ensemble. *Nature Climate Change*, *3*(5), 471–476. https://doi.org/10.1038/nclimate1791

Hersbach, H. (2000). Decomposition of the continuous ranked probability score for ensemble prediction systems. *Weather and Forecasting*, *15*(5), 559–570. https://doi.org/10.1175/1520-0434(2000)015<0559:DOTCRP>2.0.CO;2

Hersbach, Hans, Bell, B., Berrisford, P., Hirahara, S., Horányi, A., Muñoz-Sabater, J., Nicolas, J., Peubey, C., Radu, R., Schepers, D., Simmons, A., Soci, C., Abdalla, S., Abellan, X., Balsamo, G., Bechtold, P., Biavati, G., Bidlot, J., Bonavita, M., … Thépaut, J. (2020). The ERA5 global reanalysis. *Quarterly Journal of the Royal Meteorological Society*, *146*(730), 1999–2049. https://doi.org/10.1002/qj.3803

Hertel, L., Collado, J., Sadowski, P., Ott, J., & Baldi, P. (2020). Sherpa: Robust hyperparameter optimization

for machine learning. *SoftwareX, 12*, 100591. https://doi.org/10.1016/j.softx.2020.100591

Hewamalage, H., Bergmeir, C., & Bandara, K. (2021). Recurrent Neural Networks for Time Series Forecasting: Current status and future directions. *International Journal of Forecasting*, *37*(1), 388–427. https://doi.org/10.1016/j.ijforecast.2020.06.008

Hibbert, A., Royston, S. J., Horsburgh, K. J., Leach, H., & Hisscott, A. (2015). An empirical approach to improving tidal predictions using recent real-time tide gauge data. *Journal of Operational Oceanography*, *8*(1), 40–51. https://doi.org/10.1080/1755876x.2015.1014641

Hinkel, J., Feyen, L., Hemer, M., Le Cozannet, G., Lincke, D., Marcos, M., Mentaschi, L., Merkens, J. L., de Moel, H., Muis, S., Nicholls, R. J., Vafeidis, A. T., van de Wal, R. S. W., Vousdoukas, M. I., Wahl, T., Ward, P. J., & Wolff, C. (2021). Uncertainty and Bias in Global to Regional Scale Assessments of Current and Future Coastal Flood Risk. *Earth's Future*, *9*(7), e2020EF001882. https://doi.org/10.1029/2020EF001882

Hinkel, Jochen, & Klein, R. J. T. (2009). Integrating knowledge to assess coastal vulnerability to sea-level rise: The development of the DIVA tool. *Global Environmental Change*, *19*(3), 384–395. https://doi.org/10.1016/J.GLOENVCHA.2009.03.002

Hinkel, Jochen, Lincke, D., Vafeidis, A. T., Perrette, M., Nicholls, R. J., Tol, R. S. J., Marzeion, B., Fettweis, X., Ionescu, C., & Levermann, A. (2014a). Coastal flood damage and adaptation costs under 21st century sea-level rise. *Proceedings of the National Academy of Sciences of the United States of America*, *111*(9), 3292–3297. https://doi.org/10.1073/pnas.1222469111

Hinkel, Jochen, Nicholls, R. J., Tol, R. S. J., Wang, Z. B., Hamilton, J. M., Boot, G., Vafeidis, A. T., McFadden, L., Ganopolski, A., & Klein, R. J. T. (2013). A global analysis of erosion of sandy beaches and sea-level rise: An application of DIVA. *Global and Planetary Change*, *111*, 150–158. https://doi.org/10.1016/J.GLOPLACHA.2013.09.002

Hinkel, Jochen, Nicholls, R. J., Vafeidis, A. T., Tol, R. S. J., & Avagianou, T. (2010). Assessing risk of and adaptation to sea-level rise in the European Union: an application of DIVA. *Mitigation and Adaptation Strategies for Global Change*, *15*(7), 703–719. https://doi.org/10.1007/s11027-010-9237-y

Hinkel, Jochen, van Vuuren, D. P., Nicholls, R. J., & Klein, R. J. T. (2013). The effects of adaptation and mitigation on coastal flood impacts during the 21st century. An application of the DIVA and IMAGE models. *Climatic Change*, *117*(4), 783–794. https://doi.org/10.1007/s10584-012-0564-8

Hochreiter, S., & Schmidhuber, J. (1997). Long Short-Term Memory. *Neural Computation*, *9*, 1735–1780.

Höffken, J., Vafeidis, A. T., MacPherson, L. R., & Dangendorf, S. (2020). Effects of the Temporal Variability of Storm Surges on Coastal Flooding. *Frontiers in Marine Science*, *7*(February), 1–14. https://doi.org/10.3389/fmars.2020.00098

Hoitink, A. J. F., & Jay, D. A. (2016). *Reviews of Geophysics Tidal river dynamics: Implications for deltas*. https://doi.org/10.1002/2015RG000507

Hope, A. P., Salawitch, R. J., Canty, T. P., Tribett, W. R., & Bennett, B. F. (2017). *Paris INDCs*. https://doi.org/10.1007/978-3-319-46939-3_3

Horsburgh, K. J., & Wilson, C. (2007). Tide-surge interaction and its role in the distribution of surge residuals in the North Sea. *Journal of Geophysical Research: Oceans*, *112*(8), 1–13. https://doi.org/10.1029/2006JC004033

Horstman, E. M., Dohmen-Janssen, C. M., Narra, P. M. F., van den Berg, N. J. F., Siemerink, M., & Hulscher, S. J. M. H. (2014). Wave attenuation in mangroves: A quantitative approach to field observations. *Coastal Engineering*, *94*, 47–62. https://doi.org/10.1016/j.coastaleng.2014.08.005

Hu, Y., Schmeits, M. J., Jan van Andel, S., Verkade, J. S., Xu, M., Solomatine, D. P., & Liang, Z. (n.d.). A

Stratified Sampling Approach for Improved Sampling from a Calibrated Ensemble Forecast Distribution. *Journal of Hydrometeorology*, *17*(9), 2405–2417. https://doi.org/10.1175/JHM-D-15-0205.1

Huang, B., Zhao, B., & Song, Y. (2018). Urban land-use mapping using a deep convolutional neural network with high spatial resolution multispectral remote sensing imagery. *Remote Sensing of Environment*, *214*, 73–86. https://doi.org/10.1016/J.RSE.2018.04.050

Huizinga, J., Moel, H. de, & Szewczyk, W. (2017). Global flood depth-damage functions: Methodology and the database with guidelines. *JRC Working Papers*, *JRC105688*.

Idier, D., Bertin, X., Thompson, P., & Pickering, M. D. (2019a). Interactions Between Mean Sea Level, Tide, Surge, Waves and Flooding: Mechanisms and Contributions to Sea Level Variations at the Coast. *Surveys in Geophysics*, *40*(6), 1603–1630. https://doi.org/10.1007/s10712-019-09549-5

Idier, D., Paris, F., Cozannet, G. Le, Boulahya, F., & Dumas, F. (2017). Sea-level rise impacts on the tides of the European Shelf. *Continental Shelf Research*, *137*, 56–71. https://doi.org/10.1016/j.csr.2017.01.007

Ikeuchi, H., Hirabayashi, Y., Yamazaki, D., Muis, S., Ward, P. J., Winsemius, H. C., Verlaan, M., & Kanae, S. (2017). Compound simulation of fluvial floods and storm surges in a global coupled river-coast flood model: Model development and its application to 2007 Cyclone Sidr in Bangladesh. *Journal of Advances in Modeling Earth Systems*, *9*(4), 1847–1862. https://doi.org/10.1002/2017MS000943

Innamorati, C., Ritschel, T., Weyrich, T., & Mitra, N. J. (2019). Learning on the Edge: Investigating Boundary Filters in CNNs. *International Journal of Computer Vision 2019 128:4*, *128*(4), 773–782. https://doi.org/10.1007/S11263-019-01223-Y

Ishii, M., & Kimoto, M. (2009). Reevaluation of historical ocean heat content variations with time-varying XBT and MBT depth bias corrections. *Journal of Oceanography*, *65*(3), 287–299. https://doi.org/10.1007/s10872-009-0027-7

Jackson, L. P., & Jevrejeva, S. (2016). A probabilistic approach to 21st century regional sea-level projections using RCP and High-end scenarios. *Global and Planetary Change*, *146*, 179–189. https://doi.org/10.1016/j.gloplacha.2016.10.006

Janoušek, M. (2011). *ERA-Interim Daily Climatology*. https://confluence.ecmwf.int/download/attachments/24316422/daily_climatology_description.pdf?version=1&modificationDate=1362057125198&api=v2

Jennerjahn, T. C., Gilman, E., Krauss, K. W., Lacerda, L. D., Nordhaus, I., & Wolanski, E. (2017). Mangrove Ecosystems under Climate Change. *Mangrove Ecosystems: A Global Biogeographic Perspective: Structure, Function, and Services*, 211–244. https://doi.org/10.1007/978-3-319-62206-4_7

Jevrejeva, S., Grinsted, A., & Moore, J. C. (2014). Upper limit for sea level projections by 2100. *Environmental Research Letters*, *9*(10), 104008. https://doi.org/10.1088/1748-9326/9/10/104008

Jongman, B. (2018). Effective adaptation to rising flood risk. *Nature Communications*, *9*(1), 1986. https://doi.org/10.1038/s41467-018-04396-1

Jongman, B., Ward, P. J., & Aerts, J. C. J. H. (2012). Global exposure to river and coastal flooding: Long term trends and changes. *Global Environmental Change*, *22*(4), 823–835. https://doi.org/10.1016/J.GLOENVCHA.2012.07.004

Jonkman, S. N., Hillen, M. M., Nicholls, R. J., Kanning, W., & van Ledden, M. (2013). Costs of Adapting Coastal Defences to Sea-Level Rise— New Estimates and Their Implications. *Journal of Coastal Research*, *290*, 1212–1226. https://doi.org/10.2112/JCOASTRES-D-12-00230.1

Karpatne, A., Atluri, G., Faghmous, J. H., Steinbach, M., Banerjee, A., Ganguly, A., Shekhar, S., Samatova,

N., & Kumar, V. (2017). Theory-guided data science: A new paradigm for scientific discovery from data. *IEEE Transactions on Knowledge and Data Engineering*, *29*(10), 2318–2331. https://doi.org/10.1109/TKDE.2017.2720168

Kashinath, K., Mustafa, M., Albert, A., Wu, J. L., Jiang, C., Esmaeilzadeh, S., Azizzadenesheli, K., Wang, R., Chattopadhyay, A., Singh, A., Manepalli, A., Chirila, D., Yu, R., Walters, R., White, B., Xiao, H., Tchelepi, H. A., Marcus, P., Anandkumar, A., ... Prabhat. (2021). Physics-informed machine learning: Case studies for weather and climate modelling. In *Philosophical Transactions of the Royal Society A: Mathematical, Physical and Engineering Sciences* (Vol. 379, Issue 2194). Royal Society Publishing. https://doi.org/10.1098/rsta.2020.0093

Kim, S., Matsumi, Y., Pan, S., & Mase, H. (2016). A real-time forecast model using artificial neural network for after-runner storm surges on the Tottori coast, Japan. *Ocean Engineering*, *122*, 44–53. https://doi.org/10.1016/j.oceaneng.2016.06.017

Kim, S. W., Melby, J. A., Nadal-Caraballo, N. C., & Ratcliff, J. (2015). A time-dependent surrogate model for storm surge prediction based on an artificial neural network using high-fidelity synthetic hurricane modeling. *Natural Hazards*, *76*(1), 565–585. https://doi.org/10.1007/s11069-014-1508-6

Kirwan, M. L., Guntenspergen, G. R., D'Alpaos, A., Morris, J. T., Mudd, S. M., & Temmerman, S. (2010a). Limits on the adaptability of coastal marshes to rising sea level. *Geophysical Research Letters*, *37*(23), n/a-n/a. https://doi.org/10.1029/2010GL045489

Klein Goldewijk, K., Beusen, A., & Janssen, P. (2010). Long-term dynamic modeling of global population and built-up area in a spatially explicit way: HYDE 3.1. *The Holocene*, *20*(4), 565–573. https://doi.org/10.1177/0959683609356587

Klein Goldewijk, K., Beusen, A., Van Drecht, G., & De Vos, M. (2011). The HYDE 3.1 spatially explicit database of human-induced global land-use change over the past 12,000 years. *Global Ecology and Biogeography*, *20*(1), 73–86. https://doi.org/10.1111/j.1466-8238.2010.00587.x

Koks, E. E., Rozenberg, J., Zorn, C., Tariverdi, M., Vousdoukas, M., Fraser, S. A., Hall, J. W., & Hallegatte, S. (2019). A global multi-hazard risk analysis of road and railway infrastructure assets. *Nature Communications 2019 10:1*, *10*(1), 1–11. https://doi.org/10.1038/s41467-019-10442-3

Kooi, H., Bakr, M., de Lange G., den Haan E., Erkens, G. (2018). *A user guide to SUB-CR: A modflow land subsidence and aquifer system compaction package that includes creep.*

Kratzert, F., Klotz, D., Brenner, C., Schulz, K., & Herrnegger, M. (2018). *Rainfall – runoff modelling using Long Short-Term Memory (LSTM) networks*. 6005–6022.

Kriegler, E., Bauer, N., Popp, A., Humpenöder, F., Leimbach, M., Strefler, J., Baumstark, L., Bodirsky, B. L., Hilaire, J., Klein, D., Mouratiadou, I., Weindl, I., Bertram, C., Dietrich, J.-P., Luderer, G., Pehl, M., Pietzcker, R., Piontek, F., Lotze-Campen, H., ... Edenhofer, O. (2017). Fossil-fueled development (SSP5): An energy and resource intensive scenario for the 21st century. *Global Environmental Change*, *42*, 297–315. https://doi.org/10.1016/J.GLOENVCHA.2016.05.015

Kron, W. (2013). *Coasts: the high-risk areas of the world*. https://doi.org/10.1007/s11069-012-0215-4

Kron, W. (2005). Flood Risk=Hazard • Values • Vulnerability. https://doi.org/10.1080/02508060508691837

Lawson, E. T., Gordon, C., & Schluchter, W. (2012). The dynamics of poverty–environment linkages in the coastal zone of Ghana. *Ocean & Coastal Management*, *67*, 30–38. https://doi.org/10.1016/J.OCECOAMAN.2012.05.023

Lee, T. L. (2008). Back-propagation neural network for the prediction of the short-term storm surge in Taichung harbor, Taiwan. *Engineering Applications of Artificial Intelligence*, *21*(1), 63–72. https://doi.org/10.1016/j.engappai.2007.03.002

Leichenko, R., & Silva, J. A. (2014). Climate change and poverty: vulnerability, impacts, and alleviation

strategies. *Wiley Interdisciplinary Reviews: Climate Change*, *5*(4), 539–556. https://doi.org/10.1002/WCC.287

Lenk, S., Rybski, D., Heidrich, O., Dawson, R. J., & Kropp, J. P. (2017). Costs of sea dikes–regressions and uncertainty estimates. *Nat-Hazards-Earth-Syst-Sci.Net*.

Lenk, Stephan, Rybski, D., Heidrich, O., Dawson, R. J., & Kropp, J. P. (2017). Costs of sea dikes – regressions and uncertainty estimates. *Natural Hazards and Earth System Sciences*, *17*(5), 765–779. https://doi.org/10.5194/nhess-17-765-2017

Lewis, M., Schumann, G., Bates, P., & Horsburgh, K. (2013). Understanding the variability of an extreme storm tide along a coastline. *Estuarine, Coastal and Shelf Science*, *123*, 19–25. https://doi.org/10.1016/j.ecss.2013.02.009

Lewis, R. R. (2005). Ecological engineering for successful management and restoration of mangrove forests. *Ecological Engineering*, *24*(4), 403–418. https://doi.org/10.1016/J.ECOLENG.2004.10.003

Lin, N., & Chavas, D. (2012). On hurricane parametric wind and applications in storm surge modeling. *Journal of Geophysical Research: Atmospheres*, *117*(D9), n/a-n/a. https://doi.org/10.1029/2011JD017126

Lincke, D., & Hinkel, J. (2018). Economically robust protection against 21st century sea-level rise. *Global Environmental Change*, *51*, 67–73. https://doi.org/10.1016/J.GLOENVCHA.2018.05.003

Lincke, D., & Hinkel, J. (2021). Coastal Migration due to 21st Century Sea-Level Rise. *Earth's Future*, *9*(5), e2020EF001965. https://doi.org/10.1029/2020EF001965

Little, C. M., Horton, R. M., Kopp, R. E., Oppenheimer, M., Vecchi, G. A., & Villarini, G. (2015). Joint projections of US East Coast sea level and storm surge. *Nature Climate Change*, *5*(12), 1114–1120. https://doi.org/10.1038/nclimate2801

Lovelock, C. E., & Brown, B. M. (2019). Land tenure considerations are key to successful mangrove restoration. *Nature Ecology & Evolution 2019 3:8*, *3*(8), 1135–1135. https://doi.org/10.1038/s41559-019-0942-y

Lovelock, C. E., Cahoon, D. R., Friess, D. A., Guntenspergen, G. R., Krauss, K. W., Reef, R., Rogers, K., Saunders, M. L., Sidik, F., Swales, A., Saintilan, N., Thuyen, L. X., & Triet, T. (2015). The vulnerability of Indo-Pacific mangrove forests to sea-level rise. *Nature 2015 526:7574*, *526*(7574), 559–563. https://doi.org/10.1038/nature15538

Löw, P. (2018). *Hurricanes cause record losses in 2017 - The year in figures (Munich Re NatCatSERVICE)*.

Lyddon, C., Brown, J. M., Leonardi, N., & Plater, A. J. (2018). Flood Hazard Assessment for a Hyper-Tidal Estuary as a Function of Tide-Surge-Morphology Interaction. *Estuaries and Coasts*, *41*(6), 1565–1586. https://doi.org/10.1007/s12237-018-0384-9

Maes, J., & Jacobs, S. (2017). Nature-Based Solutions for Europe's Sustainable Development. *Conservation Letters*, *10*(1), 121–124. https://doi.org/10.1111/CONL.12216

Malakar, P., Kesarkar, A. P., Bhate, J. N., Singh, V., & Deshamukhya, A. (2020). *Comparison of Reanalysis Data Sets to Comprehend the Evolution of Tropical Cyclones Over North Indian Ocean*. 1–15. https://doi.org/10.1029/2019EA000978

Mandel, A., Tiggeloven, T., Lincke, D., Koks, E., Ward, P., & Hinkel, J. (2021). Risks on global financial stability induced by climate change: the case of flood risks. *Climatic Change*, *166*(1–2), 1–24. https://doi.org/10.1007/S10584-021-03092-2/TABLES/2

Marchand, M. (2008). *Mangrove restoration in Vietnam: Key considerations and a practical guide*. Deltares. https://repository.tudelft.nl/islandora/object/uuid%3A98b5ba43-1452-4631-81dc-ad043ef3992c

Marcos, M., M., C. F., A., B., & S., D. (2015). Long-term variations in global sea level extremes. *Journal of Geophysical Research: Oceans*, *120*, 8115–8134. https://doi.org/10.1002/2015JC011173

Marsooli, R., Lin, N., Emanuel, K., & Feng, K. (2019). Climate change exacerbates hurricane flood hazards along US Atlantic and Gulf Coasts in spatially varying patterns. *Nature Communications*, *10*(1), 1–9. https://doi.org/10.1038/s41467-019-11755-z

Matsugu, M., Mori, K., Mitari, Y., & Kaneda, Y. (2003). Subject independent facial expression recognition with robust face detection using a convolutional neural network. *Neural Networks*, *16*(5–6), 555–559. https://doi.org/10.1016/S0893-6080(03)00115-1

McGranahan, G., Balk, D., & Anderson, B. (2007). The rising tide: assessing the risks of climate change and human settlements in low elevation coastal zones. *Environment and Urbanization*, *19*(1), 17–37. https://doi.org/10.1177/0956247807076960

McInnes, K. L., White, C. J., Haigh, I. D., Hemer, M. A., Hoeke, R. K., Holbrook, N. J., Kiem, A. S., Oliver, E. C. J., Ranasinghe, R., Walsh, K. J. E., Westra, S., & Cox, R. (2016). Natural hazards in Australia: sea level and coastal extremes. *Climatic Change*, *139*(1), 69–83. https://doi.org/10.1007/s10584-016-1647-8

Mckee, K. L., Cahoon, D. R., & Feller, I. C. (2007). Caribbean mangroves adjust to rising sea level through biotic controls on change in soil elevation. *Global Ecology and Biogeography*, *16*(5), 545–556. https://doi.org/10.1111/j.1466-8238.2007.00317.x

McLeman, R., & Smit, B. (2006). Migration as an Adaptation to Climate Change. *Climatic Change*, *76*(1–2), 31–53. https://doi.org/10.1007/s10584-005-9000-7

McLeman, Robert. (2018). Migration and displacement risks due to mean sea-level rise. *74*(3), 148–154. https://doi.org/10.1080/00963402.2018.1461951

Mcowen, C. J., Weatherdon, L. V, Bochove, J.-W. Van, Sullivan, E., Blyth, S., Zockler, C., Stanwell-Smith, D., Kingston, N., Martin, C. S., Spalding, M., & Fletcher, S. (2017). A global map of saltmarshes. *Biodiversity Data Journal*, *5*, e11764. https://doi.org/10.3897/BDJ.5.e11764

Menéndez, P., Losada, I. J., Torres-Ortega, S., Narayan, S., & Beck, M. W. (2020a). The Global Flood Protection Benefits of Mangroves. *Scientific Reports*, *10*(1), 4404. https://doi.org/10.1038/s41598-020-61136-6

Merkens, J.-L., Lincke, D., Hinkel, J., Brown, S., & Vafeidis, A. T. (2018). Regionalisation of population growth projections in coastal exposure analysis. *Climatic Change*, *151*(3–4), 413–426. https://doi.org/10.1007/s10584-018-2334-8

Meyer, V., Haase, D., & Scheuer, S. (2009). Flood Risk Assessment in European River Basins—Concept, Methods, and Challenges Exemplified at the Mulde River. *Integrated Environmental Assessment and Management*, *5*(1), 17. https://doi.org/10.1897/IEAM_2008-031.1

Miller, L., & Douglas, B. C. (2004). Mass and volume contributions to twentieth-century global sea level rise. *Nature*, *428*(6981), 406–409. https://doi.org/10.1038/nature02309

Mirza, M. M. Q. (2011). Climate change, flooding in South Asia and implications. *Regional Environmental Change*, *11*(SUPPL. 1), 95–107. https://doi.org/10.1007/S10113-010-0184-7/TABLES/8

Mitsch, W. J., Bernal, B., & Hernandez, M. E. (2015). Ecosystem services of wetlands. In *International Journal of Biodiversity Science, Ecosystem Services and Management* (Vol. 11, Issue 1, pp. 1–4). Taylor and Francis Ltd. https://doi.org/10.1080/21513732.2015.1006250

Mitsch, W. J., & Hernandez, M. E. (2013). Landscape and climate change threats to wetlands of North and Central America. *Aquatic Sciences*, *75*(1), 133–149. https://doi.org/10.1007/S00027-012-0262-7/FIGURES/5

Muis, S., Apecechea, M. I., Dullaart, J., de Lima Rego, J., Madsen, K. S., Su, J., Yan, K., & Verlaan, M. (2020). A High-Resolution Global Dataset of Extreme Sea Levels, Tides, and Storm Surges, Including Future Projections. *Frontiers in Marine Science*, *7*, 263. https://doi.org/10.3389/fmars.2020.00263

Muis, S., Güneralp, B., Jongman, B., Aerts, J. C. J. H., & Ward, P. J. (2015). Flood risk and adaptation strategies under climate change and urban expansion: A probabilistic analysis using global data. *Science of The Total Environment*, *538*, 445–457. https://doi.org/10.1016/J.SCITOTENV.2015.08.068

Muis, S., Haigh, I. D., Guimarães Nobre, G., Aerts, J. C. J. H., & Ward, P. J. (2018). Influence of El Niño-Southern Oscillation on Global Coastal Flooding. *Earth's Future*, *6*(9), 1311–1322. https://doi.org/10.1029/2018EF000909

Muis, S., Lin, N., Verlaan, M., Winsemius, H. C., Ward, P. J., & Aerts, J. C. J. H. (2019). Spatiotemporal patterns of extreme sea levels along the western North-Atlantic coasts. *Scientific Reports*, *9*(1), 1–12. https://doi.org/10.1038/s41598-019-40157-w

Muis, S., Verlaan, M., Nicholls, R. J., Brown, S., Hinkel, J., Lincke, D., Vafeidis, A. T., Scussolini, P., Winsemius, H. C., & Ward, P. J. (2017). A comparison of two global datasets of extreme sea levels and resulting flood exposure. *Earth's Future*, *5*(4), 379–392. https://doi.org/10.1002/2016EF000430

Muis, S., Verlaan, M., Winsemius, H. C., Aerts, J. C. J. H., & Ward, P. J. (2016b). A global reanalysis of storm surges and extreme sea levels. *Nature Communications*, *7*(1), 1–12. https://doi.org/10.1038/ncomms11969

Narayan, S, Thomas, C., ... J. M.-C., & 2019, U. (2019). Valuing the Flood Risk Reduction Benefits of Florida's Mangroves. *The Nature Conservancy*. https://www.researchgate.net/profile/Siddharth-Narayan/publication/336903145_Valuing_the_Flood_Risk_Reduction_Benefits_of_Florida's_Mangroves/links/5db9f68245851514 35d612e6/Valuing-the-Flood-Risk-Reduction-Benefits-of-Floridas-Mangroves.pdf

Narayan, Siddharth, Beck, M. W., Reguero, B. G., Losada, I. J., van Wesenbeeck, B., Pontee, N., Sanchirico, J. N., Ingram, J. C., Lange, G.-M., & Burks-Copes, K. A. (2016). The Effectiveness, Costs and Coastal Protection Benefits of Natural and Nature-Based Defences. *PLOS ONE*, *11*(5), e0154735. https://doi.org/10.1371/journal.pone.0154735

Narayan, Siddharth, Beck, M. W., Wilson, P., Thomas, C. J., Guerrero, A., Shepard, C. C., Reguero, B. G., Franco, G., Ingram, J. C., & Trespalacios, D. (2017). The Value of Coastal Wetlands for Flood Damage Reduction in the Northeastern USA. *Scientific Reports*, *7*(1), 9463. https://doi.org/10.1038/s41598-017-09269-z

Nasir, V., & Sassani, F. (2021). A review on deep learning in machining and tool monitoring: methods, opportunities, and challenges. *The International Journal of Advanced Manufacturing Technology 2021*, 1–27. https://doi.org/10.1007/S00170-021-07325-7

Neumann, B., Vafeidis, A. T., Zimmermann, J., & Nicholls, R. J. (2015b). Future Coastal Population Growth and Exposure to Sea-Level Rise and Coastal Flooding - A Global Assessment. *PLOS ONE*, *10*(3), e0118571. https://doi.org/10.1371/journal.pone.0118571

Nguyen, T. P., Van Tam, N., Quoi, L. P., & Parnell, K. E. (2016). Community perspectives on an internationally funded mangrove restoration project: Kien Giang province, Vietnam. *Ocean & Coastal Management*, *119*, 146–154. https://doi.org/10.1016/J.OCECOAMAN.2015.10.008

Nicholls, R., Hanson, S., Herweijer, C., & Patmore, N. (2008). *Ranking port cities with high exposure and vulnerability to climate extremes*.

Nicholls, R. J., & Cazenave, A. (2010b). Sea-level rise and its impact on coastal zones. *Science*, *328*(5985), 1517–1520. https://doi.org/10.1126/science.1185782

Nicholls, R. J., Cazenave, A., Emanuel, K., Lin, N., Moel, H. de, & Michel-Kerjan, E. O. (2010). Sea-level rise and its impact on coastal zones. *Science (New York, N.Y.)*, *328*(5985), 1517–1520. https://doi.org/10.1126/science.1185782

Nicholls, R. J., Tol, R. S. J., & Vafeidis, A. T. (2008). Global estimates of the impact of a collapse of the West Antarctic ice sheet: an application of FUND. *Climatic Change*, *91*(1–2), 171–191. https://doi.org/10.1007/s10584-008-9424-y

Nuswantoro, R., Diermanse, F., & Molkenthin, F. (2016). Probabilistic flood hazard maps for Jakarta derived from a stochastic rain-storm generator. *Journal of Flood Risk Management*, *9*(2), 105–124. https://doi.org/10.1111/jfr3.12114

O'Neill, B. C., Kriegler, E., Ebi, K. L., Kemp-Benedict, E., Riahi, K., Rothman, D. S., van Ruijven, B. J., van Vuuren, D. P., Birkmann, J., Kok, K., Levy, M., & Solecki, W. (2017). The roads ahead: Narratives for shared socioeconomic pathways describing world futures in the 21st century. *Global Environmental Change*, *42*, 169–180. https://doi.org/10.1016/j.gloenvcha.2015.01.004

O'Neill, B. C., Kriegler, E., Riahi, K., Ebi, K. L., Hallegatte, S., Carter, T. R., Mathur, R., & van Vuuren, D. P. (2014). A new scenario framework for climate change research: The concept of shared socioeconomic pathways. *Climatic Change*, *122*(3), 387–400. https://doi.org/10.1007/s10584-013-0905-2

Olanrewaju, C. C., Chitakira, M., Olanrewaju, O. A., & Louw, E. (2019). Impacts of flood disasters in Nigeria: A critical evaluation of health implications and management. *Jamba: Journal of Disaster Risk Studies*, *11*(1). https://doi.org/10.4102/JAMBA.V11I1.557

Olazabal, M., Ruiz De Gopegui, M., Tompkins, E. L., Venner, K., & Smith, R. (2019). A cross-scale worldwide analysis of coastal adaptation planning. *Environmental Research Letters*, *14*(12), 124056. https://doi.org/10.1088/1748-9326/AB5532

Oppenheimer, M., Glavovic, B. C., Hinkel, J., van de Wal, R., Magnan, A. K., Biesbroek, R., Buchanan, M. K., Abe-Ouchi, A., Gupta, K., Pereira, J., Glavovic, B., Hinkel, J., van de Wal, R., Magnan, A., Abd-Elgawad, A., Cai, R., Cifuentes-Jara, M., DeConto, R., Pörtner, H., ... Weyer, N. (2019). *Sea Level Rise and Implications for Low-Lying Islands, Coasts and Communities. In: IPCC Special Report on the Ocean and Cryosphere in a Changing Climate [H.-O. Pörtner, D.C. Roberts, V. Masson-Delmotte, P. Zhai, M. Tignor, E. Poloczanska, K. Mintenbeck, A.* Poh Poh Wong.

OSM. (2015). *Open Street Map*.

Pappenberger, F., Ramos, M. H., Cloke, H. L., Wetterhall, F., Alfieri, L., Bogner, K., Mueller, A., & Salamon, P. (2015). How do I know if my forecasts are better? Using benchmarks in hydrological ensemble prediction. *Journal of Hydrology*, *522*, 697–713. https://doi.org/10.1016/j.jhydrol.2015.01.024

Pappenberger, Florian, Cloke, H. L., Parker, D. J., Wetterhall, F., Richardson, D. S., & Thielen, J. (2015). The monetary benefit of early flood warnings in Europe. *Environmental Science & Policy*, *51*, 278–291. https://doi.org/10.1016/J.ENVSCI.2015.04.016

Pedregosa, F., Michel, V., Grisel OLIVIERGRISEL, O., Blondel, M., Prettenhofer, P., Weiss, R., Vanderplas, J., Cournapeau, D., Pedregosa, F., Varoquaux, G., Gramfort, A., Thirion, B., Grisel, O., Dubourg, V., Passos, A., Brucher, M., Perrot andÉdouardand, M., Duchesnay, andÉdouard, & Duchesnay EDOUARDDUCHESNAY, Fré. (2011). Scikit-learn: Machine Learning in Python. In *Journal of Machine Learning Research* (Vol. 12). http://scikit-learn.sourceforge.net.

Pekel, J.-F., Cottam, A., Gorelick, N., & Belward, A. S. (2016). High-resolution mapping of global surface water and its long-term changes. *Nature*, *540*(7633), 418–422. https://doi.org/10.1038/nature20584

Pesaresi, M., Ehrlich, D., Florczyk, A. J., Freire, S., Julea, A., Kemper, T., & Syrris, V. (2016). The global human settlement layer from landsat imagery. *International Geoscience and Remote Sensing Symposium (IGARSS)*, *2016-Novem*, 7276–7279. https://doi.org/10.1109/IGARSS.2016.7730897

Phan, K. L., Stive, M. J. F., Zijlema, M., Truong, H. S., & Aarninkhof, S. G. J. (2019). The effects of wave non-linearity on wave attenuation by vegetation. *Coastal Engineering*, *147*, 63–74. https://doi.org/10.1016/J.COASTALENG.2019.01.004

Phillips, J. D. (2018). Coastal wetlands, sea level, and the dimensions of geomorphic resilience. *Geomorphology*, *305*, 173–184. https://doi.org/10.1016/J.GEOMORPH.2017.03.022

Pickering, M. D., Wells, N. C., Horsburgh, K. J., & Green, J. A. M. (2012). The impact of future sea-level rise on the European Shelf tides. *Continental Shelf Research*, *35*, 1–15. https://doi.org/10.1016/J.CSR.2011.11.011

Pörtner, H.-O., Roberts, D. C., Alegría, A., Nicolai, M., Okem, A., Petzold, J., Rama, B., & Weyer, N. M. (2019). *The Ocean and Cryosphere in a Changing Climate A Special Report of the Intergovernmental Panel on Climate Change Edited by*.

Powell, N., Osbeck, M., Bach, S., & Canh Toan, V. U. (2011). *Mangrove Restoration and Rehabilitation for Climate Change Adaptation in Vietnam World Resources Report Case Study*. http://www.worldresourcesreport.org/http://www.worldresourcesreport.org

Pullen, T., Allsop, N. W. H., Bruce, T., Kortenhaus, A., Schüttrumpf, H., & Van der Meer, J. W. (2007). EurOtop, European Overtopping Manual - Wave overtopping of sea defences and related structures: Assessment manual. *Also Published as Special Volume of Die Küste*.

Pycroft, J., Abrell, J., & Ciscar, J.-C. (2016). The Global Impacts of Extreme Sea-Level Rise: A Comprehensive Economic Assessment. *Environmental and Resource Economics*, *64*(2), 225–253. https://doi.org/10.1007/s10640-014-9866-9

Raftery, A. E., Zimmer, A., Frierson, D. M. W., Startz, R., & Liu, P. (2017). Less than 2 °C warming by 2100 unlikely. *Nature Climate Change*, *7*(9), 637–641. https://doi.org/10.1038/nclimate3352

Rahman, M. M., & Mahmud, M. A. (2018). Economic feasibility of mangrove restoration in the Southeastern Coast of Bangladesh. *Ocean & Coastal Management*, *161*, 211–221. https://doi.org/10.1016/J.OCECOAMAN.2018.05.009

Rakib, M. A., Sasaki, J., Matsuda, H., & Fukunaga, M. (2019). Severe salinity contamination in drinking water and associated human health hazards increase migration risk in the southwestern coastal part of Bangladesh. *Journal of Environmental Management*, *240*, 238–248. https://doi.org/10.1016/J.JENVMAN.2019.03.101

Reichstein, M., Camps-Valls, G., Stevens, B., Jung, M., Denzler, J., Carvalhais, N., & Prabhat. (2019). Deep learning and process understanding for data-driven Earth system science. *Nature*, *566*(7743), 195–204. https://doi.org/10.1038/s41586-019-0912-1

Resio, D. T., & Westerink, J. J. (2008). *Modeling the physics of storm surges - Physics Today September 2008 Modeling the physics of storm surges - Physics Today September 2008*. *7*(September), 3–9.

Riahi, K., van Vuuren, D. P., Kriegler, E., Edmonds, J., O'Neill, B. C., Fujimori, S., Bauer, N., Calvin, K., Dellink, R., Fricko, O., Lutz, W., Popp, A., Cuaresma, J. C., KC, S., Leimbach, M., Jiang, L., Kram, T., Rao, S., Emmerling, J., … Tavoni, M. (2017). The Shared Socioeconomic Pathways and their energy, land use, and greenhouse gas emissions implications: An overview. *Global Environmental Change*, *42*, 153–168. https://doi.org/10.1016/J.GLOENVCHA.2016.05.009

Roberts, C. D., Senan, R., Molteni, F., Boussetta, S., Mayer, M., & Keeley, S. P. E. (2018). Climate model configurations of the ECMWF Integrated Forecasting System (ECMWF-IFS cycle 43r1) for HighResMIP. *Geoscientific Model Development*, *11*(9), 3681–3712. https://doi.org/10.5194/gmd-11-3681-2018

Rueda, A., Vitousek, S., Camus, P., Tomás, A., Espejo, A., Losada, I. J., Barnard, P. L., Erikson, L. H., Ruggiero, P., Reguero, B. G., & Mendez, F. J. (2017). A global classification of coastal flood hazard climates associated with large-scale oceanographic forcing. *Scientific Reports*, *7*(1), 5038.

https://doi.org/10.1038/s41598-017-05090-w

Saintilan, N., Khan, N. S., Ashe, E., Kelleway, J. J., Rogers, K., Woodroffe, C. D., & Horton, B. P. (2020). Thresholds of mangrove survival under rapid sea level rise. *Science*, *368*(6495), 1118–1121. https://doi.org/10.1126/SCIENCE.ABA2656/SUPPL_FILE/ABA2656_SAINTILAN_SM.PDF

Saintilan, N., Rogers, K., Kelleway, J. J., Ens, E., & Sloane, D. R. (2019). Climate Change Impacts on the Coastal Wetlands of Australia. *Wetlands*, *39*(6), 1145–1154. https://doi.org/10.1007/S13157-018-1016-7/FIGURES/3

Salik, K. M., Jahangir, S., Zahdi, W. ul Z., & Hasson, S. ul. (2015). Climate change vulnerability and adaptation options for the coastal communities of Pakistan. *Ocean & Coastal Management*, *112*, 61–73. https://doi.org/10.1016/J.OCECOAMAN.2015.05.006

Santiago-Collazo, F. L., Bilskie, M. V., & Hagen, S. C. (2019). A comprehensive review of compound inundation models in low-gradient coastal watersheds. *Environmental Modelling and Software*, *119*(June), 166–181. https://doi.org/10.1016/j.envsoft.2019.06.002

Schanze, J. (2006). Flood Risk Management - a Basic Framework. In *Flood Risk Management: Hazards, Vulnerability and Mitigation Measures* (pp. 1–20). Springer Netherlands. https://doi.org/10.1007/978-1-4020-4598-1_1

Schmitt, K., Albers, T., Pham, T. T., & Dinh, S. C. (2013). Site-specific and integrated adaptation to climate change in the coastal mangrove zone of Soc Trang Province, Viet Nam. *Journal of Coastal Conservation*, *17*(3), 545–558. https://doi.org/10.1007/S11852-013-0253-4/FIGURES/7

Schuerch, M., Spencer, T., Temmerman, S., Kirwan, M. L., Wolff, C., Lincke, D., McOwen, C. J., Pickering, M. D., Reef, R., Vafeidis, A. T., Hinkel, J., Nicholls, R. J., & Brown, S. (2018). Future response of global coastal wetlands to sea-level rise. *Nature*, *561*(7722), 231–234. https://doi.org/10.1038/s41586-018-0476-5

Schulte, I., Eggers, J., Nielsen, J. Ø., & Fuss, S. (2021). What influences the implementation of natural climate solutions? A systematic map and review of the evidence. *Environmental Research Letters*, *17*(1), 013002. https://doi.org/10.1088/1748-9326/AC4071

Scussolini, P., Aerts, J. C. J. H., Jongman, B., Bouwer, L. M., Winsemius, H. C., De Moel, H., & Ward, P. J. (2016). FLOPROS: an evolving global database of flood protection standards. *Natural Hazards and Earth System Sciences*, *16*(5), 1049–1061. https://doi.org/10.5194/nhess-16-1049-2016

Seddon, N., Chausson, A., Berry, P., Girardin, C. A. J., Smith, A., & Turner, B. (2020). Understanding the value and limits of nature-based solutions to climate change and other global challenges. *Philosophical Transactions of the Royal Society B*, *375*(1794). https://doi.org/10.1098/RSTB.2019.0120

Serafin, K.A., Ruggiero, P., Parker, K., & Hill, D. . (2019). What's streamflow got to do with it? A probabilistic simulation of the competing oceanographic and fluvial processes driving along-river extreme water levels. *Natural Hazards and Earth System Sciences*, *January*.

Serafin, Katherine A., Ruggiero, P., & Stockdon, H. F. (2017). The relative contribution of waves, tides, and nontidal residuals to extreme total water levels on U.S. West Coast sandy beaches. *Geophysical Research Letters*, *44*(4), 1839–1847. https://doi.org/10.1002/2016GL071020

Shen, C. (2018). A Transdisciplinary Review of Deep Learning Research and Its Relevance for Water Resources Scientists. *Water Resources Research*, *54*(11), 8558–8593. https://doi.org/10.1029/2018WR022643

Shepard, C. C., Crain, C. M., & Beck, M. W. (2011). The Protective Role of Coastal Marshes: A Systematic Review and Meta-analysis. *PLoS ONE*, *6*(11), e27374. https://doi.org/10.1371/journal.pone.0027374

Small, C., & Nicholls, R. J. (2003). A Global Analysis of Human Settlement in Coastal Zones. In *Journal of Coastal Research* (Vol. 19, pp. 584–599). Coastal Education & Research Foundation, Inc. https://doi.org/10.2307/4299200

Soanes, L. M., Pike, S., Armstrong, S., Creque, K., Norris-Gumbs, R., Zaluski, S., & Medcalf, K. (2021). Reducing the vulnerability of coastal communities in the Caribbean through sustainable mangrove management. *Ocean & Coastal Management*, *210*, 105702. https://doi.org/10.1016/J.OCECOAMAN.2021.105702

Solaymani, S., & Kari, F. (2014). Poverty evaluation in the Malaysian Fishery Community. *Ocean & Coastal Management*, *95*, 165–175. https://doi.org/10.1016/J.OCECOAMAN.2014.04.017

Spalding, M. D., and M. L. (2021). The State of the World's Mangroves. *Global Mangrove Alliance*.

Spalding, M. D., Mcivor, A. L., Beck, M. W., Koch, E. W., Möller, I., Reed, D. J., Rubinoff, P., Spencer, T., Tolhurst, T. J., Wamsley, T. V., van Wesenbeeck, B. K., Wolanski, E., & Woodroffe, C. D. (2014). Coastal ecosystems: A critical element of risk reduction. *Conservation Letters*, *7*(3), 293–301. https://doi.org/10.1111/conl.12074

Spalding, M., & Parrett, C. L. (2019). Global patterns in mangrove recreation and tourism. *Marine Policy*, *110*, 103540. https://doi.org/10.1016/J.MARPOL.2019.103540

Steele, J. E., Sundsøy, P. R., Pezzulo, C., Alegana, V. A., Bird, T. J., Blumenstock, J., Bjelland, J., Engø-Monsen, K., De Montjoye, Y. A., Iqbal, A. M., Hadiuzzaman, K. N., Lu, X., Wetter, E., Tatem, A. J., & Bengtsson, L. (2017). Mapping poverty using mobile phone and satellite data. *Journal of The Royal Society Interface*, *14*(127). https://doi.org/10.1098/RSIF.2016.0690

Su, J., Friess, D. A., & Gasparatos, A. (2021). A meta-analysis of the ecological and economic outcomes of mangrove restoration. *Nature Communications 2021 12:1*, *12*(1), 1–13. https://doi.org/10.1038/s41467-021-25349-1

Sun, W., & Su, F. (2017). A novel companion objective function for regularization of deep convolutional neural networks. *Image and Vision Computing*, *60*, 58–63. https://doi.org/10.1016/j.imavis.2016.11.012

Sutanudjaja, E. H., Van Beek, R., Wanders, N., Wada, Y., Bosmans, J. H. C., Drost, N., Van Der Ent, R. J., De Graaf, I. E. M., Hoch, J. M., De Jong, K., Karssenberg, D., López López, P., Peßenteiner, S., Schmitz, O., Straatsma, M. W., Vannametee, E., Wisser, D., & Bierkens, M. F. P. (2018). PCR-GLOBWB 2: A 5 arcmin global hydrological and water resources model. *Geoscientific Model Development*, *11*(6), 2429–2453. https://doi.org/10.5194/gmd-11-2429-2018

Sutton-Grier, A. E., Wowk, K., & Bamford, H. (2015). Future of our coasts: The potential for natural and hybrid infrastructure to enhance the resilience of our coastal communities, economies and ecosystems. *Environmental Science & Policy*, *51*, 137–148. https://doi.org/10.1016/J.ENVSCI.2015.04.006

Syvitski, J. P. M., Kettner, A. J., Overeem, I., Hutton, E. W. H., Hannon, M. T., Brakenridge, G. R., Day, J., Vörösmarty, C., Saito, Y., Giosan, L., & Nicholls, R. J. (2009). Sinking deltas due to human activities. *Nature Geoscience*, *2*(10), 681–686. https://doi.org/10.1038/ngeo629

Tadesse, M., & Wahl, T. (2021). A Database of Global Storm Surge Reconstruction (GSSR). *Scientific Data*, 1–10. https://doi.org/10.1038/s41597-021-00906-x

Tadesse, M., Wahl, T., Cid, A., & Lambert, E. (2020). *Data-Driven Modeling of Global Storm Surges*. *7*(April), 1–19. https://doi.org/10.3389/fmars.2020.00260

Tatem, A., Gething, P., Pezzulo, C., Weiss, D., & Bhatt, S. (2013). Pilot High-Resolution Poverty Maps. *University of Southampton/Oxford*.

Tatem, A. J., Garcia, A. J., Snow, R. W., Noor, A. M., Gaughan, A. E., Gilbert, M., & Linard, C. (2013).

Millennium development health metrics: Where do Africa's children and women of childbearing age live? *Population Health Metrics*, *11*(1), 1–11. https://doi.org/10.1186/1478-7954-11-11/FIGURES/4

Tebaldi, C., Strauss, B. H., & Zervas, C. E. (2012). Modelling sea level rise impacts on storm surges along US coasts. *Environmental Research Letters*, *7*(1), 014032. https://doi.org/10.1088/1748-9326/7/1/014032

Temmerman, S., Meire, P., Bouma, T. J., Herman, P. M. J., Ysebaert, T., & De Vriend, H. J. (2013). Ecosystem-based coastal defence in the face of global change. *Nature*, *504*(7478), 79–83. https://doi.org/10.1038/nature12859

Teng, J., Jakeman, A. J., Vaze, J., Croke, B. F. W., Dutta, D., & Kim, S. (2017). Flood inundation modelling: A review of methods, recent advances and uncertainty analysis. *Environmental Modelling and Software*, *90*, 201–216. https://doi.org/10.1016/j.envsoft.2017.01.006

Tiggeloven, T., Couasnon, A., van Straaten, C., Muis, S., & Ward, P. J. (2021). Exploring deep learning capabilities for surge predictions in coastal areas. *Scientific Reports 2021 11:1*, *11*(1), 1–15. https://doi.org/10.1038/s41598-021-96674-0

Tiggeloven, T., De Moel, H., Winsemius, H. C., Eilander, D., Erkens, G., Gebremedhin, E., Diaz Loaiza, A., Kuzma, S., Luo, T., Iceland, C., Bouwman, A., Van Huijstee, J., Ligtvoet, W., & Ward, P. J. (2019). Global scale benefit-cost analysis of coastal flood adaptation to different flood risk drivers. *Natural Hazards and Earth System Sciences Discussions*. https://doi.org/10.5194/nhess-2019-330

Tiggeloven, T., Moel, H. de, Zelst, V. van, Wesenbeeck, B. K. van, Winsemius, H. C., Eilander, D., & Ward, P. (2022). The benefits of coastal adaptation through conservation of foreshore vegetation. *Journal of Flood Risk Management*.

Tol, R. S. J. (2002). Estimates of the Damage Costs of Climate Change. Part 1: Benchmark Estimates. *Environmental and Resource Economics*, *21*(1), 47–73. https://doi.org/10.1023/A:1014500930521

Tong, S. (2017). Flooding-related displacement and mental health. *The Lancet Planetary Health*, *1*(4), e124–e125. https://doi.org/10.1016/S2542-5196(17)30062-1

Trinh, B. N., Thielen-del Pozo, J., & Thirel, G. (2013). The reduction continuous rank probability score for evaluating discharge forecasts from hydrological ensemble prediction systems. *Atmospheric Science Letters*, *14*(2), 61–65. https://doi.org/10.1002/asl2.417

Turner, R. K., Burgess, D., Hadley, D., Coombes, E., & Jackson, N. (2007). A cost–benefit appraisal of coastal managed realignment policy. *Global Environmental Change*, *17*(3–4), 397–407. https://doi.org/10.1016/J.GLOENVCHA.2007.05.006

UNFCCC. (2021). *Nationally determined contributions under the Paris Agreement Synthesis report by the secretariat*.

United Nations Framework Convention on Climate Change. (2015). *COP21 Paris agreement*.

United Nations Office for Disaster Risk Reduction. (2015). *Sendai framework for disaster risk reduction 2015–2030*. http://www.unisdr.org/we/inform/publications/43291

United Nations Office for Disaster Risk Reduction. (2016). *Report of the open-ended intergovernmental expert working group on indicators and terminology relating to disaster risk reduction*.

Vafeidis, A. T., Schuerch, M., Wolff, C., Spencer, T., Merkens, J. L., Hinkel, J., Lincke, D., Brown, S., & Nicholls, R. J. (2019). Water-level attenuation in global-scale assessments of exposure to coastal flooding: a sensitivity analysis. *Natural Hazards and Earth System Sciences*, *19*(5), 973–984. https://doi.org/10.5194/nhess-19-973-2019

Valenzuela, R. B., Yeo-Chang, Y., Park, M. S., & Chun, J. N. (2020). Local People's Participation in

Mangrove Restoration Projects and Impacts on Social Capital and Livelihood: A Case Study in the Philippines. *Forests 2020, Vol. 11, Page 580*, *11*(5), 580. https://doi.org/10.3390/F11050580

van den Brink, H. W., Können, G. P., Opsteegh, J. D., van Oldenborgh, G. J., & Burgers, G. (2004). Improving 104-year surge level estimates using data of the ECMWF seasonal prediction system. *Geophysical Research Letters*, *31*(17), 1–4. https://doi.org/10.1029/2004GL020610

Van Huijstee, J., Van Bemmel, B., Bouwman, A., & Van Rijn, F. (2018a). *TOWARDS AN URBAN PREVIEW Modelling future urban growth with 2UP Background Report Towards and Urban Preview: Modelling future urban growth with 2UP.*

Van Huijstee, J., Van Bemmel, B., Bouwman, A., & Van Rijn, F. (2018b). *Towards and Urban Preview: Modelling future urban growth with 2UP, Background Report.*

van Rooijen, A. A., McCall, R. T., van Thiel de Vries, J. S. M., van Dongeren, A. R., Reniers, A. J. H. M., & Roelvink, J. A. (2016). Modeling the effect of wave-vegetation interaction on wave setup. *Journal of Geophysical Research: Oceans*, *121*(6), 4341–4359. https://doi.org/10.1002/2015JC011392

van Vuuren, D. P., Kriegler, E., O'Neill, B. C., Ebi, K. L., Riahi, K., Carter, T. R., Edmonds, J., Hallegatte, S., Kram, T., Mathur, R., & Winkler, H. (2014). A new scenario framework for Climate Change Research: scenario matrix architecture. *Climatic Change*, *122*(3), 373–386. https://doi.org/10.1007/s10584-013-0906-1

van Wesenbeeck, B. K., de Boer, W., Narayan, S., van der Star, W. R. L., & de Vries, M. B. (2017). Coastal and riverine ecosystems as adaptive flood defenses under a changing climate. *Mitigation and Adaptation Strategies for Global Change*, *22*(7), 1087–1094. https://doi.org/10.1007/s11027-016-9714-z

van Zelst, V. T. M., Dijkstra, J. T., van Wesenbeeck, B. K., Eilander, D., Morris, E. P., Winsemius, H. C., Ward, P. J., & de Vries, M. B. (2021). Cutting the costs of coastal protection by integrating vegetation in flood defences. *Nature Communications*, *12*(6533). https://doi.org/https://doi.org/10.1038/s41467-021-26887-4

Villarreal-Rosas, J., Vogl, A. L., Sonter, L. J., Possingham, H. P., & Rhodes, J. R. (2021). Trade-offs between efficiency, equality and equity in restoration for flood protection. *Environmental Research Letters*, *17*(1), 014001. https://doi.org/10.1088/1748-9326/AC3797

Vitousek, S., Barnard, P. L., Fletcher, C. H., Frazer, N., Erikson, L., & Storlazzi, C. D. (2017). Doubling of coastal flooding frequency within decades due to sea-level rise. *Scientific Reports*, *7*(1), 1–9. https://doi.org/10.1038/s41598-017-01362-7

Vousdoukas, M. I., Bouziotas, D., Giardino, A., Bouwer, L. M., Mentaschi, L., Voukouvalas, E., & Feyen, L. (2018). Understanding epistemic uncertainty in large-scale coastal flood risk assessment for present and future climates. *Natural Hazards and Earth System Sciences*, *18*(8), 2127–2142. https://doi.org/10.5194/nhess-18-2127-2018

Vousdoukas, M. I., Mentaschi, L., Voukouvalas, E., Bianchi, A., Dottori, F., & Feyen, L. (2018). Climatic and socioeconomic controls of future coastal flood risk in Europe. *Nature Climate Change*, *8*(9), 776–780. https://doi.org/10.1038/s41558-018-0260-4

Vousdoukas, M. I., Mentaschi, L., Voukouvalas, E., Verlaan, M., & Feyen, L. (2017). Extreme sea levels on the rise along Europe's coasts. *Earth's Future*, *5*(3), 304–323. https://doi.org/10.1002/2016EF000505

Vousdoukas, M. I., Mentaschi, L., Voukouvalas, E., Verlaan, M., Jevrejeva, S., Jackson, L. P., & Feyen, L. (2018). Global probabilistic projections of extreme sea levels show intensification of coastal flood hazard. *Nature Communications*, *9*(1), 2360. https://doi.org/10.1038/s41467-018-04692-w

Vousdoukas, M. I., Ranasinghe, R., Mentaschi, L., Plomaritis, T. A., Athanasiou, P., Luijendijk, A., & Feyen, L. (2020). Sandy coastlines under threat of erosion. *Nature Climate Change*, *10*(3), 260–263. https://doi.org/10.1038/s41558-020-0697-0

Vousdoukas, M. I., Voukouvalas, E., Annunziato, A., Giardino, A., & Feyen, L. (2016). Projections of extreme storm surge levels along Europe. *Climate Dynamics*, *47*(9–10), 3171–3190. https://doi.org/10.1007/s00382-016-3019-5

Vousdoukas, M. I., Voukouvalas, E., Mentaschi, L., Dottori, F., Giardino, A., Bouziotas, D., Bianchi, A., Salamon, P., & Feyen, L. (2016a). Developments in large-scale coastal flood hazard mapping. *Natural Hazards and Earth System Sciences*, *16*(8), 1841–1853. https://doi.org/10.5194/nhess-16-1841-2016

Vuik, V., Jonkman, S. N., Borsje, B. W., & Suzuki, T. (2016a). Nature-based flood protection: The efficiency of vegetated foreshores for reducing wave loads on coastal dikes. *Coastal Engineering*, *116*, 42–56. https://doi.org/10.1016/j.coastaleng.2016.06.001

Vuik, V., Jonkman, S. N., Borsje, B. W., & Suzuki, T. (2016b). Nature-based flood protection: The efficiency of vegetated foreshores for reducing wave loads on coastal dikes. *Coastal Engineering*, *116*, 42–56. https://doi.org/10.1016/j.coastaleng.2016.06.001

Vuik, Vincent, van Vuren, S., Borsje, B. W., van Wesenbeeck, B. K., & Jonkman, S. N. (2018a). Assessing safety of nature-based flood defenses: Dealing with extremes and uncertainties. *Coastal Engineering*, *139*, 47–64. https://doi.org/10.1016/j.coastaleng.2018.05.002

Wahl, T., Haigh, I. D., Nicholls, R. J., Arns, A., Dangendorf, S., Hinkel, J., & Slangen, A. B. A. (2017). Understanding extreme sea levels for broad-scale coastal impact and adaptation analysis. *Nature Communications 2017 8:1*, *8*(1), 1–12. https://doi.org/10.1038/ncomms16075

Wamsley, T. V., Cialone, M. A., Smith, J. M., Atkinson, J. H., & Rosati, J. D. (2010). The potential of wetlands in reducing storm surge. *Ocean Engineering*, *37*(1), 59–68. https://doi.org/10.1016/J.OCEANENG.2009.07.018

Wang, W., Liu, H., Li, Y., & Su, J. (2014). Development and management of land reclamation in China. *Ocean & Coastal Management*, *102*, 415–425. https://doi.org/10.1016/J.OCECOAMAN.2014.03.009

Wani, M. A., Bhat, F. A., Afzal, S., & Khan, A. I. (2020). *Advances in Deep Learning* (Vol. 57). Springer Singapore. https://doi.org/10.1007/978-981-13-6794-6

Ward, P. J., Marfai, M. A., Yulianto, F., Hizbaron, D. R., & Aerts, J. C. J. H. (2011). Coastal inundation and damage exposure estimation: a case study for Jakarta. *Natural Hazards*, *56*(3), 899–916. https://doi.org/10.1007/s11069-010-9599-1

Ward, Philip J., Jongman, B., Aerts, J. C. J. H., Bates, P. D., Botzen, W. J. W., DIaz Loaiza, A., Hallegatte, S., Kind, J. M., Kwadijk, J., Scussolini, P., & Winsemius, H. C. (2017). A global framework for future costs and benefits of river-flood protection in urban areas. *Nature Climate Change*, *7*(9), 642–646. https://doi.org/10.1038/nclimate3350

Ward, Philip J., Jongman, B., Weiland, F. S., Bouwman, A., Van Beek, R., Bierkens, M. F. P., Ligtvoet, W., & Winsemius, H. C. (2013). Assessing flood risk at the global scale: Model setup, results, and sensitivity. *Environmental Research Letters*, *8*(4). https://doi.org/10.1088/1748-9326/8/4/044019

Ward, Philip J., Winsemius, H. C., Kuzma, S., Luo, T., Bierkens, M. F. P., Bouwman, A., de Moel, H., Diaz Loaizaa, A., Eilander, D., Englhardt, J., Erkens, G., Gebremedhind, E., Iceland, C., Kooi, H., Ligtvoet, W., Muis, S., Scussolini, P., Sutanudjaja, E. H., van Beek, R., ... Tiggeloven, T. (n.d.). *Aqueduct Floods Methodology Technical Note*.

Ward, Philip J, Strzepek, K. M., Pauw, W. P., Brander, L. M., Hughes, G. A., & Aerts, J. C. J. H. (2010). Partial costs of global climate change adaptation for the supply of raw industrial and municipal water: a methodology and application. *Environmental Research Letters*, *5*(4), 044011. https://doi.org/10.1088/1748-9326/5/4/044011

Ward, R. D., Friess, D. A., Day, R. H., & Mackenzie, R. A. (2017). Impacts of climate change on mangrove ecosystems: a region by region overview. *Http://Dx.Doi.Org/10.1002/Ehs2.1211*, *2*(4), 1211.

https://doi.org/10.1002/EHS2.1211

Willard, J., Jia, X., Xu, S., Steinbach, M., & Kumar, V. (2020). Integrating Physics-Based Modeling with Machine Learning: A Survey. *ArXiv*, *1*, 34. http://arxiv.org/abs/2003.04919

Williams, J., Irazoqui Apecechea, M., Saulter, A., & Horsburgh, K. J. (2018). Radiational tides: Their double-counting in storm surge forecasts and contribution to the Highest Astronomical Tide. *Ocean Science*, *14*(5), 1057–1068. https://doi.org/10.5194/os-14-1057-2018

Wing, O. E. J., Bates, P. D., Neal, J. C., Sampson, C. C., Smith, A. M., Quinn, N., Shustikova, I., Domeneghetti, A., Gilles, D. W., Goska, R., & Krajewski, W. F. (2019). A New Automated Method for Improved Flood Defense Representation in Large-Scale Hydraulic Models. *Water Resources Research*, *55*(12), 11007–11034. https://doi.org/10.1029/2019WR025957

Winsemius, H. C., Aerts, J. C. J. H., Van Beek, L. P. H., Bierkens, M. F. P., Bouwman, A., Jongman, B., Kwadijk, J. C. J., Ligtvoet, W., Lucas, P. L., Van Vuuren, D. P., & Ward, P. J. (2016). Global drivers of future river flood risk. *Nature Climate Change*, *6*(4), 381–385. https://doi.org/10.1038/nclimate2893

Winsemius, H. C., Jongman, B., Veldkamp, T. I. E., Hallegatte, S., Bangalore, M., & Ward, P. J. (2018). Disaster risk, climate change, and poverty: assessing the global exposure of poor people to floods and droughts. *Environment and Development Economics*, *23*(3), 328–348. https://doi.org/10.1017/S1355770X17000444

Winterwerp, J. C., Erftemeijer, P. L. A., Suryadiputra, N., Van Eijk, P., & Zhang, L. (2013). Defining eco-morphodynamic requirements for rehabilitating eroding mangrove-mud coasts. *Wetlands*, *33*(3), 515–526. https://doi.org/10.1007/s13157-013-0409-x

Wolff, C., Vafeidis, A. T., Lincke, D., Marasmi, C., & Hinkel, J. (2016). Effects of Scale and Input Data on Assessing the Future Impacts of Coastal Flooding: An Application of DIVA for the Emilia-Romagna Coast. *Frontiers in Marine Science*, *3*, 41. https://doi.org/10.3389/fmars.2016.00041

Woodworth, P. L., Hunter, J. R., Marcos, M., Caldwell, P., Menéndez, M., & Haigh, I. (2017). Towards a global higher-frequency sea level dataset. *Geoscience Data Journal*, *3*(2), 50–59. https://doi.org/10.1002/gdj3.42

Woodworth, Philip L., Melet, A., Marcos, M., Ray, R. D., Wöppelmann, G., Sasaki, Y. N., Cirano, M., Hibbert, A., Huthnance, J. M., Monserrat, S., & Merrifield, M. A. (2019a). Forcing Factors Affecting Sea Level Changes at the Coast. *Surveys in Geophysics 2019 40:6*, *40*(6), 1351–1397. https://doi.org/10.1007/S10712-019-09531-1

Worthington, T., Spalding, M., Herr, D., Hingorani, S., & Landis, E. (2018). Mangrove Restoration Potential: A global map highlighting a critical opportunity. *Geological Survey*. https://doi.org/10.17863/CAM.39153

Wu, W., Westra, S., & Leonard, M. (2017). A basis function approach for exploring the seasonal and spatial features of storm surge events. *Geophysical Research Letters*, 1–10. https://doi.org/10.1002/2017GL074357

Xingjian, S., Zhourong, C., Hao, W., Dit-Yan, Y., Wai-kin, W., & Wang-chun, W. (2015). Convolutional LSTM Network: A Machine Learning Approach for Precipitation Nowcasting. *Advances in Neural Information Processing Systems*, *2015*, 802–810.

Yamazaki, D., Ikeshima, D., Tawatari, R., Yamaguchi, T., O'Loughlin, F., Neal, J. C., Sampson, C. C., Kanae, S., & Bates, P. D. (2017). A high-accuracy map of global terrain elevations. *Geophysical Research Letters*, *44*(11), 5844–5853. https://doi.org/10.1002/2017GL072874

Yin, J., Yu, D., Yin, Z., Wang, J., & Xu, S. (2013). Modelling the combined impacts of sea-level rise and land subsidence on storm tides induced flooding of the Huangpu River in Shanghai, China. *Climatic Change*, *119*(3–4), 919–932. https://doi.org/10.1007/s10584-013-0749-9

Zeng, Y., Friess, D. A., Sarira, T. V., Siman, K., & Koh, L. P. (2021). Global potential and limits of mangrove blue carbon for climate change mitigation. *Current Biology*, *31*(8), 1737-1743.e3. https://doi.org/10.1016/J.CUB.2021.01.070

Zhang, K., Liu, H., Li, Y., Xu, H., Shen, J., Rhome, J., & Smith, T. J. (2012). The role of mangroves in attenuating storm surges. *Estuarine, Coastal and Shelf Science*, *102–103*, 11–23. https://doi.org/10.1016/J.ECSS.2012.02.021

zu Ermgassen, P. S. E., Mukherjee, N., Worthington, T. A., Acosta, A., Rocha Araujo, A. R. da, Beitl, C. M., Castellanos-Galindo, G. A., Cunha-Lignon, M., Dahdouh-Guebas, F., Diele, K., Parrett, C. L., Dwyer, P. G., Gair, J. R., Johnson, A. F., Kuguru, B., Savio Lobo, A., Loneragan, N. R., Longley-Wood, K., Mendonça, J. T., … Spalding, M. (2020). Fishers who rely on mangroves: Modelling and mapping the global intensity of mangrove-associated fisheries. *Estuarine, Coastal and Shelf Science*, *247*, 106975. https://doi.org/10.1016/J.ECSS.2020.106975

List of Publications

Publications on which this thesis is based

Tiggeloven, T., Couasnon, A., van Straaten, C., Muis, S., & Ward, P. J. (2021). Exploring deep learning capabilities for surge predictions in coastal areas. *Scientific Reports 2021 11:1*, *11*(1), 1–15. https://doi.org/10.1038/s41598-021-96674-0

Tiggeloven, T., de Moel, H., Winsemius, H. C., Eilander, D., Erkens, G., Gebremedhin, E., Diaz Loaiza, A., Kuzma, S., Luo, T., Iceland, C., Bouwman, A., Van Huijstee, J., Ligtvoet, W., & Ward, P. J. (2019). Global scale benefit-cost analysis of coastal flood adaptation to different flood risk drivers. *Natural Hazards and Earth System Sciences, 20(4), 1025-1044.*

Tiggeloven, T., de Moel, H., Zelst, V. van, Wesenbeeck, B. K. van, Winsemius, H. C., Eilander, D., & Ward, P. (2022). The benefits of coastal adaptation through conservation of foreshore vegetation. *Journal of Flood Risk Management, e12790.*

Tiggeloven, T., Mortensen, E.S., de Moel, H., van Zelst, V. T., van Wesenbeeck, B. K., Worthington, T., Spalding, M. & Ward, P. J. T Mangrove restoration and coastal flood adaptation: a global perspective. *In review.*

Tiggeloven, T., de Moel, H. & Ward, P. J. Hybrid solutions and global coastal flood risk management. *In review*

Other publications

Mandel, A., **Tiggeloven, T.**, Lincke, D., Koks, E., Ward, P., & Hinkel, J. (2021). Risks on global financial stability induced by climate change: the case of flood risks. *Climatic Change*, *166*(1–2), 1–24. https://doi.org/10.1007/S10584-021-03092-2/TABLES/2

Ignjacevic, P., Botzen, W. W., Estrada, F., Kuik, O., Ward, P., & **Tiggeloven, T.** (2020). CLIMRISK-RIVER: Accounting for local river flood risk in estimating the economic cost of climate change. Environmental Modelling & Software, 132, 104784.

Knittel, N., Tesselaar, M., Botzen W., Bachner, G., **Tiggeloven, T.** Bearing the indirect costs of flood risk: A macroeconomic assessment of different insurance systems in Europe under climate change. In review with *Economic Systems Research.*

Paszkowski, A., **Tiggeloven, T.**, Borgomeo, E., Hall, J. Disparities in exposure to geomorphic hazards in Bangladesh. In review with *Nature Communications.*

Tesselaar, M., Botzen, W. W., Haer, T., Hudson, P., **Tiggeloven, T.**, & Aerts, J. C. (2020). Regional inequalities in flood insurance affordability and uptake under climate change. Sustainability, 12(20), 8734.

Ward, P. J., Daniell, J., Duncan, M., Dunne, A., Hananel, C., Hochrainer-Stigler, S., Tijssen, A., Torresan, S., Ciurean, R., Gill, J. C., Sillmann, J., Couasnon, A., Koks, E., Padrón-Fumero, N., Tatman, S., Tronstad Lund, M., Adesiyun, A., Aerts, J. C. J. H., Alabaster, A., Bulder, B., Campillo Torres, C., Critto, A., Hernández-Martín, R., Machado, M., Mysiak, J., Orth, R., Palomino Antolín, I., Petrescu, E.-C., Reichstein, M., **Tiggeloven, T.**, Van Loon, A. F., Vuong Pham, H., and de Ruiter, M. C.: Invited perspectives: A research agenda towards disaster risk management pathways in multi-(hazard-)risk assessment, Nat. Hazards Earth Syst. Sci., 22, 1487–1497, https://doi.org/10.5194/nhess-22-1487-2022, 2022.

Acknowledgments

It goes without saying that the PhD journey can be quite demanding and exhaustive. There is always this constant pressure of feeling that you are falling behind schedule, that the work you do will never be good enough and up to some fictional self-determined standard, or that you must make sacrifices, mentally or socially, to accomplish the insanely undoable tight deadlines you set for yourself, because goodness knows why, we add a little more pressure on ourselves. Almost everybody feels the same way at a certain stage in the PhD, but still this journey can feel quite solitary and desolate. Surely you are thinking you must be the only one struggling considering the fact that you are only hearing about everybody's accomplishments. As for my personal life and probably similarly to many others, I also underwent quite some difficult moments during the PhD years. I almost slipped into a burnout, I have sacrificed a lot up to the point that I now look back and cannot find myself anymore. I have caused pain to others because I have chosen the PhD above everything else. I have looked at code so much that looking into a specific model still brings up a physical nauseous feeling, and I have given myself for this PhD until I had no more tears left to cry.

Throughout the PhD I have thus been wondering that if I had to choose between doing it all over again or making the decision to follow my career path elsewhere, would I go through this again? Was this all worth it? I find this question very difficult to answer, and solely looking into the struggles to obtain the PhD, I am tending towards no. However, seeing all the wonderful and lovely connections I have made, sharing so many precious moments and having the immense privilege of getting all the support of the fantastic people in my life that stood with me throughout this arduous journey, then I ask myself the question again and the answer easily shifts to yes, it's definitely worth it. I wouldn't even have to sleep on this question anymore given how many amazing people I have met and how many connections that grew even stronger during this time. I'm so happy to see that people are now more open about their struggles in academia, or in life in general, and that there is this community you can really feel part of. But it grieves me every time I see people going through the same struggles and detrimentally sacrificing themselves in a similar way I have. I hope you all will be kind with yourself. We are there for each other, and remember that through thick and thin, in moments of joy and moments of hardship, reach out! Betting on love will not only dissolve the lumps of selfishness or solitariness but will break the dams that distance us.

I'm eternally grateful to everyone that took the time to talk about mental health, to support me during the PhD, putting a much appreciated and sometimes very needed smile on my face, organising all the fun social activities and experiences, and for enduring me always bothering you all for a talk at random office hours. I sincerely love you all. Thank you for all the love and support you gave me throughout this journey. I will definitely pay you all back in full and then give some more love!

Thank you especially to my supervisors Philip and Hans. Without the patience, the countless discussions and all the room you gave me for showing imperfection while always cheerfully supporting me, I would not have made it. Without your guidance I

sincerely doubt if I would be able to find the path to finishing the PhD. Philip you are the best supervisor I could have imagined. You have always been open for discussing important matters and helping me make compromises while safeguarding me for always trying to do too many things. Always thinking along, mindful of one's feelings and being decisive when needed, has been the perfect recipe for helping me shape my career. Mostly, I happily look back at the wonderful trip in NOLA or all our talks about music. I'm super happy I get to continue enjoying working with you for some time still. Hans, without all the hours and devotion during our discussions, I would seriously have had to double the time for the PhD. I remember when I took your maths course more than 10 years ago and since then I always thought you were the best teacher I ever had. I am so grateful to have been given the opportunity to pick your brain so many times during my PhD and of course for all the fun on our fieldwork trips. Many times, we have been wandering around Diekirch to look for decent food or trying to finish insanely big desserts. All the other members of the reading commission, thank you for accepting to read and approving the thesis. Wouter, I always enjoy discussing work with you, and I'm hoping we can continue this. Dim, I hope there will be an opportunity to work together with you to explore a machine learning application.

Alle liefde en ondersteuning die ik van jullie heb gehad is niet uit te drukken in woorden. Jullie zijn altijd met me aan het meedenken geweest, ook al was ik gestrest of had ik andere dingen aan mijn hoofd. Altijd geven jullie mij ruimte, stabiliteit en genegenheid wanneer ik het nodig hebt. Dankjewel Mam, Pap, Meggie en Rinze en natuurlijk kleine Novi. Mam, ik koester alle mooie gesprekken die we hebben gehad over hoe we samen mentaal sterker en fijner in het leven kunnen staan. Ik ben blij dat ik jouw doorzettingsvermogen, kracht en het durven in het diepe gegooid te worden heb overgedragen gekregen. Pap, jouw precisie, geduldigheid en nieuwsgierigheid heeft me geschapen en gezorgd dat ik in het leven sta waar ik nu ben. Beiden hebben jullie mij geleerd dat liefde geven en altruïsme uiteindelijk zal uitmonden in geluk, affiniteit en harmonie. Mijn perfecte grote zus waar ik altijd naar opkijk, houdt haar broertje nog altijd nauw in de gaten of alles goed gaat. Ik waardeer al onze gesprekken, de zondagochtend uitjes met Novi, en ik heb tijdens deze periode heel erg genoten van onze gezamenlijke passie voor koken en een feest maken van elke kleine gelegenheidjes. Rinze met jouw humor, luchtigheid en geïnteresseerdheid voel ik me altijd speciaal. Alle liefdevolle momentjes met Novi hebben mij altijd een hard nodige glimlach op mijn gezicht gegeven.

Het is echt een onwijs grote eer dat je het artwork van het proefschrift wilde ontwikkelen! Het was een prachtige samenwerking met vele inspirerende discussies. Het resultaat is mooier dan ik ooit had durven dromen. Mirjam, bedankt voor dit allemaal. Ilko, bedankt voor alle hulp bij het vormgeven van de digitale cover en boekenlegger. We gaan snel weer een keer wat leuks doen!

Without having such wonderful friends giving me so much pleasures in my life, the most trivial journey in life will become tedious and tiresome. William, ik waardeer het enorm dat je altijd een stabiele factor bent in mijn leven, voor alle klimsessies meerdere keren per week, voor de gezellige lunches met kleine Elliot, voor altijd alle interesse in mijn leven. Toen we elkaar ontmoette, meer dan een half leven geleden, wist ik al dat

onze band speciaal was en ben blij je nog zoveel te kunnen zien in mijn leven. Keanie, van studiegenoot tot huisgenoot tot een van de meest dierbare personen in mijn leven. Ik waardeer al onze gedeelde nerdy interesses en de mooie gesprekken, bijvoorbeeld tijdens onze ochtendwandelingen voor werk. Niets is zo dynamisch en gezellig als vrienden zijn met jou Jeroen. Ik geniet enorm van al onze mooie momentjes, je humor, en vastberadenheid om van alles een gezellig moment te maken. Michelle, ik ken niemand zo veerkrachtig en sterk als jij. Ik bewonder jouw passie en liefdevolle houding in het leven. Alle humor, bordspel avontuurtjes, en onze gezamenlijke passie voor experimenteren met koken (plus decoratie!!) hebben mij veel luchtigheid gegeven en ik hoop dat ik dit ook kan bieden voor jou. Kevin, alle hard nodige tripjes in Malaga en onze losgaan momentjes tijdens het muziek maken laten me altijd beter voelen. Ik waardeer het echt enorm om iemand te hebben in mijn leven die altijd, hoe dan ook, meteen voor me klaar staat mocht er wat zijn. Dennis en Maarten de Vries, ik koester al onze fijne en diepgaande discussies, tot in de late uurtjes, over het leven, gezondheid, werk en muziek. Ik denk dat we nooit uitgepraat zullen raken. Vanaf het moment dat we elkaar ontmoette tijdens VoorUit was het een ware sensatie. Alle talloze fijne avondjes uit, (corona) thuisfeestjes, filmavondjes, vaste agenda zoals museumnacht, festivals en feestdagen, geven mij een ware Friends gevoel. Dankjewel Marieke, Kayleigh en Jonas. Chen thank you for all the fun dinners and the best guidance to make my (im)perfect dumplings. Kathy, your enthusiasm, and energy in life always give me a cheerful feeling. All the yoga sessions during the lockdown kept me sane and on track for the PhD. Maarten Buwalda, we zien elkaar niet vaak, maar als we elkaar zien bloeit onze ware vriendschap weer op. Rutger en Domo dank voor alle gekkigheid en de klimuitjes naar Fontainebleau!

Tim and Anaïs, the sweetest friends, thank you so much for accepting to be my paranymphs and already making me feel special with all your enthusiasm and involvement. Anaïs, to me our collaboration is how science and academia should work. Authoring a paper as shared first author with you, that is part of this thesis, is still the most accomplished and fun achievement I have done. Doing every step together, from coding to writing, was an enlightening experience that not only was super fun, it also hugely improved the quality of science and reduced production time. I enjoyed all of our home officing days, dinners and your devilishly fun company, making you a dear friend. Tim, your positivity and wholehearted devotion for collective happiness inspires me. I'm so happy to see we are becoming such good friends. Since drinking a beer on a couple meter high boulder in the middle of the night in France, it has been set in stone. I truly cannot wait when the time comes for you to become a 'real' doctor too! Maybe then you can finally beat me with chess.

Amelie, it has been such a pleasure to be working with you. The last three years have shown that persistence through online communication and meetings can result in something we both are absolutely proud of. I'm so excited to continue our research agenda and hopefully we can live up to all our big ideas! It feels special that out of all the time collaborating a valuable friendship has evolved. I'm super happy that out of sheer luck I happened to be in Oxford to join your PhD party. Who knows what the future brings regarding Vietnam.

I cannot even count how many times spontaneously we got to hang out together. I feel like the spring of 2021 has been a crazy one. One that was filled with social activities, parties, start of the curry nights, and countless others. I have never laughed so much in my life and enjoyed all those social outings and it all revolved around you Camille, Elvia and Rhoda! I treasure the best and, I think also, longest brunch day I ever had were we really bonded. Camille, your spontaneity and disquisitive mind, drives you as a person and this is what makes you special. I always love to philosophise with you. You make me feel like family. Elvia (and of course Kenny) have made me feel at home with all those super fun home office days during lockdown. I think in a short amount of time we were able to cross off every nice food places in de Pijp. I still laugh out of pure joy every time I hear the song Traag. Rhoda it's always so much fun to spend time with you. I really treasure all the fun conversations, and of course the witty games to make fun of one another.

Henrique, I really treasure how good friends we become in such a short timeframe. I so much enjoy all our shared interests, making music together, and all our meaningful talks in which I'm amazed how fast a deeper understanding we create for each other. You always make me feel happy and like kindred spirits. Ana you are the best friend, a friend to share the same plants with (Blij and Feliz), share the best music, and share the spectacular homemade food. I'm keeping you to your end of the promise you made to make all the sweets, water the plants and send nice music! Eric thank you so much for all the fun outings, wherever you are, everybody follows in a trail of joy. It's always exciting spending time with you and I'm happy to be sad boys together. I'm really glad we finally did go to the NbS conference with a flamboyant twist. Alessia, thank you so much for all the fun working experiences, the meaningful talks, the connection, the friendship, and your expert judgments with thesis help or life in general. With your generosity and virtues, I sincerely think that the world would be a happier, brighter, and colourful place if it follows you as an example.

The best quote about the PhD, or life in general, "Sometimes you have good days, and sometimes you have bad weeks" is something to live by. Liselotte I so much enjoyed all our fieldwork trips, the fancy food we ate in Kampen or in Tenerife, always to share of course! I always admire your sense of staying in reality. Marleen, I think I consider you my first real professional colleague where you work on similar interests together, and this means a lot to me. I so hope we get to travel a lot more together, just because we need to finish all the Gilmore Girls episodes! Jens, the more I get to know you, the more amazed I am by your beautiful personality. I'm happy we get to hang out a lot.

It wouldn't be the best office room in the world without Nadia, Gabi, Kostas and Giorgia! Thank you for showing me around and for welcoming me when I walked in the office very shyly for the first time. You all showed me how to make the office days more fun and lighter. All the enthusiasm helped me have joy in the work we do. And of course, Nadia your humour and sending of gifs are spot on! Thank you, Max, Pedja en Lars for all the fun times together in the IVM band, the countless hours of practice, and of course our amazing trip to Serbia. Max I super enjoy that we still work together. And Lotte I think we have made some fun anecdotes on the Serbia trip.

It wouldn't be a normal office day when you are not asked to do some fun (outdoor) activity after work, be that climbing, volleyball, swimming, going for a drink, or all the other things. I super enjoy this environment so much. The IVM bouldering vibe is captivating. The devotion to play yet another match of volleyball is alluring. And the willingness to connect as colleagues but also as friends is beautiful. Niels, I always admire your infamously twisted kneebars and of course not to forget your thoughtful and sweet personality! Marthe, I have enjoyed all the wonderful moments during bouldering, work, and all personal talks. Joel, your sweetness and warm-heartedness brings me joy. I love sharing obscure music with you. Tamara, I super enjoy all the bouldering trips and conversing with you. I hope we can live up to Joel's pinky promises lots of more times to come. There are few people in the world where you can take a three-week trip together (from camping to conference to fieldwork), and still laugh so loud at the end of it, Ileen, I super enjoyed those good times together and sitting on the train being fed up with all but everything together. From supervising your thesis, through working together as colleagues, to becoming friends, Sophie, I still have not seen any of your tv-famous baking skills but I'm sure this will change very soon. Lena, I super enjoy your lovely personality, and hope we get to do many more dinners together with all our social plans. Heidi, there are few people super kind from the heart and one of them is you. Thank you for all the lovely outings, postcards, and concert plans to come. Hanna, your joyfulness, and energy is a delight to see. Sem, I always super enjoy having discussions with you and then finding out we share so many similarities. I'm sad you cannot be at the defence but we for sure will make up for it. Tristian, beach volleyball won't be fun if you are not at the opposite of the field. Teun, I'm always happy to see you at all the social outings or the fun camping trip we did.

I'm blessed to be part of so many PhD councils (VU PhD council, IVM PhD council, Sense PhD council and PNN) during the past few years. Shaping academic culture to be more viable and less prone to mental health related issues, is strenuous, but a cause worth fighting for. Thank you, Margot and Nina, for setting up the VU PhD council together and all the inspiring discussions and our devotion to make a change in academia. Thank you, Perline, Nadia, Nicole, Fiona, and Rick. Thank you Fernie for all the connections you made for us and enthusiastically advocating our agenda to several VU-level consultations. Thank you, Jeroen Geurts, for always giving me and other young academics the opportunity to express themselves. It was super fun to have been able to install the IVM PhD council and I'm proud to see that it is going stronger ever since. Thank you Xiaoran and Rebecca (and Lies) for all the wonderful talks and sharing amazing ideas.

The last year would not be so much fun and inspiring without the VU MYRIAD team! I super enjoyed all the trips we did and the devotion we have to advance the multi-hazard research. Judith and Ruoying, the enthusiasm and energy you bring to the office is making work fun and enlightening. Elco, all the fun interaction with you I hold dear, be that at the Kampen fieldworks, discussing work/life related issues or trashing on Slack. Anne, I really admire your ambition to shape academia in a more diverse and all inclusive way, and I'm happy we get to talk about this together sometimes. Thank you Julius for sharing special MYRIAD experiences during those trips.

Thank you also to all the EG people that treated me sometimes as their own with regards to social events. Katharina, when you are around the sun is always shining. Tagada will be boring and dull without you, Perrine, I really treasure our beach trip on the bike in Montpellier together and life is always fun when you are around. Alex I always so much enjoy being sassy together. The day going to the Bird brewery and the walks in the forest is something I still hold dear, thank you Cecilia, Claudia and Floris. Walking in the office would not be so fun without encountering you Pierre. Thank you for all the fun times and good discussions Jonas and Job.

The IVM wouldn't be this special and illuminating place it is now without you. Maurizio, your eating habits very much inspire me to the moon. Irene, I hope soon our conversation open up more than talking about poster caseholders. Vita, where did the time go, since we always had fun sitting next to each other in the office. Mark, I know your life and eating habits have considerably changed (for the better) to a more collective behaviour after going to Tenerife with the staff. Raed, with your fun and bubbly personality there is always something to cheer about. Marjolijn, thank you for making the office a lively place to work in and of course always withstanding my not so bright questions. Neele, I really enjoy our passion for doing sportsy activities after work and happy to see you at many social outings or seeing you unexpectedly at VU meetings. Sanne, I'm so happy to have been able to work with you during fieldworks, it always feels like a great collaboration where I can learn a lot. Leen, I'm happy we got to bond over PhD related matters, and even happier I got to be your PhD buddy. Lars, I really enjoy working together and supervising the students. Dirk, I always admire your knowledge and love for code we share together. Rex, I really enjoy your vibe and passion for games. Andres, thank you for all the help at the start of the PhD and showing that office life also can be without taking everything too literally. Chiem, I treasure that I was able to pick your brain a lot on the paper we did together. Sadhana, thank you for always having a sunny vibe in the office and the nice talks we had in Potsdam/Berlin. Huazhi, I always feel good when you are around. Tim Williams, the talks about brewing always makes me want to do more of this. Toon, the countless times of having a drink after office hours were always fun. Kina, the Kampen fieldwork wouldn't be as fun without you there. Thank you also to all the others where I shared meaningful discussions/experiences with. That includes you, Alejandra, Anne Elise, Atoesa, Bep, Caterina, Fei, Iris, Job, Joshua, Kate, Lisa, Liz, Lotte, Marijn, Marlies, Max, Michelle, Nina, Noelle, Paolo, Sem, Sunshine, Tadzio, Ted, Thijs, Yue.

I'm happy to have made a lot of connections outside of the IVM as well through conferences, fieldwork and project meetings. Thank you all for the social activities and inspiring discussions. Thank you for all the connections I've made through MYRIAD, the Hydrology students during the fun fieldworks, or the MSc students that wanted to do the thesis with me. Teun, choosing to do a thesis with me twice is an honour. Thank you as well Agnes, Beck, Cas, Fergus, Floris, Gwen, Josse, Louie, Pietro, Sascha, Tim and Wessel. It was a delight to work with you. Thank you Evelyn and Samuel for the fun times during Potsdam and Berlin, and happy to see you again from time to time. Vincent and Bregje, I really enjoy working with you and happy you were willing to contribute on several papers. Thank you Arno and Willem for all the fun working experiences and also thank you to the rest of the Aqueduct team.

Met trots kijk ik terug op alle fijne en lieve momenten waar je naast me stond tijdens de afgelopen vijf jaar. Door jou heb ik me nooit alleen gevoeld, want bij zware en donkere tijden scheen jij altijd het licht op mijn pad dat ik achtervolgde. Tijdens mijlpalen wist je altijd een waar feest te maken en zonder jouw kennis en visie op het leven was ik nooit de persoon met zelfverzekerdheid geworden dat ik vandaag de dag ben. Met vastberadenheid en gezond realiteitsbesef heb je geholpen om dit product te maken. Vanuit het diepste punt van mijn hart ben ik dankbaar jou in mijn leven te hebben. Rael, je bent prachtig in je authenticiteit en ik weet zeker dat de wereld nooit genoeg van je krijgt. Met jouw energie, passie en humor weet je altijd elke situatie in te kleuren met pret, genegenheid en geborgenheid.

About the author

Timothy Tiggeloven was born in Amsterdam, the Netherlands on 19th of July 1991. He holds a BSc degree in Earth and Economic and a MSc degree in Hydrology from the Vrije Universiteit Amsterdam (VU). In his MSc thesis project, Timothy explored the interaction between water storage capacity and evaporation in sand dams, collaborating with South Eastern Kenya University (SEKU) during his fieldwork in Kitui (Kenya).

In September 2017, Timothy joined the Institute for Environmental Studies (IVM) at the Vrije Universiteit Amsterdam as a junior researcher, working on flood risk assessment at the global scale. During this position, Timothy and colleagues closely collaborated with the World Resource Institute (WRI), PlanBureau voor Leefomgeving (PBL), Deltares, and Universiteit Utrecht to develop the Aqueduct Flood Analyzer tool. This tool estimates coastal and riverine flood risk at the global scale and analyses the benefits and costs of investing in flood protection. In April 2018, Timothy started his PhD on Nature-based Solutions for coastal flood risk management, a position funded by the NWO-VIDI grant awarded to prof. dr. Philip J. Ward.

Over the course of the PhD, Timothy has been extensively engaged in capacity building and policy development with human resources, teacher staff, (etc.), through his active contribution within the PhD community at the VU. With a group of PhDs, he (re-)established the VU PhD council. During his role as chair of the VU PhD council, Timothy took part of a sounding board on PhD policy related matters for the VU Network of Graduate Schools (NoGS) and VU central research policy meetings (VUO). Furthermore, he participated as a member of the Promovendi Network Nederland (PNN) and the SENSE PhD council. Additionally, he co-founded the IVM PhD council in which he initiated the buddy system among other things. Timothy is still active as a member of the taskforce for the Awards & Recognition team of the VU and advises on the development of the PhD policy roadmap.

Throughout his PhD, Timothy (co-)authored several papers in international peer-reviewed journals and presented his work at several international scientific conferences including EGU, AGU, FloodRisk2020, Nature-based Solutions Oxford. In his current postdoc position at the IVM, Timothy focusses on multi-hazard risk and the interaction of dynamics in vulnerability and disasters using novel methods, such as deep learning. For this position, he works as project management support for the Horizon2020 project MYRIAD-EU.